Title
Studies in Gold-Heteroatom Bonds: Synthesis, Reactivity, and Application to Catalysis

Author
Johnson, Miles William

Publication Date
2014

Peer reviewed|Thesis/dissertation

Studies in Gold-Heteroatom Bonds:
Synthesis, Reactivity, and Application to Catalysis

by

Miles William Johnson

A dissertation submitted in partial satisfaction of the

requirements for the degree of

Doctor of Philosophy

in

Chemistry

in the

Graduate Division

of the

University of California, Berkeley

Committee in charge:

Professor Robert G. Bergman, Co-Chair
Professor F. Dean Toste, Co-Chair
Professor Stuart Linn

Fall 2014

Abstract

Studies in Gold—Heteroatom Bonds:
Synthesis, Reactivity, and Application to Catalysis

by

Miles William Johnson

Doctor of Philosophy in Chemistry

University of California, Berkeley

Professors Robert G. Bergman and F. Dean Toste, Co-Chairs

Understanding the interaction between gold and its ligands is essential in exploiting this versatile metal in many areas of chemistry. Organogold chemistry and the reactivity of gold-carbon bonds, particularly in the context of catalysis, have been extensively investigated over the past two decades. Markedly less research has been dedicated to gold-heteroatom bonds. A desire to understand these bonds has resulted in four studies with vastly different goals and conceptual underpinnings, but that are unified by utilizing gold's interaction with X-type heteroatom ligands.

Chapter 1 is the starting point of this broader study, and relates the preparation and study of the first terminal gold(I) amides and phosphides. A series of N-heterocyclic carbene-supported complexes was synthesized and the reactivity of these new compounds explored. It was determined that gold(I) amides are unlikely to intervene as catalytic intermediates, as has been suggested in the literature, and that they exhibit high nucleophilicity and basicity toward a number of substrates. Gold(I) phosphides were identified as intermediates in a catalytic phosphide alkylation, the first example of C-P bond formation using a homogeneous gold catalyst. These experimental studies were further supported by computational studies to gain insight into the bonding between gold and heteroatoms.

Chapter 2 documents the bottom-to-top construction of a catalytic cycle for the synthesis of sulfinate derivatives from boronic acids and metabisulfite. This study exploited the well-documented insertion of sulfur dioxide into Au-C bonds, transmetallation of Au-O bonds with boronic acids, and the lability of sulfinate ligands to construct a catalytic cycle that allows access to a variety of sulfonyl compounds *via* common sulfinate intermediates. The potential utility of this method is demonstrated in the facile construction of a chemical library of sulfones and sulfonamides from a single sulfinate intermediate.

Chapter 3 is based on the surprisingly poor bonding between the azide anion and gold(I). Instead of discounting gold azides as catalysts or pre-catalysts, the opportunity to form carbon-azide bonds was seized; since azides are unlikely to poison a gold catalyst but are excellent nucleophiles, an enantioselective hydroazidation of allenes was developed, the first documented hydroazidation that does not proceed *via* conjugate addition.

Chapter 4 marks a departure from gold(I). In this final study, heteroatom bonds are used to stabilize gold(III) in a pincer ligand framework. A series of gold(III) iminothiolate, carboxylate, and amidate complexes was prepared. The synthesis of structurally similar compounds offered the opportunity to determine if, and to what extent, different heteroatoms decreased the reduction potential of gold(III). The findings from this project may inform ligand design for the myriad applications of gold(III)

Table of Contents

Abstract 1
Table of Contents i
Acknowledgements ii

Chapter 1. Synthesis and Reactivity of Gold(I) Amide and Phosphide Complexes 1
Introduction 2
Results and Discussion 3
Conclusion 10
Experimental 12
References 21
DFT Calculations 23
NMR Spectra 36
X-Ray Crystallographic Tables 51

Chapter 2. Application of Fundamental Organometallic Chemistry to the Development of a Gold-Catalyzed Synthesis of Sulfinate Derivatives 71
Introduction 72
Results and Discussion 75
Conclusion 82
Experimental 83
References 94
NMR Spectra 95
X-Ray Crystallographic Tables 101

Chapter 3. Development of an Enantioselective Hydroazidation of Allenes Catalyzed by Gold(I) 107
Introduction 108
Results and Discussion 110
Conclusion 113
Experimental 115
References 117

Chapter 4. Synthesis of Stable Gold(III) Pincer Complexes with Anionic Heteroatom Donors 119
Introduction 120
Results and Discussion 120
Conclusion 124
Experimental 125
References 132
NMR Spectra 134
X-Ray Crystallographic Tables 148

Acknowledgements

The friends and mentors that I have found have been the best part of my graduate experience. So many people were involved in helping me reach my goals and completing my doctoral studies. One page of thanks is not enough.

I would first like to thank my advisors, Profs. F. Dean Toste and Robert G. Bergman. They gave me immense support and freedom throughout my time at Berkeley. The mentoring they provided and patience they showed have served as a guide for the type of educator I aspire to be. Their distinct but complementary approaches toward education and research provided me with an enriching graduate experience that I cannot imagine having received with any other advisor(s).

My undergraduate research advisor Prof. C. Wade Downey helped me find my passion for organic chemistry and for that I am overwhelmingly grateful. I would not be writing this thesis without the mentoring that he has given me over the past nine years.

The staff of UC Berkeley Chemistry played an integral role in my graduate career. First and foremost, I thank Anneke Runtupalit for her friendship, advice, and unparalleled administrative support. Drs. Antonio DiPasquale, Chris Canlas, Kathleen Durkin, and Xingzheng Yang kindly dedicated their time to helping me analyze and better understand the compounds that I made.

I am thankful for the opportunity to work with and befriend over 120 labmates. My classmates Chen Zhao, Thomas Gianetti, Hunter Shunantona, Vivian Lin, and Jason Ji have been with me through classes, practice quals, problem sets, and literature presentations; I cannot imagine getting through all of it without them. There are too many post-docs to thank all of them individually, but I must single out Drs. Jürgen Koller, Neal Mankad, Matthew Winston, Hosea Nelson, and Mark Crimmin for the countless pieces of advice, helpful discussion, training, and friendship they have given me. Finally, I would like to acknowledge Drs. Miriam Bowring, Aaron Lackner, and Casey Brown. I could not have asked for better graduate student mentors and friends.

The work that I have done was in part collaborative. Scott Bagley gave me the opportunity to work on a fascinating problem and showed me an industrial perspective on chemistry. Dimitri Khrakovsky generously provided catalysts for the hydroazidation project. Finally, I must acknowledge Sophie Shevick who worked with me as an undergraduate researcher. She not only was a part of three of my projects but also a great labmate and constant reminder of why I have pursued a career in chemistry.

In a department of over 400 people, you can make a lot of friends in five years. Thank you Olivia Lee, Allegra Liberman-Martin, Jessica Kisunzu, Stephanie Jones, Chelsea Gordon, Teera "Annie" Chantarojsiri, Christo Sevov, Billy Hart-Cooper, Micah Ziegler, and Caitlin Stevens for your friendship.

My family has, and continues to be, an integral part of my life and education. I thank my mom and dad for all their love and support, and for providing me with the opportunities that have allowed me to make it this far. Thank you Nia for being a terrific little sister and great friend.

Lastly, I want to thank Priscilla Erickson. Thank you Priscilla for your love and friendship. I never thought that I would meet someone who understands me so well and who could bring so much joy to my life. My greatest discovery at Berkeley has been the indescribable happiness that I have found with you.

Chapter 1. Synthesis and Reactivity of Gold(I) Amide and Phosphide Complexes

Introduction

The transition metal-heteroatom bond is ubiquitous in organometallic and inorganic chemistry. This linkage is often found in coordination complexes where a heteroatom-based ligand stabilizes a metal through a dative interaction, a phenomenon that has been under study for over a century. More recently, late transition metal complexes bearing X-type heteroatom ligands have been a center of intense investigation.[1,2] This class of compounds plays a pivotal role in bio-inorganic systems[3] and as intermediates in catalytic processes, such as the Buchwald-Hartwig coupling,[4] amination of C—H bonds,[5,6] and hydroamination (Figure 1).[7]

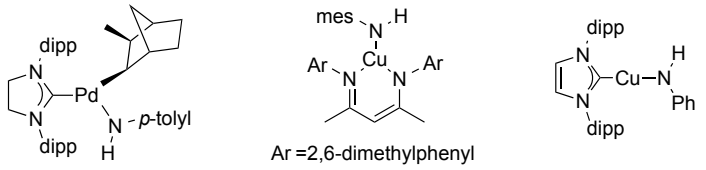

Figure 1. Intermediates in amino alkylation (left),[8] amino arylation (center),[5] and hydroamination (right)[7]

Within the transition series, Au—X bonds have received relatively little attention despite the gains made in gold catalysis over the past decade.[9,10] The study of gold complexes has focused mainly on the formation of C-X (X = C, N, O) bonds *via* organometallic intermediates, *i.e.* the bond is formed from a Au-C and not a Au-X intermediate. Some reports have invoked Au(III)-N bonds as intermediates in amination reactions (Figure 2), [11,12] and others have proposed this for Au(I) by analogy,[13-15] but without structural data to substantiate the claim.

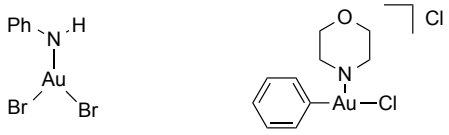

Figure 2. Proposed gold amide intermediates in hydroamination (left)[11] and arylamination (right)[12]

The study of Au(I) heteroatom bonds is of great fundamental interest as well. Since gold is the most electronegative transition metal (2.54 by the Pauling scale) and possesses the largest ionic radius (1.51 Å for Au(I)), it should be expected to form bonds with more covalent character with most light p-block elements and yet experience more d-π/p-π repulsion relative to other transition metals.[16,17] This latter factor should be further enhanced by the filled 5*d* orbitals and their expansion due to relativistic effects. [18] The reactivity of late-metal heteroatom bonds has been attributed to d-π/p-π repulsion (Figure 3) and the ionic character of the M-X bond,[19] making Au(I)-X bonds of particular interest since repulsive forces and the ionic character of the bond do not track as they do in the case of other M-X bonds.

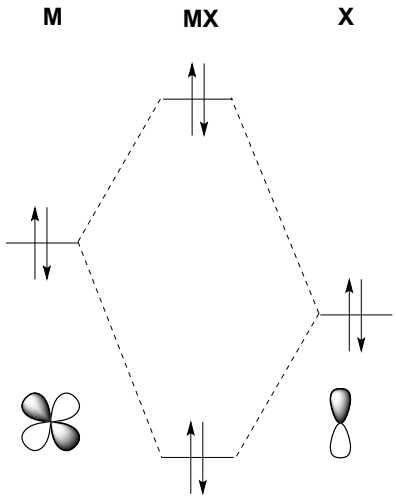

Figure 3. Molecular orbital depiction of d-π/p-π repulsion.

Gold(I) pnictogenides represent a class of compounds that are ideal for the in-depth study of gold—heteroatom bonds. Those that are reported in the literature exist as μ-phosphides[20-22] and –amides[23] (Figure 4), suggesting that terminal species are disfavored, presumably due to the high nucleophilicity and Lewis basicity of the sterically unhindered heteroatom and the linear geometry of gold(I). A single terminal gold(III) amide had been characterized crystallographically prior to the work described here.[24] The reactivity of this electron-deficient anilido complex has not been explored to date.

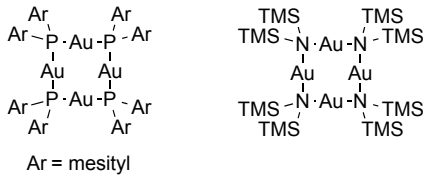

Figure 4. Representative examples of tetrameric gold(I) phosphide[21] and amide complexes.[23]

Results and Discussion

The existence of bridging gold(I) pnictogenide complexes is a testament to the potential reactivity of the corresponding monomers and makes clear the need for a sterically encumbered supporting ligand. Based on its frequent use in gold catalysis[25] and ability to stabilize gold(I) hydroxides[26] and alkoxides,[27] N-heterocyclic carbene (NHC) ligands were chosen, specifically IPr (1,3-bis(2,6-diisopropylphenyl)imidazole-2-ylidene) to stabilize new gold pnictogenides. Amido ligands were installed by a metathetical route from IPrAuCl and a lithium amide (Scheme 1). The diisopropyl amido (**1**) and anilido (**2**) complexes were characterized crystallographically to confirm that indeed monomeric terminal amido complexes had been prepared (Figure 5). Complex **1** is of particular interest since other group 11 metal amides require aryl substitution on nitrogen for stability (*vide infra*). This compound shows no signs of decomposition, including β-hydride elimination as seen with other transition metal amides,[28,29] even after prolonged heating. The *t*-Bu substituted complex (**3**) is observable spectroscopically but is not

isolable, presumably due to the unhindered but electron-rich amido ligand. An anilido complex supported by the less sterically encumbered IMes (1,3-bis(2,4,6-trimethylphenyl)imidazole-2-ylidene) ligand was also synthesized (**4**).

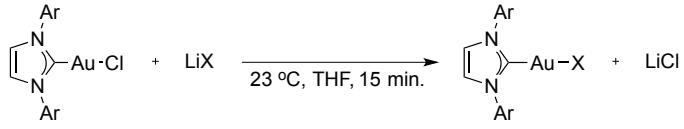

1 X = N(*i*-Pr)$_2$, 72% yield, Ar = dipp
2 X = N(H)Ph, 62% yield, Ar = dipp
3 X = N(H)*t*-Bu, 68% yield,[a] Ar = dipp
4 X = N(H)Ph, 57% yield, Ar = mes

[a]Yield was determined by ^{1}H NMR with hexamethylbenzene as an internal standard.

Scheme 1. Synthesis of gold(I) amides.

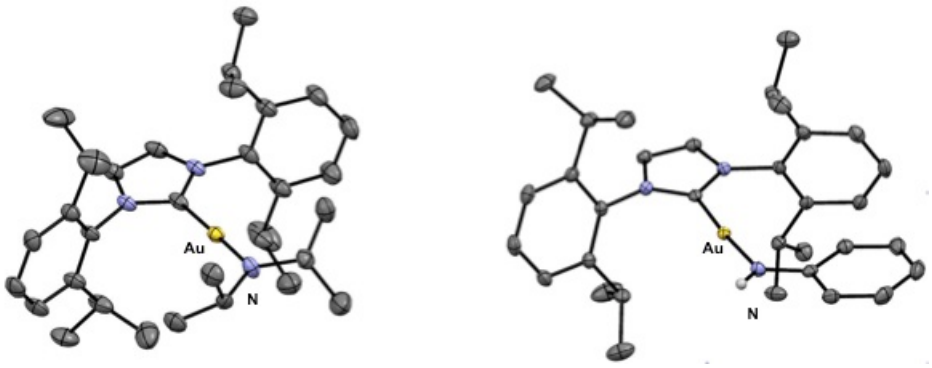

Figure 5. Solid-state structures of complexes **1** and **2** (50% probability ellipsoids). Hydrogen atoms (except for N—H of **2**) and solvent molecules have been omitted for clarity.

Reactivity studies were conducted to gauge the nucleophilicity of this new series of compounds. Focus was placed primarily on **1** as it was found to be more reactive than **2** in preliminary studies. The reaction of **1** with benzyl bromide resulted in formation of IPrAuBr (**5**) (98% isolated yield) and *N,N*-diisopropylbenzylamine (eq 1). This amination did not proceed when benzyl chloride was used as the electrophile. Aminoauration to form **6** was observed upon treatment of **1** with acrylonitrile (eq 2), a typical hydroamination substrate in transition-metal catalysis.[7,30] The regiochemistry of the reaction was verified unambiguously by single crystal X-ray diffraction and suggests that the transformation takes place *via* a conjugate addition mechanism (Figure 6). Attempts to liberate the aminated product catalytically were unsuccessful. The stability of **6** stands in stark contrast to analogous proposed copper intermediates in highly efficient hydroaminations of Michael acceptors.[31] This is likely due to the strength of the Au—C bond and the low kinetic basicity of Au(I)—C$_{sp3}$ bonds,[32] and could explain the superior catalysis observed with copper catalysts compared to isostructural gold complexes in hydroamination.[30]

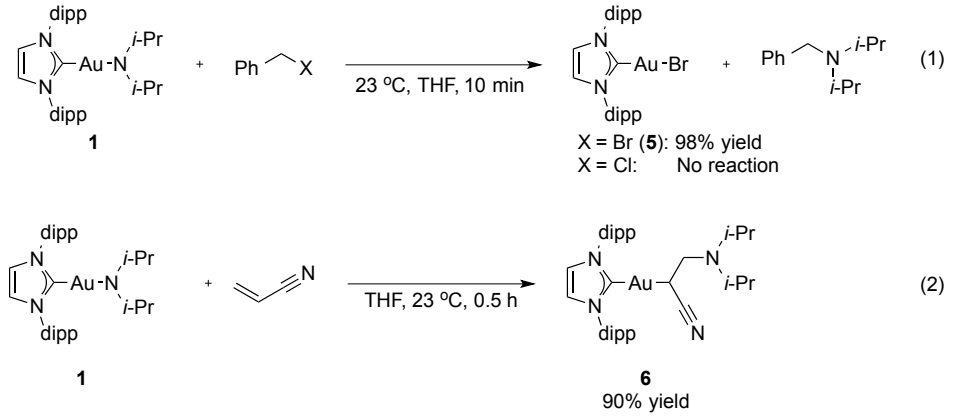

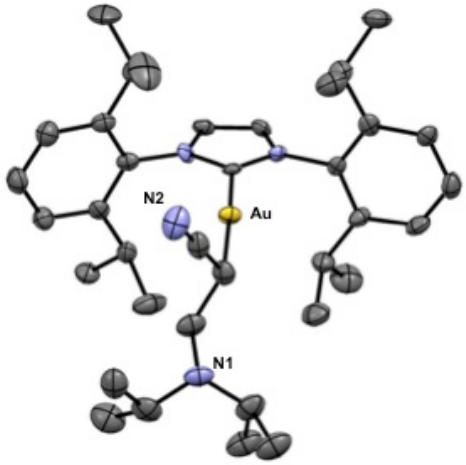

Figure 6. Solid-state structure of complex **6** (50% probability ellipsoids). Hydrogen atoms have been excluded for clarity.

Complex **1** reacts with heteroallenes to form a variety of unique complexes (Scheme 2). Reaction with di(*p*-tolyl)carbodiimide and ethyl isocyante results in gold guanidinate (**7**) and ureate (**8**) complexes, respectively. Perhaps of greater interest is reaction of **1** with carbon dioxide to form a gold carbamate (**9**). Like other transition metal carbamates, **9** could only be characterized spectroscopically due to its instability.[33,34] Isotope labeling using ^{13}C-enriched carbon dioxide allowed for identification of the carbonyl resonance at δ 161 ppm in the ^{13}C NMR spectrum. The carbonyl resonance of **9** was identified as the strong stretch at $\nu = 1578$ cm^{-1} as this signal was replaced with one at 1527 cm^{-1} for the heavier isotopologue (see Experimental). Gold hydrocarbyl complexes have previously been shown to be unreactive toward CO_2,[35] suggesting that formation of **9** takes place *via* nucleophilic attack rather than insertion.

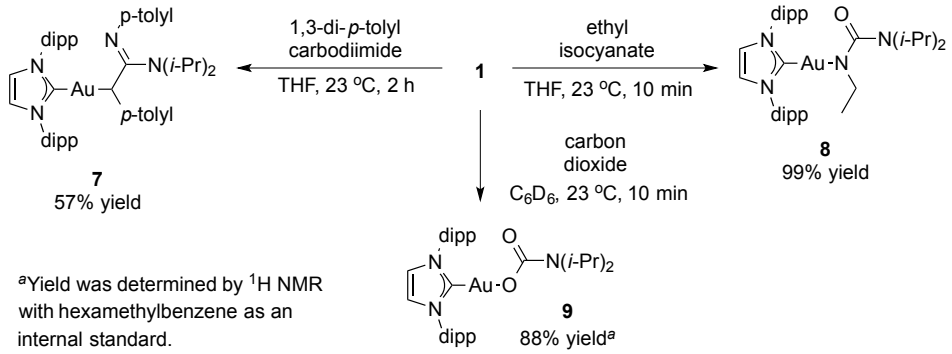

Scheme 2. Reaction of **1** with heteroallenes.

The isolation of discrete gold(I) amides permitted the first direct evaluation of their ability to intervene as catalytic intermediates in hydroamination reactions. An innersphere mechanism has been proposed in some reports[11,13-15] but an outersphere mechanism has been supported with kinetic studies.[36] Neither side of the debate, however, has had the opportunity to react an amide with a substrate. Treatment of **1** with a variety of olefins and alkynes leads to no reaction even at 75 °C (eq 3). Additionally, **1** deprotonates fluorene (pK_a 23 in THF)[37] to form the alkyl gold complex **10** in high yield (eq 4). These data taken together suggest that amination of unactivated, unsaturated substrates from an amide complex formed by deprotonation of the corresponding amine complex is unlikely, and support an outersphere mechanism for gold-catalyzed amination.

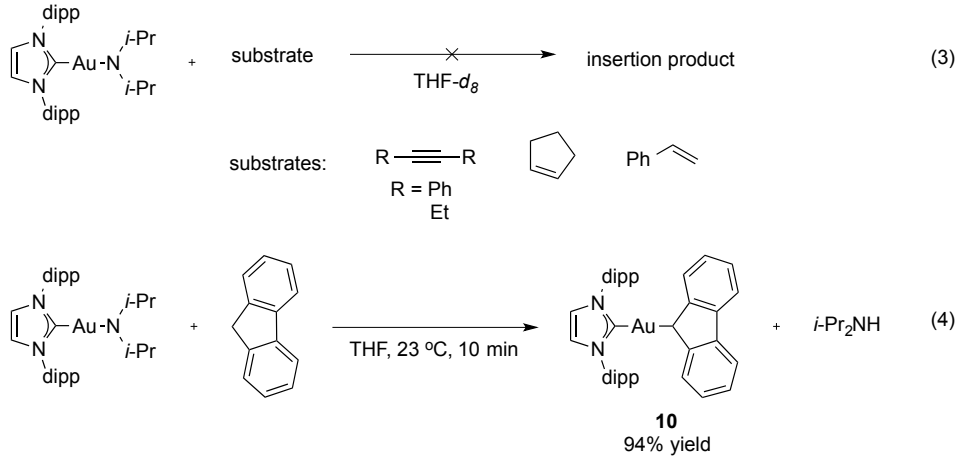

A number of attempts were made to integrate complexes **1** and **4** into a catalytic cycle for the alkylation of amines with the ultimate goal of effecting monoalkylation of secondary amines. However, a strong base is required to generate amido complexes from amines. These bases could in turn be alkylated by electrophiles, such as alkyl halides, or cause elimination of the leaving group for substrates bearing acidic protons. Coordination of the leaving group to gold also posed a problem as leaving groups such as triflate would not ligate strongly to gold but the alkyl triflate substrate would be unstable and prone to attack by base. These results further illustrate the unlikelihood of gold(I) amides as catalytic intermediates.

Following synthetic studies with gold(I) amides, the preparation of gold(I) phosphides was undertaken. Salt metathesis in initial studies proved ineffective. Halide

abstraction from IPrAuCl followed by reaction of diphenylphosphine was then attempted. From this reaction was crystallized a μ-phosphide complex even without addition of base (Figure 7). The synthetic route was then adjusted to include bulky dimesityl (**11**) and di-*t*-Bu phosphines (**12**) (Scheme 3). These phosphine complexes were deprotonated to form the desired phosphides in high yield. Complex **13** was crystallized from diethyl ether and confirmed by X-ray diffraction to be the first reported terminal group 11 phosphide (Note: An NHC-supported copper phosphide has been characterized crystallographically but was never reported in the literature).[38] Due to its instability, **14** could only be characterized spectroscopically.

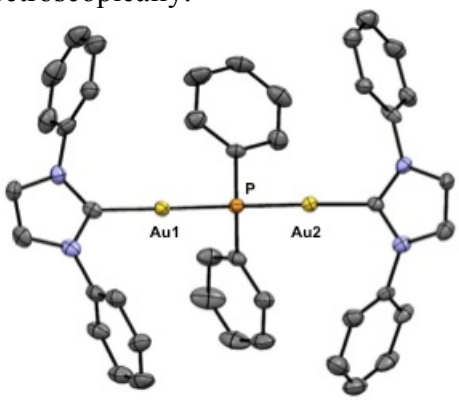

Figure 7. Solid-state structure of a μ-phosphide (50% probability ellipsoids). Solvent molecules, hydrogens, BF_4^-, and isopropyl groups have been omitted for clarity.

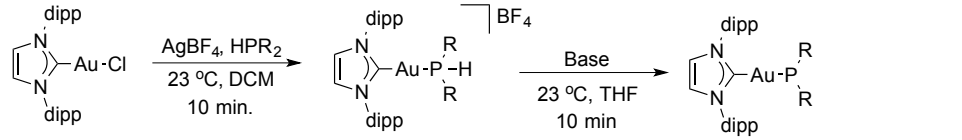

11 R = Mes, 89% yield
12 R = *t*-Bu, 95% yield

13 R = Mes, 96% with KHMDS
14 R = *t*-Bu, 85% with NaO(*t*-amyl)[a]

[a]Yield was determined by ^{1}H NMR with hexamethylbenzene as an internal standard.

Scheme 3. Synthesis of gold(I) phosphides.

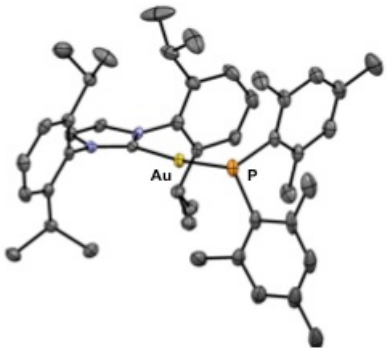

Figure 8. Solid-state structure of **13** (50% probability ellipsoids). Hydrogens have been omitted for clarity.

Phosphines often serve as supporting ligands for gold but are rarely synthesized catalytically using the same metal. There are reports of ruthenium[39] and palladium

phosphides[40] acting as key intermediates in the phosphination of alkyl halides. We hypothesized that gold phosphides should exhibit similar reactivity. Indeed, reaction of benzyl chloride with di-*t*-butylphosphine in the presence of **12** results in 5.5 turnovers of catalyst to form the corresponding trialkyl product (eq 5). No reaction is observed in the absence of catalyst. Each intermediate in the proposed catalytic cycle was isolated or observed spectroscopically (Figure 9), with the species identified as the catalyst resting state (**15**) being synthesized independently (eq 6). Though the reaction is low yielding and cannot be compared to state-of-the-art methods, it marks the first example of C—P bond formation by a homogeneous gold catalyst.

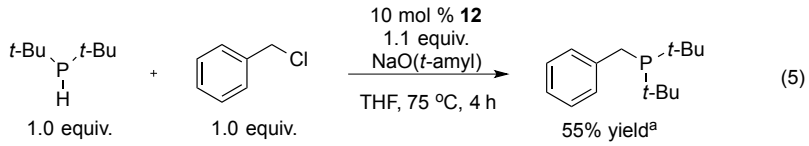

(5)

[a]Yield was determined by ^{1}H NMR with hexamethylbenzene as an internal standard.

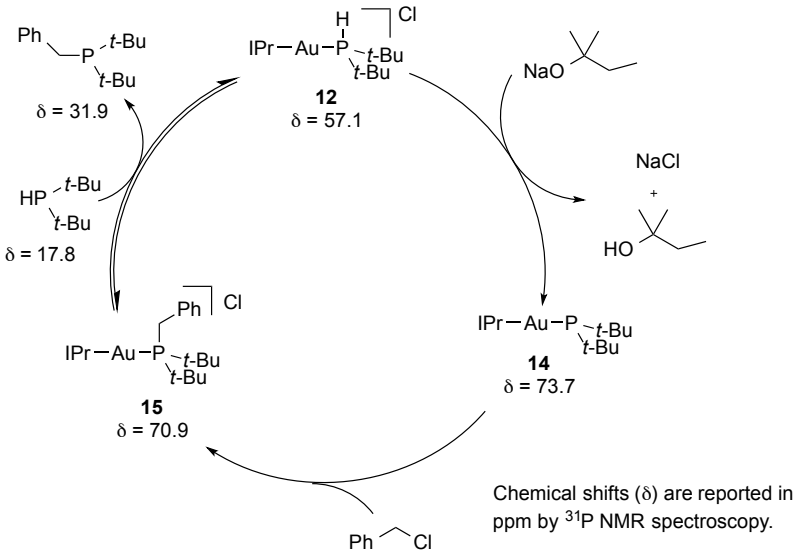

Figure 9. Proposed mechanism for the catalytic alkylation of HP(*t*-Bu)$_2$.

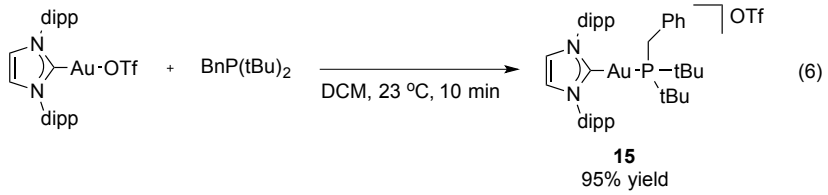

(6)

A priority in this investigation was to examine the structures and electronic properties of terminal gold(I) pnictogenides. We first examined the crystal structures of complexes **1** and **13**, and their conjugate acids **16** and **11**, respectively (Table 1 and Figure 10). The ionic Au—N bond (1.967(4) Å) of **1** was more than 0.1 Å shorter than its dative counterpart (2.0921(2) Å) **16**, similar to what has been observed with ruthenium amides/amines,[41,42] whereas the Au—P bond of the phosphide complex **13** (2.3195(9) Å) was slightly longer than that of the phosphine complex **11** (2.279(2) Å). With regard to

geometry around the heteroatom, both **16** and **11** were pyramidal. Upon net deprotonation, **16** became planar at nitrogen (**1**) whereas **11** became more pyramidalized (**13**). These data suggested that lone pair repulsion from the heteroatom is weaker than electrostatic attraction between the metal center and nitrogen for the case of **1**, whereas d-π/p-π is likely the cause for bond elongation for **11**.

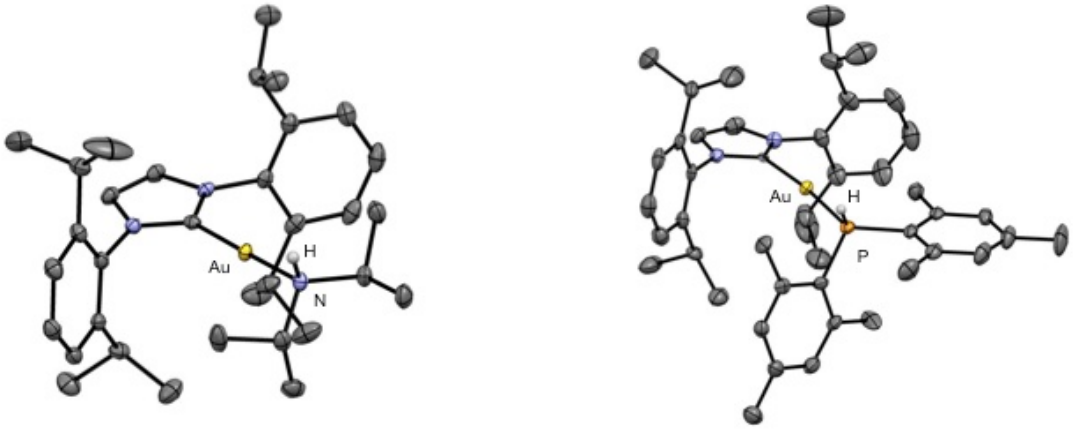

Figure 10. Solid-state structure of complexes **16** (left) and **11** (right) (50% probability ellipsoids). All solvent molecules, counter ions, and hydrogens (except X—H hydrogens) have been omitted for clarity.

	Amide (1)	**Amine (16)**	**Phosphide (13)**	**Phosphine (11)**
Au—X (Å)	1.967(4)	2.091(2)	2.3195(9)	2.279(2)
Σ angles (°)	360	340	317	343

Table 1. Bond lengths and angles of pnictogenide complexes and their conjugate acids

Computational studies were undertaken in order to gain insight into the bonding of the gold pnictogenides. Issues of particular interest were the hybridization at the pnictogen and the degree of ionic character in the Au—X bond. Complexes **1**, **3**, **13**, and **14** were compared against IPrAuO*t*-Bu (**17**) and IPrAuNTf$_2$ (**18**). Complex **17** was chosen based on its established reactivity toward acids while complex **18** was analyzed since it posses an Au—N bond but the triflimido ligand is considered weakly bound.[43] Natural population analysis predicted that the amido complexes have ionic bonds with a difference in charge between the metal and nitrogen greater than 1.0 (Table 2). These values approach those calculated for complexes **17** and **18**. In contrast, the phosphide complexes were found to have highly covalent bonds as evidenced by a difference in charge of less than 0.2 between gold and phosphorus. With both the phosphido and amido complexes, the HOMO was identified as the lone pair at the heteroatom residing in sp and p orbitals, respectively. Natural localized molecular orbital (NLMO) calculations[44] for **1** and **2** indicate that the Au—N bond consists of an sp^2-hybridized nitrogen representing 82% of the bonds' character. This stands in contrast to the phosphides in which phosphorus contributes only 30% (**13**) and 33% (**14**) to the Au—P bond, which is in line with both the similar electronegativities and charges at each atom. What is perhaps most interesting about the bonding encountered in the amides is that less than 3% of the primary interaction between gold and nitrogen is attributed to second order interactions. Since late metal amides have always been anilides, the planarity at nitrogen has been attributed to delocalization of the nitrogen lone pair into the aryl ring.[45]

In the case of **1**, planarity is observed both in the solid state and computationally, which suggests that this is due to the electrostatic benefit of concentrating electron density at an orbital of high s-character, *i.e.* sp^2 as opposed to sp^3.

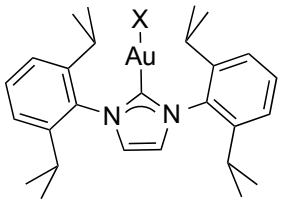

X[b]		q(Au)[c]	q(X)[c]	Δq(Au-X)[d]	% Contribution[e]
N(*i*-Pr)$_2$	**1**	0.25	-0.81	1.06	62
NH(Ph)	**2**	0.34	-0.90	1.24	40
NH(*t*-Bu)	**3**	0.29	-1.00	1.29	67
P(Mes)$_2$	**13**	0.16	0.15	0.01	49
P(*t*-Bu)$_2$	**14**	0.09	0.15	0.05	61
O*t*-Bu	**17**	0.32	-0.85	1.17	71
NTf$_2$	**18**	0.35	-1.00	1.35	< 13

[a] Natural charge based on NBO analysis and occupancy on population analysis BPV86/LANL2DZ/ 6-311G++d,p [b] X = pnictogen. [c] *q* = charge. [d] Δ*q* = difference in charge between Au and X. [e] Percent contribution of X to the HOMO.

Table 2. Charge distribution and natural population analysis of Au—heteroatom complexes.[a]

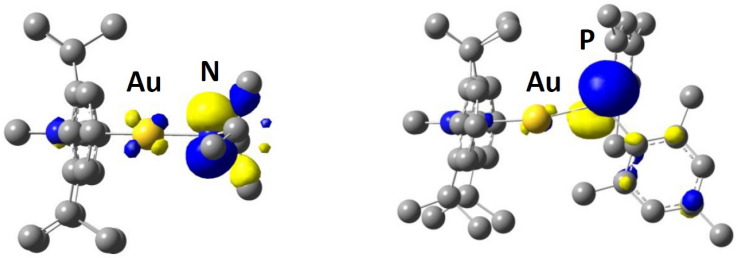

Figure 11. Calculated HOMO (BPV86/LANL2DZ/6-311++G(d,p), 0.06 isocontour) of **1** (left) and **5** (right)

Conclusions

For the first time terminal gold(I) amides and phosphides have been synthesized, their reactivity probed, and their solid state structures elucidated. Both classes of complexes were found to be highly nucleophilic and capable of reacting with a number of electrophiles. The viability of amides as catalytic intermediates was shown to be unlikely as illustrated by the high kinetic basicity of a diisopropyl amido complex and its lack of reactivity toward various unsaturated molecules. Phosphides, however, were identified as intermediates in the catalytic alkylation of secondary phosphines. In addition, to

synthetic investigation, a computational study was conducted, the results for which shed light on the structure, bonding and reactivity of gold(I) pnictogenides. These findings will hopefully serve as a guide in the development of C—X bond-forming reactions with gold and provide a more complete picture of late transition metal—heteroatom bonding.

Experimental

General Information

Unless otherwise noted, all manipulations were performed in an inert atmosphere (N_2) glovebox. Glassware was oven-dried overnight or flame-dried under vacuum. All NMR spectra were obtained at ambient temperature using Bruker AV-600, DRX-500, AV-500, AVB-400, AVQ-400, or AV-300 spectrometers. ^{1}H NMR chemical shifts (δ) are reported in parts per million (ppm) relative to residual solvent peaks (3.58 and 1.73 ppm for THF-d_8, 5.32 ppm for CD_2Cl_2, 7.16 ppm for C_6D_6). ^{13}C NMR chemical shifts were also reported relative to residual solvent peaks (67.57 and 25.37 ppm for THF-d_8, 54.00 ppm for CD_2Cl_2, 128.06 for C_6D_6). Infrared (IR) spectra were recorded on a Nicolet Avatar FT-IR spectrometer. High-resolution mass spectral data were obtained from the Micromass/Analytical Facillity operated by the College of Chemistry, University of California, Berkeley using Thermo LTQ-FT (ESI) and Fisons VG70 (FAB). X-ray structural analyses were obtained at the University of California, Berkeley CHEXRAY facility (details in the X-ray section below). Combustion analysis data were obtained at the Micro-Mass Facility at the University of California, Berkeley.

Materials

Reagents were purchased from commercial suppliers, checked for purity and used without further purification unless otherwise noted. Pentane, hexane, diethyl ether, toluene, tetrahydrofuran, and methylene chloride were dried and purified by passage through a column of activated alumina (type A2, 12 x 32, UOP LLC), and sparged with N_2 prior to use. Ethyl isocyanate, acrylonitrile, fluorene, benzyl chloride and bromide, and all amines were purified according to literature methods prior to use.[46] Methylene chloride-d_2 was distilled from CaH_2 and degassed prior to use. Tetrahydrofuran-d_8 was passed through a short plug of activated alumina and stored over activated 3 Å molecular sieves prior to use. All lithium amides were prepared by addition of *n*-BuLi in hexane to an excess of amine followed by concentration to yield the corresponding products as white solids. In purifications utilizing syringe filters, filters of 0.2 μm porosity from National Scientific were used. The compounds IPrAuCl,[47] IPrAuOTf,[48] and BnP(*t*-Bu)$_2$[49] were synthesized by literature methods.

(IPr)gold(I) diisopropylamide (1)

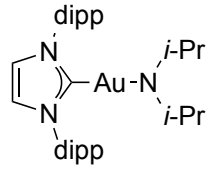

To a 20-mL scintillation vial was added IPrAuCl (201 mg, 0.323 mmol) and THF (12 mL). Lithium diisopropylamide (35.5 mg, 0.331 mmol) was added as a solid to the vigorously stirred solution. The reaction mixture immediately turned clear and yellow. After being stirred for 10 min, the solution was concentrated to yield a pale yellow solid. The solid was dissolved in hexane and passed through a syringe filter twice. The hexane solution was concentrated to yield the desired product as a yellow powder (160 mg, 0.23 mmol, 72% yield). X-ray quality crystals were obtained from a concentrated hexane solution of **1** stored at -35 °C. ^{1}H NMR (500 MHz, THF-d_8): δ(ppm) 7.44-7.40 (m, 4 H), 7.28 (d, 4 H, J = 8.0 Hz), 3.16 (sept., 2 H, J = 6.5 Hz), 2.73 (sept., 4 H, J = 7.0 Hz), 1.39 (d, 12 H, 7.0 Hz), 1.20 (d, 12 H, 7.0 Hz), 0.50 (d, 12 H, J =

6.0 Hz). ^{13}C NMR (125 MHz, THF-d_8): δ(ppm) 186.2, 146.9, 136.7, 130.6, 124.7, 123.4, 55.2, 29.8, 28.8, 24.7, 24.6. IR (ATR): ν_{max}(cm^{-1}): 2961, 2867, 1462, 1362,1188, 1061, 946, 804,762. HRMS(*m/z*): calculated for $C_{33}H_{50}AuN_3$ 686.3743, found 686.3743.

(IPr)gold(I) anilide (2)

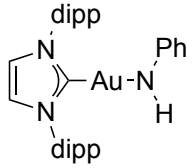

To a 20-mL scintillation vial was added IPrAuCl (106 mg, 0.170 mmol) and THF (6 mL). Lithium anilide (17.0 mg, 0.172 mmol) was added to the vigorously stirred solution. After being stirred for 10 minutes, the solution was concentrated to a white solid. The solid was dissolved in toluene and passed through a syringe filter. The resulting solution was concentrated to a white solid that that was then recrystallized from diethyl ether to yield the desired product as X-ray quality crystals (71.3 mg, 0.105 mmol, 62% yield). ^{1}H NMR (500 MHz, THF-d_8): δ(ppm) 7.56 (s, 2 H, imidazole), 7.53 (t, 2 H, *J* = 8.0 Hz, *p*-H), 7.56 (d, 4 H, *J* = 7.5 Hz, *m*-H), 6.43 (t, 2 H, *J* = 7.6 Hz, anilide aryl), 585-5.80 (m, 3 H, anilide aryl), 3.49 (s, 1 H, N-*H*), 2.71 (sept., 4 H, J = 7.0 Hz, IPr C(*H*)Me$_2$), 1.36 (d, 12 H, *J* = 6.5 Hz, IPr C(H)*Me*$_2$), 1.23 (d, 12 H, *J* = 6.5 Hz, IPr C(H)*Me*$_2$). ^{13}C NMR (125 MHz, THF-d_8): δ(ppm) 182.0, 160.5, 147.1, 136.2, 131.1, 128.6, 124.9, 124.4, 115.4, 110.8, 29.9, 24.8, 24.4. IR (ATR): ν_{max}(cm^{-1}) 2959, 2926, 2867, 1587, 1486, 1460, 1352, 1182, 802, 743, 689. HRMS(*m/z*): calculated for $C_{33}H_{42}AuN_3$ 678.3117, found 678.3130. Anal. Calcd. for $C_{33}H_{42}AuN_3$: C, 58.49; H, 6.25; N, 6.20. Found: C, 58.80; H, 6.41; N, 5.88.

Generation of (IPr)gold(I) *t*-butylamide (3)

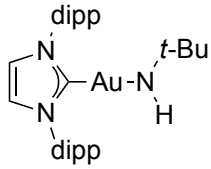

IPrAuCl (10.0 mg, 0.016 mmol) and hexamethylbenzene (1.1 mg, 0.007 mmol) were dissolved in THF-d_8 and transferred to a J. Young NMR tube. The spectrum of this mixture was then obtained. Lithium *t*-butylamide (1.3 mg, 0.016 mmol) was dissolved in THF-d_8 and transferred to the NMR tube. The reaction mixture immediately changed from colorless to bright orange and then to colorless again. The product was present in 68% yield as determined by reference to the internal standard. ^{1}H NMR (300 MHz, THF-d_8): δ(ppm) 7.45-7.42 (m, 4 H, aryl), 7.29 (d, 4 H, *J* = 7.8 Hz, *m*-H), 2.71 (sept., 4 H, *J* = 6.9 Hz, IPr C(*H*)Me$_2$), 1.38 (d, 12 H, *J* = 6.6 Hz, IPr C(H)*Me*$_2$), 1.20 (d, 12 H, *J* = 6.9 Hz, IPr C(H)*Me*$_2$), 0.68 (s, 9 H, *t*-Bu). The N—H proton was not observed.

IMes)gold(I) anilide (4)

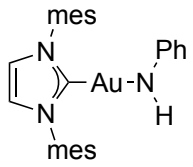

To a stirred suspension of IMesAuCl (100.9 mg, 0.188 mmol) and THF (7 mL) in a 20-mL scintillation vial was added lithium anilide (20.0 mg, 0.202 mmol). After being stirred for ten min, the homogenous clear solution was concentrated to yield an off-white solid. The solid was dissolved in toluene (10 mL) and filtered through a syringe filter. An overnight recrystallization at -35°C in toluene yielded the desired product as off-white crystals (63.5 mg, 57% yield). ^{1}H NMR (600 MHz, THF-d_8): δ(ppm) 7.41 (s, 2H, imidazole), 7.07 (s, 4H, mes), 6.47 (t, 2H, *J* = 7.7 Hz, anilide *m*-H), 5.90 (d, 2H, *J* = 7.6 Hz, anilide *o*-H), 5.86 (t, 1H, *J* = 7.1 Hz, anilide *p*-H), 3.46 (s, 1H, N-*H*), 2.37 (s, 6H, *p*-Me), 2.16 (s, 12H, *o*-Me). ^{13}C (150 MHz, THF-d_8): δ(ppm) 180.2, 140.1, 138.6, 136.1, 130.1, 128.6, 123.2, 115.5, 110.9, 21.4, 18.2. IR (ATR): ν_{max}(cm^{-1})

3133, 3013, 2913, 1596, 1580. 1485, 1304, 855, 732. HRMS (*m/z*): calculated for $C_{27}H_{30}N_3Au$ 593.2105, found 593.2115. Anal. Calcd. for $C_{27}H_{30}AuN_3$: C, 54.64; H, 5.09; N, 7.08. Found: C, 56.22; H, 5.23; N, 6.64.

IPrAuBr (5)

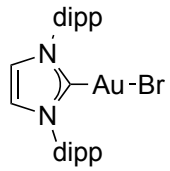

To a weighed vial containing **1** (50 mg, 0.073 mmol) and a Teflon stir bar was added THF (2 mL). Benzyl bromide (25 mg, 0.15 mmol) was added via syringe and the reaction mixture was stirred at 23 °C for 4 h. The reaction mixture was concentrated and the resulting solid washed with pentane (2 x 1 mL). The product was isolated as a white solid (47 mg, 0.072 mmol, 98%). The ^{1}H NMR spectrum of **8** matches that found in the literature. [50] The identity of the organic fragment (N,N-diisopropyl-benzylamine) was confirmed by ^{1}H NMR by comparison to a sample synthesized by a literature method. [51]

Complex 6

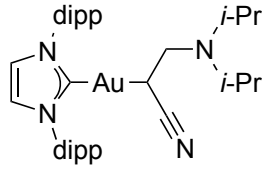

To a vial containing **1** (50.1 mg, 0.073 mmol) and a Teflon stir bar was added THF (2 mL). Acrylonitrile (7.8 mg, 0.15 mmol) was added via syringe and the reaction mixture was stirred for 30 min. The reaction mixture was concentrated to yield a crude solid that was washed with hexane (2 mL). Removing the remaining solvent under vacuum yielded a pale yellow solid (48.8 mg, 0.066 mmol, 90% yield). X-ray quality crystals were obtained from a concentrated solution of **9** in diethyl ether stored at -35 °C. ^{1}H NMR (500 MHz, THF-d_8): δ(ppm) 7.54 (s, 2H, imidazole), 7.48 (t, 2 H, J = 7.8 Hz, *p*-H), 7.33 (d, 4 H, 7.5 Hz, *m*-H), 2.88 (sept., 2 H, J = 6.5 Hz, N-C(*H*)Me$_2$), 2.65 (sept., 4 H, J = 6.8 Hz, IPr C(H)*Me*$_2$), 2.38 (dd, 1 H, J = 13.5 Hz, 10.0 Hz, N-C(*H*)$_2$), 2.26 (dd, 1 H, J = 14.0 Hz, 5.0 Hz, N-C(*H*)$_2$), 1.50 (dd, 1 H, J = 10.0 Hz, 5.0 Hz, Au-C(*H*)), 1.37 (dd, 12 H, J = 7.0 Hz, 1.5 Hz, IPr C(*H*)Me$_2$), 1.22 (dd, 12 H, J = 6.5 Hz, 1.5 Hz, IPr C(*H*)Me$_2$), 0.81 (d, 12 H, J = 8.0 Hz, IPr C(*H*)Me$_2$), 0.75 (d, 12 H, 7.0 Hz, N-C(*H*)Me$_2$). ^{13}C NMR (125 MHz, THF-d_8): δ(ppm) 193.9, 146.8, 146.8, 136.0, 131.1, 128.5, 124.9, 124.8, 124.5, 48.1, 47.7, 29.8, 29.8, 22.1, 21.0, 20.0. IR (ATR): ν_{max}(cm^{-1}) 2961, 2928, 2868, 2191, 1462, 1415, 1384, 1363, 1329, 1204, 1180, 803, 757. HRMS(*m/z*): calculated for $C_{36}H_{53}AuN_4$ 739.4009, found 739.4021. Anal. Calcd. for $C_{36}H_{53}AuN_4$: C, 58.53; H, 7.22; N, 7.58. Found: C, 58.21; H, 6.68; N, 8.21.

Complex 7

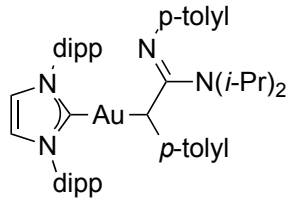

Compound **1** (51.4 mg, 0.750 mmol) and 1,3-*p*-tolylcarbodiimide (16.5 mg, 0.742 mmol) were added to a weighed vial containing a stir bar and THF (2 mL), and the solution was stirred for 2 h. The reaction mixture was concentrated, leaving a solid. The sparingly soluble solid was dissolved in diethyl ether (3 mL) and precipitated upon addition of pentane (10 mL). The mother liquor was decanted and residual solvent removed under vacuum to give the product as a pale yellow powder (39 mg, 0.043 mmol, 57% yield). ^{1}H NMR (500 MHz, THF-d_8): δ(ppm) 7.57 (t, 2 H, J = 7.8 Hz, IPr *p*-H), 7.56 (s, 2 H, imidazole), 7.37 (d, 4 H, 8.0 Hz, IPr *m*-H), 6.44 (d, 2 H, J = 8.0 Hz, *p*-tolyl aryl), 6.38, (d, 2 H, J = 8.0 Hz, *p*-tolyl aryl), 6.33 (d, 2 H, J = 8.0 Hz, *p*-tolyl aryl), 6.05 (d, 2 H, J = 7.5 Hz, *p*-tolyl aryl), 3.70 (sept., 2 H, J = 7.0 Hz, NC(*H*)Me$_2$), 2.65 (sept., 4 H, J = 7.0 Hz,

IPr C(*H*)Me_2), 2.05 (s, 3 H, *p*-tolyl Me), 2.00 (s, 3 H, *p*-tolyl Me), 1.26 (d, 12 H, *J* = 7.0 Hz, IPr C(H)*Me_2*), 1.20 (d, 12 H, *J* = 7.0 Hz, IPr C(H)*Me_2*), 1.03 (d, 12 H, *J* = 7.0 Hz, NC(H)*Me_2*). IR (ATR) ν_{max}(cm^{-1}): 2961, 2922, 2866, 1551, 1498, 1460, 1288, 1148, 813, 759. ^{13}C NMR (125 MHz, THF-*d_8*): δ(ppm) 178.5, 156.9, 153.4, 150.3, 146.8, 136.1, 131.2, 129.1, 128.8,126.9, 125.1, 124.7, 123.4, 122.6, 117.6, 46.8, 29.9, 26.0, 24.8, 24.6, 21.2, 20.8. HRMS (*m/z*): calculated for $C_{48}H_{65}N_5Au$ 908.4900, found 908.4928. Anal. Calcd. for $C_{48}H_{64}AuN_5$: C, 63.49; H, 7.10; N, 7.71. Found: C, 62.68; H, 7.03; N, 7.31.

Complex 8

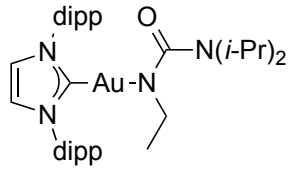

To a weighed vial containing **1** (51.8 mg, 0.076 mmol) and a Teflon stir bar was added THF (2 mL). Ethyl isocyanate (10.8 mg, 0.151 mmol) was added via syringe and the reaction mixture was stirred for 10 min at 23 °C. The product was isolated as a white solid upon concentration (56.6 mg, 0.075 mmol, 99% yield). ^{1}H NMR (500 MHz, THF-*d_8*): δ(ppm) 7.56 (s, 2 H, imidazole), 7.47 (t, 2 H, *J* = 7.8 Hz, *p*-H), 7.33 (d, 4 H, *J* = 8.0 Hz, *m*-H), 3.36 (sept., 2 H, *J* = 6.8 Hz,), 2.87 (q, 2 H, *J* = 7.0 Hz, N-C*H_2*), 2.69 (sept., 4 H, *J* = 7.0 Hz, IPr C(*H*)Me_2), 1.36 (d, 12 H, *J* = 7.0 Hz, IPr C(H)*Me_2*), 1.21 (d, 12 H, *J* = 7.0 Hz, IPr C(H)*Me_2*), 0.75 (d, 12 H, *J* = 6.5 Hz, N-C(H)*Me_2*), 0.45 (t, 3 H, *J* = 7.3 Hz, NCH_2CH_3). ^{13}C NMR (125 MHz, THF-*d_8*): δ(ppm) 179.4, 167.9, 146.8, 136.4, 131.2, 125.0, 124.7, 47.1, 44.2, 29.9, 24.8, 24.5, 22.2, 18.3. IR (ATR) ν_{max}(cm^{-1}) 2960, 2926, 2868, 1572, 1552, 1467, 1418, 1328, 1159, 801, 765. HRMS (*m/z*): calculated for $C_{36}H_{55}AuN_4O$ 757.4114, found 757.4118. Anal. Calcd. for $C_{36}H_{55}AuN_4O$: C, 57.13; H, 7.33; N, 7.40. Found: C, 56.96; H, 7.13; N, 7.25.

Complex 9

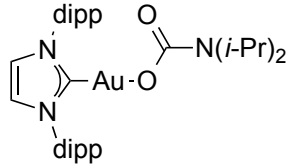

Compound **1** (5.6 mg, 0.008 mmol) and 1,3,5-trimethoxybenzene (1.0 mg, 0.006 mmol) were dissolved in benzene-*d_6* and transferred to a J.-Young tube. The reaction mixture was subjected to one freeze-pump-thaw cycle and the evacuated tube opened to carbon dioxide (1 atm). Upon closure and inversion of the tube, the reaction mixture instantly changed from yellow to colorless. The product was present in 88% yield as determined by reference to the internal standard. ^{1}H NMR (500 MHz, Benzene-*d_6*): δ(ppm) 7.10 (t, 2 H, *J* = 7.7 Hz, IPr *p*-H), 7.00 (d, 4 H, 7.8 Hz, IPr *m*-H), 6.30 (s, 2 H, imidazole), 4.02-3.77 (m, 2 H, NC(*H*)Me_2), 2.61 (sept., 4 H, 6.9 Hz, IPr C(*H*)Me_2), 1.52 (d, 12 H, *J* = 6.9 Hz, IPr C(H)*Me_2*), 1.10 (d, 12 H, *J* = 7.8 Hz, C(H)*Me_2*), 1.05 (d, 12 H, *J* = 6.8 Hz, IPr C(H)*Me_2*).). ^{13}C (150 MHz, Benzene-*d_6*): 171.3, 161.4, 145.7, 134.7, 130.8, 128.4, 122.7, 29.2, 24.7, 24.1, 21.8. IR (C_6D_6) ν_{max}(cm^{-1}): 2970, 2928, 1577 (C=O), 1478, 1418, 1364, 1299, 1221.

Comparison of ^{12}C-[9] and ^{13}C-[9] IR spectra.

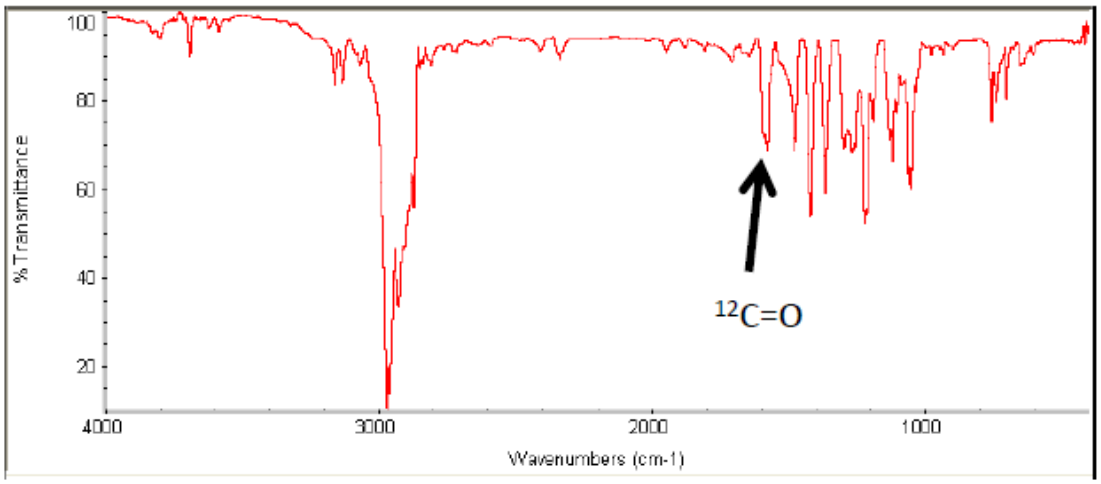

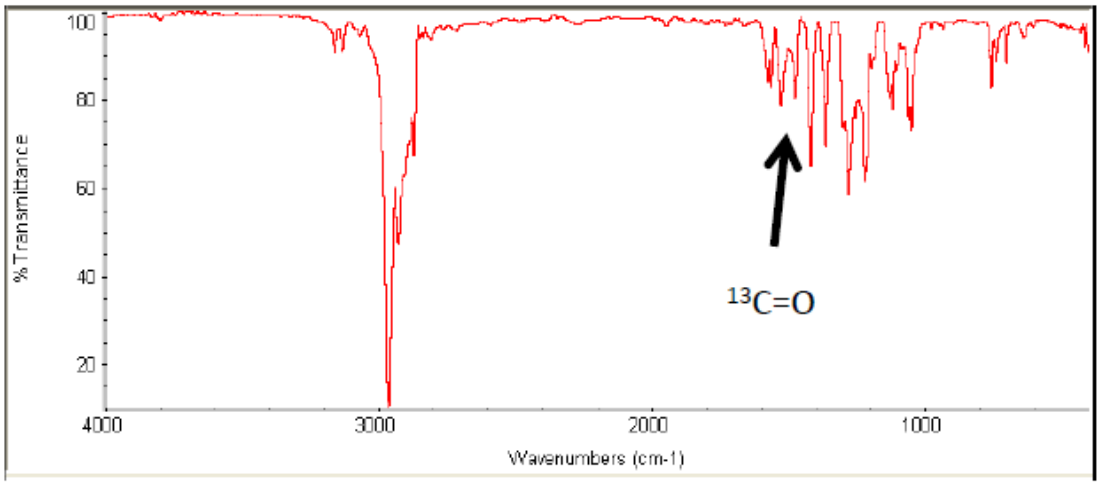

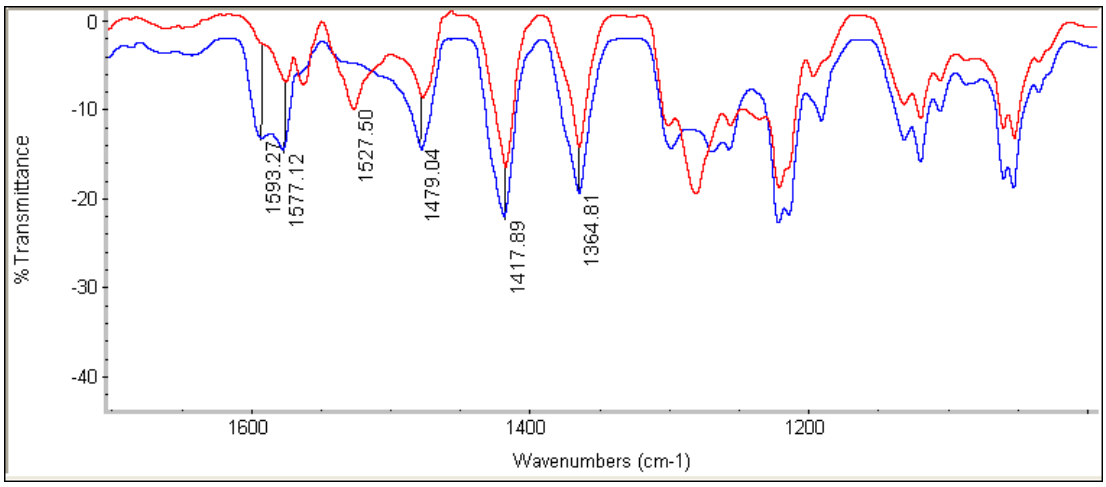

Red: ^{13}C-[9]; Blue ^{12}C-[9]

Complex 10

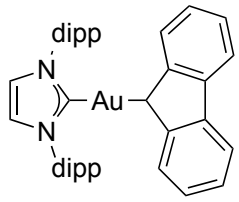

To a weighed vial containing **1** (51.9 mg, 0.076 mmol) and a Teflon stir bar was added THF (2 mL). Fluorene (12.2 mg, 0.073 mmol) was added and the solution immediately turned from yellow to colorless. After being stirred for 10 minutes, the reaction mixture was concentrated and the crude product washed with pentane (1 mL). The product was isolated as a white solid (51.8 mg, 0.069 mmol, 94% yield). ^{1}H NMR (500 MHz, THF-d_8): δ(ppm) 7.61-7.57 (m, 2 H, aryl), 7.42 (t, 2 H, J = 7.8 Hz, aryl), 7.41 (s, 2 H, imidazole), 7.19 (d, 4 H, J = 7.5 Hz, aryl), 6.87-6.81 (m, 6 H, aryl), 3.99 (s, 1 H, Au-C(*H*)), 2.43 (sept., 4 H, J = 6.8 Hz, IPr C(*H*)Me$_2$), 1.11 (d, 12 H, J = 7.0 Hz, IPr C(H)*Me*$_2$), 1.02 (d, 12 H, J = 6.5 Hz, IPr C(H)*Me*$_2$). ^{13}C NMR (125 MHz, THF-d_8): δ(ppm) 193.0, 153.9, 146.6, 138.3, 135.9, 130.8, 124.6, 124.4, 124.2,124.0, 121.3, 119.2, 49.8, 29.6, 24.6, 24.3. IR (ATR) ν_{max}(cm^{-1}): 2963, 2927, 2868, 1471, 1382,1329, 1217, 1191, 903, 743. HRMS(*m/z*): calculated for $C_{40}H_{45}AuN_2Li$ [M-Li$^+$] 757.3403, found 757.3402. Anal. Calcd. for $C_{40}H_{45}AuN_2$: C, 63.99; H, 6.04; N, 3.73. Found: C, 63.58; H, 5.96; N, 3.93.

Complex 11

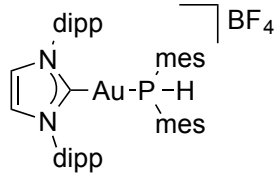

IPrAuCl (99.7 mg, 0.161 mmol) was added to a solution of bis(2,4,6-trimethylphenyl)phosphine (45.0 mg, 0.166 mmol) and $AgBF_4$ (32.4 mg, 0.164) in methylene chloride (5 mL). Silver chloride precipitated immediately. After being stirred for 10 minutes, the reaction mixture was filtered through a syringe filter and the resulting solution was concentrated to a white solid. The solid was dissolved in methylene chloride (~1 mL) and precipitated using pentane. The mother liquor was decanted and the resulting product washed with hexane (1 mL) to leave a white powder (136 mg, 0.144 mmol, 89% yield). X-ray quality crystals were obtained from a methylene chloride solution of **4** layered with hexane and stored at -35 °C. ^{1}H NMR(500 MHz, CD_2Cl_2): δ(ppm) 7.60 (t, 2H, J = 7.3 Hz, IPr *p*-H), 7.44, (s, 2 H, imidazole), 7.31 (d, 4 H, 8.0 Hz, IPr *m*-H), 6.82 (d, 4 H, J_{H-P} = 4.0 Hz, mes), 6.78, (d, 1 H, J_{H-P} = 395.5 Hz, P-*H*), 2.45 (sept., 4 H, J = 7.0 Hz, IPr C(*H*)Me$_2$), 2.25 (s, 6 H, mes *p*-H), 1.90 (s, 12 H, *o*-H), 1.22 (d, 12 H, J = 7.0 Hz, IPr C(H)*Me*$_2$), 1.09 (d, 12 H, J = 7.0 Hz, IPr C(H)*Me*$_2$). ^{13}C NMR (125 MHz, CD_2Cl_2): δ(ppm) 191.9, 191.1, 146.3, 133.8, 131.7, 125.0, 125.0, 124.9, 34.3, 34.1, 30.5, 30.4, 29.4, 25.0, 24.4. ^{31}P{^{1}H} NMR (162 MHz, CD_2Cl_2): δ(ppm) 42.0. ^{19}F{^{1}H} (376 MHz, CD_2Cl_2) -152.6. IR (ATR): ν_{max}(cm^{-1}) 2963, 1604, 1458, 1422, 1385, 1050, 851, 805, 759, 705. HRMS(*m/z*): calculated for $C_{42}H_{61}AuN_2P$ [M-BF_4] 855.4076, found 855.4093. Anal. Calcd. for $C_{45}H_{59}AuBF_4N_2P$: C, 57.33; H, 6.31; N, 2.97. Found: C, 56.55; H, 6.30; N, 2.90.

Complex 12

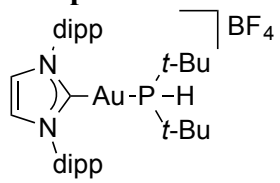

Compound **5** was synthesized analogously to **4** but with di-*t*-butylphosphine (24.5 mg, 0.167 mmol). The product was isolated as a white solid (125 mg, 0.153 mmol, 95% yield). X-ray quality crystals were grown from a methylene chloride solution layered with pentane and stored at -35 °C. ^{1}H NMR (500 MHz, CD_2Cl_2): δ(ppm) 7.55 (t, 2 H, J = 8.0 Hz, *p*-H), 7.45 (s, 2 H, imidazole), 7.34 (d, 4 H, 8.0 Hz, *m*-H), 4.55 (d, 1 H, J_{H-P} = 359.5 Hz, P-*H*), 2.52 (sept., 4 H, J = 7.0 Hz, IPr C(*H*)Me$_2$) 1.28

(d, 12 H, 7.0 Hz, IPr C(H)*Me*$_2$), 1.26 (d, 12 H, 7.0 Hz, IPr C(H)*Me*$_2$), 1.00 (d, 18 H, $J_{H\text{-}P}$ = 16.5 Hz, *t*-Bu). ^{13}C NMR (125 MHz, CD_2Cl_2): δ(ppm) 146.3, 133.8, 131.7, 125.0 (d, *J* = 3.3 Hz), 124.9, 34.2 (d, *J* = 26.4), 30.4 (d, *J* = 5.4 Hz), 29.4, 25.0, 24.4. ^{31}P{^{1}H} NMR (162, CD_2Cl_2): δ(ppm) 57.1. ^{19}F{^{1}H} NMR (376 MHz, CD_2Cl_2): 152.6. IR (ATR): ν_{max}(cm^{-1}) 2964, 2870, 1471, 1420, 1365, 1049, 809, 763. HRMS(*m/z*): calculated for $C_{35}H_{55}AuN_2P$ [M-BF_4] 731.3763, found 731.3744. Anal. Calcd. for $C_{35}H_{55}AuBF_4N_2P$: C, 51.35; H, 6.77; N, 3.42. Found: C, 51.54; H, 6.77; N, 3.43.

Complex 13

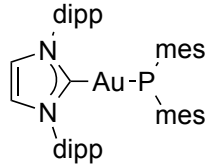

KHMDS (11.6 mg, 0.058 mmol) was stirred vigorously in THF (3 mL). To the basic solution was added **11** (49.7 mg, 0.053 mmol) in THF (2 mL) dropwise. The reaction mixture turned yellow immediately. After being stirred for 5 minutes, the reaction mixture was concentrated to give a yellow solid. The solid was dissolved in diethyl ether and passed through a syringe filter, and the resulting solution was concentrated to a yellow solid. The solid was washed with pentane (~l mL) and the residual solvent removed under vacuum to yield the desired product as a yellow powder (43.6 mg, 0.051 mmol, 96% yield) X-ray quality crystals were grown from a concentrated diethyl ether solution stored at -35 °C. ^{1}H NMR (600 MHz, THF-d_8): δ(ppm) 7.53 (s, 2 H, imidazole), 7.48 (t, 2 H, *J* = 7.5 Hz, IPr *p*-H), 7.25 (d, 4 H, *J* = 7.8 Hz, IPr *m*-H), 6.44 (s, 4 H, mes), 2.59 (sept., 4 H, *J* = 6.9 Hz, C(*H*)Me$_2$), 2.09 (s, 6 H, mes *p*-Me), 1.80 (s, 12 H, mes *o*-Me), 1.16 (d, 12 H, *J* = 3.0 Hz, C(H)*Me*$_2$), 1.15 (d, 12 H, *J* = 2.5 Hz, C(H)*Me*$_2$). ^{13}C NMR (500 MHz, THF-d_8): δ(ppm) 146.7, 143.3, 143.1, 141.8, 141.7, 136.2, 133.0, 131.0, 128.9, 128.8, 124.8, 124.3, 29.8, 24.6, 24.5, 21.1. ^{31}P{^{1}H} NMR (162 MHz, THF-d_8): δ(ppm) -52.7. IR (ATR): ν_{max}(cm^{-1}) 3146, 3024, 2960, 2866, 1554, 1461, 1409, 1350, 847, 802, 758. HRMS (*m/z*): calculated for $C_{45}H_{58}N_2AuP$ 854.4003, found 854.4001. Anal. Calcd. for $C_{45}H_{58}AuN_2P$: C, 63.22; H, 6.84; N, 3.28. Found: C, 63.02; H, 6.88; N, 3.17.

Complex 14

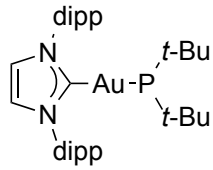

Complex **12** (7.2 mg, 0.009 mmol) and hexamethylbenzene (0.6 mg, 0.004 mmol) were transferred to a J. Young NMR tube using THF-d_8 (0.5 mL). The ^{1}H NMR spectrum of the reaction mixture was then obtained. The contents of the tube were added dropwise to a vigorously stirred solution of sodium *t*-amylate (1.3 mg, 0.012 mmol) in THF-d_8 (0.2 mL). The reaction mixture immediately turned pale yellow and was returned to the NMR tube, and a second spectrum was acquired. Complex **7** was present in 85% yield as determined by reference to the internal standard. ^{1}H NMR (500 MHz, THF-d_8): δ(ppm) 7.52 (s, 2 H, imidazole), 7.43 (t, 2 H, *J* = 7.5 Hz, IPr *p*-H), 7.29 (d, 4 H, *J* = 7.5 Hz, IPr *m*-H), 2.70 (sept., 4 H, *J* = 6.8 Hz, C(*H*)Me$_2$), 1.38 (d, 12 H, *J* = 6.5 Hz, C(H)*Me*$_2$), 1.20 (d, 12 H, *J* = 7.0 Hz, C(H)*Me*$_2$), 0.89 (d, 18 H, $J_{P\text{-}H}$ = 10.5 Hz, *t*-Bu). ^{31}P{^{1}H} NMR (162 MHz, THF-d_8): δ(ppm): 73.6.

Complex 15

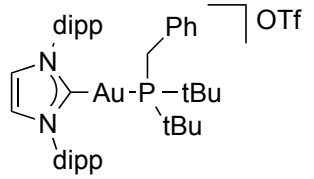

To a weighed vial was added IPrAuOTf (30.1 mg, 0.041 mmol), methylene chloride (2 mL), and di(*t*-butyl)benzylphosphine (13.1 mg, 0.055 mmol). The reaction mixture was stirred for 10 min and then concentrated to a solid. The crude solid was washed with hexane (2 mL) to give the desired product as a white powder (38.2 mg, 0.039 mmol, 95% yield). ^{1}H NMR (500 MHz, THF-d_8): δ(ppm) 7.97 (s, 2 H, imidazole), 7.60 (t, 2 H, J = 7.8 Hz, IPr *p*-H), 7.45 (d, 4 H, J = 8.0 Hz, *m*-H), 7.15-7.03 (m, 5 H, phenyl), 3.36 (d, 2 H, $J_{H\text{-}P}$ = 11.5, PCH_2), 2.71 (sept., 4 H, J = 7.0 Hz, C(*H*)Me$_2$), 1.32 (d, 12 H, 6.5 Hz, C(H)*Me*$_2$), 1.26 (d, 12 H, J = 7.0 Hz, C(H)*Me*$_2$), 0.99 (d, 18 H, $J_{H\text{-}P}$ = 15.0 Hz, *t*-Bu). ^{13}C NMR (125 MHz, THF-d_8): δ(ppm) 146.8, 135.6 (d, J = 4.1 Hz), 135.4, 132.0, 131.3 (d, J = 5.6 Hz), 129.9, 127.6, 126.9, 125.4, 36.9 (d, J = 23.6), 30.1 (d, J = 17.5 Hz), 30.0, 28.3 (d, J = 23.4 Hz), 24.9, 24.6. ^{31}P{^{1}H} NMR (162 Hz, CD_2Cl_2): δ(ppm) 70.9. IR (ATR) ν_{max}(cm^{-1}): 2963, 2870, 1466, 1455, 1259, 1224, 1149, 1029, 809, 761, 636. HRMS(*m/z*): calculated for $C_{42}H_{61}N_2AuP$ [M-OTf] 821.4233, found 821.4213. Anal. Calcd. for $C_{43}H_{61}AuF_3N_2O_3PS$: C, 53.19; H, 6.33; N, 2.89. Found: C, 53.57; H, 6.36; N, 2.81.

Complex 16

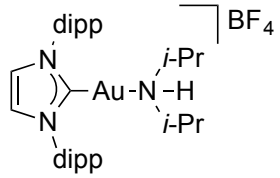

To a vial was added $AgBF_4$ (70.6 mg, 0.357 mmol), diisopropylamine (42.7 mg, 0.422 mmol), and methylene chloride (10 mL). IPrAuCl (200 mg, 0.322 mmol) was added to the reaction mixture, leading to the immediate precipitation of AgCl. Following 10 min. of stirring, the reaction mixture was filtered through two syringe filters and concentrated to yield the product as a white solid (237 mg, 0.306 mmol, 95% yield). X-ray quality crystals were grown from a methylene chloride solution layered with pentane and stored at -35 °C. ^{1}H NMR (500 MHz, CD_2Cl_2): δ(ppm) 7.54 (t, 2 H, J = 7.5 Hz, *p*-H), 7.39(s, 2 H, imidazole), 7.35 (d, 4 H, J = 10 Hz, *m*-H), 3.50 (br s,1 H, N-*H*), 3.18-3.09 (m, 2 H, NC(*H*)Me$_2$), 2.51 (sept., 4 H, J = 5.0 Hz, IPr NC(*H*)Me$_2$), 1.31 (d, 12 H, J = 5.0 Hz, C(H)*Me*$_2$), 1.24 (d, 12 H, J = 10 Hz, C(H)*Me*$_2$), 0.85 (d, 3 H, 5.0 Hz, NC(H)*Me*$_2$), 0.78 (d, 3 H, 5.0 Hz, NC(H)*Me*$_2$). ^{13}C NMR (125 MHz, CD_2Cl_2): δ(ppm) 173.1, 146.3, 134.2, 131.5, 124.9, 124.6, 51.6, 29.4, 24.6, 24.5, 22.8, 22.3. ^{19}F{^{1}H} NMR (376 MHz, CD_2Cl_2): δ(ppm) 151.4. HRMS(*m/z*): calculated for $C_{33}H_{51}AuN_3$ 686.3743, found 686.3744.

Catalytic Benzylation of Di(*t*-butyl)phosphine

Hexamethylbenzene (2.9 mg, 0.006 mmol) and sodium *t*-amylate (2.9 mg, 0.026 mmol) were dissolved in THF-d_8 and transferred to a J. Young NMR tube. Benzyl chloride (3.0 mg, 0.024 mmol) and di(t-butyl)phosphine (3.6 mg, 0.024 mmol) were added via syringe to the reaction mixture. The ^{1}H NMR spectrum of the mixture was taken. Compound **4** (2.0 mg, 0.002 mmol) in THF-d_8 was added to the tube. The tube was promptly inverted to ensure mixing, resulting in a pale yellow reaction mixture. A ^{1}H NMR spectrum of the mixture was obtained every two hours after heating continuously at 75 °C. Conversion was determined by comparison of the benzyl protons of the starting material and product relative to the internal standard. The identity of the

product was confirmed by comparison of the spectra of the reaction mixture to the spectrum of an authentic sample of di(*t*-butyl)benzylphosphine [49] in THF-d_8.

Ligand Exchange of Complex 4 with d_5-Aniline

A J. Young tube was charged with complex **4** (6.8 mg, 0.010 mmol), C_6D_6 (0.5 mL), and hexamethylbenzene (0.8 mg, 0.005 mmol). A ^{1}H NMR spectrum of the mixture was taken. Aniline-d_5 (5.0 μL, 5.5 equiv.) was added to the reaction mixture via syringe. A second spectrum was collected immediately following addition. A statistical amount (~80%) of free aniline was observed.

References

1. Fulton, J. R.; Holland, A. W.; Fox, D. J.; Bergman, R. G. *Acc. Chem. Res.* **2002***, 35*, 44.
2. Glueck, D. S. *Dalton Transactions* **2008**, 5276.
3. Lancaster, K. M.; Roemelt, M.; Ettenhuber, P.; Hu, Y.; Ribbe, M. W.; Neese, F.; Bergmann, U.; DeBeer, S. *Science* **2011***, 334*, 974.
4. Shekhar, S.; Ryberg, P.; Hartwig, J. F.; Mathew, J. S.; Blackmond, D. G.; Strieter, E. R.; Buchwald, S. L. *J. Am. Chem. Soc.* **2006***, 128*, 3584.
5. Gephart, R. T.,III; Huang, D. L.; Aguila, M. J. B.; Schmidt, G.; Shahu, A.; Warren, T. H. Catalytic C-H Amination with Aromatic Amines. *Angew. Chem., Int. Ed.* **2012***, 51*, 6488-.
6. Wiese, S.; Badiei, Y. M.; Gephart, R. T.; Mossin, S.; Varonka, M. S.; Melzer, M. M.; Meyer, K.; Cundari, T. R.; Warren, T. H *Angew. Chem., Int. Ed.* **2012***, 51*, 6488.
7. Munro-Leighton, C.; Blue, E. D.; Gunnoe, T. B. *J. Am. Chem. Soc.* **2006***, 128*, 1446-1447.
8. Hanley, P. S.; Marquard, S. L.; Cundari, T. R.; Hartwig, J. F. *J. Am. Chem. Soc.* **2012***, 134*, 15281.
9. Corma, A.; Leyva-Perez, A.; Sabater, M. J. *Chem. Rev.* **2011***, 111*, 1657.
10. Shapiro, N. D.; Toste, F. D. *Synlett* **2010**, 675.
11. Nishina, N.; Yamamoto, Y.. *Angew. Chem., Int. Ed.* **2006***, 45*, 3314-3317.
12. Lavy, S.; Miller, J. J.; Pazicky, M.; Rodrigues, A.; Rominger, F.; Jaekel, C.; Serra, D.; Vinokurov, N.; Limbach, M. *Adv. Synth. Catal.* **2010***, 352*, 2993.
13. Kinjo, R.; Donnadieu, B.; Bertrand, G. *Angew. Chem., Int. Ed.* **2011***, 50*, 5560-5563.
14. Lavallo, V.; Frey, G. D.; Donnadieu, B.; Soleilhavoup, M.; Bertrand, G. *Angew. Chem., Int. Ed* **2008***, 47*, 5224-5228.
15. Zeng, X.; Soleilhavoup, M.; Bertrand, G. *Org. Lett.* **2009***, 11*, 3166.
16. Mayer, J. M. *Comments Inorg. Chem.* **1988***, 8*, 125.
17. Caulton, K. G. *New J. Chem.* **1994***, 18*, 25.
18. Gorin, D. J.; Toste, F. D. *Nature* **2007***, 446*, 395.
19. Holland, P. L.; Andersen, R. A.; Bergman, R. G. *Comments Inorg. Chem.* **1999***, 21*, 115.
20. Stefanescu, D. M.; Yuen, H. F.; Glueck, D. S.; Golen, J. A.; Zakharov, L. N.; Incarvito, C. D.; Rheingold, A. L. *Inorg. Chem.* **2003***, 42*, 8891.
21. Stefanescu, D. M.; Yuen, H. F.; Glueck, D. S.; Golen, J. A.; Rheingold, A. L. *Angew. Chem., Int. Ed.* **2003***, 42*, 1046.
22. Lane, E. M.; Chapp, T. W.; Hughes, R. P.; Glueck, D. S.; Feland, B. C.; Bernard, G. M.; Wasylishen, R. E.; Rheingold, A. L. *Inorg. Chem.* **2010***, 49*, 3950.
23. Bunge, S. D.; Just, O.; Rees, W. S. *Angew. Chem., Int. Ed.* **2000***, 39*, 3082.
24. Cinellu, M. A.; Minghetti, G.; Pinna, M. V.; Stoccoro, S.; Zucca, A.; Manassero, M. *Eur. J. Inorg. Chem.* **2003**, 2304.
25. Marion, N.; Nolan, S. P. *Chem. Soc. Rev.* **2008***, 37*, 1776.
26. Gaillard, S.; Slawin, A. M. Z.; Nolan, S. P. *Chem. Commun.* **2010***, 46*, 2742.
27. Laitar, D. S.; Muller, P.; Gray, T. G.; Sadighi, J. P. *Organometallics* **2005***, 24*, 4503.
28. Diamond, S. E.; Mares, F. *J. Organomet. Chem.* **1977***, 142*, C55.
29. Hartwig, J. F.; Richards, S.; Baranano, D.; Paul, F. *J. Am. Chem. Soc.* **1996***, 118*, 3626.

30. Corberán, R.; Marrot, S.; Dellus, N.; Merceron-Saffon, N.; Kato, T.; Peris, E.; Baceiredo, A. *Organometallics* **2008***, 28*, 326.
31. Munro-Leighton, C.; Delp, S. A.; Blue, E. D.; Gunnoe, T. B. *Organometallics* **2007***, 26*, 1483.
32. Roth, K. E.; Blum, S. A. *Organometallics* **2010***, 29*, 1712.
33. Cowan, R. L.; Trogler, W. C. *J. Am. Chem. Soc.* **1989***, 111*, 4750.
34. Joslin, F. L.; Johnson, M. P.; Mague, J. T.; Roundhill, D. M. *Organometallics* **1991***, 10*, 2781.
35. Johnson, M. T.; van Rensburg, J. M. J.; Axelsson, M.; Ahlquist, M. S. G.; Wendt, O. F. *Chem. Sci.* **2011***, 2*, 2373.
36. Wang, Z. J.; Benitez, D.; Tkatchouk, E.; Goddard, W. A.,III; Toste, F. D. *J. Am. Chem. Soc.* **2010***, 132*, 13064.
37. Streitwieser, A.; Wang, D. Z.; Stratakis, M.; Facchetti, A.; Gareyev, R.; Abbotto, A.; Krom, J. A.; Kilway, K. V. *Can. J. Chem.* **1998***, 76*, 765.
38. Laitar, D. S. *Synthetic and Catalytic Studies of Group 11 N-Heterocyclic Carbene Complexes (Thesis).* Massachusetts Institute of Technology. August 1, 2006.
39. Chan, V. S.; Chiu, M.; Bergman, R. G.; Toste, F. D. *J. Am. Chem. Soc.* **2009***, 131*, 6021.
40. Blank, N. F.; Moncarz, J. R.; Brunker, T. J.; Scriban, C.; Anderson, B. J.; Amir, O.; Glueck, D. S.; Zakharov, L. N.; Golen, J. A.; Incarvito, C. D.; Rheingold, A. L. *J. Am. Chem. Soc.* **2007***, 129*, 6847.
41. Kaplan, A. W.; Ritter, J. C. M.; Bergman, R. G. *J. Am. Chem. Soc.* **1998***, 120*, 6828-6829.
42. Fulton, J. R.; Bouwkamp, M. W.; Bergman, R. G. *J. Am. Chem. Soc.* **2000***, 122*, 8799-8800.
43. Ricard, L.; Gagosz, F. *Organometallics* **2007***, 26*, 4704-4707.
44. Weinhold, F.; Landis, C. *Valency and Bonding: A Natural Bond Orbital Donor-Acceptor Perspective;* Cambridge University Press: 2005.
45. Goj, L. A.; Blue, E. D.; Delp, S. A.; Gunnoe, T. B.; Cundari, T. R.; Pierpont, A. W.; Petersen, J. L.; Boyle, P. D. *Inorg. Chem.* **2006***, 45*, 9032-9045.
46. Armarego, W.; Chai, C. *Purification of Laboratory Chemicals, 6th Edition;* 2009.
47. Mauleon, P.; Zeldin, R. M.; Gonzalez, A. Z.; Toste, F. D. *Am. Chem. Soc.* **2009***, 131*, 6348-6349.
48. Tsui, E. Y.; Mueller, P.; Sadighi, J. P. *Angew. Chem., Int. Ed* **2008***, 47*, 8937.
49. Ionkin, A. S.; Marshall, W. J.; Adelman, D. J.; Fones, B. B.; Fish, B. M.; Schiffhauer, M. F. *Organometallics* **2006***, 25*, 2978.
50. de Fremont, P.; Singh, R.; Stevens, E. D.; Petersen, J. L.; Nolan, S. P. *Organometallics* **2007***, 26*, 1376.
51. Xiang, S.; Xu, J.; Yuan, H.; Huang, P. *Synlett* **2010**, 1829.

DFT Calculations

Density functional calculations were performed at the UC Berkeley Molecular Graphics and Computional Facility using the Gaussian09 suite.[7] Calculations were conducted using the BPV86 functional and LANL2DZ basis set for Au. The 6-311++G(d,p) basis set was used for all other atoms during geometry optimization, frequency, energy, NBO, and NLMO calculations. Optimized XYZ coordinates for all calculated molecules are enumerated below.

(IPr)gold(I) diisopropylamide (1)

Center Number	Atomic Number	Atomic Type	Coordinates (Angstroms) X	Y	Z
1	79	0	0.000089	1.033261	0.000091
2	7	0	1.086069	-1.809786	-0.022296
3	7	0	-1.086473	-1.809603	0.021704
4	7	0	0.000394	3.059113	0.000294
5	6	0	-0.000133	-0.954227	-0.000161
6	6	0	-0.681130	-3.144977	0.013334
7	1	0	-1.394881	-3.960699	0.028048
8	6	0	0.680497	-3.145088	-0.014341
9	1	0	1.394105	-3.960931	-0.029334
10	6	0	2.471767	-1.397017	-0.066644
11	6	0	3.091073	-1.241231	-1.327586
12	6	0	4.445948	-0.870601	-1.342392
13	1	0	4.952951	-0.736128	-2.300814
14	6	0	5.151836	-0.664403	-0.155178
15	1	0	6.204254	-0.372549	-0.189936
16	6	0	4.514035	-0.827482	1.076471
17	1	0	5.074582	-0.662127	1.999718
18	6	0	3.160971	-1.198166	1.151255
19	6	0	2.347286	-1.455939	-2.642521
20	1	0	1.308457	-1.728785	-2.400945
21	6	0	2.958289	-2.619620	-3.451911
22	1	0	3.998329	-2.402999	-3.744114
23	1	0	2.381172	-2.788768	-4.374957
24	1	0	2.961676	-3.557288	-2.874599
25	6	0	2.297991	-0.160044	-3.477697
26	1	0	1.819736	0.653391	-2.912629
27	1	0	1.721870	-0.323778	-4.402388
28	1	0	3.308539	0.170291	-3.767410
29	6	0	2.495004	-1.378491	2.511846
30	1	0	1.440242	-1.640837	2.337551
31	6	0	3.141191	-2.536319	3.302298
32	1	0	4.198843	-2.325559	3.528014
33	1	0	3.101477	-3.482549	2.740568

34	1	0	2.618449	-2.685624	4.260520
35	6	0	2.510124	-0.069333	3.327133
36	1	0	3.539087	0.255658	3.550391
37	1	0	1.989514	-0.211936	4.287491
38	1	0	2.004769	0.739957	2.779639
39	6	0	-2.472104	-1.396640	0.066367
40	6	0	-3.161489	-1.197468	-1.151374
41	6	0	-4.514499	-0.826646	-1.076289
42	1	0	-5.075185	-0.661050	-1.999409
43	6	0	-5.152067	-0.663726	0.155500
44	1	0	-6.204447	-0.371762	0.190495
45	6	0	-4.445996	-0.870221	1.342555
46	1	0	-4.952823	-0.735863	2.301087
47	6	0	-3.091169	-1.241011	1.327449
48	6	0	-2.495752	-1.377549	-2.512108
49	1	0	-1.441023	-1.640168	-2.338034
50	6	0	-3.142284	-2.534994	-3.302830
51	1	0	-4.199917	-2.323941	-3.528365
52	1	0	-3.102713	-3.481405	-2.741394
53	1	0	-2.619687	-2.684123	-4.261159
54	6	0	-2.510712	-0.068134	-3.326995
55	1	0	-3.539642	0.257126	-3.550015
56	1	0	-1.990251	-0.210546	-4.287463
57	1	0	-2.005131	0.740889	-2.779318
58	6	0	-2.347200	-1.456101	2.642218
59	1	0	-1.308377	-1.728776	2.400425
60	6	0	-2.958028	-2.620127	3.451251
61	1	0	-3.998059	-2.403691	3.743620
62	1	0	-2.380811	-2.789567	4.374181
63	1	0	-2.961392	-3.557583	2.873596
64	6	0	-2.297899	-0.160510	3.477857
65	1	0	-1.819766	0.653165	2.913031
66	1	0	-1.721649	-0.324549	4.402413
67	1	0	-3.308427	0.169655	3.767833
68	6	0	1.219325	3.858644	0.131201
69	1	0	1.076923	4.801920	-0.439684
70	6	0	2.444521	3.157897	-0.469079
71	1	0	2.631673	2.198543	0.042165
72	1	0	3.347890	3.781161	-0.362793
73	1	0	2.285658	2.945552	-1.536959
74	6	0	1.489855	4.257367	1.601565
75	1	0	0.611671	4.757590	2.039415
76	1	0	2.351288	4.943049	1.689457
77	1	0	1.695664	3.354560	2.199718
78	6	0	-1.218249	3.859063	-0.130755
79	1	0	-1.075400	4.802469	0.439783
80	6	0	-2.443603	3.158919	0.469912

81	1	0	-2.630979	2.199401	-0.040940
82	1	0	-3.346832	3.782349	0.363431
83	1	0	-2.284706	2.946958	1.537863
84	6	0	-1.488783	4.257388	-1.601223
85	1	0	-0.610411	4.757059	-2.039326
86	1	0	-2.349928	4.943413	-1.689272
87	1	0	-1.695055	3.354460	-2.199036

(IPr)gold(I) anilide (2)

Center Number	Atomic Number	Atomic Type	Coordinates (Angstroms) X	Y	Z
1	79	0	-0.272905	-0.936341	0.000112
2	6	0	0.752376	0.764120	0.000049
3	6	0	1.298629	2.982155	-0.000069
4	1	0	1.108163	4.049156	-0.000145
5	6	0	2.465374	2.276615	0.000049
6	1	0	3.498575	2.604281	0.000088
7	6	0	3.078774	-0.160348	0.000040
8	6	0	3.535143	-0.660452	1.240647
9	6	0	4.486537	-1.693800	1.210049
10	1	0	4.855663	-2.107492	2.151459
11	6	0	4.960361	-2.205054	0.000115
12	1	0	5.698854	-3.010351	0.000144
13	6	0	4.486693	-1.693745	-1.209859
14	1	0	4.855942	-2.107397	-2.151239
15	6	0	3.535306	-0.660392	-1.240536
16	6	0	3.028897	-0.137074	2.581734
17	1	0	2.297470	0.660605	2.380535
18	6	0	4.172190	0.479481	3.415608
19	1	0	4.930940	-0.274931	3.677482
20	1	0	3.778336	0.895981	4.356228
21	1	0	4.680927	1.289453	2.870048
22	6	0	2.293630	-1.242952	3.367531
23	1	0	2.967390	-2.082061	3.603796
24	1	0	1.443638	-1.637507	2.790597
25	1	0	1.908379	-0.844479	4.319435
26	6	0	3.029241	-0.136955	-2.581672
27	1	0	2.297745	0.660675	-2.380539
28	6	0	4.172616	0.479725	-3.415342
29	1	0	4.681239	1.289679	-2.869647
30	1	0	3.778869	0.896280	-4.355981
31	1	0	4.931439	-0.274626	-3.677178
32	6	0	2.294150	-1.242828	-3.367644
33	1	0	1.909080	-0.844339	-4.319616

34	1	0	1.444051	-1.637418	-2.790893
35	1	0	2.967980	-2.081916	-3.603792
36	6	0	-1.144832	2.400749	-0.000164
37	6	0	-1.797962	2.576876	1.240842
38	6	0	-3.151502	2.951593	1.209820
39	1	0	-3.688659	3.090717	2.150796
40	6	0	-3.822245	3.139982	-0.000397
41	1	0	-4.875755	3.429526	-0.000489
42	6	0	-3.151394	2.951214	-1.210496
43	1	0	-3.688465	3.090052	-2.151564
44	6	0	-1.797855	2.576479	-1.241281
45	6	0	-1.100919	2.360497	2.580686
46	1	0	-0.052377	2.092475	2.377535
47	6	0	-1.093607	3.647641	3.432290
48	1	0	-0.619961	4.485614	2.897526
49	1	0	-0.538510	3.482254	4.369275
50	1	0	-2.115752	3.957429	3.702425
51	6	0	-1.735730	1.183538	3.351172
52	1	0	-1.195556	1.008701	4.295280
53	1	0	-1.704460	0.256683	2.759036
54	1	0	-2.788348	1.390964	3.601407
55	6	0	-1.100681	2.359723	-2.580996
56	1	0	-0.052121	2.091900	-2.377674
57	6	0	-1.093471	3.646583	-3.433029
58	1	0	-2.115642	3.956171	-3.703301
59	1	0	-0.538321	3.480946	-4.369939
60	1	0	-0.619936	4.484784	-2.898525
61	6	0	-1.735278	1.182420	-3.351130
62	1	0	-1.704009	0.255795	-2.758635
63	1	0	-1.194949	1.007271	-4.295091
64	1	0	-2.787877	1.389648	-3.601603
65	6	0	-2.632710	-2.934675	0.000045
66	6	0	-3.585046	-1.879621	0.000131
67	1	0	-3.221706	-0.847358	0.000122
68	6	0	-4.955566	-2.142727	0.000229
69	1	0	-5.657137	-1.303260	0.000301
70	6	0	-5.444026	-3.459343	0.000245
71	1	0	-6.517557	-3.658053	0.000328
72	6	0	-4.517473	-4.513345	0.000158
73	1	0	-4.869021	-5.549246	0.000175
74	6	0	-3.144337	-4.262757	0.000066
75	1	0	-2.438947	-5.100597	0.000018
76	7	0	2.119844	0.925162	0.000022
77	7	0	0.261825	2.049597	-0.000051
78	7	0	-1.278047	-2.691386	-0.000021
79	1	0	-0.727150	-3.548662	-0.000054

(IPr)gold(I) bis(2,4,6-trimethlyphenyl)phosphide(13)

Center Number	Atomic Number	Atomic Type	Coordinates (Angstroms) X	Y	Z
1	79	0	0.092697	-0.273240	-0.219365
2	15	0	-2.021486	-1.004680	-1.037556
3	6	0	1.989530	0.452166	0.133164
4	6	0	4.256884	0.731653	0.062896
5	1	0	5.279779	0.473962	-0.186406
6	6	0	3.733239	1.811560	0.710089
7	1	0	4.206618	2.685140	1.143271
8	6	0	1.442903	2.568076	1.372070
9	6	0	0.891557	3.602365	0.583509
10	6	0	0.060086	4.531595	1.230454
11	1	0	-0.389015	5.340413	0.650126
12	6	0	-0.209116	4.433055	2.596849
13	1	0	-0.861325	5.165807	3.077959
14	6	0	0.347090	3.396103	3.348259
15	1	0	0.123799	3.323461	4.415256
16	6	0	1.186799	2.438428	2.755702
17	6	0	1.182690	3.749313	-0.906581
18	1	0	1.715775	2.844251	-1.236621
19	6	0	2.105251	4.959986	-1.169487
20	1	0	2.342573	5.037336	-2.242567
21	1	0	3.053512	4.878236	-0.615492
22	1	0	1.619238	5.900471	-0.863637
23	6	0	-0.110378	3.844652	-1.739695
24	1	0	-0.780280	2.994684	-1.544499
25	1	0	0.133353	3.855275	-2.813796
26	1	0	-0.668085	4.769235	-1.521398
27	6	0	1.782087	1.320663	3.607531
28	1	0	2.368494	0.664710	2.945597
29	6	0	2.744017	1.882165	4.676795
30	1	0	3.555317	2.472161	4.222784
31	1	0	3.199893	1.061379	5.252989
32	1	0	2.213920	2.535884	5.387728
33	6	0	0.681485	0.452344	4.250056
34	1	0	0.069012	1.034370	4.956959
35	1	0	1.131612	-0.383107	4.809477
36	1	0	0.010923	0.033186	3.485862
37	6	0	3.342694	-1.357087	-0.966172
38	6	0	3.158554	-1.404519	-2.366519
39	6	0	3.365489	-2.640611	-3.001417
40	1	0	3.226633	-2.714114	-4.082286

41	6	0	3.743599	-3.773080	-2.278208
42	1	0	3.897582	-4.723639	-2.794411
43	6	0	3.924225	-3.693256	-0.895889
44	1	0	4.218739	-4.586138	-0.339610
45	6	0	3.727000	-2.485797	-0.205726
46	6	0	2.778619	-0.182536	-3.196910
47	1	0	2.566961	0.646390	-2.504312
48	6	0	3.950398	0.251422	-4.104675
49	1	0	4.859269	0.465095	-3.520735
50	1	0	3.683423	1.160280	-4.667118
51	1	0	4.198963	-0.534241	-4.836082
52	6	0	1.495916	-0.425360	-4.016997
53	1	0	1.213444	0.492139	-4.557089
54	1	0	0.658209	-0.714477	-3.364789
55	1	0	1.636653	-1.219564	-4.767761
56	6	0	3.950667	-2.430168	1.303635
57	1	0	3.623238	-1.440560	1.658914
58	6	0	5.449144	-2.577173	1.648238
59	1	0	5.833993	-3.559602	1.331018
60	1	0	5.604038	-2.490311	2.735457
61	1	0	6.059667	-1.805650	1.154284
62	6	0	3.111865	-3.484759	2.053217
63	1	0	2.041495	-3.380633	1.826182
64	1	0	3.246267	-3.372764	3.140807
65	1	0	3.417048	-4.509265	1.787813
66	6	0	-3.001099	0.589211	-0.919124
67	6	0	-3.230036	1.302996	-2.129772
68	6	0	-3.980302	2.490723	-2.109104
69	1	0	-4.149829	3.021279	-3.052563
70	6	0	-4.523553	3.009127	-0.925866
71	6	0	-4.265558	2.314385	0.263465
72	1	0	-4.651954	2.713492	1.207937
73	6	0	-3.513533	1.126930	0.295347
74	6	0	-2.677161	0.829329	-3.456400
75	1	0	-2.915156	-0.229937	-3.638929
76	1	0	-1.576996	0.900827	-3.484955
77	1	0	-3.077200	1.435827	-4.283344
78	6	0	-5.373963	4.259380	-0.934181
79	1	0	-5.099500	4.928986	-1.763778
80	1	0	-5.273614	4.821291	0.007394
81	1	0	-6.443642	4.013760	-1.053466
82	6	0	-3.247130	0.488088	1.636051
83	1	0	-3.531553	1.167084	2.453858
84	1	0	-2.176623	0.239665	1.732812
85	1	0	-3.798217	-0.456615	1.762279
86	6	0	-2.949296	-2.219286	0.032837
87	6	0	-2.341440	-3.034216	1.029014

88	6	0	-3.113286	-3.982018	1.725894
89	1	0	-2.624845	-4.583504	2.500407
90	6	0	-4.472867	-4.184615	1.467504
91	6	0	-5.049488	-3.418400	0.445160
92	1	0	-6.103321	-3.574027	0.188870
93	6	0	-4.323056	-2.463969	-0.282709
94	6	0	-0.877863	-2.947886	1.382566
95	1	0	-0.584809	-1.916120	1.649128
96	1	0	-0.236308	-3.237656	0.533373
97	1	0	-0.644008	-3.612515	2.228464
98	6	0	-5.278729	-5.212724	2.228386
99	1	0	-5.516065	-6.086683	1.597570
100	1	0	-6.237678	-4.796502	2.577005
101	1	0	-4.729150	-5.579191	3.108414
102	6	0	-5.036626	-1.748886	-1.407368
103	1	0	-5.985165	-2.254484	-1.642866
104	1	0	-4.412421	-1.733367	-2.316606
105	1	0	-5.259435	-0.698526	-1.163136
106	7	0	2.352250	1.625664	0.746957
107	7	0	3.183774	-0.088945	-0.280376

(IPr)gold(I) di-*t*-butyl phosphide (14)

Center Number	Atomic Number	Atomic Type	Coordinates (Angstroms) X	Y	Z
1	79	0	0.099265	0.724407	-0.193715
2	15	0	0.358564	3.033098	-0.729611
3	6	0	-0.169783	-1.322643	0.010706
4	6	0	-1.126021	-3.397989	0.129023
5	1	0	-1.939180	-4.114668	0.150665
6	6	0	0.225617	-3.569496	0.186551
7	1	0	0.830672	-4.465090	0.271016
8	6	0	2.221382	-2.054047	0.140740
9	6	0	2.928021	-2.041373	-1.082574
10	6	0	4.315602	-1.829236	-1.022997
11	1	0	4.892022	-1.804236	-1.950524
12	6	0	4.966786	-1.642820	0.197941
13	1	0	6.046496	-1.476748	0.219988
14	6	0	4.240757	-1.663984	1.390779
15	1	0	4.759755	-1.511844	2.339828
16	6	0	2.851518	-1.872816	1.392496
17	6	0	2.243030	-2.224860	-2.433270
18	1	0	1.180596	-2.446625	-2.247345
19	6	0	2.831714	-3.416516	-3.217100
20	1	0	3.888590	-3.247353	-3.477684

21	1	0	2.278820	-3.563364	-4.158406
22	1	0	2.774858	-4.351297	-2.637835
23	6	0	2.300623	-0.923681	-3.260999
24	1	0	1.830545	-0.089753	-2.717790
25	1	0	1.771736	-1.055098	-4.218469
26	1	0	3.341300	-0.641317	-3.487711
27	6	0	2.081137	-1.869855	2.710039
28	1	0	1.040312	-2.156771	2.493499
29	6	0	2.644275	-2.899844	3.710939
30	1	0	2.662755	-3.913992	3.282580
31	1	0	2.024038	-2.924174	4.620952
32	1	0	3.671172	-2.647165	4.019139
33	6	0	2.048583	-0.453374	3.321765
34	1	0	3.064753	-0.099943	3.559326
35	1	0	1.463198	-0.450529	4.255123
36	1	0	1.591096	0.265304	2.624301
37	6	0	-2.671763	-1.432333	-0.045183
38	6	0	-3.210060	-1.113945	-1.312488
39	6	0	-4.501385	-0.560696	-1.342842
40	1	0	-4.946638	-0.298307	-2.305319
41	6	0	-5.223090	-0.340846	-0.168011
42	1	0	-6.225210	0.091882	-0.216493
43	6	0	-4.666493	-0.672518	1.069061
44	1	0	-5.239571	-0.494596	1.982221
45	6	0	-3.378769	-1.225809	1.161541
46	6	0	-2.460407	-1.358863	-2.618913
47	1	0	-1.470601	-1.770687	-2.368849
48	6	0	-3.191714	-2.401943	-3.491532
49	1	0	-4.188987	-2.043696	-3.793029
50	1	0	-3.326127	-3.355759	-2.957812
51	1	0	-2.617567	-2.601908	-4.410183
52	6	0	-2.226707	-0.045845	-3.393197
53	1	0	-1.655596	-0.243979	-4.314058
54	1	0	-1.659322	0.677000	-2.787684
55	1	0	-3.179362	0.423514	-3.686504
56	6	0	-2.799402	-1.574763	2.530416
57	1	0	-1.791505	-1.989816	2.375950
58	6	0	-3.641776	-2.656876	3.239037
59	1	0	-4.662132	-2.298155	3.448425
60	1	0	-3.181148	-2.932065	4.201117
61	1	0	-3.728174	-3.568732	2.627971
62	6	0	-2.646840	-0.321264	3.415976
63	1	0	-2.006711	0.431178	2.932985
64	1	0	-2.193089	-0.589968	4.383275
65	1	0	-3.622277	0.146542	3.623565
66	6	0	2.082286	3.576509	-0.033280
67	6	0	3.084779	2.544012	-0.591410

68	1	0	4.118230	2.863870	-0.362593
69	1	0	2.995701	2.452168	-1.686215
70	1	0	2.927011	1.546450	-0.151992
71	6	0	2.215103	3.623105	1.498375
72	1	0	1.944727	2.657459	1.951943
73	1	0	1.578178	4.401540	1.945119
74	1	0	3.259951	3.855604	1.782027
75	6	0	2.448016	4.954518	-0.629254
76	1	0	1.782668	5.753785	-0.273009
77	1	0	2.391164	4.936204	-1.728660
78	1	0	3.480915	5.228255	-0.342801
79	6	0	-1.072438	3.914399	0.233935
80	6	0	-2.336998	3.533019	-0.567575
81	1	0	-3.228409	4.000905	-0.110771
82	1	0	-2.493455	2.441981	-0.572378
83	1	0	-2.266270	3.871835	-1.612928
84	6	0	-1.271179	3.469611	1.696099
85	1	0	-0.402243	3.703956	2.326509
86	1	0	-1.439661	2.383282	1.748363
87	1	0	-2.150882	3.980514	2.134471
88	6	0	-0.909359	5.446380	0.180586
89	1	0	-1.829493	5.934108	0.553026
90	1	0	-0.731768	5.799796	-0.847315
91	1	0	-0.078523	5.795710	0.812585
92	7	0	0.792832	-2.297321	0.114381
93	7	0	-1.351122	-2.025500	0.024725

IPrAuO*t*-Bu

Center Number	Atomic Number	Atomic Type	Coordinates (Angstroms) X	Y	Z
1	79	0	-0.071339	-1.131751	0.025034
2	7	0	1.465908	1.452233	-0.026031
3	7	0	-0.669925	1.841953	-0.045529
4	6	0	0.245266	0.814323	-0.017898
5	6	0	-0.032095	3.082332	-0.069699
6	1	0	-0.589450	4.011631	-0.092586
7	6	0	1.308991	2.837385	-0.057398
8	1	0	2.159157	3.509665	-0.067929
9	6	0	2.752388	0.784923	-0.007957
10	6	0	3.352090	0.504306	1.240458
11	6	0	4.614822	-0.111028	1.225975
12	1	0	5.104301	-0.348296	2.173392
13	6	0	5.248436	-0.433358	0.024268

14	1	0	6.229089	-0.914983	0.037028
15	6	0	4.626755	-0.150780	-1.193597
16	1	0	5.125407	-0.419107	-2.127876
17	6	0	3.364315	0.463417	-1.240508
18	6	0	2.675092	0.815864	2.571698
19	1	0	1.719009	1.317784	2.356118
20	6	0	3.520336	1.779213	3.431047
21	1	0	4.484510	1.327330	3.713565
22	1	0	2.986421	2.029520	4.361538
23	1	0	3.734494	2.717857	2.896626
24	6	0	2.348378	-0.482628	3.339625
25	1	0	1.713879	-1.149955	2.737119
26	1	0	1.816039	-0.249811	4.275673
27	1	0	3.266317	-1.031895	3.603624
28	6	0	2.699275	0.729212	-2.587650
29	1	0	1.743678	1.242484	-2.398183
30	6	0	3.554894	1.657245	-3.475021
31	1	0	4.519525	1.192000	-3.733146
32	1	0	3.768418	2.614113	-2.973682
33	1	0	3.029231	1.875128	-4.418271
34	6	0	2.373213	-0.595441	-3.309904
35	1	0	3.290987	-1.157688	-3.545638
36	1	0	1.849489	-0.395358	-4.258310
37	1	0	1.731145	-1.237526	-2.688315
38	6	0	-2.108613	1.674115	-0.047398
39	6	0	-2.786293	1.638335	1.192147
40	6	0	-4.183360	1.494535	1.159736
41	1	0	-4.738744	1.456505	2.099806
42	6	0	-4.871931	1.394791	-0.051044
43	1	0	-5.958550	1.280321	-0.052405
44	6	0	-4.174524	1.439224	-1.260050
45	1	0	-4.723095	1.358452	-2.201412
46	6	0	-2.777135	1.580815	-1.288880
47	6	0	-2.063894	1.742791	2.532221
48	1	0	-0.989643	1.872252	2.328560
49	6	0	-2.534628	2.975130	3.333402
50	1	0	-3.600118	2.897787	3.602488
51	1	0	-2.401034	3.906206	2.760939
52	1	0	-1.961176	3.064043	4.269739
53	6	0	-2.220872	0.446775	3.354079
54	1	0	-3.276963	0.255127	3.602947
55	1	0	-1.662813	0.524299	4.300765
56	1	0	-1.837820	-0.421904	2.798314
57	6	0	-2.045413	1.626463	-2.627113
58	1	0	-0.970119	1.742446	-2.421075
59	6	0	-2.489549	2.840572	-3.470537
60	1	0	-3.555888	2.774727	-3.739480

61	1	0	-1.912241	2.887190	-4.407585
62	1	0	-2.339291	3.787479	-2.929006
63	6	0	-2.221520	0.308105	-3.408377
64	1	0	-1.861326	-0.549979	-2.822001
65	1	0	-1.653338	0.344280	-4.351477
66	1	0	-3.278712	0.129428	-3.662092
67	8	0	-0.179243	-3.154679	0.069906
68	6	0	-1.396257	-3.890858	0.083936
69	6	0	-0.982310	-5.377420	0.105250
70	1	0	-1.859448	-6.045509	0.117567
71	1	0	-0.375175	-5.607995	-0.783555
72	1	0	-0.370645	-5.581207	0.997491
73	6	0	-2.225340	-3.563310	1.344653
74	1	0	-1.617550	-3.737277	2.246286
75	1	0	-2.527051	-2.502906	1.330717
76	1	0	-3.137566	-4.181202	1.411239
77	6	0	-2.232404	-3.601198	-1.181280
78	1	0	-2.530555	-2.539802	-1.198451
79	1	0	-1.630989	-3.805363	-2.080879
80	1	0	-3.146826	-4.218047	-1.222499

IPrAuNTf$_2$

Center Number	Atomic Number	Atomic Type	Coordinates (Angstroms) X	Y	Z
1	79	0	0.178301	-0.004169	-0.002341
2	16	0	3.119421	0.809101	1.199206
3	16	0	3.086075	-0.915009	-1.213845
4	9	0	2.215053	3.076853	0.050624
5	9	0	3.970311	3.332395	1.341488
6	9	0	4.195138	2.464390	-0.658170
7	9	0	3.849027	-3.466100	-1.359567
8	9	0	2.118060	-3.148432	-0.049780
9	9	0	4.125630	-2.602315	0.635372
10	8	0	2.139994	1.047693	2.273287
11	8	0	4.453704	0.269469	1.474315
12	8	0	4.435059	-0.417882	-1.497207
13	8	0	2.093610	-1.124068	-2.282149
14	7	0	-2.616479	1.116765	-0.159768
15	7	0	-2.651953	-1.030948	0.162552
16	7	0	2.290415	-0.039399	-0.005721
17	6	0	-1.800797	0.028979	0.000248
18	6	0	-3.955455	0.740049	-0.097833
19	1	0	-4.756649	1.462132	-0.203661

20	6	0	-3.977749	-0.609678	0.104252
21	1	0	-4.802342	-1.304571	0.212377
22	6	0	-2.161582	2.479958	-0.369155
23	6	0	-1.999154	3.314966	0.759176
24	6	0	-1.585100	4.636435	0.523147
25	1	0	-1.442717	5.310270	1.370899
26	6	0	-1.343581	5.098407	-0.772081
27	1	0	-1.017469	6.128977	-0.930582
28	6	0	-1.511167	4.245719	-1.865004
29	1	0	-1.312161	4.616422	-2.873033
30	6	0	-1.925858	2.914635	-1.692917
31	6	0	-2.250547	2.842211	2.188287
32	1	0	-2.534656	1.778655	2.151020
33	6	0	-0.975044	2.945263	3.050393
34	1	0	-0.145795	2.363860	2.622175
35	1	0	-1.172085	2.564019	4.064865
36	1	0	-0.641735	3.990628	3.149024
37	6	0	-3.424415	3.611359	2.832135
38	1	0	-3.194471	4.684429	2.927596
39	1	0	-3.627211	3.223033	3.842705
40	1	0	-4.347330	3.519228	2.238421
41	6	0	-2.093923	2.009122	-2.909885
42	1	0	-2.444088	1.025640	-2.558642
43	6	0	-0.747861	1.785381	-3.630580
44	1	0	-0.335835	2.733075	-4.012071
45	1	0	-0.881922	1.108845	-4.489121
46	1	0	-0.002296	1.336024	-2.958011
47	6	0	-3.162760	2.558840	-3.878522
48	1	0	-4.132844	2.698704	-3.376689
49	1	0	-3.309182	1.862678	-4.719339
50	1	0	-2.861310	3.530415	-4.300923
51	6	0	-2.242135	-2.408626	0.370330
52	6	0	-2.109887	-3.248021	-0.758658
53	6	0	-1.738760	-4.582433	-0.524031
54	1	0	-1.620656	-5.260281	-1.372325
55	6	0	-1.509254	-5.052542	0.770465
56	1	0	-1.216563	-6.093269	0.927828
57	6	0	-1.646420	-4.195328	1.864102
58	1	0	-1.457302	-4.572748	2.871552
59	6	0	-2.017941	-2.851383	1.693401
60	6	0	-2.350534	-2.767034	-2.186903
61	1	0	-2.594541	-1.693572	-2.149081
62	6	0	-3.555733	-3.492465	-2.823682
63	1	0	-3.366517	-4.573539	-2.918333
64	1	0	-3.748965	-3.098310	-3.833878
65	1	0	-4.471570	-3.364966	-2.225562
66	6	0	-1.084697	-2.918138	-3.056098

67	1	0	-0.231704	-2.368346	-2.632847
68	1	0	-1.273104	-2.529708	-4.069483
69	1	0	-0.791622	-3.975296	-3.156690
70	6	0	-2.153268	-1.941138	2.910856
71	1	0	-2.476921	-0.948112	2.561069
72	6	0	-3.232003	-2.459160	3.885876
73	1	0	-4.208430	-2.571636	3.389479
74	1	0	-3.353810	-1.758233	4.726657
75	1	0	-2.956278	-3.438511	4.307870
76	6	0	-0.797068	-1.756143	3.623562
77	1	0	-0.410322	-2.715311	4.002842
78	1	0	-0.906338	-1.075780	4.482590
79	1	0	-0.042935	-1.328717	2.946244
80	6	0	3.397053	2.539173	0.414268
81	6	0	3.313493	-2.652018	-0.427851

NMR Spectra

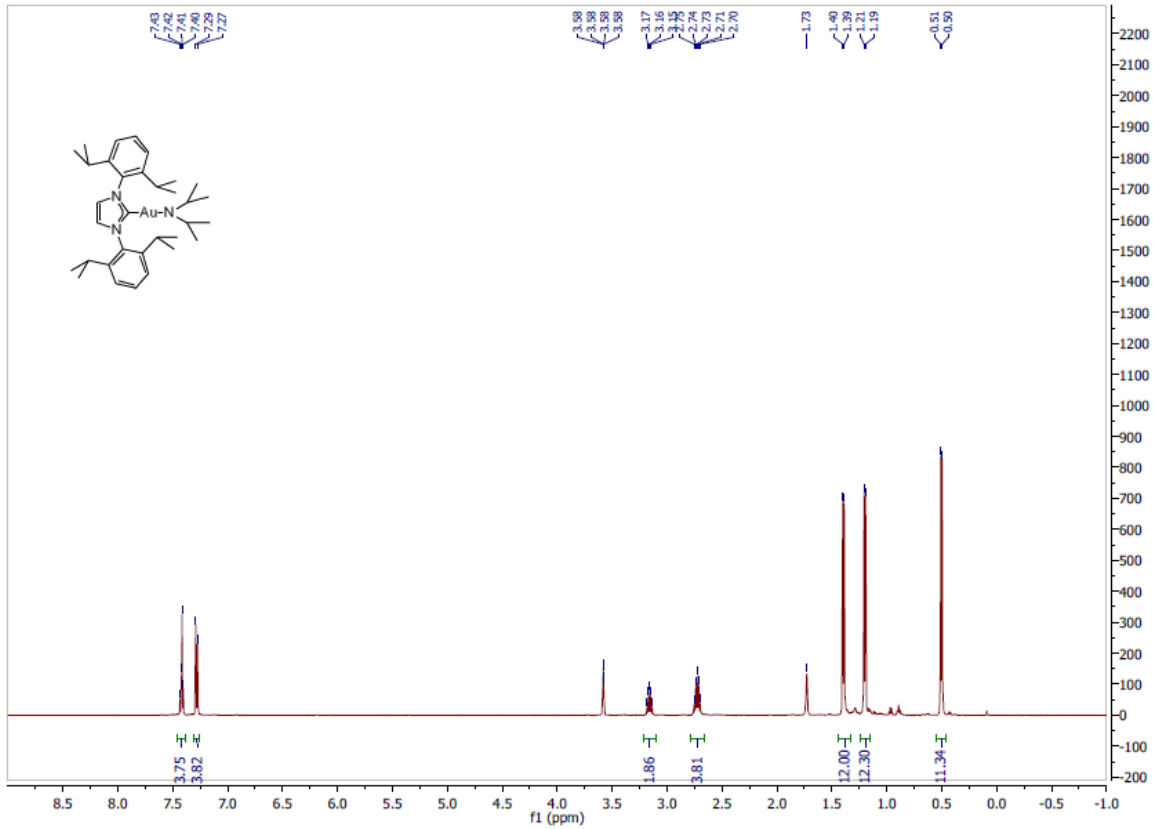
7.43
7.42
7.41
7.40
7.29
7.27
3.58
3.58
3.58
3.58
3.58
3.17
3.16
3.15
2.74
2.73
2.71
2.70
1.73
1.40
1.39
1.21
1.19
0.51
0.50
Au-N
3.75
3.82
1.86
3.81
12.00
12.30
11.34
f1 (ppm)

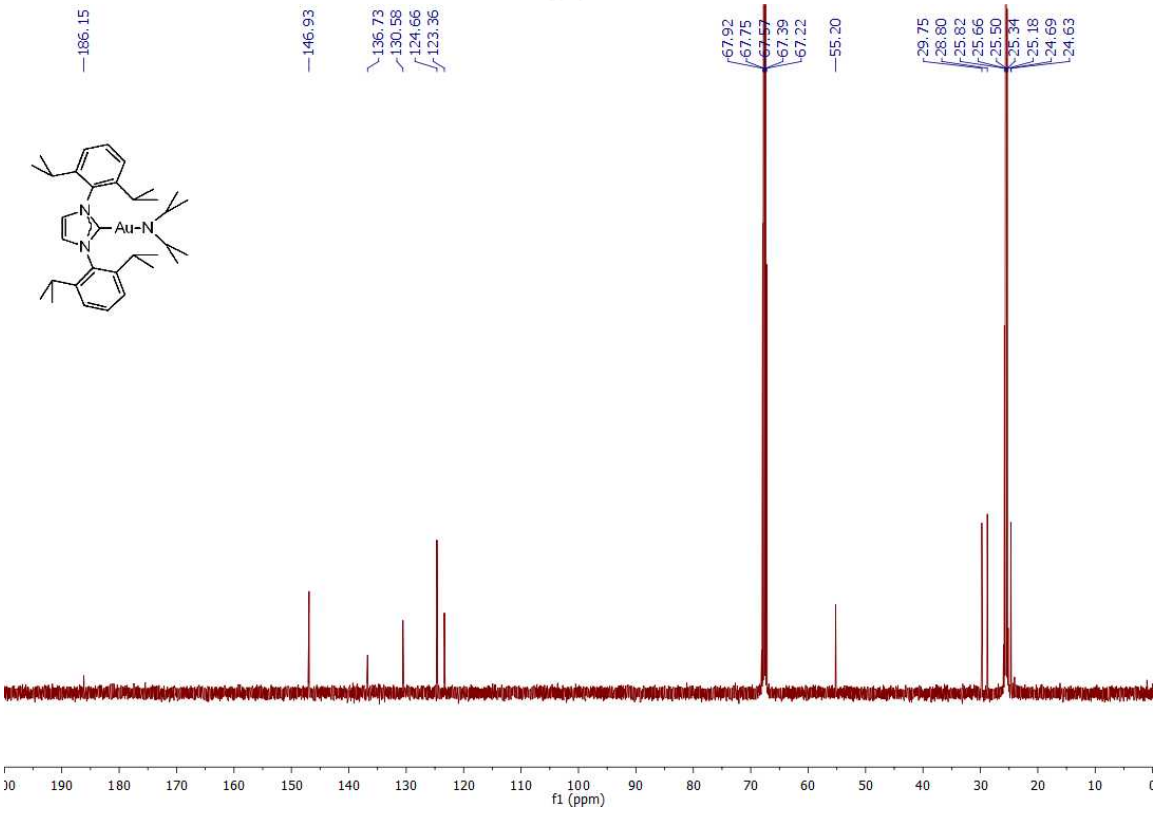
186.15
146.93
136.73
130.58
124.66
123.36
67.92
67.75
67.57
67.39
67.22
55.20
29.75
28.80
25.82
25.66
25.50
25.34
25.18
24.69
24.63
Au-N
f1 (ppm)

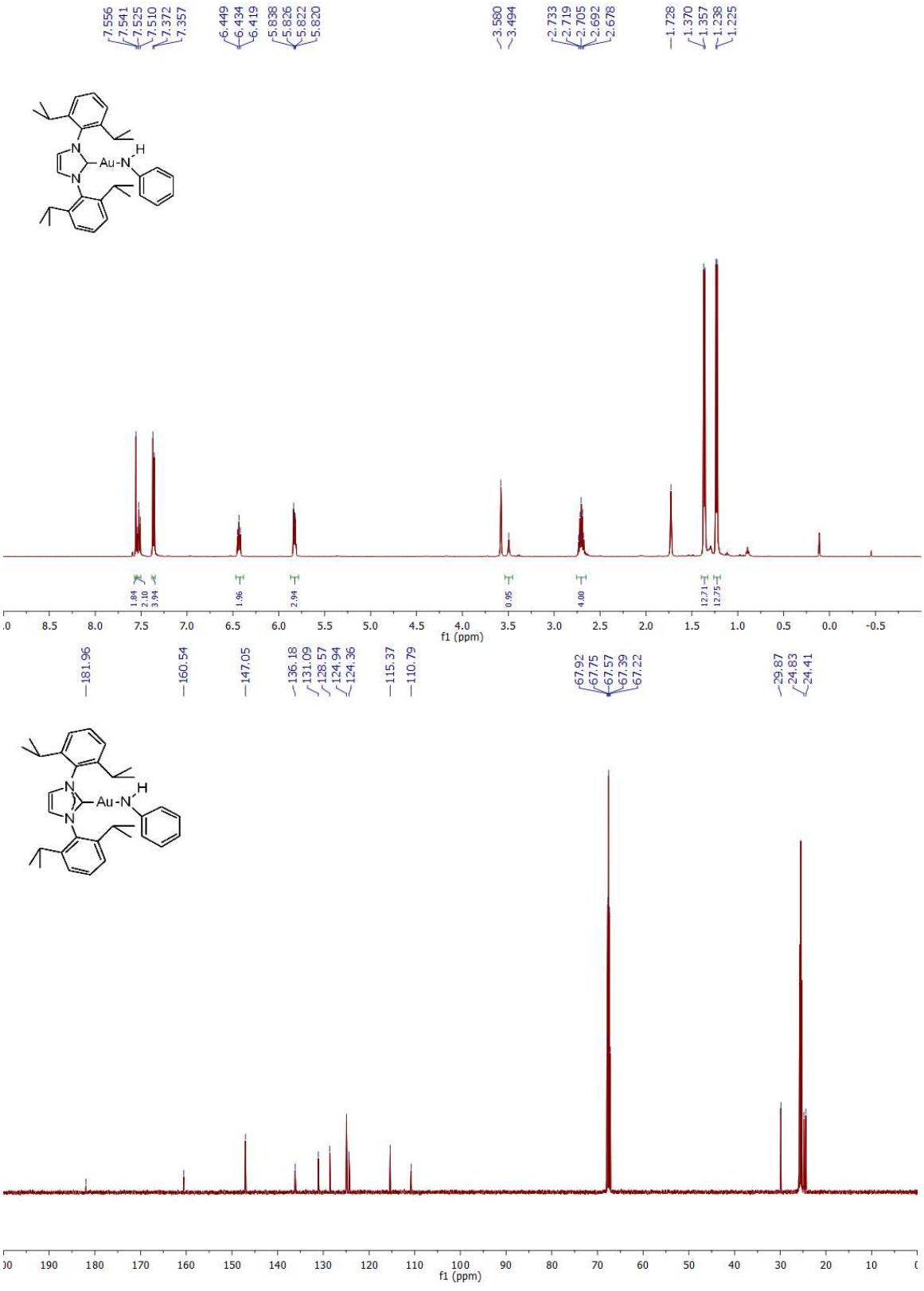
7.556
7.541
7.525
7.510
7.372
7.357
6.449
6.434
6.419
5.838
5.826
5.822
5.820
3.580
3.494
2.733
2.719
2.705
2.692
2.678
1.728
1.370
1.357
1.238
1.225
Au-N
H
1.84
2.10
3.94
1.96
2.94
0.95
4.00
12.71
12.75
f1 (ppm)
181.96
160.54
147.05
136.18
131.09
128.57
124.94
124.36
115.37
110.79
67.92
67.75
67.57
67.39
67.22
29.87
24.83
24.41
Au-N
H
f1 (ppm)

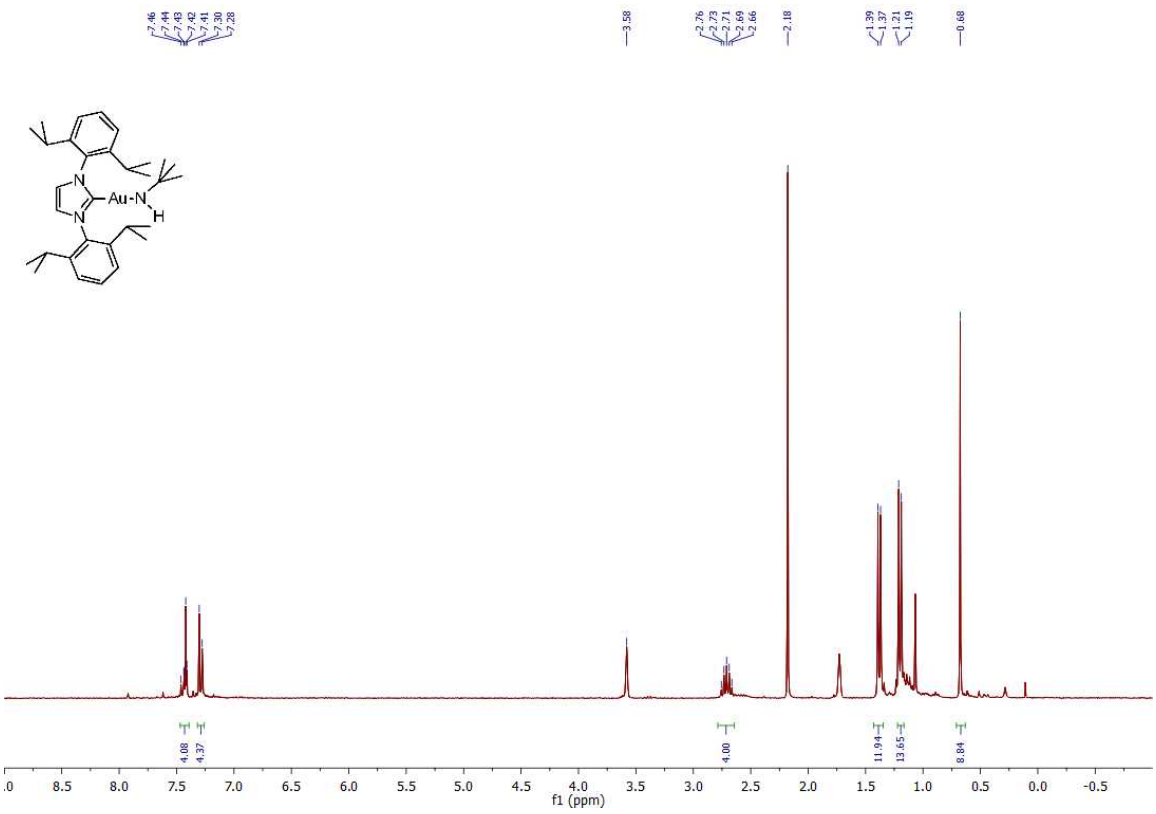
7.46
7.44
7.43
7.42
7.41
7.30
7.28
3.58
2.76
2.73
2.71
2.69
2.66
2.18
1.39
1.37
1.21
1.19
0.68
Au-N
H
4.08
4.37
4.00
11.94
13.65
8.84
f1 (ppm)

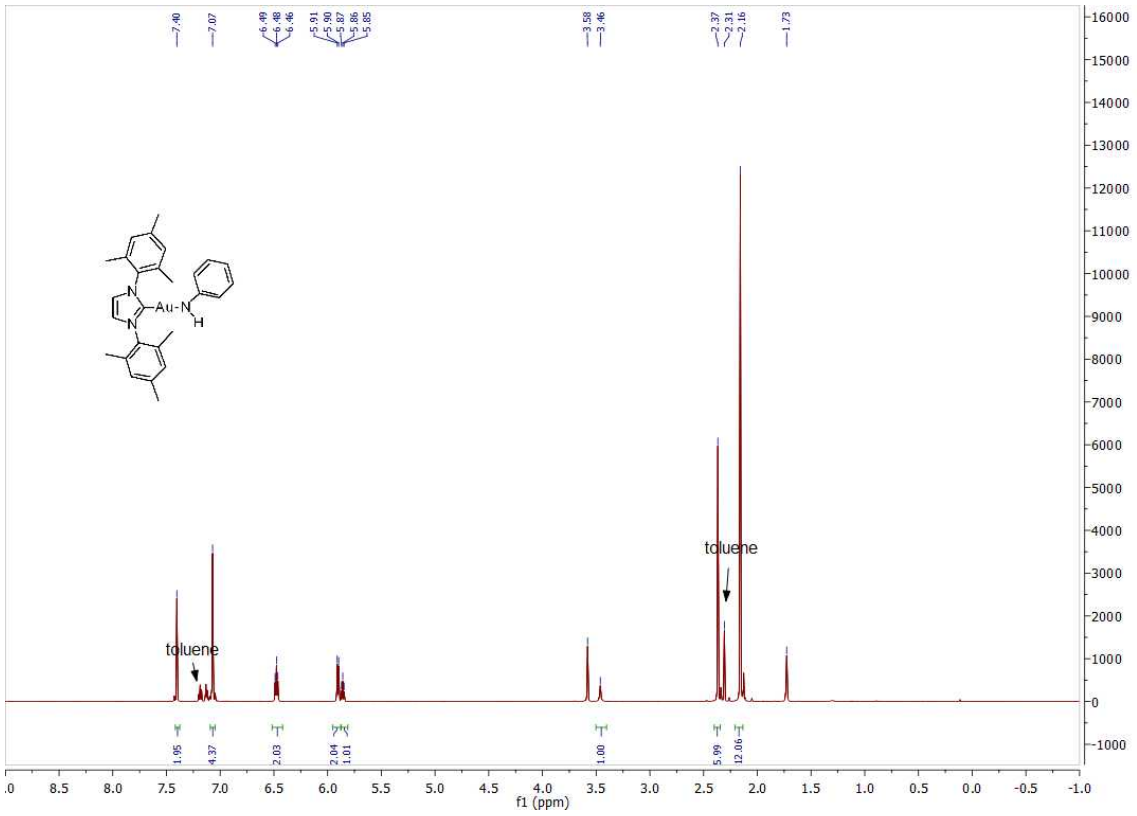
7.40
7.07
6.49
6.48
6.46
5.91
5.90
5.87
5.86
5.85
3.58
3.46
2.37
2.31
2.16
1.73
toluene
toluene
1.95
4.37
2.03
2.04
1.01
1.00
5.99
12.06
f1 (ppm)

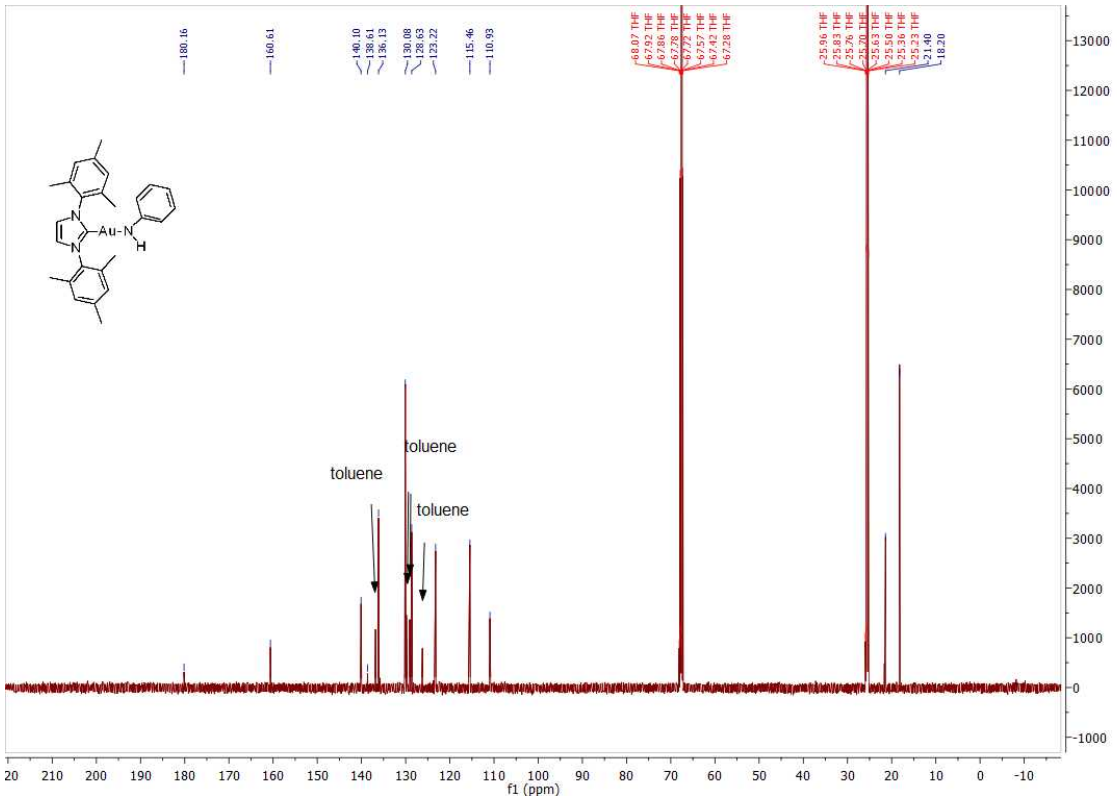
180.16
160.61
140.10
138.61
136.13
130.08
128.63
123.22
115.46
110.93
68.07 THF
67.92 THF
67.86 THF
67.78 THF
67.72 THF
67.57 THF
67.43 THF
67.28 THF
25.96 THF
25.83 THF
25.76 THF
25.70 THF
25.63 THF
25.50 THF
25.36 THF
25.23 THF
21.40
18.20
toluene
toluene
toluene
f1 (ppm)

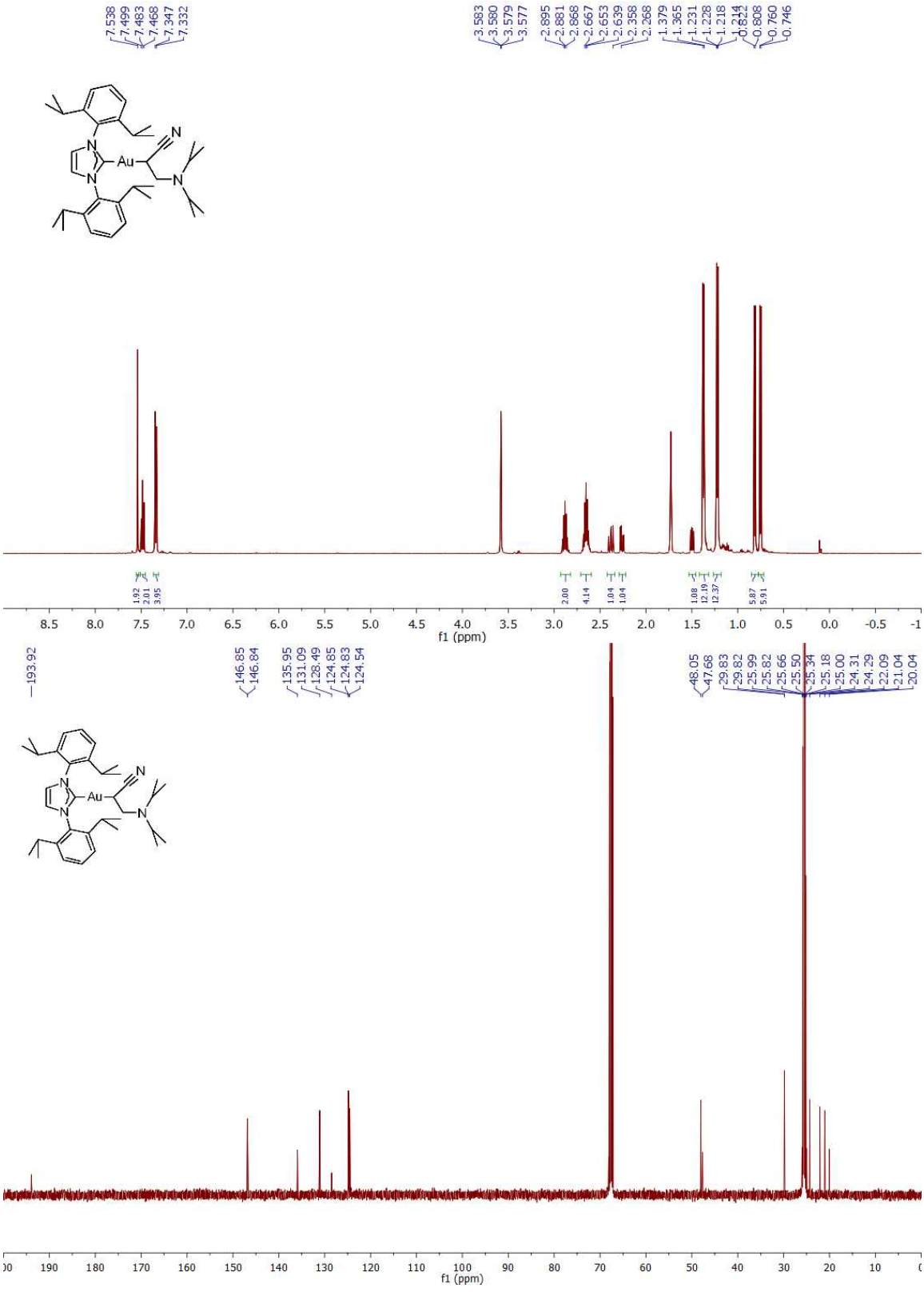
7.538
7.499
7.483
7.468
7.347
7.332
3.583
3.580
3.579
3.577
2.895
2.881
2.868
2.667
2.653
2.639
2.358
2.268
1.379
1.365
1.231
1.228
1.218
1.214
0.822
0.808
0.760
0.746
Au
N
f1 (ppm)
193.92
146.85
146.84
135.95
131.09
128.49
124.85
124.83
124.54
48.05
47.68
29.83
29.82
25.99
25.82
25.66
25.50
25.34
25.18
25.00
24.31
24.29
22.09
21.04
20.04
f1 (ppm)

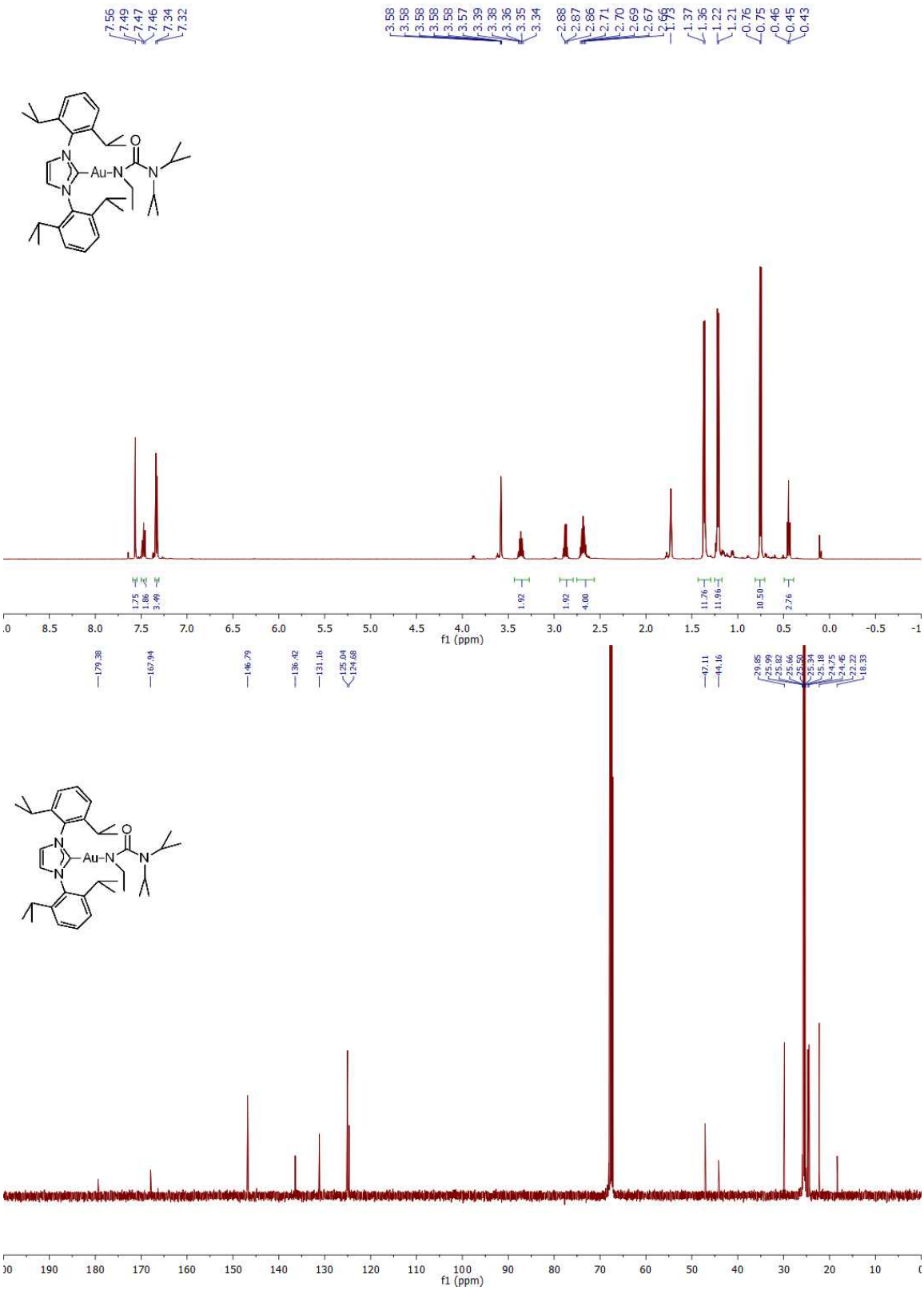
7.56
7.49
7.47
7.46
7.34
7.32
3.58
3.58
3.58
3.58
3.58
3.57
3.39
3.38
3.36
3.35
3.34
2.88
2.87
2.86
2.71
2.70
2.69
2.67
1.93
1.37
1.36
1.22
1.21
0.76
0.75
0.46
0.45
0.43
Au-N
O
N
1.75
1.86
3.49
1.92
1.92
4.00
11.76
11.96
10.50
2.76
f1 (ppm)
179.38
167.94
146.79
136.42
131.16
125.04
124.68
47.11
44.16
29.85
25.99
25.82
25.66
25.50
25.34
25.18
24.75
24.46
22.22
18.33
f1 (ppm)

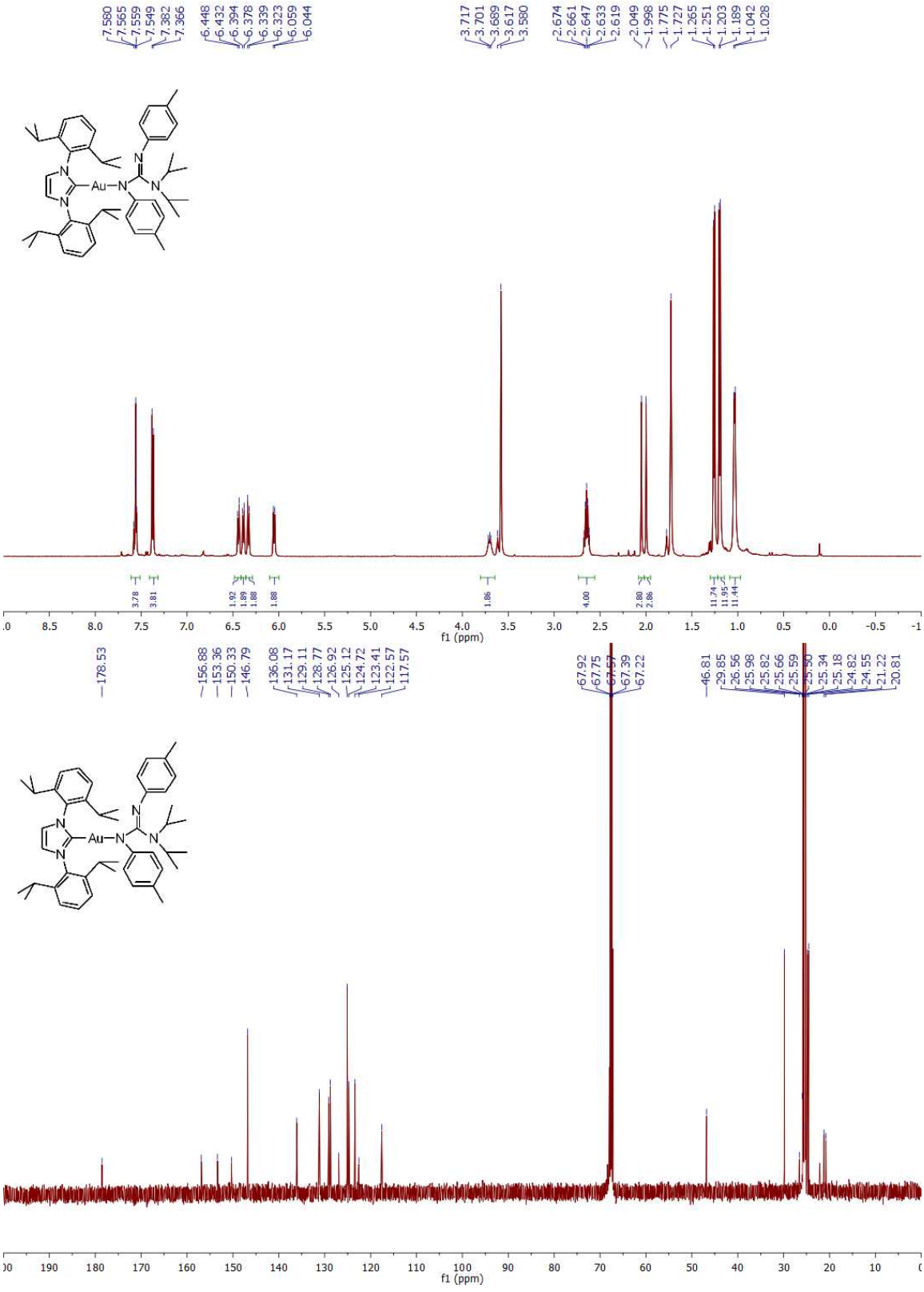
7.580
7.565
7.559
7.549
7.382
7.366
6.448
6.432
6.394
6.378
6.339
6.323
6.059
6.044
3.717
3.701
3.689
3.617
3.580
2.674
2.661
2.647
2.633
2.619
2.049
1.998
1.775
1.727
1.265
1.251
1.203
1.189
1.042
1.028
Au
N
3.78
3.81
1.92
1.89
1.88
1.88
1.86
4.00
2.80
2.86
11.74
11.95
11.44
f1 (ppm)
178.53
156.88
153.36
150.33
146.79
136.08
131.17
129.11
128.77
126.92
125.12
124.72
123.41
122.57
117.57
67.92
67.75
67.57
67.39
67.22
46.81
29.85
26.56
25.98
25.82
25.66
25.59
25.50
25.34
25.18
24.82
24.55
21.22
20.81
f1 (ppm)

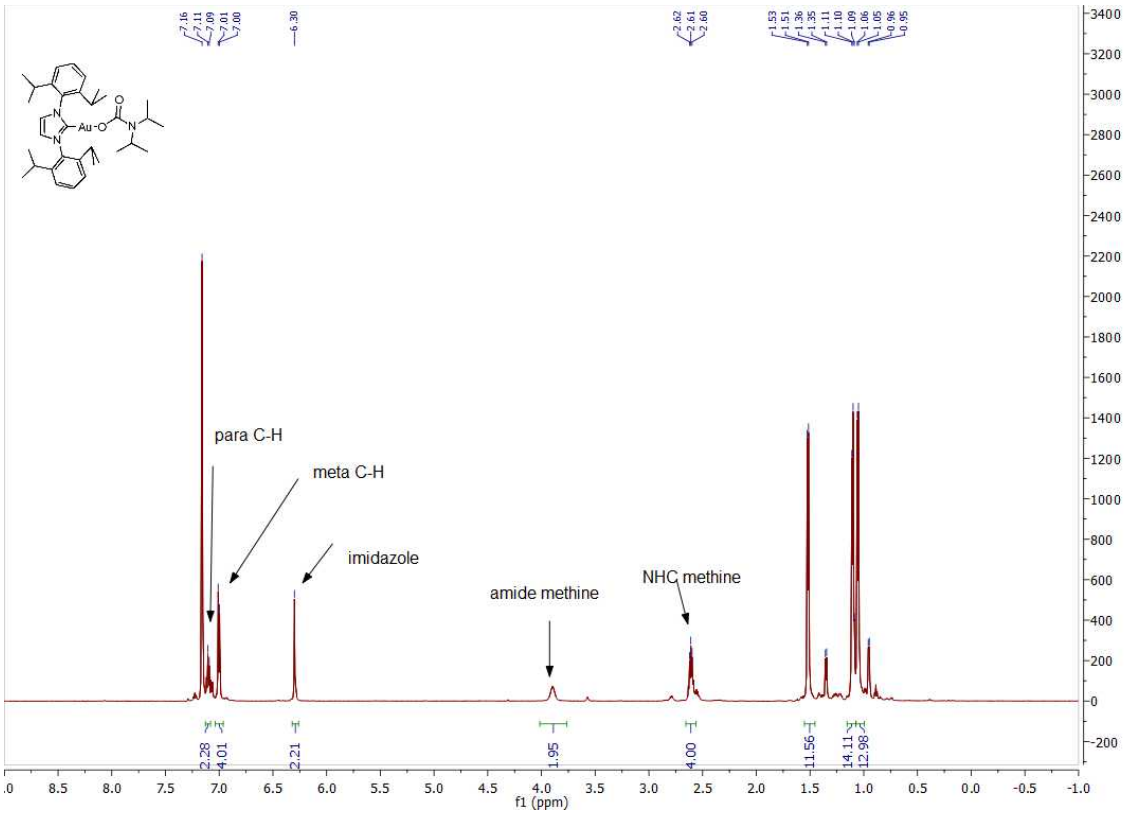
para C-H
meta C-H
imidazole
amide methine
NHC methine
f1 (ppm)

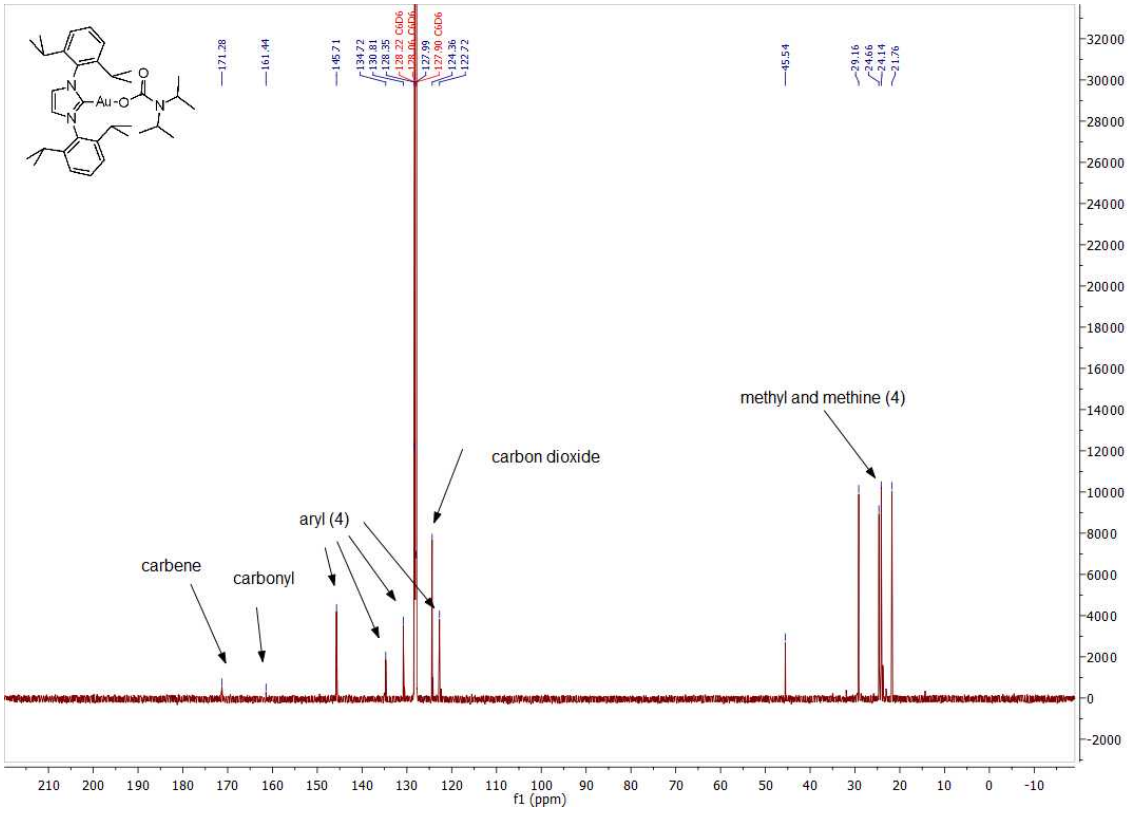
carbene
carbonyl
aryl (4)
carbon dioxide
methyl and methine (4)
f1 (ppm)

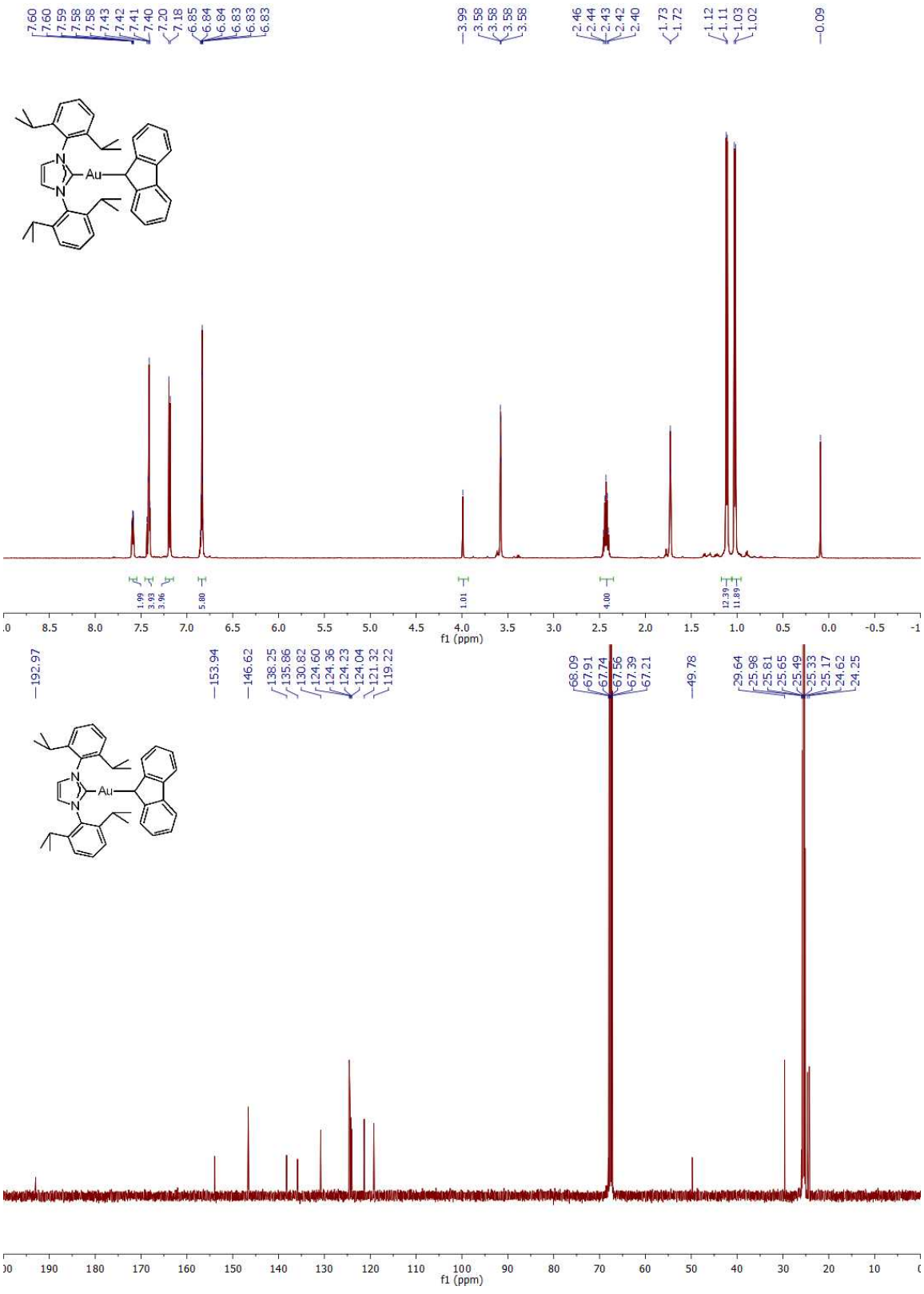
7.60
7.60
7.59
7.58
7.58
7.58
7.43
7.42
7.41
7.40
7.20
7.18
6.85
6.84
6.84
6.83
6.83
6.83
3.99
3.58
3.58
3.58
3.58
2.46
2.44
2.43
2.42
2.40
1.73
1.72
1.12
1.11
1.03
1.02
0.09
Au
1.99
3.03
3.06
5.80
1.01
4.00
12.39
11.89
f1 (ppm)
192.97
153.94
146.62
138.25
135.86
130.82
124.60
124.36
124.23
124.04
121.32
119.22
68.09
67.91
67.74
67.56
67.39
67.21
49.78
29.64
25.98
25.81
25.65
25.49
25.33
25.17
24.62
24.25
Au
f1 (ppm)

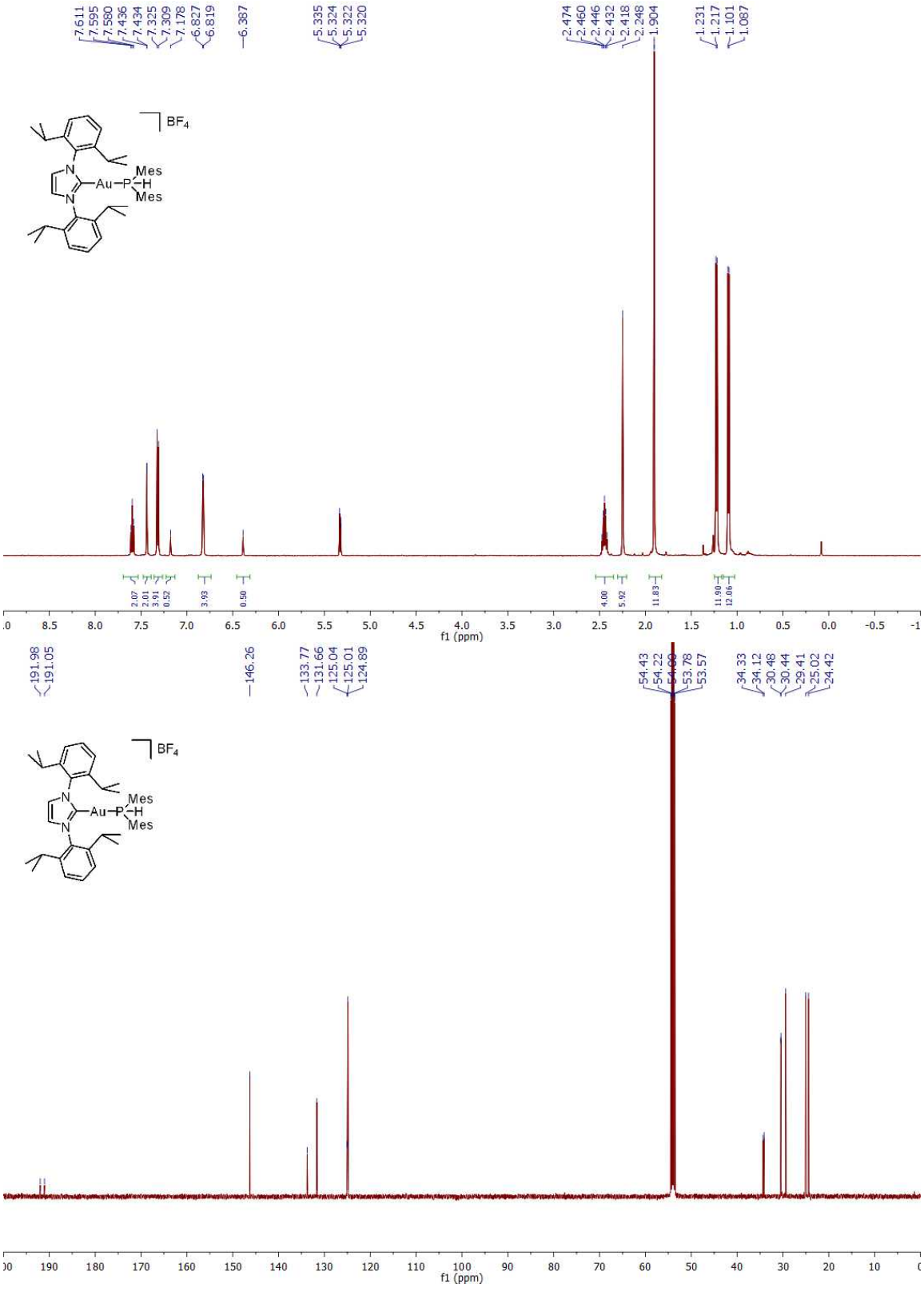
7.611
7.595
7.580
7.436
7.434
7.325
7.309
7.178
6.827
6.819
6.387
5.335
5.324
5.322
5.320
2.474
2.460
2.446
2.432
2.418
2.248
1.904
1.231
1.217
1.101
1.087
BF4
Au
P
H
Mes
Mes
2.07
2.01
3.91
0.52
3.93
0.50
4.00
5.92
11.83
11.90
12.06
f1 (ppm)
191.98
191.05
146.26
133.77
131.66
125.04
125.01
124.89
54.43
54.22
54.00
53.78
53.57
34.33
34.12
30.48
30.44
29.41
25.02
24.42
BF4
Au
P
H
Mes
Mes
f1 (ppm)

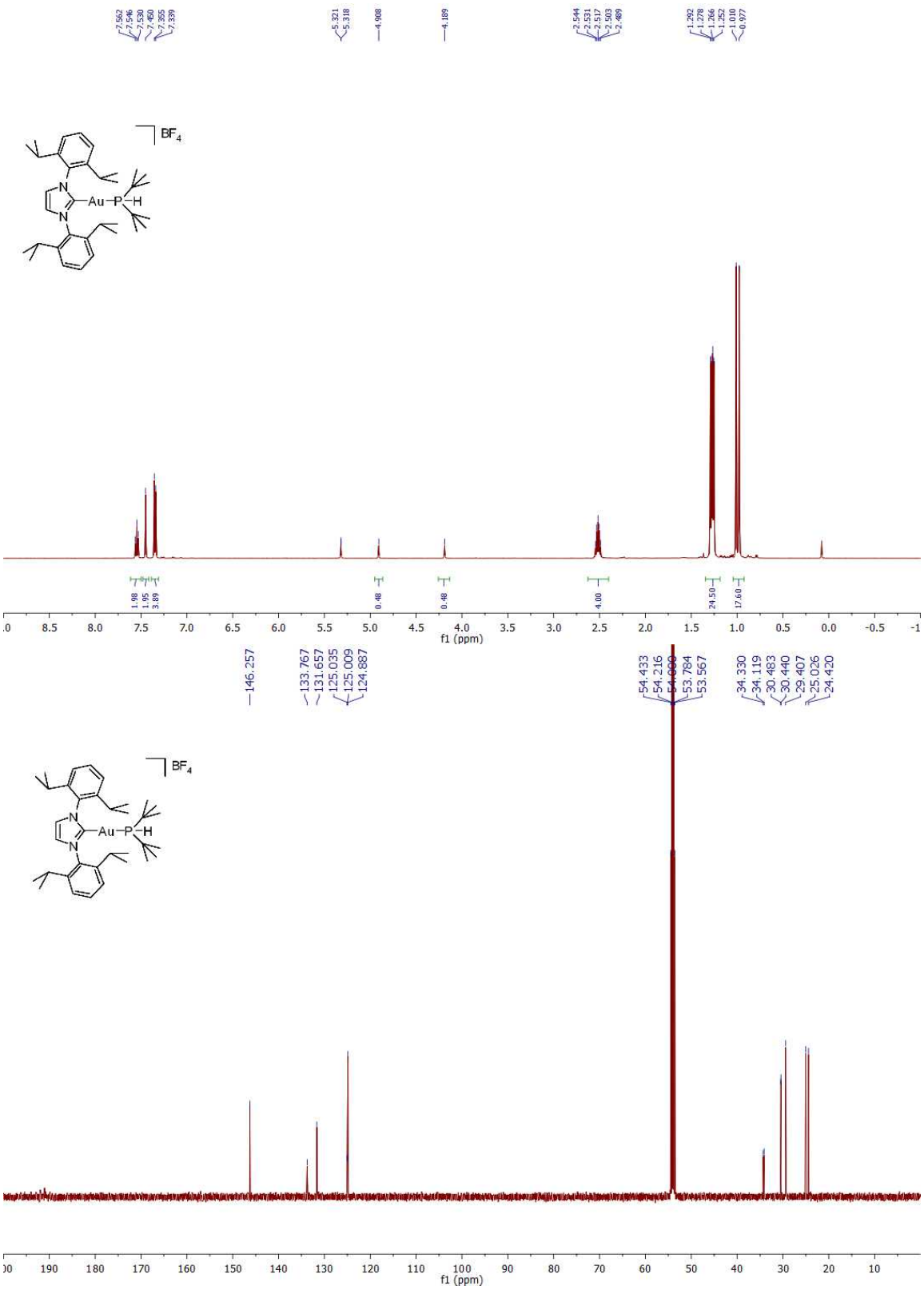
7.562
7.546
7.530
7.460
7.355
7.339
5.321
5.318
4.908
4.189
2.544
2.531
2.517
2.503
2.489
1.292
1.278
1.266
1.252
1.010
0.977
BF4
Au
P
H
1.98
1.95
3.89
0.48
0.48
4.00
24.50
17.60
f1 (ppm)
146.257
133.767
131.657
125.035
125.009
124.887
54.433
54.216
54.000
53.784
53.567
34.330
34.119
30.483
30.440
29.407
25.026
24.420
BF4
Au
P
H
f1 (ppm)

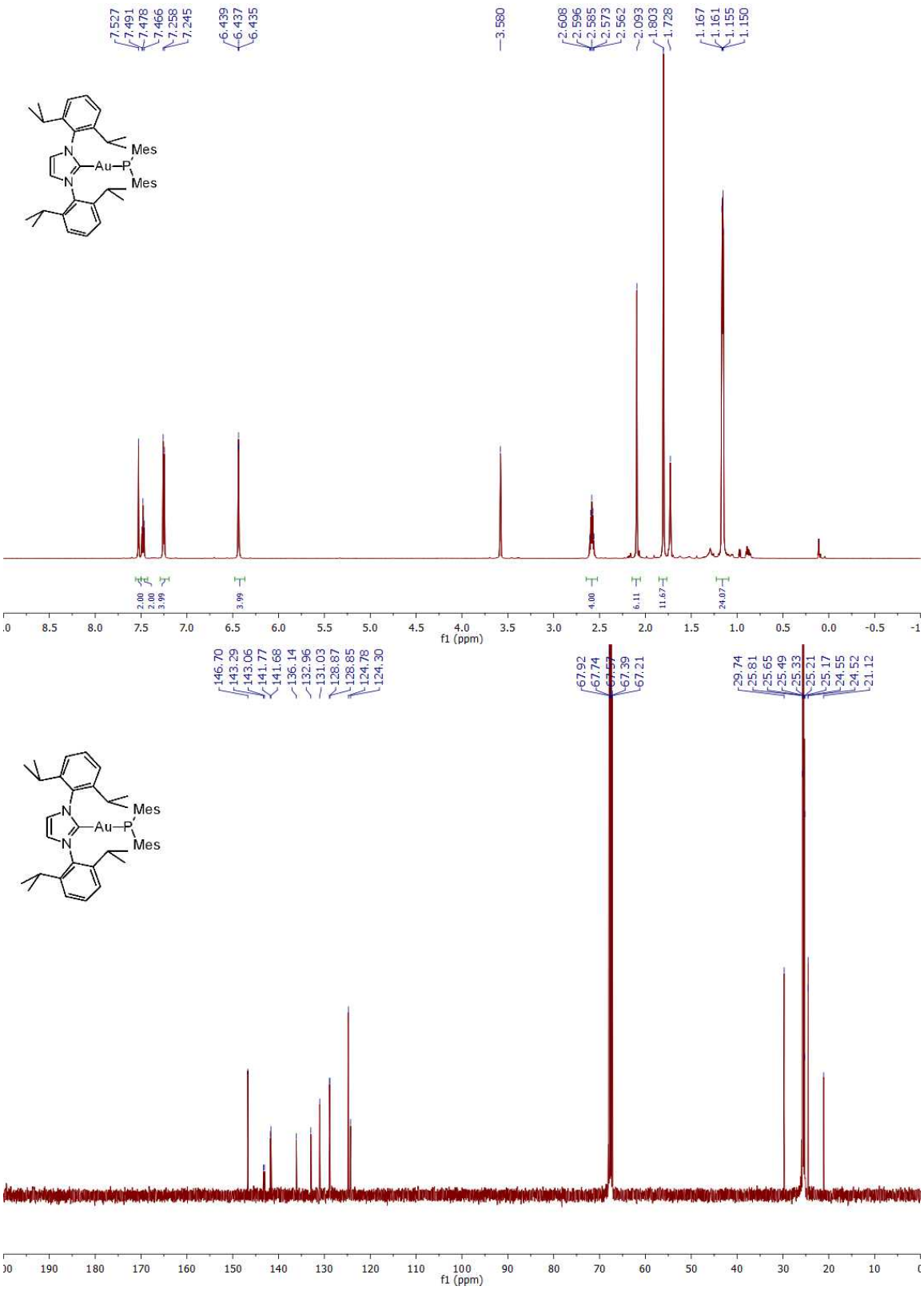
7.527
7.491
7.478
7.466
7.258
7.245
6.439
6.437
6.435
3.580
2.608
2.596
2.585
2.573
2.562
2.093
1.803
1.728
1.167
1.161
1.155
1.150
Mes
Au
P
Mes
2.00
2.00
3.99
3.99
4.00
6.11
11.67
24.07
f1 (ppm)
146.70
143.29
143.06
141.77
141.68
136.14
132.96
131.03
128.87
128.85
124.78
124.30
67.92
67.74
67.57
67.39
67.21
29.74
25.81
25.65
25.49
25.33
25.21
25.17
24.55
24.52
21.12
Mes
Au
P
Mes
f1 (ppm)

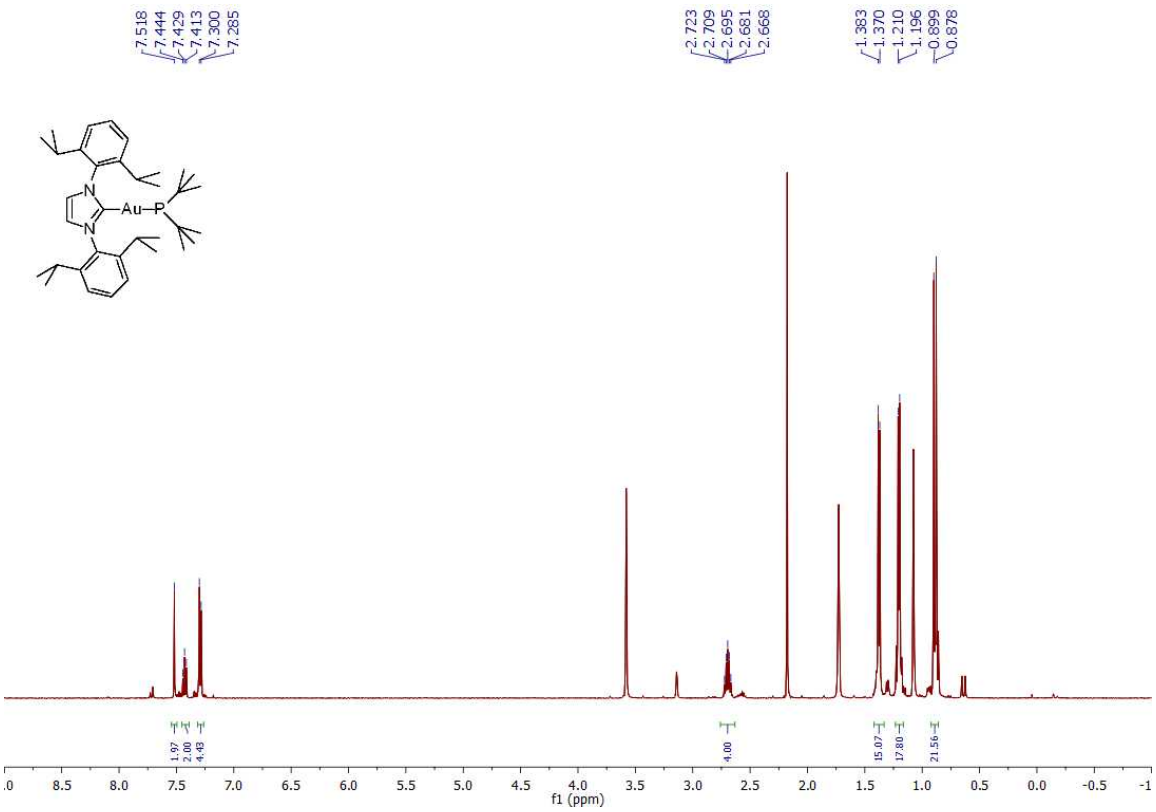
7.518
7.444
7.429
7.413
7.300
7.285
2.723
2.709
2.695
2.681
2.668
1.383
1.370
1.210
1.196
0.899
0.878
Au
P
N
N
1.97
2.00
4.48
4.00
15.07
17.80
21.56
f1 (ppm)

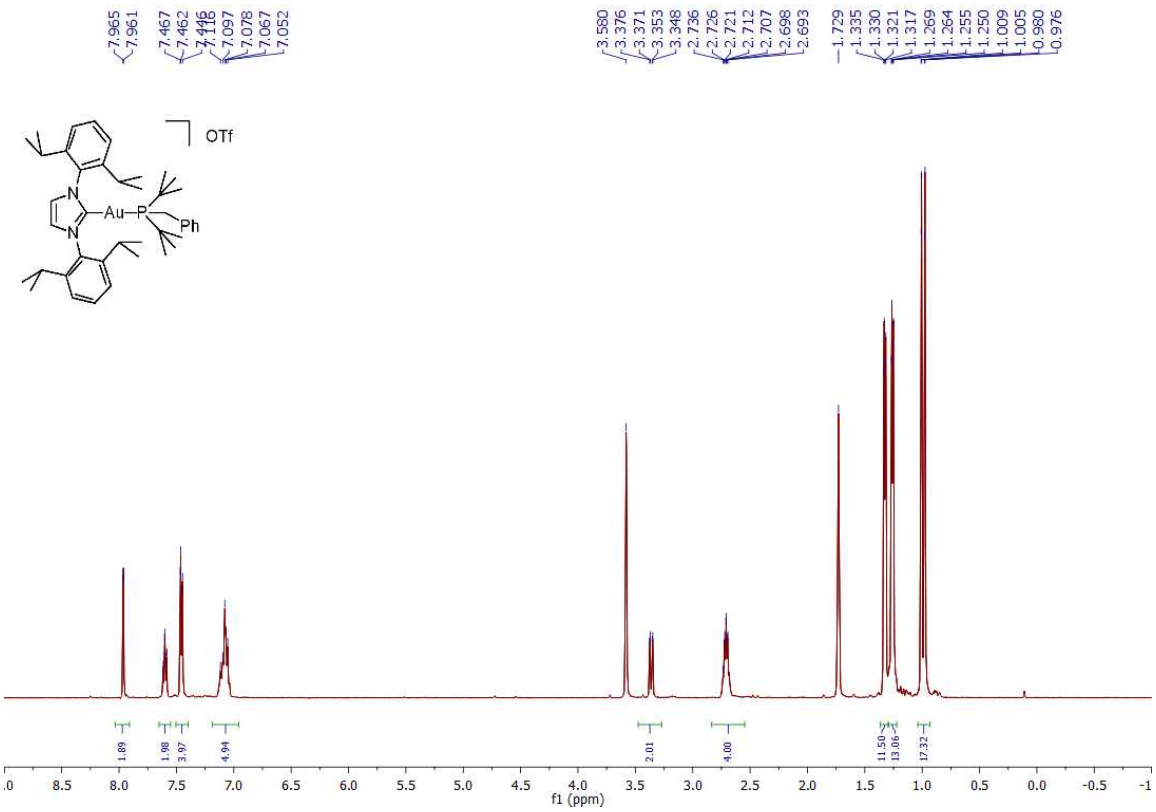
7.965
7.961
7.467
7.462
7.116
7.097
7.078
7.067
7.052
3.580
3.376
3.371
3.353
3.348
2.736
2.726
2.721
2.712
2.707
2.698
2.693
1.729
1.335
1.330
1.321
1.317
1.269
1.264
1.255
1.250
1.009
1.005
0.980
0.976
OTf
Au
P
Ph
1.89
1.98
3.97
4.94
2.01
4.00
11.50
13.06
17.32
f1 (ppm)

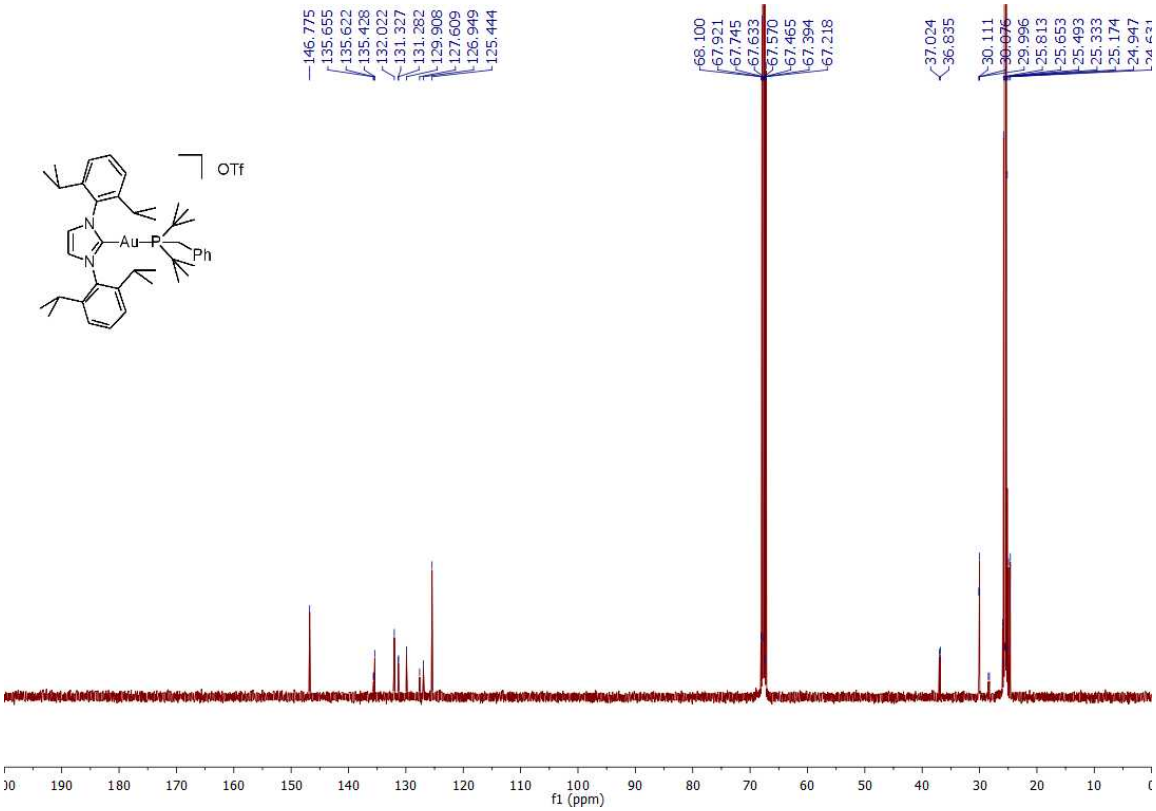
146.775
135.655
135.622
135.428
132.022
131.327
131.282
129.908
127.609
126.949
125.444
68.100
67.921
67.745
67.633
67.570
67.465
67.394
67.218
37.024
36.835
30.111
30.076
29.996
25.813
25.653
25.493
25.333
25.174
24.947
OTf
Au
P
Ph
f1 (ppm)

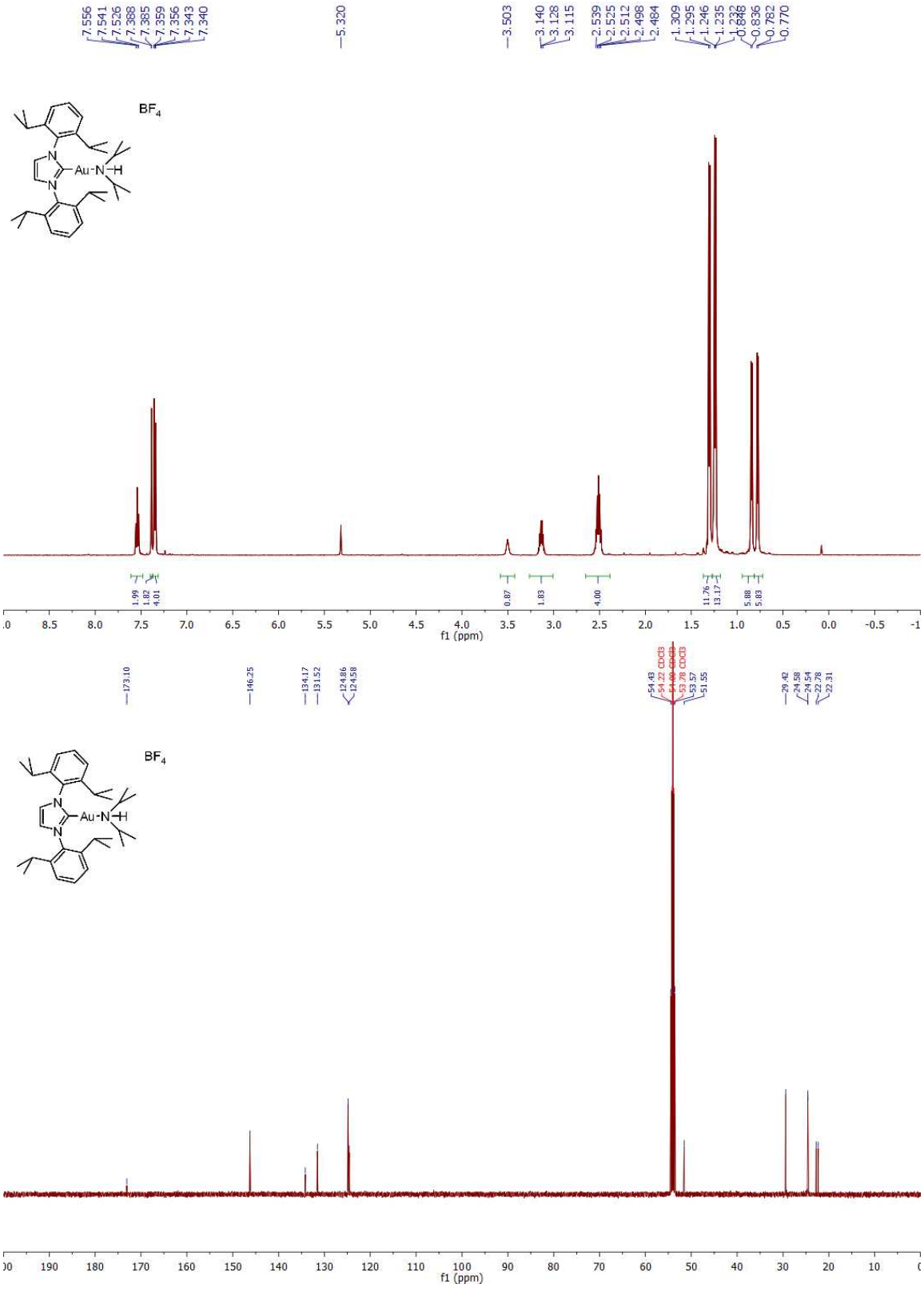
7.556
7.541
7.526
7.388
7.385
7.359
7.356
7.343
7.340
5.320
3.503
3.140
3.128
3.115
2.539
2.525
2.512
2.498
2.484
1.309
1.295
1.246
1.235
0.848
0.836
0.782
0.770
BF4
Au-N-H
1.99
1.82
4.01
0.87
1.83
4.00
11.76
13.17
5.88
5.83
f1 (ppm)
173.10
146.25
134.17
131.52
124.86
124.58
54.43
54.22 CDCl3
53.78 CDCl3
53.57
51.55
29.42
29.58
29.54
27.78
22.31
BF4
Au-N-H
f1 (ppm)

X-Ray Crystallographic Tables

Complex 1

Table 1. Crystal data and structure refinement for ipraunipr2.

Identification code	npm028	
Empirical formula	C33 H50 Au N3	
Formula weight	685.73	
Temperature	100(2) K	
Wavelength	0.71073 ≈	
Crystal system	Monoclinic	
Space group	P2(1)/c	
Unit cell dimensions	a = 12.5384(10) ≈	a= 90∞.
	b = 13.4689(11) ≈	b= 93.3730(10)∞.
	c = 19.1735(15) ≈	g = 90∞.
Volume	3232.4(4) $\approx^3$	
Z	4	
Density (calculated)	1.409 Mg/m^3	
Absorption coefficient	4.575 mm^{-1}	
F(000)	1392	
Crystal size	0.40 x 0.25 x 0.10 mm^3	
Theta range for data collection	1.63 to 27.10∞.	
Index ranges	-16<=h<=16, -17<=k<=17, -24<=l<=24	
Reflections collected	94771	
Independent reflections	7128 [R(int) = 0.0294]	
Completeness to theta = 27.10∞	99.9 %	
Absorption correction	Semi-empirical from equivalents	
Max. and min. transmission	0.6576 and 0.2619	
Refinement method	Full-matrix least-squares on F^2	
Data / restraints / parameters	7128 / 0 / 346	
Goodness-of-fit on F^2	1.176	
Final R indices [I>2sigma(I)]	R1 = 0.0297, wR2 = 0.0891	
R indices (all data)	R1 = 0.0329, wR2 = 0.0937	
Largest diff. peak and hole	3.194 and -1.824 $e.\approx^{-3}$	

Table 2. Atomic coordinates (x 10^4) and equivalent isotropic displacement parameters ($\approx^2$x 10^3)
for ipraunipr2. U(eq) is defined as one third of the trace of the orthogonalized U^{ij} tensor.

	x	y	z	U(eq)
Au(1)	7565(1)	5877(1)	2444(1)	20(1)
N(1)	6780(3)	5425(2)	969(2)	22(1)
N(2)	7940(3)	6587(2)	984(2)	23(1)
N(3)	7622(3)	5791(3)	3470(2)	27(1)
C(1)	7452(3)	5954(3)	1424(2)	23(1)
C(2)	7588(4)	6455(3)	291(2)	27(1)
C(3)	6857(4)	5727(3)	283(2)	26(1)
C(4)	6060(3)	4652(3)	1173(2)	23(1)
C(5)	6377(4)	3659(3)	1113(2)	28(1)
C(6)	5636(4)	2933(3)	1268(3)	34(1)
C(7)	4633(4)	3185(3)	1473(3)	33(1)
C(8)	4352(4)	4176(3)	1542(3)	29(1)
C(9)	5061(3)	4936(3)	1401(2)	26(1)
C(10)	7509(4)	3386(3)	934(3)	36(1)
C(11)	7571(5)	2415(4)	521(3)	43(1)
C(12)	8235(4)	3327(5)	1598(4)	54(2)
C(13)	4771(4)	6021(3)	1495(2)	28(1)
C(14)	4210(6)	6443(4)	842(3)	60(2)
C(15)	4120(6)	6205(5)	2123(3)	54(2)
C(16)	8760(3)	7287(3)	1217(2)	26(1)
C(17)	9809(4)	6943(3)	1327(3)	31(1)
C(18)	10585(4)	7641(4)	1533(3)	40(1)
C(19)	10324(4)	8631(4)	1620(3)	42(1)
C(20)	9277(4)	8940(4)	1507(3)	37(1)
C(21)	8469(3)	8284(3)	1301(2)	27(1)
C(22)	10116(4)	5862(3)	1228(3)	36(1)
C(23)	10877(5)	5771(4)	633(4)	61(2)
C(24)	10575(5)	5409(4)	1906(3)	51(1)
C(25)	7312(4)	8631(3)	1192(2)	28(1)
C(26)	7224(4)	9698(3)	931(3)	38(1)

C(27)	6749(4)	8534(4)	1875(3)	39(1)
C(28)	6994(3)	5062(3)	3836(2)	23(1)
C(29)	6638(4)	4204(3)	3372(3)	35(1)
C(30)	5993(4)	5533(4)	4144(3)	37(1)
C(31)	8242(4)	6465(3)	3949(2)	29(1)
C(32)	8520(4)	7423(4)	3580(3)	38(1)
C(33)	9256(4)	6003(4)	4288(4)	49(1)

Complex 2

Table 1. Crystal data and structure refinement for ipraun(h)ph.

Identification code	npm031	
Empirical formula	C37 H50 Au N3 O	
Formula weight	749.77	
Temperature	100(2) K	
Wavelength	0.71073 ≈	
Crystal system	Monoclinic	
Space group	P2(1)/n	
Unit cell dimensions	a = 12.5675(7) ≈	a= 90∞.
	b = 19.0611(10) ≈	b= 108.9710(10)∞.
	c = 14.9662(8) ≈	g = 90∞.
Volume	3390.4(3) $\approx^3$	
Z	4	
Density (calculated)	1.465 Mg/m^3	
Absorption coefficient	4.371 mm^{-1}	
F(000)	1512	
Crystal size	0.50 x 0.50 x 0.30 mm^3	
Theta range for data collection	1.79 to 27.48∞.	
Index ranges	-16<=h<=16, -24<=k<=24, -19<=l<=19	
Reflections collected	130079	
Independent reflections	7777 [R(int) = 0.0332]	
Completeness to theta = 27.48∞	100.0 %	
Absorption correction	Semi-empirical from equivalents	
Max. and min. transmission	0.3539 and 0.2186	
Refinement method	Full-matrix least-squares on F^2	
Data / restraints / parameters	7777 / 0 / 391	
Goodness-of-fit on F^2	1.109	
Final R indices [I>2sigma(I)]	R1 = 0.0161, wR2 = 0.0373	
R indices (all data)	R1 = 0.0184, wR2 = 0.0390	
Largest diff. peak and hole	1.088 and -1.012 e.$\approx^{-3}$	

Table 2. Atomic coordinates (x 10^4) and equivalent isotropic displacement parameters ($\approx^2$x 10^3)
for ipraun(h)ph. U(eq) is defined as one third of the trace of the orthogonalized U^{ij} tensor.

	x	y	z	U(eq)
Au(1)	-180(1)	1621(1)	8768(1)	12(1)
C(1)	729(2)	2151(1)	9896(1)	13(1)
C(2)	1155(2)	2735(1)	11291(1)	16(1)
C(3)	2064(2)	2771(1)	11003(1)	17(1)
C(4)	2540(2)	2344(1)	9595(1)	15(1)
C(5)	3084(2)	1701(1)	9602(1)	17(1)
C(6)	3828(2)	1665(1)	9087(2)	22(1)
C(7)	4013(2)	2241(1)	8588(2)	25(1)
C(8)	3447(2)	2864(1)	8587(1)	22(1)
C(9)	2691(2)	2933(1)	9090(1)	18(1)
C(10)	2894(2)	1076(1)	10163(1)	21(1)
C(11)	3670(3)	1112(1)	11183(2)	42(1)
C(12)	3032(2)	370(1)	9734(2)	36(1)
C(13)	2005(2)	3598(1)	9031(1)	21(1)
C(14)	2615(2)	4264(1)	8901(2)	31(1)
C(15)	884(2)	3529(1)	8227(2)	30(1)
C(16)	-751(2)	2165(1)	10642(1)	15(1)
C(17)	-843(2)	1564(1)	11155(1)	16(1)
C(18)	-1926(2)	1381(1)	11139(1)	20(1)
C(19)	-2854(2)	1772(1)	10636(1)	22(1)
C(20)	-2730(2)	2363(1)	10142(1)	21(1)
C(21)	-1670(2)	2578(1)	10136(1)	17(1)
C(22)	170(2)	1104(1)	11637(1)	18(1)
C(23)	191(2)	828(1)	12601(1)	24(1)
C(24)	202(2)	489(1)	10983(2)	27(1)
C(25)	-1547(2)	3233(1)	9601(1)	21(1)
C(26)	-1978(2)	3880(1)	9983(2)	30(1)
C(27)	-2143(2)	3146(1)	8536(2)	30(1)
C(28)	-2274(2)	895(1)	7553(1)	16(1)

C(29)	-2776(2)	1040(1)	8250(1)	19(1)
C(30)	-3888(2)	865(1)	8115(2)	23(1)
C(31)	-4546(2)	534(1)	7296(2)	27(1)
C(32)	-4059(2)	367(1)	6612(2)	25(1)
C(33)	-2948(2)	538(1)	6734(1)	21(1)
C(34)	187(2)	1909(1)	6268(2)	26(1)
C(35)	1364(2)	1722(1)	6933(2)	24(1)
C(36)	1389(2)	922(1)	6917(2)	33(1)
C(37)	452(2)	743(1)	6011(2)	31(1)
N(1)	1790(1)	2411(1)	10147(1)	14(1)
N(2)	351(1)	2349(1)	10608(1)	13(1)
N(3)	-1199(1)	1100(1)	7660(1)	17(1)
O(1)	-391(1)	1258(1)	5948(1)	26(1)

Complex 6

Table 1. Crystal data and structure refinement for iprau(acrylonitrile)n(ipr)2.

Identification code	npm038_twin5	
Empirical formula	C36 H53 Au N4	
Formula weight	738.79	
Temperature	100(2) K	
Wavelength	0.71073 ≈	
Crystal system	Monoclinic	
Space group	P2(1)/c	
Unit cell dimensions	a = 10.8111(8) ≈	a= 90∞.
	b = 20.7615(16) ≈	b= 103.247(3)∞.
	c = 16.2556(12) ≈	g = 90∞.
Volume	3551.6(5) $\approx^3$	
Z	4	
Density (calculated)	1.382 Mg/m^3	
Absorption coefficient	4.170 mm^{-1}	
F(000)	1504	
Crystal size	0.10 x 0.10 x 0.03 mm^3	
Theta range for data collection	1.94 to 27.61∞.	
Index ranges	-14<=h<=13, 0<=k<=26, 0<=l<=20	
Reflections collected	9829	
Independent reflections	9937 [R(int) = 0.0000]	
Completeness to theta = 27.61∞	93.8 %	
Absorption correction	Semi-empirical from equivalents	
Max. and min. transmission	0.8851 and 0.6805	
Refinement method	Full-matrix least-squares on F^2	
Data / restraints / parameters	9937 / 25 / 383	
Goodness-of-fit on F^2	1.142	
Final R indices [I>2sigma(I)]	R1 = 0.0692, wR2 = 0.1596	
R indices (all data)	R1 = 0.0981, wR2 = 0.1791	
Largest diff. peak and hole	5.469 and -2.708 e.$\approx^{-3}$	

Table 2. Atomic coordinates (x 10^4) and equivalent isotropic displacement parameters ($\approx^2$x 10^3)
for iprau(acrylonitrile)n(ipr)2. U(eq) is defined as one third of the trace of the orthogonalized U^{ij} tensor.

	x	y	z	U(eq)
	8665(1)	2141(1)	3924(1)	23(1)
C(1)	9486(9)	2610(5)	5000(6)	19(2)
C(2)	10275(9)	2806(5)	6385(6)	23(2)
C(3)	10111(10)	3380(5)	5985(6)	21(2)
C(4)	9242(9)	3754(4)	4527(5)	17(2)
C(5)	10137(10)	3994(5)	4093(6)	25(2)
C(6)	9768(10)	4520(5)	3564(6)	26(2)
C(7)	8569(12)	4781(6)	3462(7)	34(3)
C(8)	7708(11)	4525(6)	3891(7)	32(3)
C(9)	8012(10)	3997(5)	4424(6)	25(2)
C(10)	11427(11)	3664(6)	4167(6)	30(2)
C(11)	12483(11)	4158(7)	4241(8)	44(3)
C(12)	11347(13)	3240(7)	3405(8)	46(3)
C(13)	7045(11)	3706(6)	4854(7)	33(3)
C(14)	6483(14)	4197(7)	5343(9)	51(4)
C(15)	6014(12)	3347(6)	4211(9)	43(3)
C(16)	9883(9)	1646(5)	5912(6)	22(2)
C(17)	10888(10)	1283(5)	5778(6)	28(2)
C(18)	10832(12)	620(6)	5899(7)	36(3)
C(19)	9833(12)	341(6)	6165(7)	36(3)
C(20)	8843(11)	722(5)	6289(7)	30(2)
C(21)	8849(10)	1384(5)	6180(6)	23(2)
C(22)	12019(12)	1588(7)	5506(8)	41(3)
C(23)	13249(12)	1471(8)	6190(11)	63(4)
C(24)	12116(16)	1352(8)	4642(10)	66(5)
C(25)	7744(11)	1789(5)	6315(7)	30(2)
C(26)	7271(11)	1600(6)	7098(7)	31(3)
C(27)	6627(12)	1756(8)	5526(7)	49(4)
C(28)	7587(11)	1637(5)	2881(7)	33(3)

C(29)	8365(12)	1189(6)	2575(7)	34(3)
C(30)	6463(11)	1325(6)	3152(7)	37(3)
C(31)	4839(12)	523(6)	2578(7)	42(3)
C(32)	4619(15)	386(8)	3462(9)	58(4)
C(33)	5609(14)	-2(6)	2297(8)	47(3)
C(34)	4559(13)	1692(7)	2198(8)	43(3)
C(35)	3652(13)	1845(8)	2781(8)	52(4)
C(36)	3773(14)	1616(8)	1285(8)	55(4)
N(1)	9636(7)	3245(4)	5140(4)	16(2)
N(2)	9879(8)	2335(4)	5783(5)	21(2)
N(3)	9008(12)	814(5)	2345(6)	47(3)
N(4)	5414(9)	1142(5)	2467(6)	35(2)

Complex 11

Table 1. Crystal data and structure refinement for [ipraup(h)mes2][bf4].

Identification code	npm041	
Empirical formula	C36 H64 Au B Cl6 F4 N2 P	
Formula weight	1052.34	
Temperature	100(2) K	
Wavelength	0.71073 ≈	
Crystal system	Monoclinic	
Space group	P2/n	
Unit cell dimensions	a = 11.8034(6) ≈	a= 90∞.
	b = 8.9229(4) ≈	b= 92.9920(10)∞.
	c = 50.327(3) ≈	g = 90∞.
Volume	5293.3(4) $\approx^{3}$	
Z	4	
Density (calculated)	1.321 Mg/m^{3}	
Absorption coefficient	3.150 mm^{-1}	
F(000)	2124	
Crystal size	0.50 x 0.50 x 0.35 mm^{3}	
Theta range for data collection	1.62 to 25.37∞.	
Index ranges	-14<=h<=14, -10<=k<=10, -60<=l<=60	
Reflections collected	95868	
Independent reflections	10326 [R(int) = 0.0320]	
Completeness to theta = 25.37∞	99.8 %	
Absorption correction	Semi-empirical from equivalents	
Max. and min. transmission	0.332 and 0.226	
Refinement method	Full-matrix least-squares on F^{2}	
Data / restraints / parameters	10326 / 6 / 526	
Goodness-of-fit on F^{2}	1.204	
Final R indices [I>2sigma(I)]	R1 = 0.0790, wR2 = 0.1853	
R indices (all data)	R1 = 0.0822, wR2 = 0.1876	
Largest diff. peak and hole	3.680 and -4.165 $e.\approx^{-3}$	

Table 2. Atomic coordinates (x 10^4) and equivalent isotropic displacement parameters ($\approx^2$x 10^3)
for [ipraup(h)mes2][bf4]. U(eq) is defined as one third of the trace of the orthogonalized U^{ij} tensor.

	x	y	z	U(eq)
C(1)	3782(7)	3073(9)	3550(2)	14(2)
C(2)	2495(8)	1475(12)	3378(2)	27(2)
C(3)	3216(9)	1830(13)	3187(2)	30(2)
C(4)	4953(9)	3463(12)	3171(2)	25(2)
C(5)	4831(10)	4893(13)	3068(2)	31(2)
C(6)	5778(12)	5502(14)	2951(2)	42(3)
C(7)	6777(12)	4709(16)	2944(3)	47(3)
C(8)	6862(11)	3297(15)	3052(3)	45(3)
C(9)	5952(10)	2622(13)	3168(2)	34(3)
C(10)	3731(11)	5809(14)	3076(2)	40(3)
C(11)	3158(17)	5930(20)	2797(3)	75(5)
C(12)	3881(13)	7330(18)	3204(3)	60(4)
C(13)	6063(11)	1070(13)	3296(3)	40(3)
C(14)	6579(14)	-54(17)	3109(4)	72(5)
C(15)	6732(13)	1162(16)	3564(3)	58(4)
C(16)	2388(8)	2208(11)	3863(2)	21(2)
C(17)	1482(8)	3165(12)	3911(2)	25(2)
C(18)	1093(9)	3157(13)	4166(2)	30(2)
C(19)	1565(10)	2242(14)	4362(2)	34(3)
C(20)	2454(9)	1303(13)	4306(2)	29(2)
C(21)	2891(9)	1272(12)	4056(2)	25(2)
C(22)	980(9)	4191(12)	3695(2)	32(2)
C(23)	-312(10)	4008(17)	3655(3)	49(3)
C(24)	1321(13)	5841(16)	3753(4)	66(5)
C(25)	3856(9)	209(11)	3994(2)	24(2)
C(26)	3404(11)	-1392(14)	3958(3)	47(3)
C(27)	4827(10)	252(13)	4199(3)	37(3)
C(28)	5923(8)	4207(11)	4440(2)	21(2)
C(29)	6923(8)	3327(12)	4458(2)	25(2)

C(30)	7070(9)	2301(13)	4669(2)	29(2)
C(31)	6249(9)	2123(12)	4854(2)	28(2)
C(32)	5251(8)	2941(12)	4821(2)	24(2)
C(33)	5060(8)	3970(10)	4618(2)	20(2)
C(34)	7811(10)	3412(15)	4255(3)	45(3)
C(35)	6442(11)	1051(13)	5084(2)	35(3)
C(36)	3941(8)	4775(13)	4595(2)	29(2)
C(37)	6899(8)	6692(11)	4119(2)	22(2)
C(38)	7374(8)	6799(11)	3866(2)	22(2)
C(39)	8304(8)	7754(11)	3840(2)	26(2)
C(40)	8782(9)	8540(13)	4051(3)	35(3)
C(41)	8299(9)	8449(13)	4296(3)	36(3)
C(42)	7366(9)	7532(11)	4336(2)	27(2)
C(43)	6945(9)	5965(13)	3625(2)	29(2)
C(44)	9788(11)	9563(16)	4013(4)	58(4)
C(45)	6894(10)	7492(15)	4607(2)	39(3)
C(46)	10000(20)	8130(30)	2850(5)	89(7)
C(47)	10090(20)	3130(30)	2642(5)	91(7)
B(1)	2700(30)	290(30)	2516(8)	44(8)
B(2)	270(30)	9760(40)	4956(7)	49(8)
N(1)	4000(7)	2816(10)	3302(2)	23(2)
N(2)	2866(7)	2248(9)	3604(2)	21(2)
F(1)	2181(12)	-293(16)	2721(3)	40(3)
F(2)	2500	1805(15)	2500	60(3)
F(3)	3790(13)	86(18)	2621(3)	49(4)
F(4)	405(14)	9300(20)	5190(3)	59(4)
F(5)	-1000(20)	9220(30)	5000(5)	89(6)
F(6)	698(17)	8790(20)	4769(4)	72(5)
P(1)	5666(2)	5523(3)	4171(1)	19(1)
Au(1)	4698(1)	4325(1)	3830(1)	19(1)
Cl(1)	8670(6)	7827(9)	2679(1)	109(3)
Cl(2)	9923(6)	8539(8)	3187(1)	106(2)
Cl(3)	9024(7)	1725(11)	2612(2)	132(3)
Cl(4)	10208(7)	3864(10)	2945(2)	122(3)
Cl(5)	1303(8)	6980(11)	4473(2)	67(3)
Cl(6)	-477(9)	5259(12)	4675(2)	77(3)

C(48)	570(40)	6610(60)	4782(10)	94(14)

Complex 12

Table 1. Crystal data and structure refinement for [ipraup(h)tbu2]bf4.

Identification code	npm023	
Empirical formula	C37 H59 Au B Cl4 F4 N2 P	
Formula weight	988.41	
Temperature	100(2) K	
Wavelength	0.71073 ≈	
Crystal system	Triclinic	
Space group	P-1	
Unit cell dimensions	a = 11.9915(6) ≈	a= 96.5550(10)∞.
	b = 12.2396(6) ≈	b= 108.3860(10)∞.
	c = 16.7165(9) ≈	g = 105.0960(10)∞.
Volume	2195.71(19) ≈^{3}	
Z	2	
Density (calculated)	1.495 Mg/m^3	
Absorption coefficient	3.685 mm^{-1}	
F(000)	1116	
Crystal size	0.50 x 0.40 x 0.30 mm^3	
Theta range for data collection	1.31 to 27.28∞.	
Index ranges	-15<=h<=15, -15<=k<=15, -21<=l<=21	
Reflections collected	82038	
Independent reflections	9761 [R(int) = 0.0269]	
Completeness to theta = 27.28∞	98.8 %	
Absorption correction	Semi-empirical from equivalents	
Max. and min. transmission	0.331 and 0.186	
Refinement method	Full-matrix least-squares on F^2	
Data / restraints / parameters	9761 / 0 / 469	
Goodness-of-fit on F^2	1.197	
Final R indices [I>2sigma(I)]	R1 = 0.0725, wR2 = 0.1608	
R indices (all data)	R1 = 0.0778, wR2 = 0.1644	
Largest diff. peak and hole	16.029 and -6.444 e.≈$^{-3}$	

Table 2. Atomic coordinates (x 10^4) and equivalent isotropic displacement parameters ($\approx^2$x 10^3)
for [ipraup(h)tbu2]bf4. U(eq) is defined as one third of the trace of the orthogonalized U^{ij} tensor.

	x	y	z	U(eq)
Au(1)	-11(1)	6618(1)	7350(1)	25(1)
P(1)	-1437(2)	4850(2)	7137(2)	28(1)
B(1)	3925(9)	2938(9)	7575(7)	26(2)
C(1)	1226(6)	8176(6)	7454(5)	13(1)
C(2)	2915(7)	9732(6)	7849(5)	17(2)
C(3)	2009(7)	9942(7)	7220(5)	19(2)
C(4)	-242(7)	8788(7)	6352(5)	18(2)
C(5)	-479(7)	8296(6)	5496(5)	18(2)
C(6)	-1685(8)	8064(7)	4908(5)	23(2)
C(7)	-2585(8)	8302(8)	5179(6)	28(2)
C(8)	-2315(8)	8807(8)	6036(6)	26(2)
C(9)	-1117(7)	9065(7)	6646(5)	22(2)
C(10)	495(8)	7985(7)	5203(5)	23(2)
C(11)	528(9)	8369(9)	4371(6)	33(2)
C(12)	298(11)	6679(8)	5088(7)	37(2)
C(13)	-828(8)	9631(8)	7571(5)	25(2)
C(14)	-982(10)	10839(9)	7622(7)	37(2)
C(15)	-1614(9)	8867(9)	7983(6)	34(2)
C(16)	3042(7)	8066(6)	8602(5)	17(1)
C(17)	3502(7)	7222(7)	8329(5)	21(2)
C(18)	4050(8)	6655(7)	8946(6)	25(2)
C(19)	4145(8)	6946(8)	9789(6)	28(2)
C(20)	3700(8)	7811(8)	10049(6)	25(2)
C(21)	3130(7)	8390(7)	9461(5)	19(2)
C(22)	3420(8)	6902(7)	7400(5)	24(2)
C(23)	4710(9)	7030(9)	7366(7)	37(2)
C(24)	2554(9)	5667(8)	6967(6)	35(2)
C(25)	2586(7)	9296(7)	9738(5)	21(2)
C(26)	3519(9)	10206(9)	10532(6)	33(2)

C(27)	1399(9)	8712(9)	9891(7)	35(2)
C(28)	-2941(8)	4703(8)	6294(6)	27(2)
C(29)	-2599(10)	5194(11)	5568(7)	45(3)
C(30)	-3668(10)	5340(11)	6613(8)	46(3)
C(31)	-3704(11)	3404(10)	5921(9)	57(3)
C(32)	-1478(9)	4443(9)	8162(7)	35(2)
C(33)	-200(11)	4378(12)	8623(10)	61(4)
C(34)	-1714(13)	5412(12)	8708(8)	56(3)
C(35)	-2467(10)	3293(10)	8025(9)	50(3)
C(36)	2491(10)	2526(9)	9253(8)	40(2)
C(37)	4567(12)	10301(11)	6225(8)	52(3)
Cl(1)	1440(2)	1936(2)	9748(2)	43(1)
Cl(2)	3035(3)	4028(2)	9535(3)	57(1)
Cl(3)	5613(3)	10246(3)	7215(2)	54(1)
Cl(4)	4000(4)	8955(4)	5505(3)	72(1)
F(1)	2656(5)	2772(5)	7344(4)	36(1)
F(2)	4601(6)	4079(5)	7904(5)	46(2)
F(3)	4140(7)	2523(8)	6844(4)	62(2)
F(4)	4270(6)	2296(5)	8188(4)	48(2)
N(1)	972(6)	8967(5)	6988(4)	14(1)
N(2)	2416(6)	8640(6)	7976(4)	17(1)

Complex 13

Table 1. Crystal data and structure refinement for ipraupmes2.

Identification code	npm032	
Empirical formula	C45 H58 Au N2 P	
Formula weight	854.87	
Temperature	100(2) K	
Wavelength	0.71073 ≈	
Crystal system	Orthorhombic	
Space group	Pbca	
Unit cell dimensions	a = 14.8187(6) ≈	a= 90∞.
	b = 19.5498(8) ≈	b= 90∞.
	c = 28.0267(11) ≈	g = 90∞.
Volume	8119.4(6) ≈^{3}	
Z	8	
Density (calculated)	1.399 Mg/m^3	
Absorption coefficient	3.695 mm^{-1}	
F(000)	3456	
Crystal size	0.10 x 0.10 x 0.10 mm^3	
Theta range for data collection	1.87 to 33.14∞.	
Index ranges	-22<=h<=19, -28<=k<=28, -43<=l<=43	
Reflections collected	280900	
Independent reflections	15119 [R(int) = 0.0359]	
Completeness to theta = 33.14∞	97.7 %	
Absorption correction	Semi-empirical from equivalents	
Max. and min. transmission	0.7089 and 0.7089	
Refinement method	Full-matrix least-squares on F^2	
Data / restraints / parameters	15119 / 0 / 456	
Goodness-of-fit on F^2	1.147	
Final R indices [I>2sigma(I)]	R1 = 0.0402, wR2 = 0.0793	
R indices (all data)	R1 = 0.0704, wR2 = 0.0922	
Largest diff. peak and hole	5.832 and -2.610 e.≈$^{-3}$	

Table 2. Atomic coordinates (x 10^4) and equivalent isotropic displacement parameters ($\approx^2$x 10^3)
for ipraupmes2. U(eq) is defined as one third of the trace of the orthogonalized U^{ij} tensor.

	x	y	z	U(eq)
Au(1)	3040(1)	2382(1)	788(1)	16(1)
P(1)	1678(1)	2610(1)	1164(1)	21(1)
C(1)	4247(2)	2299(2)	441(1)	16(1)
C(2)	5353(2)	2142(2)	-111(1)	20(1)
C(3)	5755(2)	2340(2)	296(1)	20(1)
C(4)	5211(2)	2729(2)	1097(1)	22(1)
C(5)	5115(3)	3440(2)	1128(1)	27(1)
C(6)	5242(3)	3734(2)	1577(2)	35(1)
C(7)	5498(3)	3343(2)	1965(1)	33(1)
C(8)	5616(3)	2641(2)	1917(1)	26(1)
C(9)	5486(2)	2321(2)	1479(1)	20(1)
C(10)	4894(3)	3885(2)	703(2)	32(1)
C(11)	5670(5)	4379(3)	596(2)	70(2)
C(12)	4011(4)	4263(3)	763(2)	57(2)
C(13)	5614(2)	1554(2)	1416(1)	21(1)
C(14)	6302(3)	1244(2)	1762(1)	28(1)
C(15)	4706(3)	1188(2)	1463(1)	26(1)
C(16)	3771(2)	2018(2)	-398(1)	17(1)
C(17)	3372(2)	2597(2)	-603(1)	20(1)
C(18)	2789(2)	2482(2)	-985(1)	25(1)
C(19)	2612(3)	1833(2)	-1151(1)	26(1)
C(20)	3019(3)	1274(2)	-940(1)	24(1)
C(21)	3611(2)	1349(2)	-556(1)	19(1)
C(22)	3599(2)	3319(2)	-434(1)	22(1)
C(23)	4453(4)	3593(3)	-671(2)	44(1)
C(24)	2828(3)	3824(2)	-485(2)	49(1)
C(25)	4040(3)	731(2)	-315(1)	22(1)
C(26)	4132(3)	113(2)	-645(2)	29(1)
C(27)	3490(3)	534(2)	128(1)	32(1)

C(28)	2042(2)	3203(2)	1641(1)	21(1)
C(29)	1863(3)	3904(2)	1584(1)	26(1)
C(30)	2110(3)	4371(2)	1938(2)	31(1)
C(31)	2547(3)	4164(2)	2352(1)	31(1)
C(32)	2737(3)	3472(2)	2404(1)	28(1)
C(33)	2504(2)	2988(2)	2060(1)	24(1)
C(34)	1394(3)	4171(2)	1141(2)	37(1)
C(35)	2813(4)	4669(3)	2734(2)	48(1)
C(36)	2774(3)	2257(2)	2141(2)	32(1)
C(37)	1128(2)	1907(2)	1496(1)	25(1)
C(38)	1364(3)	1209(2)	1469(1)	26(1)
C(39)	885(3)	727(3)	1735(2)	36(1)
C(40)	156(3)	896(3)	2018(2)	44(1)
C(41)	-104(3)	1574(3)	2023(2)	43(1)
C(42)	348(3)	2085(3)	1767(1)	34(1)
C(43)	2106(3)	953(2)	1154(2)	35(1)
C(44)	-347(5)	360(3)	2300(2)	69(2)
C(45)	-30(3)	2798(3)	1771(2)	43(1)
N(1)	5075(2)	2423(2)	629(1)	16(1)
N(2)	4430(2)	2120(2)	-22(1)	16(1)

Chapter 2. Application of Fundamental Organometallic Chemistry to the Development of a Gold-Catalyzed Synthesis of Sulfinate Derivatives

Introduction

Sulfonyl compounds play a crucial role in drug development and sufonyl groups are a salient feature in many well-known pharmaceuticals. Since the discovery of the first sulfonamide-based antibiotic Prontosil in the 1930s,[1] sulfonyl compounds have been a key target in drug design and development. The search for expeditious, atom-economical, and practical syntheses of sulfones and sulfonamides continues to drive method development both in the academic and industrial arenas.

Stoichiometric synthesis of these compounds is well established and integral to organic synthesis.[2] The sulfonyl moiety play a crucial role in drug design and in the development of reagents for synthesis as well, *e.g.,* the Julia-Lythgoe olefination. However, the methods employed to make these compounds suffer from a host of drawbacks (Figure 1). Two common methods for accessing sulfinate salts are *via* alkylation of sulfur dioxide with organometallic reagents or oxidation of thiols to sulfinic acids followed by deprotonation (Figure 1, A). However, these routes require a toxic gas and pyrophoric reagents, or malodorous starting materials that are prone to over-oxidation, respectively. From these sulfinate salts, sulfones can be synthesized through alkylation though with the possibility of the sulfinate ester as a byproduct (Figure 1, B). Sulfonyl halides may also be formed and treated with nucleophiles, but adventitious water can result in undesired formation of sulfonic acids (Figure 1, C).

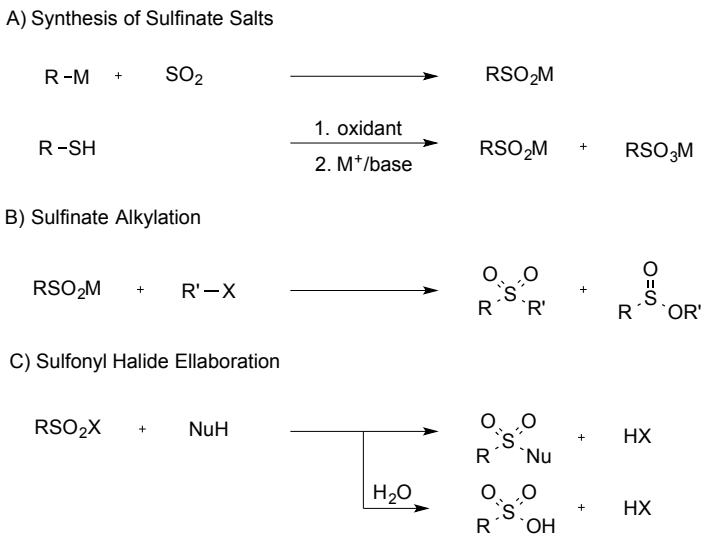

Figure 1. Stoichiometric synthesis of sulfinate salts and their derivatives.

One aspect of the development of new sulfonylation technologies is the creation and employment of SO_2 surrogates (Figure 2). Though the incorporation of a sulfonyl group into a compound is most direct, *i.e.* atom-economical, with SO_2, , this compound is a gas under ambient conditions and requires careful handling due to its toxicity. As an alternative, SO_2 may be released from one of its affordable and readily available surrogates, namely DABSO[3] and metabisulfite. The former, developed by the Willis group, is commercially available, easy to handle and has demonstrated its utility in a number of stoichiometric and catalytic reactions.[4,5] Metabisulfite is perhaps an even

more appealing source of SO_2 due to its low cost (0.3% the cost of DABSO) and proven efficacy in sulfonylation.[6] Use of one of these safe, bench-stable reagents is paramount in discovering new practical methods for sulfonyl installation.

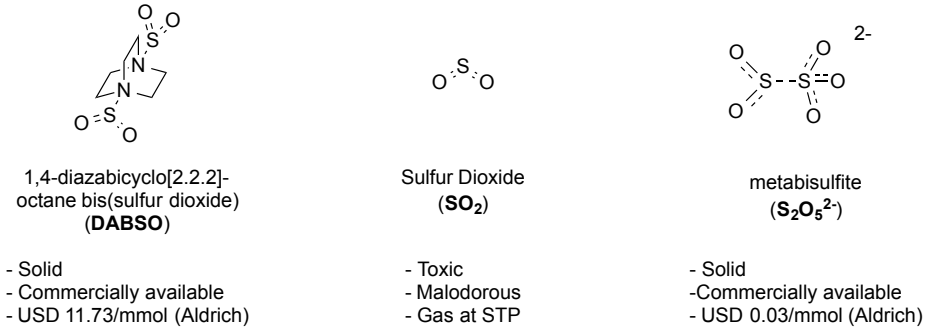

Figure 2. Sources of sulfur dioxide.

Another key aspect of sulfonylation chemistry is the transition from stoichiometric to catalytic methods. Immense gains have been made in this respect over the past decade (Figure 2), especially with palladium and copper. An initial dependence on hydrazines and morpholines [7,8] as coupling partners has been overcome, permitting the synthesis of both sulfones and sulfonamides. An ideal reaction would involve readily available coupling partners, such as boronic acids, [9] that react with a stable SO_2 source to form a synthetic intermediate capable of further elaboration. [10]

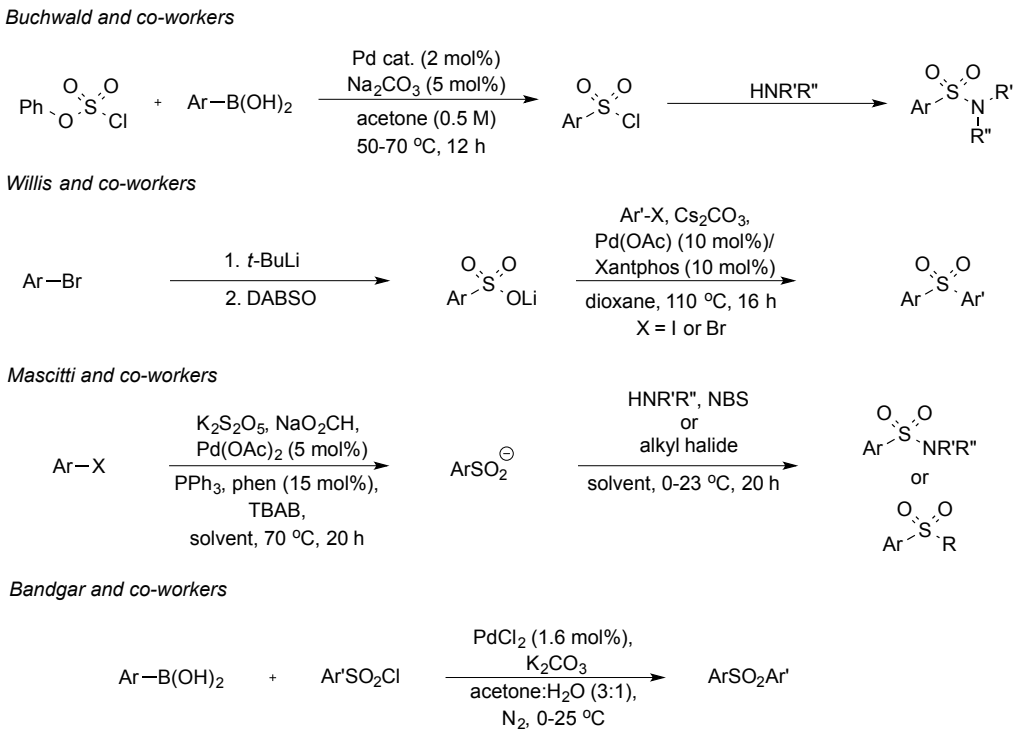

Figure 3. Transition metal-catalyzed sulfone and sulfonamide syntheses.

A metal that has not been employed in the synthesis of sulfinates and their derivatives is gold. Despite its ubiquity in the literature, gold catalysis has only produced a few examples of C—S bond formation.[11] This may be due in large part to the high affinity of sulfur for gold, making sulfur-based nucleophiles act as catalyst poisons. Indeed all sulfur nucleophiles used to date in gold-mediated reactions exist as thioethers, which bind reversibly to gold. Additionally, catalytic sufonylation presumably proceeds through a single-electron or a two-electron oxidative addition-reductive elimination cycle for copper and palladium, respectively. Gold, however, shows little propensity for single-electron processes due to the instability of mononuclear Au(II) catalysts, and cycling between the first and third oxidation states typically requires a potent oxidant such as Selectfluor,[12] which would oxidize sulfur(II) (oxidation 0.4 V) more readily than Au(I) (oxidation potential of 1.36 V). These considerations lead to two questions: Why would sulfonylation with gold be attractive and how could such a transformation be effected?

If gold were to be used as a catalyst for sulfonylation, it would not only be a conceptual advancement in this field but also a means to potentially circumvent shortcomings of other systems. Gold catalysis is appealing due to the bench-stability of the catalysts and the open-flask nature of the reactions. Gold's stability in the first oxidation state may also permit the use of the coupling partners that are subject to attack by other metals *via* oxidative addition, such as aryl halides.

To realize a catalytic sulfonylation with gold, knowledge of the metal's established reactivity is needed. Gold(I) complexes have been documented to undergo insertion of SO_2 into Au—C bonds to form gold sulfinates (Scheme 1, Step 1). This has been shown most clearly by the works of Puddephatt [13-15] and Vasapollo.[16] Schmidbaur also prepared sulfuryl complexes but from organosulfinate salts (Figure 4).[17] One could then imagine the displacement of the sulfinate ion to regenerate the Au—C bond. However, this bond is normally made using highly reactive organometallic reagents such as Grignard reagents[18] and alkyl/aryl zinc compounds.[19] These reactive compounds would react with SO_2 directly and require careful exclusion of moisture. A more appealing route would be through transmetallation between a gold-hydroxide[20] or -alkoxide[21,22] and boronic acids (Scheme 1, Steps 2 and 3). These Au—O bonds are readily formed *via* salt metathesis and boronic acids are plentiful due to the prominence of the Suzuki reaction. The literature precedent for these three elementary steps shows the potential for their inclusion in a catalytic cycle.

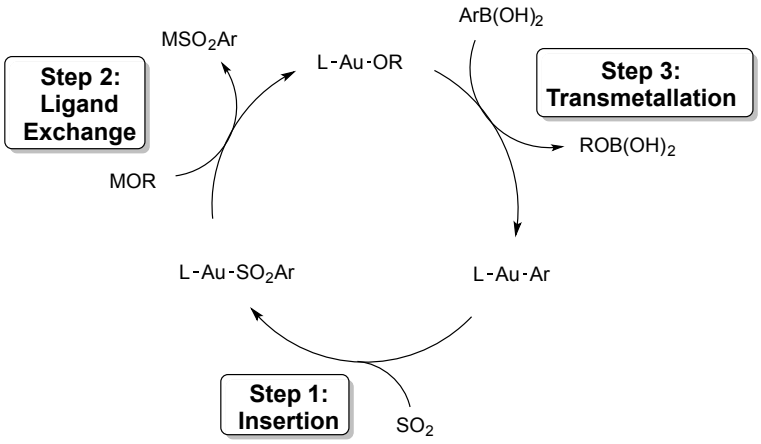

Scheme 1. Proposed catalytic cycle for the sulfination of boronic acids.

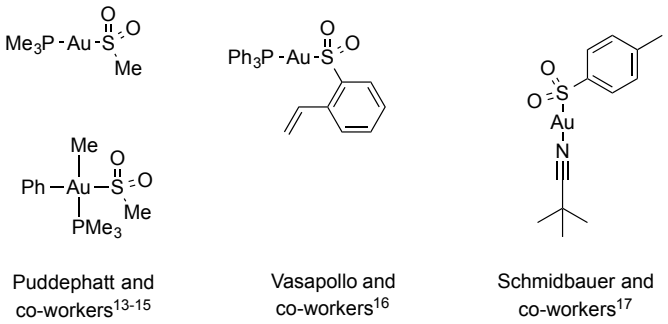

Figure 4. Reported gold organosulfinate complexes.

Herein is reported the development of a Au(I)-catalyzed sulfination method. A catalytic preparation of sulfinate salts is realized based on the fundamental reactivity of gold—heteroatom and –carbon bonds. Additionally, this method shows potential in the divergent synthesis of sulfonyl compounds from a common intermediate.

Results

The propensity of Au—C bonds to insert SO_2 was first evaluated (Figure 5). Given the potential instability of gold sulfinate complexes, a model system bearing IPr (1,3-bis(2,6-diisopropylphenyl)imidazole-2-ylidene) as the supporting ligand was chosen as it has been utilized in the stabilization of a number of reactive coordination complexes of gold(I).[21-23] Sulfur dioxide was found to cleanly insert into the Au—C bond of IPrAuPh and IPrAuBn to yield the corresponding sulfinates **1** and **2**. X-ray crystallographic analysis indicated that the sulfinate ligand was sulfur-bound rather than oxygen-bound (Figure 6), as anticipated based on the thermodynamic preference for this linkage isomer in other sulfuryl complexes.[24] Sulfur dioxide did not insert into the Au—C bond of the analogous ethyl and phenylacetylide complexes. This result tracks with the previously investigated reactivity of organometallic gold complexes with acid,[25] providing evidence that sulfur dioxide inserts by electrophilic attack at carbon (Figure 7). Additionally, treatment of IPrAuN(*i*-Pr)$_2$ led to decomposition, suggesting that accessing sulfonamides *via* gold amide intermediates would be challenging.

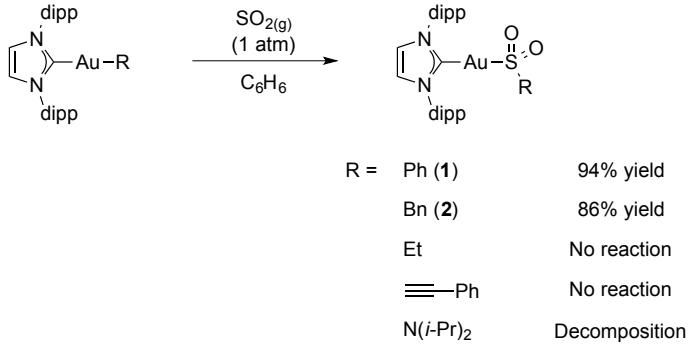

Figure 5. Scope of SO_2-insertion into IPrAuX complexes.

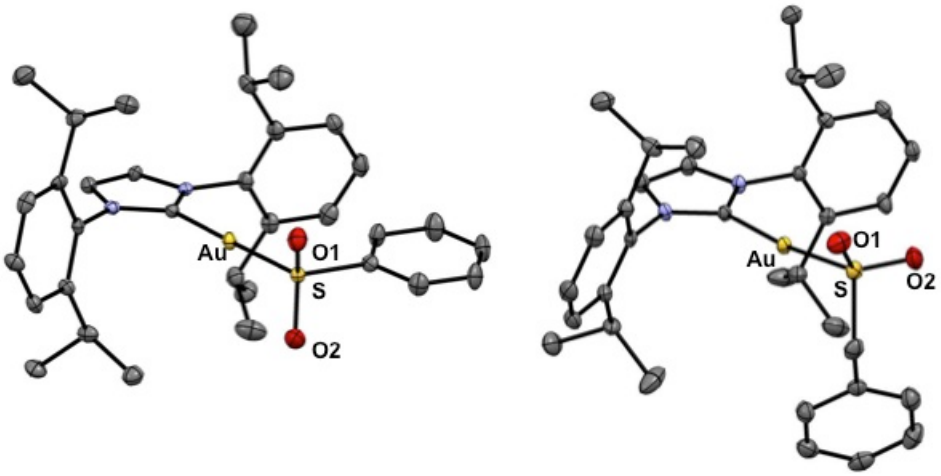

Figure 6. Solid-state structures of sulfinate complexes **1** and **2** (50% probability ellipsoids). Solvent molecules and hydrogens have been omitted for clarity.

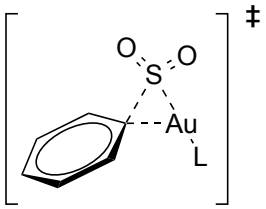

Figure 7. Proposed transition state for SO_2 insertion.

The elementary steps necessary to effect the desired sulfination were first evaluated stoichiometrically. IPrAuPh was prepared by treating IPrAuO*t*-Bu with phenyl boronic acid in benzene. This complex was then reacted with SO_2 to yield **1**. Finally, the sulfinate ligand was displaced by NaO*t*-Bu to regenerate the phenyl-substituted complex and precipitate sodium phenyl sulfinate. The viability of each of these elementary steps in a closed synthetic cycle suggested that a redox-neutral synthesis of sulfinate salts was indeed reasonable. Additionally, entry into the catalytic cycle from a gold halide

complex could be imagined based on transmetallation of this class of compounds with boronic acids in alcoholic solvent.[26]

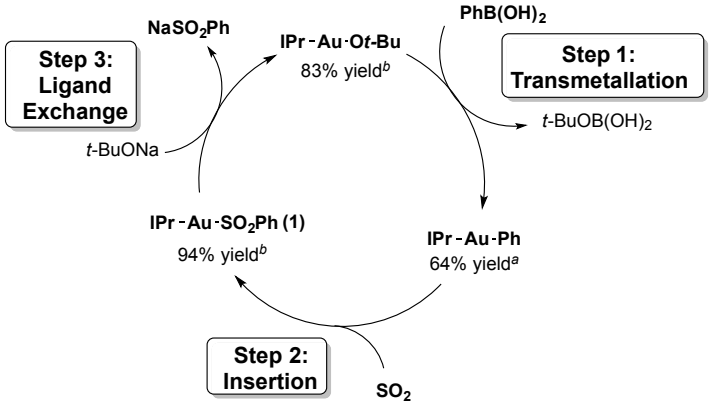

[a] Isolated yield. [b] Yields were determined by ^{1}H NMR with 1,3,5-trimethoxybenzene as an internal standard.

Scheme 2. Closed synthetic cycle for the gold-mediated synthesis of sulfinates

Reaction optimization was realized through trapping a *p*-tolyl sulfinate salt with benzyl bromide to form the sulfone **3**. Initial attempts to quantify the sulfinate salt directly were hampered by solubility and variability of the desired product resonances when compared against an authentic sample by ^{1}H NMR, presumably due to the presence of multiple counter ions and variable hydrogen bonding. Once $K_2S_2O_5$ was found to be a superior source of SO_2 in comparison to DABSO and $SO_{2(g)}$, and diisopropylethylamine was identified as a necessary base, catalyst and solvent were evaluated. Bulky, electron-rich catalysts were found to be most reactive (Figure 8). This may be attributed to increased electron density at the *ipso* carbon of the organometallic intermediate and steric protection against amine binding. With regard to solvent, the presence of methanol was found to play a major role (Figure 9). Biphasic mixtures with arene solvents provided the highest yields. Methanol likely improves solubility of the potassium metabisulfite and provides the alkoxide ligand necessary for transmetallation. The fact that low amounts of product are formed in the absence of alcohol could be attributed to the presence of ambient moisture or a second, and as of yet undetermined, mechanism being operative.

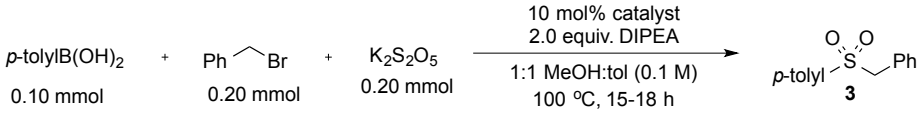

Entry	Catalyst	Yield[a]	Entry	Catalyst	Yield[a]
1	IPrAuCl	21%	5	*t*-Bu_3PAuCl	51%
2	Me_3PAuCl	18%	6	Cy-JohnPhosAuCl	34%
3	(*o*-tol)$_3$AuCl	28%	7	Mes_3PAuCl	6%
4	Cy_3PAuCl	32%			

[a]Yield determined versus 1,3,5-trimethoxybenzene as an internal standard.

Figure 8. Reaction optimization with regard to catalyst.

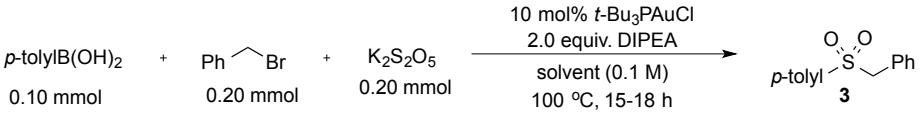

Entry	Solvent	Yield[a]	Entry	Solvent	Yield[a]
1	1:1 MeOH:$PhCF_3$	37%	8	1:1 MeOH:*p*-xylene	27%
2	1:1 MeOH:PhF	36%	9	1:1 MeOH:benzene	42%
3	1:1 MeOH:PhCl	32%	10	1:1 H_2O:tol	5%
4	1:1 MeOH:*o*-$C_6H_4F_2$	35%	11	1:1 THF:MeOH	20%
5	1:1 MeOH:*o*-xylene	43%	12	100% DMF	trace
6	1:1 MeOH:*m*-xylene	37%	13	1:1 DMF:MeOH	10%
7	1:1 MeOH:dioxane	trace	14	1:1 tol:MeOH	51%
			15	100% toluene	28%

[a]Yield determined versus 1,3,5-trimethoxybenzene as an internal standard.

Figure 9. Reaction optimization for solvent

The role of each reagent in the reaction mixture and the efficacy of other transition metal catalysts were evaluated (Table 1). In the absence of catalyst (entry 2), no reaction was observed. Copper and palladium catalysts known to effect similar transformations exhibited no more than stoichiometric reactivity (entries 3-7). Only trace product was observed in the absence of base (entry 9), and use of the less hindered amine base triethylamine (entry 8) caused a dramatic decline in yield. These two results may indicate that base is needed for formation of a gold alkoxide but an unhindered amine could potentially ligate to gold and shut down catalysis. Though ambient moisture does not affect the reaction, addition of excess water is deleterious (entry 10). Finally, gaseous sulfur dioxide as the reaction atmosphere results in less than a single turnover of the

catalyst, which may be due to the formation of an amine-SO_2 adduct (entry 11).[27,28] Alternatively, the intermediate gold alkoxide may react with SO_2 to form a sul*fon*ate complex. The likelihood of this potential pathway is supported by the reactivity of IPrAuO*t*-Bu with SO_2, which results in an unstable compound tentatively identified as IPrAuSO_3*t*-Bu (see Experimental for further details). It should be noted that all optimization and mechanistic experiments were conducted at 0.1 M for the sake of ease of handling of small volumes but that 0.2 M was optimal for the model substrate (*vide infra*).

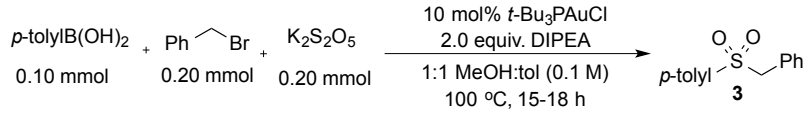

Entry	Variation from standard conditions	Yield[a]
1	none	51%
2	no catalyst	0%
3	10 mol% $Pd(OAc)_2$ as catalyst	trace
4	10 mol% $Pd(OAc)_2$/[HP*t*-Bu_3][BF_4] as catalyst	9%
5	10 mol% $Pd(PPh_3)_4$ as catalyst	trace
6	10 mol% Cu_2O as catalyst	10%
7	10 mol% CuCl as catalyst	3%
8	Et_3N in place of DIPEA	7%
9	no base	trace
10	Addition of of 10%-by-volume H_2O	4%
11	Under $SO_{2(g)}$ (1 atm) in place of air	9%

[a]Yield determined versus 1,3,5-trimethoxybenzene as an internal standard.

Table 1. Variation from standard reaction conditions.

The scope of sulfination was evaluated based on the steric environment, electronic properties, and presence of heteroatoms with regard to the boronic acid (Figure 10). The reaction yield diminished slightly as steric bulk was positioned closer to the boronic acid moiety (**3**, **5**, **6**) but was improved with increased electron-density relative to phenyl boronic acid (**7**, **11**). Boronic acids with electron-withdrawing groups and electron-deficient heterocycles showed no reactivity under catalytic conditions (**8**-**10**). 1-methyl-1H-indazole-5-boronic acid, an electron-rich heterocycle, afforded the desired sulfone **12** in comparable yield to other competent boronic acids.

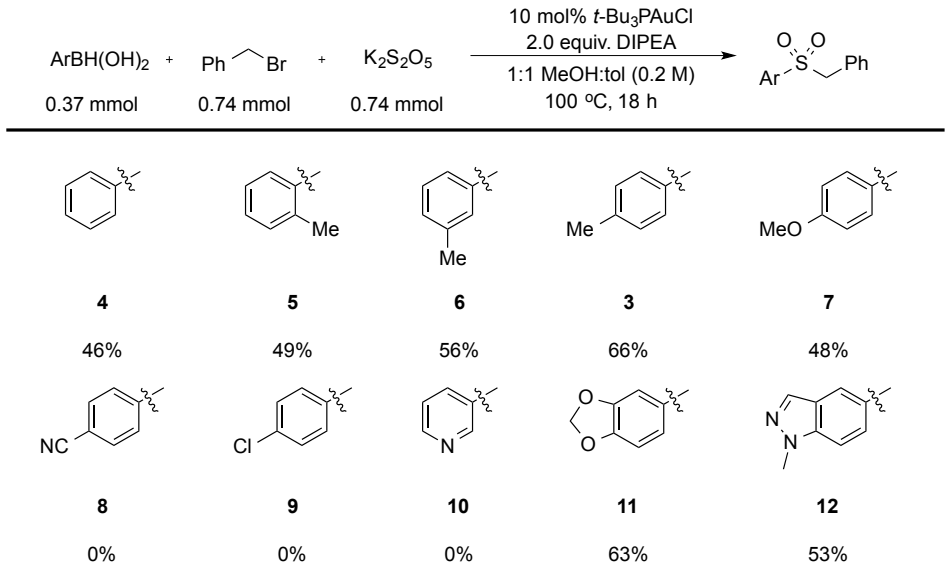

Figure 10. Scope of sulfinate synthesis in boronic acid

To access the validity of the proposed mechanism, hypothesized catalytic intermediates were synthesized and subjected to reaction conditions (Figure 11), as the heterogeneity of the reaction mixture precluded rigorous NMR kinetic studies. The *p*-tolyl (**13**) and *p*-tolyl sulfinate (**14**) complexes that were anticipated to form from *t*-Bu_3PAuCl were prepared. Each of these complexes proved to be a competent precatalyst under catalytic conditions, providing comparable yields of **3** as *t*-Bu_3PAuCl at 0.1 M. Based on the poor reactivity of electron-deficient boronic acids, it was hypothesized that SO_2-insertion was hampered by the nucleophilicity of the organometallic intermediate. Indeed, subjection of the 4-cyanophenyl complex **15** to standard reaction conditions with *p*-tolyl boronic acid as the coupling partner resulted in only 7% yield of the desired product. Additionally, reaction of **15** or IPrAu(4-CN-C_6H_4) (**16**) with $SO_{2(g)}$ resulted in no reaction, even at elevated temperatures (eq 1). Collectively, these data suggest that the proposed three-step mechanism is viable and that the electronic nature of the gold-aryl intermediate dictates the effectiveness of a given boronic acid as a coupling partner.

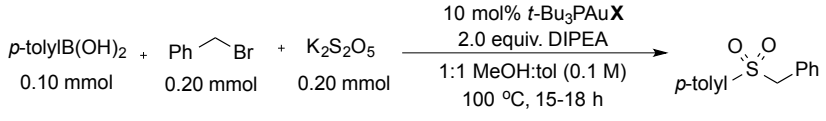

		Yield[a]
X =	*p*-tolyl (**13**)	46%
	(SO_2)*p*-tolyl (**14**)	47%
	p-CN-C_6H_4 (**15**)	7%

[a] Yield determined by NMR versus 1,3,5-trimethoxybenzene as an internal standard.

Figure 11. Subjection of proposed catalytic intermediates to reaction conditions.

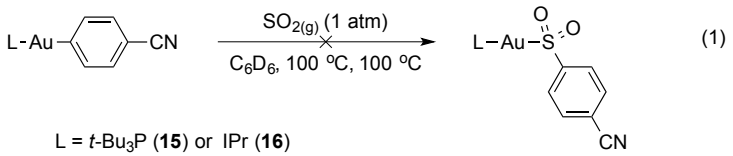

An appealing aspect of this methodology is the formation of a sulfinate salt as opposed to a more elaborate sulfonyl compound. A sulfinate salt can be reacted divergently to sulfones and sulfonamides. Treatment of commercially available sodium *p*-tolyl sulfinate under standard reaction conditions in the absence of catalyst is a testament to the reactivity of the sulfinate intermediate and shows that gold is not required beyond the sulfination step of a synthetic sequence (eq 2). Given the medicinal relevance of the indazole framework and its sulfonyl compounds,[29,30] a library of sulfones and sulfonamides was created based on a single indazolyl sulfinate intermediate (Scheme 3). This scope serves as a proof-of-concept for the potential utility of this method in a medicinal chemistry setting.

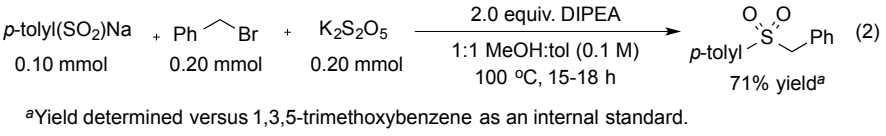

[a]Yield determined versus 1,3,5-trimethoxybenzene as an internal standard.

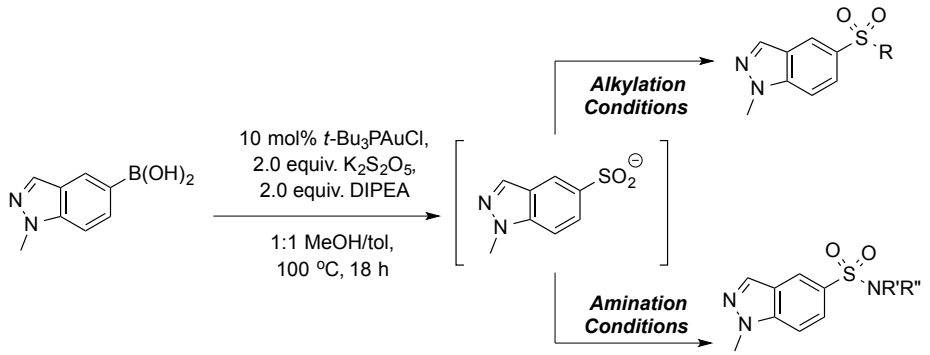

Alkylation conditions: *t*-Bu_3PAuCl (10 mol%), $K_2S_2O_5$ (2 equiv), DIPEA (2 equiv), 1:1 MeOH:tol (0.2 M), 100 °C, 18 h. then electrophile (2 equiv), 50 °C, 3 h.

Amination conditions: *t*-Bu_3PAuCl (10 mol%), $K_2S_2O_5$ (2 equiv), DIPEA (2 equiv), 1:1 MeOH:tol (0.2 M), 100 °C, 18 h. Solvent swap to THF, NCS (1 equiv), 23 °C, 1 h then amine (2 equiv.), 23 °C, 2 h.

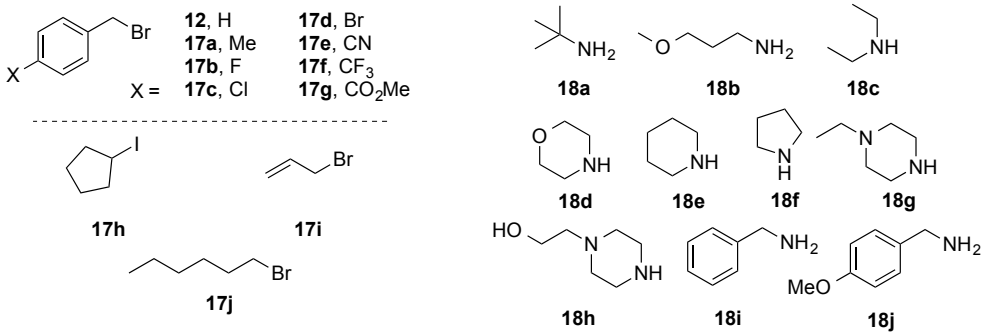

Scheme 3. Divergent synthesis of indazolyl sulfonyl compounds

Conclusion

In summary, a conceptually novel approach to the synthesis of sulfinate salts has been achieved by exploiting the reactivity of gold—heteroatom and —carbon bonds. This method stands in stark contrast to established procedures through the apparent redox neutrality of the transformation, the formation of a versatile sulfinate salt, and the robust nature of the reaction with regard to its highly stable starting materials. Further work is needed to improve the modest yields and narrow scope of this reaction, but the groundwork has been laid to explore a new avenue in gold catalysis.

Experimental

General Information

All stoichiometric reactions and the synthesis of gold(I) sulfinates were carried out in a nitrogen-filled drybox. All glassware was oven-dried overnight or flame-dried under vacuum. All NMR spectra were obtained at ambient temperature using Bruker AV-600, DRX-500, AV-500, AVB-400, AVQ-400, or AV-300 spectrometers. ^{1}H NMR chemical shifts (δ) are reported in parts per million (ppm) relative to residual solvent peaks (5.32 ppm for CD_2Cl_2, 7.26 ppm for $CDCl_3$, 7.16 ppm for C_6D_6, 2.50 DMSO-d_6). ^{13}C NMR chemical shifts were also reported relative to deuterated solvent peaks (54.00 ppm for CD_2Cl_2, 77.23 ppm for $CDCl_3$, 128.06 for C_6D_6, 39.51 ppm for DMSO-d_6). Flash chromatography was carried out on a Biotage SP purification system with Redisep Rf silica columns. Infrared (IR) spectra were recorded on a Nicolet Avatar FT-IR spectrometer. High-resolution mass spectral data for organometallic complexes were obtained from the Micromass/Analytical Facility operated by the College of Chemistry, University of California, Berkeley using a Thermo LTQ-FT (ESI) or Waters AutoSpec Premier (EI). All high-resolution mass spectral data for organic compounds were obtained at Pfizer Worldwide Medicinal Chemistry in Groton, CT on an Agilent 6220 TOF mass spectrometer. X-ray structural analyses was conducted at the University of California, Berkeley CHEXRAY facility (details in the X-ray section below). Combustion analysis data were obtained at the Micro-Mass Facility at the University of California, Berkeley.

Materials

Reagents were purchased from commercial suppliers, checked for purity and used without further purification unless otherwise noted. Pentane, hexane, diethyl ether, toluene, tetrahydrofuran, and methylene chloride were dried and purified by passage through a column of activated alumina (type A2, 12 x 32, UOP LLC), and sparged with N_2 prior to use. Methanol was purchased from Aldrich in a SureSeal bottle and used without further purification. Methylene chloride-d_2 and benzene-d_6 were distilled from CaH_2 and degassed prior to use. (Diisopropylethyl)amine (DIPEA) was distilled from CaH_2 prior to use. Benzyl bromide was passed through a short plug of activated neutral alumina prior to use. Sulfur dioxide was purchased from Praxair and stored in a toxic gas cabinet. IPrAuBn,[31] IPrAuPh,[19] IPrAuEt,[19] IPrAuC≡CPh,[32] and IPrAuO*t*-Bu[22] were synthesized according to literature procedures. IPrAuOH and *t*-Bu_3PAuCl were purchased from Strem Chemicals.

Synthesis of Gold(I) Complexes

(1,3-bis(2,6-diisopropylphenyl)imidazol-2-ylidene)gold(I) phenylsulfinate (1).

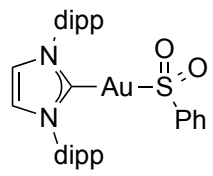

IPrAuPh (66.0 mg, 0.100 mmol) was dissolved in benzene (5 mL) and transferred to a Schlenk vessel in a nitrogen-filled glovebox. The vessel was subjected to two freeze-pump-thaw cycles and its contents placed under sulfur dioxide gas (1 atm). The reaction mixture was stirred for 16 h and concentrated *in vacuo*. The evacuated vessel was

returned to the glovebox and its contents transferred to a vial using ether. The solution was concentrated to yield the desired product as an analytically pure white solid (68.6 mg, 0.094 mmol, 94% yield). X-ray quality crystals were obtained by diffusion of pentane into a DCM solution at -25 °C. ^{1}H NMR (600 MHz, DCM-d_2): δ(ppm) 7.58 (t, J = 7.8 Hz, 2H, IPr *p*-H), 7.33 (d, J = 7.8 Hz, 4 H, IPr *m*-H), 7.30-7.26 (s + m, 3H, imidazole + Ph), 7.24-7.17 (m, 4H, Ph), 2.45 (sept., J = 6.0 Hz, 4H, C(*H*)Me$_2$), 1.23 (d, J = 6.9 Hz, 12H, C*H*$_3$), 1.21 (d, J = 6.9 Hz, 12H, C*H*$_3$). ^{13}C NMR (126 MHz, DCM-d_2): δ 180.3, 155.3, 146.2, 133.9, 131.5, 130.3, 128.9, 125.0, 124.9, 124.7, 29.4, 24.8, 24.3. IR (ATR): ν_{max}(cm^{-1}): 3151, 3065, 2960, 1471, 1457, 1198, 1096, 1050, 599. ESI-MS (*m*/*z*) calculated for [$C_{33}H_{41}O_2N_2AuS$+Na]$^+$: 749.2463, found: 749.2447. Anal. Calcd. for $C_{33}H_{41}AuN_2O_2S$: C, 54.54; H, 5.69; N, 3.85; S, 4.41. Found: C, 54.24; H, 5.74; N, 3.76; S, 4.30.

(1,3-bis(2,6-diisopropylphenyl)imidazol-2-ylidene)gold(I) benzylsulfinate (2).

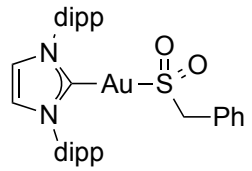

Complex **2** was synthesized analogously to complex **1** using IPrAuBn (34.2 mg, 0.051 mmol) and benzene (6 mL). The product was isolated as a white solid (32.8 mg, 0.044 mmol, 86% yield). X-ray quality crystals were grown by slow diffusion of pentane into a CD_2Cl_2 solution. ^{1}H NMR (600 MHz, DCM-d_2) δ 7.61 (t, J = 7.8 Hz, 2H, IPr *p*-H), 7.39 (d, J = 7.9, 4H, IPr *m*-H), 7.28 (s, 4H, imidazole), 7.16 – 7.11 (m, 2H, benzyl Ar), 7.08 (t, J = 7.5 Hz, 2H, benzyl Ar), 6.76 (d, J = 7.4 Hz, 2H, benzyl Ar), 3.51 (s, 2H, benzylic H), 2.49 (sept, J = 7.2 Hz, 4H, C(*H*)Me$_2$), 1.29 (d, J = 7.2 Hz, 12H, C*H*$_3$), 1.23 (d, J = 6.6 Hz, 12H). ^{13}C NMR (151 MHz, DCM-d_2) δ 180.6, 146.3, 134.0, 131.6, 131.5, 130.9, 128.7, 127.4, 125.0, 124.9, 72.4, 29.4, 24.9, 24.3. (ATR): ν_{max}(cm^{-1}): 2959, 2926, 1457, 1198, 1182, 1048, 809, 758, 521, 497. ESI-MS (*m*/*z*) calculated for [$C_{34}H_{43}O_2N_2AuS$+Na]$^+$: 763.2610, found 763.2603. Anal. Calcd. for $C_{34}H_{43}AuN_2O_2S$: C, 55.13; H, 5.85; N, 3.78; S, 4.33. Found: C, 54.82; H, 5.69; N, 3.67; S, 4.31.

(tri-*tert*-butylphosphine)gold(I) *p*-tolyl (13).

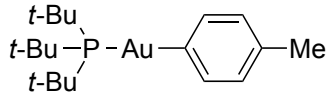

t-Bu$_3$PAuCl (175 mg, 0.402 mmol), *p*-tolylboronic acid (136 mg, 1.00 mmol), isopropanol (15 mL), and Cs_2CO_3 (337 mg, 1.03 mmol) were added to a 20-mL scintillation vial and the vial sealed with a Teflon-lined cap. The reaction mixture was heated at 50 °C for 21 h with vigorous stirring. The white suspension was concentrated to a white solid. The crude material was then suspended in benzene and passed through a thin pad of silica to yield a colorless solution. The solution was concentrated and residual solvent removed *in vacuo* to yield an analytically pure white solid (93.5 mg, 0.191 mmol, 48% yield). ^{1}H NMR (600 MHz, DCM-d_2): δ 7.34 – 7.21 (m, 2H, Ar), 7.00 (d, J = 13 Hz, 2H, Ar), 2.25 (s, 3H, tolyl Me), 1.54 (d, J_{H-P} = 12.8 Hz, 27H, *t*-Bu). ^{13}C NMR (151 MHz, DCM-d_2): δ 173.1 (d, J_{C-P} = 107.8 Hz), 139.6, 134.6, 128.4 (d, J_{C-P} = 5.7 Hz), 39.2 (d, J_{C-P} = 13.6 Hz), 32.8 (d, J_{C-P} = 4.7 Hz), 21.5. ^{31}P NMR (243 MHz, DCM-d_2): δ 92.3. IR (ATR): ν_{max}(cm^{-1}): 2950, 2912, 2865, 1600, 1470, 1251, 1170, 1025, 786, 478. EI-MS (*m*/*z*) calculated for [$C_{19}H_{34}PAu$]$^+$: 490.2065, found: 490.2064. Anal. Calcd. for $C_{19}H_{34}AuP$: C, 46.53; H, 6.99. Found: C, 46.55; H. 6.96.

(tri-*tert*-butlyphosphine)gold(I) *p*-tolysulfinate (14).

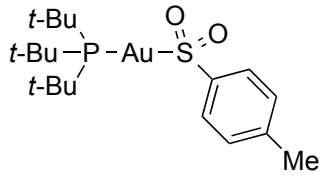

Complex **5** was synthesized analogously to complex **1** using **4** (46.9 mg, 0.096 mmol) and benzene (3 mL). The product was isolated as an analytically pure white solid (47.3 mg, 0.085 mmol, 89% yield). ^{1}H NMR (500 MHz, C_6D_6): δ 8.32 (d, $J_{H\text{-}P}$ = 8.2 Hz, 2H, Ar), 7.04 (d, $J_{H\text{-}P}$ = 8.0 Hz, 2H, Ar), 2.01 (s, 3H, tolyl methyl), 0.91 (d, $J_{H\text{-}P}$ = 13.9 Hz, 27H, *t*-Bu). ^{13}C NMR (151 MHz, C_6D_6) δ 140.2 , 129.7 , 128.4 , 126.4 , 39.0 (d, $J_{C\text{-}P}$ = 17.1 Hz), 31.9 (d, $J_{C\text{-}P}$ = 4.1 Hz), 21.2. ^{31}P NMR (162 MHz, C_6D_6) δ 87.34. IR (ATR): ν_{max}(cm^{-1}): 3018, 2948, 1478, 1189, 1170, 1091, 1045, 823, 709, 647, 576, 489. ESI-MS (*m/z*) calculated for $[C_{19}H_{34}O_2AuPS+Na]^+$: 577.1584, found: 577.1575. Anal. Calcd. for $C_{19}H_{34}AuO_2PS$: C, 41.16; H, 6.18. Found: C, 41.29; H, 6.14.

(tri-*tert*-butlyphosphine)gold(I) 4-cyanophenyl (15).

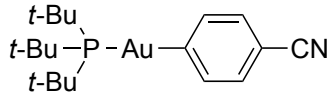

The title compound was prepared analogously to complex **3** with 4-cyanophenylboronic acid (146 mg, 1.00 mmol). The product was isolated as an analytically pure off-white solid (92.2 mg, 0.184 mmol, 46% yield). ^{1}H NMR (500 MHz, DCM-d_2): δ 7.60 (m, 2 H, Ar), 7.44 (d, *J* = 8.1 Hz, 2H), 1.54 (d, $J_{H\text{-}P}$ = 12.9 Hz, 27H). ^{13}C NMR (126 MHz, DCM-d_2): δ 165.1, 140.2, 130.3 (d, $J_{C\text{-}P}$ = 4.6 Hz), 120.7, 108.4, 54.00, 39.3 (d, $J_{C\text{-}P}$ = 14.6 Hz), 32.8 (d, $J_{C\text{-}P}$ = 4.5 Hz). ^{31}P NMR (162 MHz, DCM-d_2): δ 91.6. IR (ATR): ν_{max}(cm^{-1}): 2216 (C≡N), 1574, 1170. 808. EI-MS (*m/z*) calculated for $[C_{19}H_{31}NPAu]^+$: 501.1860, found: 501.1859. Anal. Calcd. for $C_{19}H_{31}AuNP$: C, 45.41; H, 6.23; N, 2.79. Found: C, 45.74; H, 6.51; N, 2.88.

(1,3-bis(2,6-diisopropylphenyl)imidazol-2-ylidene)gold(I) 4-cyanophenyl (16).

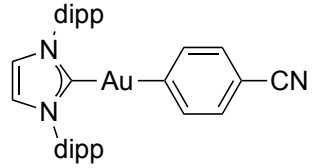

IPrAuOH (30.1 mg, 0.050 mmol) and 4-cyanophenyl boronic acid were suspended in toluene (4 mL) in a drybox and stirred for 18 h. The heterogeneous reaction mixture was passed through a plug of Celite open to air and the Celite washed with toluene (2 mL). Solvent was removed *in vacuo* to yield an analytically pure off-white solid (34.4 mg, 0.050 mmol, 100% yield). ^{1}H NMR (500 MHz, DCM-d_2) δ 7.52 (t, *J* = 7.8 Hz, 2H, IPr *p*-H), 7.33 (d, *J* = 7.8 Hz, 4H, IPr *m*-H), 7.22 (s, 2H, imidazole), 7.18 (d, *J* = 8.2 Hz, 2H), 7.09 (d, *J* = 8.2 Hz, 2H), 2.64 (sept, *J* = 6.9 Hz, 2H, C(*H*)Me$_2$), 1.38 (d, *J* = 6.9 Hz, 6H, C*H*$_3$), 1.25 (d, *J* = 6.9 Hz, 6H, C*H*$_3$). ^{13}C NMR (126 MHz, DCM-d_2) δ 195.3, 178.4, 146.4, 141.0, 135.0, 130.8, 129.7, 124.5, 123.8, 120.8, 107.5, 100.6, 54.0, 29.3, 24.8, 24.2. IR (ATR): ν_{max}(cm^{-1}): 2960, 2868, 2213 (C≡N), 1466, 1456, 805, 554. ESI-MS (*m/z*) calculated for $[C_{34}H_{40}N_3Au+Na]^+$: 710.2780, found: 710.2815. Anal. Calcd. for $C_{34}H_{40}AuN_3$: C, 59.38; H, 5.86; N, 6.11. Found: C, 59.06; H, 6.23; N, 5.92.

Stoichiometric Reactions

Conversion of IPrAuO*t*-Bu to IPrAuPh. A 20-mL scintillation vial was charged with IPrAuO*t*-Bu (49.9 mg, 0.076 mmol), phenylboronic acid (18.1 mg, 0.089 mmol), and benzene (5 mL). The reaction mixture was stirred for 75 min at ambient temperature. The vial's contents were filtered through a plug of basic alumina in air. IPrAuPh was isolated in 63% yield; its ^{1}H NMR properties matched those in the literature.[22]

Conversion of IPrAuPh to IPrAu(SO_2)Ph Monitored by ^{1}H NMR (1). IPrAuPh (6.8 mg, 0.010 mmol) and 1,3,5-trimethoxybenzene (1.1 mg, 0.007 mmol) were transferred to a J. Young tube with assistance of DCM-d_2. A ^{1}H NMR spectrum of this mixture was collected. The reaction mixture was subjected to two freeze-pump-thaw cycles on a vacuum line. The head space of the tube was then pressurized with sulfur dioxide (1 atm). A second spectrum of the reaction mixture was collected. Complex (**1**) was obtained in 95% yield by comparison with the internal standard.

Conversion of IPrAu(SO_2)Ph (1) to IPrAuO*t*-Bu Monitored by ^{1}H NMR. Complex **1** (7.4 mg, 0.010 mmol) and 1,3,5-trmethoxybenzene (1.7 mg, 0.010 mmol) were dissolved in DCM-d_2 (0.5 mL) and transferred to a J. Young tube inside a glovebox. A ^{1}H NMR spectrum of this mixture was collected. The reaction mixture was transferred to a 1-dram vial containing sodium *tert*-butoxide (2.9 mg, 0.030 mmol) and the resulting suspension was stirred for 30 min. The reaction mixture was then transferred to a J. Young tube and a second spectrum collected. IPrAuO*t*-Bu was obtained in 83% yield by comparison with the internal standard. Its ^{1}H NMR data matched those in the literature.[44]

Reaction Optimization

General Procedure: $K_2S_2O_5$ (44 mg, 0.20 mmol), boronic acid (0.10 mmol) , and *t*-Bu_3PAuCl (4.3 mg, 0.010 mmol) were added to a microwave vial followed by MeOH (0.5 mL) and toluene (0.5 mL). Benzyl bromide (24 μL, 0.20 mmol) and DIPEA (35 μL, 0.20 mmol) were added via syringe. The vial was sealed with a septum cap. The reaction mixture was heated at 100 °C for 15 to 18 h in an oil bath. The brown to black reaction mixture was concentrated by rotary evaporation. The crude solid was extracted with ethyl acetate (2 x 5 mL) from aqueous ammonium chloride (~8 mL). The organic solution was dried over sodium sulfate, and then filtered through a plug of cotton to remove desiccant and particulate matter from the reaction mixture. The ethyl acetate solution was concentrated to yield a white solid or colorless film. Trimethoxybenzene (0.025 mmol) was added to the crude product. The solid was dissolved in $CDCl_3$ and analyzed by ^{1}H NMR. Product yield was determined by comparison against a trimethoxybenzene internal standard.

Catalyst and Solvent Screen

The general procedure was applied with the exception that a different catalyst (0.010 mmol) or solvent/solvent mixture was employed in place of *t*-Bu_3PAuCl.

Aryl Coupling Partner Screen

The general procedure was applied but with varied *p*-tolyl coupling partners.

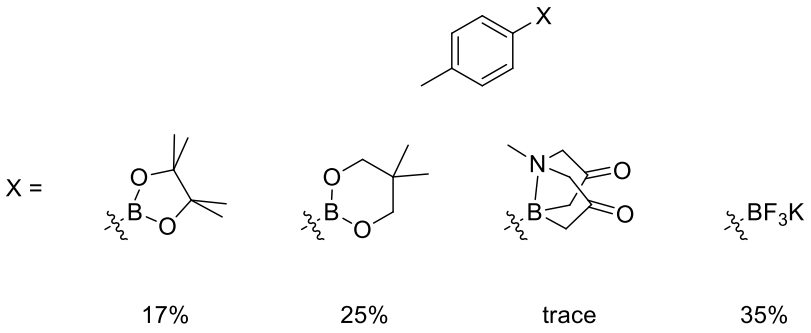

Yield determined by NMR relative to an internal standard

Varied Conditions from Standard Conditions (Table 1)

The general procedure was applied with the noted variation. In the case of Entry 12, the reaction was performed in a Schlenk vessel that was pressurized with sulfur dioxide (1 atm).

Mechanistic Experiments

Alkylation of sodium *p*-tolyl sulfinate

The standard conditions employed for reaction optimization were used but without any catalyst and with inclusion of sodium *p*-tolyl sulfinate (17.9 mg, 0.100 mmol) in place of *p*-tolyl boronic acid. *p*-tolyl(benzyl)sulfone was synthesized in 71% yield relative to the internal standard.

Catalytic viability of proposed intermediates 13, 14, and 15.

The standard conditions employed for reaction optimization were used but with complexes **13** (5.0 mg, 0.010 mmol), **14** (5.4 mg, 0.010 mmol), and **15** (5.0 mg, 0.010 mmol) in place of *t*-Bu_3PAuCl. The desired product, *p*-tolyl(benzyl)sulfone was synthesized in 45%, 46% and 7% yield, respectively, relative to the internal standard.

Reaction of IPrAuO*t*-Bu with SO_2

In a nitrogen-filled glovebox, a J. Young tube was charged with IPrAuO*t*-Bu (3.8 mg, 0.006 mmol), 1,3,5-trimethoxybenzene (~1 mg), and DCM-d_2. A ^{1}H NMR spectrum of the reaction mixture was collected (t = 0). The tube was then pressurized with SO_2 (1 atm) following two freeze-pump-thaw cycles. The ^{1}H NMR spectrum of this reaction mixture indicated a 98% mass balance with 36% conversion to a new species tentatively

assigned as the gold sulfonate IPrAuSO$_3$*t*-Bu. No further reaction was observed upon standing for 16 h.

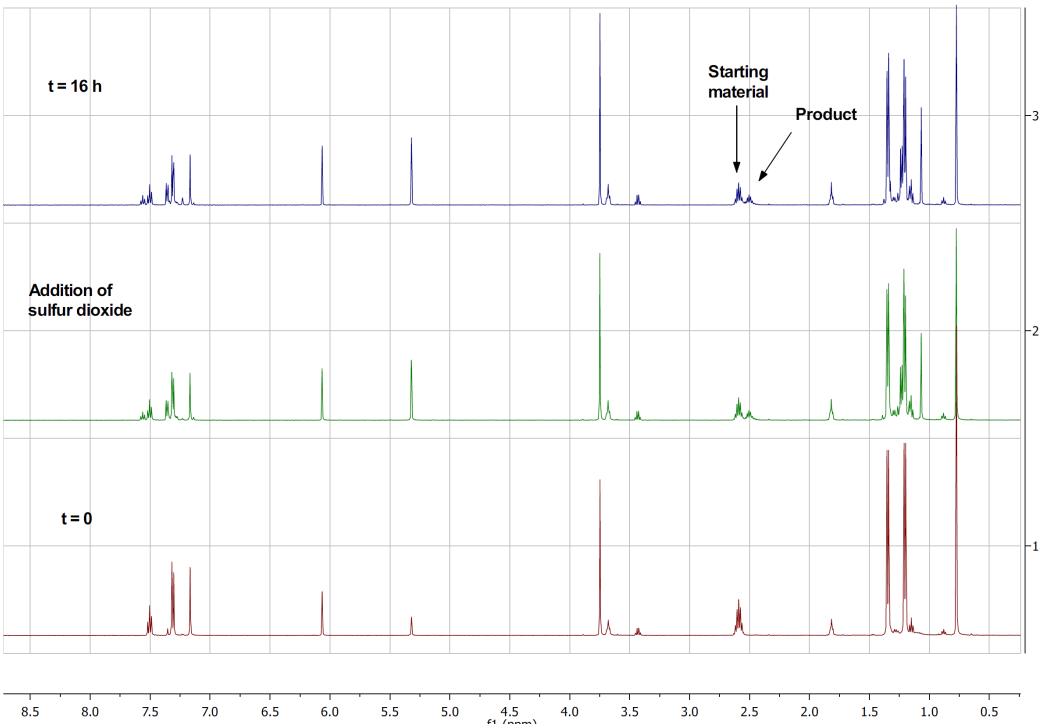

Catalytic Reactions with Varied Boronic Acids

General Procedure: A 2-dram vial with stir bar was charged with boronic acid (0.37 mmol), $K_2S_2O_5$ (167 mg, 0.74 mmol) and *t*-Bu$_3$PAuCl (16 mg, 0.037). The reagents were suspended in 1:1 PhCH$_3$/MeOH (2 mL) and treated with DIPEA (128 µL, 0.74 mmol) and benzyl bromide (88 µL, 0.74 mmol). The reaction vessel was capped with a septum-lined cap and heated in an aluminum block at 100 °C for 18 h. The reaction mixture was cooled to room temperature and the volatile materials were removed on the rotary evaporator. The resultant solids were partitioned between EtOAc (30 mL) and water (30 mL) and treated with sat. aq. NH_4Cl (3 mL). The organic phase was dried over Na_2SO_4, filtered and concentrated. The resultant crude product was purified by flash chromatography (0-60% EtOAc/heptanes gradient, 4 g silica gel) to yield the desired product.

1-(benzylsulfonyl)benzene (4). The title compound was prepared according to the General Procedure from phenyl boronic acid (50 mg, 0.37 mmol) to yield 39 mg (46 %). ^{1}H NMR (400MHz, DMSO-d$_6$) δ (ppm) 7.77 - 7.67 (m, 3H), 7.63 - 7.55 (m, 2H), 7.34 - 7.24 (m, 3H), 7.14 (dd, *J*=1.6, 7.8 Hz, 2H), 4.67 (s, 2H); ^{13}C NMR (101MHz, DMSO-d$_6$) δ (ppm) 138.32, 133.76, 130.93, 129.07, 128.65, 128.29, 128.17, 127.99, 60.65; HR-MS calcd for $C_{13}H_{13}NO_2S$ (m/z) $[M + NH_4]^+$ 250.0896, found 250.0894.

1-(benzylsulfonyl)-2-methylbenzene (5). The title compound was prepared according to the General Procedure from 2-methylphenyl boronic acid (50 mg, 0.37 mmol) to yield 45 mg (49 %). ^{1}H NMR (400MHz, DMSO-d_6) δ (ppm) 7.62 (dd, J=1.2, 7.8 Hz, 1H), 7.60 - 7.53 (m, 1H), 7.41 (d, J=7.8 Hz, 1H), 7.37 - 7.23 (m, 4H), 7.16 - 7.10 (m, 2H); ^{13}C NMR (101MHz, DMSO-d_6) δ (ppm) 138.16, 136.30, 133.82, 132.51, 130.98, 130.06, 128.46, 128.31, 128.15, 126.43, 60.58, 19.73; HR-MS calcd for $C_{14}H_{18}NO_2S$ (m/z) $[M + NH_4]^+$ 264.1053, found 264.1053.

1-(benzylsulfonyl)-3-methylbenzene (6). The title compound was prepared according to the General Procedure from 3-methylphenyl boronic acid (50 mg, 0.37 mmol) to yield 51 mg (56 %). ^{1}H NMR (400MHz, DMSO-d_6) δ (ppm) 7.54 (d, J=0.8 Hz, 1H), 7.52 - 7.41 (m, 3H), 7.36 - 7.25 (m, 3H), 7.19 - 7.12 (m, 2H), 4.63 (s, 2H), 2.36 (s, 3H); ^{13}C NMR (101MHz, DMSO-d_6) δ (ppm) 138.85, 138.32, 134.32, 130.97, 128.89, 128.65, 128.27, 128.19, 128.15, 125.11, 60.68, 20.68; HR-MS calcd for $C_{14}H_{18}NO_2S$ (m/z) $[M + NH_4]^+$ 264.1053, found 264.1055.

1-(benzylsulfonyl)-4-methylbenzene (3). The title compound was prepared according to the General Procedure from 4-methylphenyl boronic acid (50 mg, 0.37 mmol) to yield 60 mg (66 %). ^{1}H NMR (400MHz, DMSO-d_6) δ (ppm) 7.58 (d, J=8.2 Hz, 2H), 7.38 (d, J=7.8 Hz, 2H), 7.34 - 7.24 (m, 3H), 7.18 - 7.09 (m, 2H), 4.62 (s, 2H), 2.39 (s, 3H); ^{13}C NMR (101MHz, DMSO-d_6) δ (ppm) 144.21, 135.56, 130.92, 129.51, 128.78, 128.25, 128.16, 128.02, 60.76, 21.03; HR-MS calcd for $C_{14}H_{15}O_2S$ (m/z) $[M + H]^+$ 247.0787, found 247.0782.

1-(benzylsulfonyl)-4-methoxybenzene (7). The title compound was prepared according to the General procedure from 4-methoxyphenyl boronic acid (56 mg, 0.37 mmol) to yield 46 mg (48 %). ^{1}H NMR (400MHz, DMSO-d_6) δ (ppm) 7.65 - 7.53 (m, 2H), 7.35 - 7.23 (m, 3H), 7.13 (dd, J=1.8, 7.6 Hz, 2H), 7.11 - 7.05 (m, 2H), 4.59 (s, 2H), 3.83 (s, 3H); ^{13}C NMR (101MHz, DMSO-d_6) δ (ppm) 163.23, 130.96, 130.35, 129.95, 129.02, 128.31, 128.24, 114.31, 61.12, 55.80; HR-MS calcd for $C_{14}H_{15}N_2O_2S$ (m/z) $[M + H]^+$ 263.0736, found 263.0736.

5-(benzylsulfonyl)benzo[d][1,3]dioxole (11). The title compound was prepared according to the General Procedure from 3,4-methylenedioxyphenyl boronic acid (56 mg, 0.37 mmol) to yield 46 mg (48 %). ^{1}H NMR (400MHz, DMSO-d_6) δ (ppm) 7.33 - 7.27 (m, 3H), 7.22 - 7.18 (m, 2H), 7.17 - 7.13 (m, 2H), 7.05 (d, J=8.2 Hz, 1H), 6.18 (s, 2H), 4.61 (s, 2H); ^{13}C NMR (101MHz, DMSO-d_6) δ (ppm) 147.71, 131.58, 130.90, 128.87, 128.27, 128.19, 124.04, 108.17, 107.73, 102.61, 60.76; HR-MS calcd for $C_{14}H_{13}O_4S$ (m/z) $[M + H]^+$ 277.0529, found 277.0526.

5-(benzylsulfonyl)-1-methyl-1H-indazole (12). The title compound was prepared according to the General Procedure from (1-methyl-1H-indazol-5-yl)boronic acid (65 mg, 0.37 mmol) to yield 56 mg (53 %). ^{1}H NMR (400MHz, DMSO-d_6) δ (ppm) 8.27 (d, J=0.8 Hz, 1H), 8.20 - 8.11 (m, 1H), 7.82 (d, J=9.0 Hz, 1H), 7.65 (dd, J=1.6, 9.0 Hz, 1H), 7.32 - 7.21 (m, 3H), 7.11 (dd, J=1.6, 7.8 Hz, 2H), 4.67 (s, 2H), 4.10 (s, 3H); ^{13}C NMR (101MHz, DMSO-d_6) δ (ppm) 140.81, 134.58, 130.88, 130.36, 128.99, 128.22, 128.16, 124.57, 123.49, 122.44, 110.36, 61.11, 35.70; HR-MS calcd for $C_{15}H_{15}N_2O_2S$ (m/z) $[M + H]^+$ 287.0849, found 287.0846.

Divergent Synthesis of Sulfonyl Compounds

Sulfone Synthesis: A 50-mL round bottom flask was charged with 1-methyl-1H-indazol-5-ylboronic acid (651 mg, 3.70 mmol), $K_2S_2O_5$ (1.68 g, 7.40 mmol) and *t*-Bu_3PAuCl (161 mg, 0.37 mmol). The solids were suspended in 1:1 $PhCH_3$/MeOH (20 mL) and treated with DIPEA (1.29 mL, 7.40 mmol). The mixture was heated at 100 ^oC for 18h. The reaction mixture was cooled to room temperature and filtered through a pad of Celite. The pad was then rinsed with 1:1 $PhCH_3$/MeOH (10 mL). A portion of the clear filtrate (2 mL) was placed in each of 14 1-dram vials previously charged with the respective alkyl halides (2 equiv.). The solutions were heated at 50 ^oC for 4 h then cooled to room temperature. The solvent was removed by N_2 flow and the resultant solids from each reaction were taken up in 1 mL DMSO and purified by HPLC to deliver the desired library targets.

HPLC purification method: Waters Sunfire C18 19x100, 5μ; Mobile phase A:0.05% TFA in H_20 (v/v); Mobile phase B: 0.05% TFA in acetonitrile (v/v); 95.0% H_20/5.0% Acetonitrile linear to 0% H_20/100% Acetonitrile in 8.5min, HOLD at 0% H_20/100% Acetonitrile to 10.0min. Flow: 25mL/min.

1-methyl-5-((4-methylbenzyl)sulfonyl)-1H-indazole (17a). ^1H NMR (600MHz, DMSO-*d_6*) δ (ppm) 8.27 (d, J=0.8 Hz, 1H), 8.16 (d, J=1.2 Hz, 1H), 7.83 (d, J=8.6 Hz, 1H), 7.66 (dd, J=1.6, 9.0 Hz, 1H), 7.06 (d, J=7.8 Hz, 2H), 6.99 (d, J=8.2 Hz, 2H), 4.61 (s, 2H), 4.11 (s, 3H), 2.24 (s, 3H); ^{13}C NMR (101MHz, DMSO-d_6) δ (ppm) 140.80, 137.54, 134.57, 130.74, 130.46, 128.77, 125.90, 124.58, 123.45, 122.46, 110.37, 60.80, 35.70, 20.70; HR-MS calcd for $C_{16}H_{17}N_2O_2S$ (m/z) [M + H]+ 301.1005, found 301.1004.

1-methyl-5-((4-fluorobenzyl)sulfonyl)-1H-indazole (17b). ^1H NMR (600MHz, DMSO-*d_6*) δ (ppm) 8.28 (d, J=0.8 Hz, 1H), 8.16 (dd, J=0.8, 1.6 Hz, 1H), 7.83 (dd, J=0.8, 9.0 Hz, 1H), 7.63 (dd, J=1.8, 8.8 Hz, 1H), 7.22 - 7.05 (m, 4H), 4.69 (s, 2H), 4.11 (s, 3H); ^{13}C NMR (101MHz, DMSO-d_6) δ (ppm) 140.84, 134.61, 132.97, 132.89, 130.15, 125.39, 125.36, 124.56, 123.55, 122.48, 115.23, 115.02, 110.41, 60.12, 35.70; HR-MS calcd for $C_{15}H_{14}FN_2O_2S$ (m/z) [M + H]+ 305.0755, found 305.0752.

1-methyl-5-((4-chlorobenzyl)sulfonyl)-1H-indazole (17c). ^1H NMR (600MHz, DMSO-*d_6*) δ (ppm) 8.29 (d, J=0.8 Hz, 1H), 8.18 (dd, J=0.8, 1.6 Hz, 1H), 7.84 (d, J=9.0 Hz, 1H), 7.65 (dd, J=1.8, 8.8 Hz, 1H), 7.34 (d, J=8.6 Hz, 2H), 7.13 (d, J=8.6 Hz, 2H), 4.71 (s, 2H), 4.11 (s, 3H); ^{13}C NMR (101MHz, DMSO-d_6) δ (ppm) 140.85, 134.64, 133.16, 132.65, 130.16, 128.25, 128.14, 124.55, 123.57, 122.48, 110.45, 60.19, 35.71; HR-MS calcd for $C_{15}H_{14}ClN_2O_2S$ (m/z) [M + H]+ 321.0459, found 321.0460.

1-methyl-5-((4-bromobenzyl)sulfonyl)-1H-indazole (17d). ^1H NMR (600MHz, DMSO-*d_6*) δ (ppm) 8.29 (d, J=0.8 Hz, 1H), 8.19 (d, J=0.8 Hz, 1H), 7.84 (d, J=9.0 Hz, 1H), 7.65 (dd, J=1.8, 8.8 Hz, 1H), 7.47 (d, J=8.2 Hz, 2H), 7.07 (d, J=8.6 Hz, 2H), 4.70 (s, 2H), 4.11 (s, 3H); ^{13}C NMR (101MHz, DMSO-d_6) δ (ppm) 140.85, 134.64, 132.96, 131.19, 130.16, 128.54, 124.54, 123.56, 122.48, 121.82, 110.47, 60.25, 35.72; HR-MS calcd for $C_{15}H_{14}BrN_2O_2S$ (m/z) [M + H]+ 364.9954 and 366.9934, found 364.9948 and 366.9929.

4-(((1-methyl-1H-indazol-5-yl)sulfonyl)methyl)benzonitrile (17e). ^{1}H NMR (600MHz, DMSO-d_6) δ (ppm) 8.29 (d, J=0.8 Hz, 1H), 8.18 (dd, J=0.8, 1.6 Hz, 1H), 7.85 (d, J=9.0 Hz, 1H), 7.75 (d, J=8.2 Hz, 2H), 7.65 (dd, J=1.8, 8.8 Hz, 1H), 7.32 (d, J=8.6 Hz, 2H), 4.85 (s, 2H), 4.11 (s, 3H); ^{13}C NMR (101MHz, DMSO-d_6) δ (ppm) 140.88, 134.73, 134.70, 132.08, 131.84, 130.04, 124.50, 123.66, 122.49, 118.52, 111.07, 110.53, 60.66, 35.72; HR-MS calcd for $C_{16}H_{14}N_3O_2S$ (m/z) [M + H]+ 312.0801, found 312.0799.

1-methyl-5-((4-(trifluoromethyl)benzyl)sulfonyl)-1H-indazole (17f). ^{1}H NMR (600MHz, DMSO-d_6) δ (ppm) 8.29 (d, J=0.8 Hz, 1H), 8.21 (dd, J=0.8, 1.6 Hz, 1H), 7.85 (d, J=9.0 Hz, 1H), 7.71 - 7.64 (m, 3H), 7.37 (d, J=8.2 Hz, 2H), 4.85 (s, 2H), 4.11 (s, 3H); ^{13}C NMR (101MHz, DMSO-d_6) δ (ppm) 140.88, 134.65, 133.83, 131.73, 130.20, 128.87, 125.09, 125.05, 124.48, 123.59, 122.50, 110.53, 60.44, 35.72; HR-MS calcd for $C_{16}H_{14}F_3N_2O_2S$ (m/z) [M + H]+ 355.0723, found 355.0722.

methyl 4-(((1-methyl-1H-indazol-5-yl)sulfonyl)methyl)benzoate (17g). ^{1}H NMR (600MHz, DMSO-d_6) δ (ppm) 8.28 (d, J=0.8 Hz, 1H), 8.18 (d, J=0.8 Hz, 1H), 7.88 - 7.80 (m, 3H), 7.64 (dd, J=1.8, 8.8 Hz, 1H), 7.27 (d, J=8.2 Hz, 2H), 4.81 (s, 2H), 4.10 (s, 3H), 3.83 (s, 3H); ^{13}C NMR (101MHz, DMSO-d_6) δ (ppm) 165.87, 140.85, 134.66, 134.44, 131.25, 130.18, 129.35, 128.94, 124.53, 123.58, 122.47, 110.47, 60.77, 52.16, 35.71; HR-MS calcd for $C_{17}H_{17}N_2O_4S$ (m/z) [M + H]+ 345.0904, found 345.0904.

5-(cyclopentylsulfonyl)-1-methyl-1H-indazole (17h). ^{1}H NMR (600MHz, DMSO-d_6) δ (ppm) 8.38 (dd, J=0.8, 1.6 Hz, 1H), 8.31 (d, J=1.2 Hz, 1H), 7.89 (d, J=8.6 Hz, 1H), 7.82 (dd, J=1.6, 9.0 Hz, 1H), 4.12 (s, 3H), 3.77 (tt, J=6.7, 8.9 Hz, 1H), 1.95 - 1.68 (m, 4H), 1.66 - 1.44 (m, 4H); ^{13}C NMR (101MHz, DMSO-d_6) δ (ppm) 140.81, 134.55, 130.58, 124.58, 123.49, 122.74, 110.75, 63.07, 35.70, 26.81, 25.46; HR-MS calcd for $C_{13}H_{17}N_2O_2S$ (m/z) [M + H]+, 265.1005, found 265.1007.

cyclopentyl 1-methyl-1H-indazole-5-sulfinate (17h-2). (O-linked isomer) ^{1}H NMR (600MHz, DMSO-d_6) δ (ppm) 8.25 (d, J=0.8 Hz, 1H), 8.19 - 8.16 (m, 1H), 7.85 (d, J=8.6 Hz, 1H), 7.65 (dd, J=1.6, 9.0 Hz, 1H), 4.83 - 4.74 (m, 1H), 4.10 (s, 3H), 1.91 - 1.73 (m, 2H), 1.70 - 1.44 (m, 6H); ^{13}C NMR (101MHz, DMSO-d_6) δ (ppm) 140.70, 137.51, 133.97, 122.83, 121.87, 119.12, 110.76, 79.89, 35.64, 33.58, 33.18, 22.83; HR-MS calcd for $C_{13}H_{17}N_2O_2S$ (m/z) [M + H]+, 265.1005, found 265.1004.

5-(allylsulfonyl)-1-methyl-1H-indazole (17i). ^{1}H NMR (600MHz, DMSO-d_6) δ (ppm) 8.33 (dd, J=0.8, 1.6 Hz, 1H), 8.32 (d, J=0.8 Hz, 1H), 7.88 (d, J=9.0 Hz, 1H), 7.80 (dd, J=1.6, 9.0 Hz, 1H), 5.68 (tdd, J=7.3, 10.0, 17.2 Hz, 1H), 5.30 - 5.20 (m, 1H), 5.14 (dd, J=1.6, 16.8 Hz, 1H), 4.13 (d, J=7.4 Hz, 2H), 4.12 (s, 3H); ^{13}C NMR (101MHz, DMSO-d_6) δ (ppm) 140.84, 134.61, 130.50, 125.66, 124.48, 124.11, 123.41, 122.53, 110.56, 59.64, 35.71; HR-MS calcd for $C_{11}H_{13}N_2O_2S$ (m/z) [M + H]+ 237.0692, found 237.0692.

5-(hexylsulfonyl)-1-methyl-1H-indazole (17j). ^{1}H NMR (600MHz, DMSO-d_6) δ (ppm) 8.38 (d, J=1.2 Hz, 1H), 8.32 (d, J=0.8 Hz, 1H), 7.89 (d, J=9.0 Hz, 1H), 7.83 (dd, J=1.6, 9.0 Hz, 1H), 4.12 (s, 3H), 3.31 - 3.24 (m, 2H), 1.56 - 1.44 (m, 2H), 1.28 (td, J=7.3, 14.7 Hz, 2H), 1.22 - 1.13 (m, 4H), 0.84 - 0.74 (m, 3H); ^{13}C NMR (101MHz, DMSO-d_6) δ

(ppm) 140.84, 134.56, 131.08, 124.21, 123.03, 122.66, 110.78, 55.01, 35.71, 30.56, 27.02, 22.46, 21.73, 13.73; HR-MS calcd for $C_{14}H_{21}N_2O_2S$ (m/z) [M + H]+ 281.1318, found 281.1317.

Sulfonamide Synthesis: A 50-mL round bottom flask was charged with 1-methyl-1H-indazol-5-ylboronic acid (651 mg, 3.70 mmol), $K_2S_2O_5$ (1.68 g, 7.40 mmol) and *t*-Bu_3PAuCl (161 mg, 0.37 mmol). The solids were suspended in 1:1 $PhCH_3$/MeOH (20 mL) and treated with DIPEA (1.29 mL, 7.40 mmol). The mixture was heated at 100 ^oC for 18h. The reaction was cooled to room temperature and the volatiles removed under reduced pressure. The white solids were taken up in THF (10 mL) and treated with N-chloro succinimide (502 mg, 3.70 mmol) and the mixture was stirred for 1 h at room temperature. The solids were filtered off through Celite and the filter cake rinsed with THF (20 mL). The filtrate was concentrated to a volume of 20 mL and divided equally amongst 10 1-dram vials equipped with stirbars. To each of the 10 vials was added DIPEA (65 µL, 0.37 mmol) followed by 100 µL of each of the 10 amines. The individual reactions were stirred for 1 h and the THF was removed by N_2 flow. The resultant solids from each reaction were taken up in 1 mL DMSO and purified by HPLC to deliver the desired library targets.

HPLC purification method: Waters Sunfire C18 19x100, 5µ; Mobile phase A:0.05% TFA in H_20 (v/v); Mobile phase B: 0.05% TFA in acetonitrile (v/v); 95.0% H_20/5.0% Acetonitrile linear to 0% H_20/100% Acetonitrile in 8.5min, HOLD at 0% H_20/100% Acetonitrile to 10.0min. Flow: 25mL/min.

N-(tert-butyl)-1-methyl-1H-indazole-5-sulfonamide (18a). ^1H NMR (600MHz, DMSO-*d*$_6$) δ (ppm) 8.27 (d, *J* = 0.9 Hz, 1H), 8.24 (s, 1H), 7.83 - 7.77 (m, 2H), 7.38 (s, 1H), 4.08 (s, 3H), 1.07 (s, 9H); ^{13}C NMR (101MHz, DMSO-d_6) δ (ppm) 140.11, 136.43, 134.15, 123.76, 122.35, 120.57, 110.45, 53.10, 35.63, 29.70; HR-MS calcd for $C_{12}H_{18}N_3O_2S$ (m/z) [M + H]+ 268.1114, found 268.1113

N-(3-methoxypropyl)-1-methyl-1H-indazole-5-sulfonamide (18b). ^1H NMR (600MHz, DMSO-*d*$_6$) δ (ppm) 8.27 - 8.24 (m, 2H), 7.84 (d, *J* = 9.0 Hz, 1H), 7.76 (dd, *J* = 1.6, 8.9 Hz, 1H), 7.46 (t, *J* = 5.9 Hz, 1H), 4.10 (s, 3H), 3.25 (t, *J* = 6.2 Hz, 2H), 3.10 (s, 3H), 2.79 - 2.73 (m, 2H), 1.57 (quin, *J* = 6.6 Hz, 2H); ^{13}C NMR (101MHz, DMSO-d_6) δ (ppm) 140.31, 134.21, 132.40, 123.52, 122.44, 121.24, 110.71, 68.93, 57.77, 40.27, 35.65, 29.10; HR-MS calcd for $C_{12}H_{18}N_3O_3S$ (m/z) [M + H]+ 284.1063, found 284.1064

N,N-diethyl-1-methyl-1H-indazole-5-sulfonamide (18c). ^1H NMR (600MHz, DMSO-*d*$_6$) δ (ppm) 8.29 (d, *J* = 1.1 Hz, 1H), 8.26 (d, *J* = 0.7 Hz, 1H), 7.83 (d, *J* = 9.0 Hz, 1H), 7.74 (dd, *J* = 1.8, 8.8 Hz, 1H), 4.10 (s, 3H), 3.17 (q, *J* = 7.2 Hz, 4H), 1.03 (t, *J* = 7.1 Hz, 6H); ^{13}C NMR (101MHz, DMSO-d_6) δ (ppm) 140.35, 134.29, 131.76, 123.68, 122.63, 121.61, 110.75, 41.72, 35.66, 14.05; HR-MS calcd for $C_{12}H_{18}N_3O_2S$ (m/z) [M + H]+ 268.1114, found 268.1114

4-(1-methyl-1H-indazol-5-ylsulfonyl)morpholine (18d). ^1H NMR (600MHz, DMSO-*d*$_6$) δ (ppm) 8.31 (s, 1H), 8.27 (d, *J* = 1.1 Hz, 1H), 7.89 (d, *J* = 8.8 Hz, 1H), 7.70 (dd, *J* =

1.8, 8.8 Hz, 1H), 4.12 (s, 3H), 3.64 - 3.60 (m, 4H), 2.93 - 2.84 (m, 4H); ^{13}C NMR (101MHz, DMSO-d_6) δ (ppm) 140.67, 134.49, 126.40, 124.28, 122.89, 122.76, 110.71, 65.25, 45.94, 35.71; HR-MS calcd for $C_{12}H_{16}N_3O_3S$ (m/z) [M + H]+ 282.0907, found 282.0910

1-methyl-5-(piperidin-1-ylsulfonyl)-1H-indazole (18e). ^{1}H NMR (600MHz, DMSO-d_6) δ (ppm) 8.28 (s, 1H), 8.24 (d, *J* = 0.7 Hz, 1H), 7.85 (d, *J* = 8.8 Hz, 1H), 7.68 (dd, *J* = 1.5, 8.8 Hz, 1H), 4.10 (s, 3H), 2.92 - 2.83 (m, 4H), 1.52 (td, *J* = 5.7, 11.0 Hz, 4H), 1.32 (td, *J* = 5.8, 11.6 Hz, 2H); ^{13}C NMR (101MHz, DMSO-d_6) δ (ppm) 140.54, 134.38, 127.51, 124.22, 122.74, 122.44, 110.54, 46.62, 35.68, 24.66, 22.82; HR-MS calcd for $C_{13}H_{18}N_3O_2S$ (m/z) [M + H]+ 280.1114, found 280.1116

1-methyl-5-(pyrrolidin-1-ylsulfonyl)-1H-indazole (18f). ^{1}H NMR (600MHz, DMSO-d_6) δ (ppm) 8.32 - 8.29 (m, 1H), 8.28 (s, 1H), 7.84 (d, *J* =8.8 Hz, 1H), 7.79 - 7.75 (m, 1H), 4.10 (s, 3H), 3.15 (t, *J* = 6.8 Hz, 4H), 1.69 - 1.57 (m, 4H); ^{13}C NMR (101MHz, DMSO-d_6) δ (ppm) 140.52, 134.39, 128.23, 124.15, 122.69, 122.30, 110.64, 47.79, 35.67, 24.62; HR-MS calcd for $C_{12}H_{16}N_3O_2S$ (m/z) [M + H]+ 266.0958, found 266.0958

5-(4-ethylpiperazin-1-ylsulfonyl)-1-methyl-1H-indazole (18g). ^{1}H NMR (600MHz, DMSO-d_6) δ (ppm) 8.30 (d, *J* = 0.7 Hz, 1H), 8.25 (d, *J* = 1.1 Hz, 1H), 7.87 (d, *J* = 8.8 Hz, 1H), 7.69 (dd, *J* = 1.6, 8.9 Hz, 1H), 4.12 (s, 3H), 2.89 (br. s., 4H), 2.40 (br. s., 4H), 2.28 (q, *J* = 7.1 Hz, 2H), 0.90 (t, *J* = 7.2 Hz, 3H); ^{13}C NMR (101MHz, DMSO-d_6) δ (ppm) 140.61, 134.43, 126.70, 124.29, 122.72, 110.55, 51.18, 50.98, 45.95, 35.69, 11.78; HR-MS calcd for $C_{14}H_{21}N_4O_2S$ (m/z) [M + H]+ 309.1380, found 309.1380

2-(4-(1-methyl-1H-indazol-5-ylsulfonyl)piperazin-1-yl)ethanol (18h). ^{1}H NMR (600MHz, DMSO-d_6) δ (ppm) 8.31 (d, J=0.8 Hz, 1H), 8.26 - 8.24 (m, 1H), 7.88 (d, J=8.6 Hz, 1H), 7.69 (dd, J=1.6, 9.0 Hz, 1H), 4.32 (br. s., 1H), 4.12 (s, 3H), 3.39 (q, J=5.9 Hz, 2H), 2.87 (br. s., 4H), 2.46 (br. s., 4H), 2.34 (t, J=5.1 Hz, 2H); ^{13}C NMR (101MHz, DMSO-d_6) δ (ppm) 140.62, 134.44, 126.61, 124.32, 122.75, 122.72, 110.57, 59.47, 58.37, 51.93, 45.95, 35.70; HR-MS calcd for $C_{14}H_{21}N_4O_3S$ (m/z) [M + H]+ 325.1329, found 325.1331

N-benzyl-1-methyl-1H-indazole-5-sulfonamide (18i). ^{1}H NMR (600MHz, DMSO-d_6) δ (ppm) 8.30 - 8.27 (m, 1H), 8.25 (d, *J* = 0.9 Hz, 1H), 8.02 (t, *J* = 6.2 Hz, 1H), 7.87 - 7.80 (m, 1H), 7.80 - 7.75 (m, 1H), 7.29 - 7.16 (m, 5H), 4.10 (s, 3H), 3.96 (d, *J* = 6.1 Hz, 2H); ^{13}C NMR (101MHz, DMSO-d_6) δ (ppm) 140.32, 137.64, 134.23, 132.64, 128.16, 127.53, 127.06, 123.56, 122.44, 121.31, 110.68, 46.13, 35.65; HR-MS calcd for $C_{15}H_{16}N_3O_2S$ (m/z) [M + H]+ 302.0958, found 302.0955

N-(4-methoxybenzyl)-1-methyl-1H-indazole-5-sulfonamide (18j). ^{1}H NMR (600MHz, DMSO-d_6) δ (ppm) 8.27 - 8.21 (m, 2H), 7.92 (t, *J* = 6.2 Hz, 1H), 7.83 - 7.79 (m, 1H), 7.77 - 7.70 (m, 1H), 7.11 (d, *J* = 8.8 Hz, 2H), 6.78 (d, *J* = 8.8 Hz, 2H), 4.10 (s, 3H), 3.88 (d, *J* = 6.4 Hz, 2H), 3.68 (s, 3H); ^{13}C NMR (101MHz, DMSO-d_6) δ (ppm) 158.36, 140.29, 134.21, 132.71, 129.39, 128.90, 123.57, 122.42, 121.29, 113.54, 110.62, 55.00, 45.68, 35.64; HR-MS calcd for $C_{16}H_{18}N_3O_3S$ (m/z) [M + H]+ 332.1063, found 332.105

References

1. Otten, H. *J. Antimicrob. Chemother.* **1986***, 17*, 689.
2. Schubart, R. In *Sulfinic Acids and Derivaties;* **Ullmann's Encyclopedia of Industrial Chemistry**; Wiley: 2012; Vol. 34, pp 677.
3. Woolven, H.; Gonzalez-Rodriguez, C.; Marco, I.; Thompson, A. L.; Willis, M. C. *Org. Lett.* **2011***, 13*, 4876.
4. Deeming, A. S.; Russell, C. J.; Hennessy, A. J.; Willis, M. C. *Org. Lett.* **2014***, 16*, 150.
5. Rocke, B. N.; Bahnck, K. B.; Herr, M.; Lavergne, S.; Mascitti, V.; Perreault, C.; Polivkova, J.; Shavnya, A. *Org. Lett.* **2014***, 16*, 154.
6. Ye, S.; Wu, J. *Chem. Comm.* **2012***, 48*, 10037.
7. Ye, S.; Wu, J. *Chem. Comm.* **2012***, 48*, 7753-7755.
8. Nguyen, B.; Emmett, E. J.; Willis, M. C. *J. Am. Chem. Soc.* **2010***, 132*, 16372.
9. Bandgar, B. P.; Bettigeri, S. V.; Phopase, J. *Org. Lett.* **2004***, 6*, 2105.
10. Shavnya, A.; Coffey, S. B.; Smith, A. C.; Mascitti, V. *Org. Lett.* **2013***, 15*, 6226.
11. Corma, A.; Leyva-Perez, A.; Sabater, M. J. *Chem. Rev.* **2011***, 111*, 1657.
12. Brenzovich, W. E., Jr.; Benitez, D.; Lackner, A. D.; Shunatona, H. P.; Tkatchouk, E.; Goddard,William A.,,III; Toste, F. D. *Angew. Chem., Int. Ed.* **2010***, 49*, 5519.
13. Johnson, A.; Puddephatt, R. J. *J. Chem. Soc., Dalton Trans*. **1977**, 1384.
14. Johnson, A.; Puddephatt, R. J.; Quirk, J. L. *J. Chem. Soc., Chem. Commmun.* **1972**, 938.
15. Puddephatt, R. J.; Stalteri, M. A. *J. Organomet. Chem.* **1980***, 193*, C27.
16. Aresta, M.; Vasapollo, G. *J. Organomet. Chem.* **1973***, 50*, C51.
17. Rombke, P.; Schier, A.; Schmidbaur, H. *J. Chem. Soc., Dalton Trans*. **2001**, 2482.
18. Hashmi, A. S. K.; Lothschuetz, C.; Doepp, R.; Rudolph, M.; Ramamurthi, T. D.; Rominger, F. *Angew. Chem., Int. Ed.* **2009***, 48*, 8243.
19. Scott, V. J.; Labinger, J. A.; Bercaw, J. E. *Organometallics* **2010***, 29*, 4090.
20. Gaillard, S.; Slawin, A. M. Z.; Nolan, S. P. *Chem. Commun.* **2010***, 46*, 2742.
21. Laitar, D. S.; Muller, P.; Gray, T. G.; Sadighi, J. P. *Organometallics* **2005***, 24*, 4503.
22. Tsui, E. Y.; Mueller, P.; Sadighi, J. P. *Angew. Chem., Int. Ed.* **2008***, 47*, 8937.
23. Johnson, M. W.; Shevick, S. L.; Toste, F. D.; Bergman, R. G. *Chem. Sci.* **2013***, 4*, 1023.
24. Wojcicki, A. *Insertion Reactions of Transition Metal–Carbon σ-Bonded Compounds II. Sulfur Dioxide and Other Molecules;* Advance in Organometallic Chemistry; Elsevier: 1974; Vol. 12.
25. Roth, K. E.; Blum, S. A. *Organometallics* **2010***, 29*, 1712.
26. Partyka, D. V.; Zeller, M.; Hunter, A. D.; Gray, T. G. *Inorg. Chem.* **2012***, 51*, 8394.
27. Byrd, W. *Inorg. Chem.* **1962***, 1*, 762.
28. Wong, M.; Wiberg, K. *J. Am. Chem. Soc.* **1992***, 114*, 7527.
29. Rueeger, H.; Lueoend, R.; Rogel, O.; Rondeau, J.; Moebitz, H.; Machauer, R.; Jacobson, L.; Staufenbiel, M.; Desrayaud, S.; Neumann, U. *J. Med. Chem.* **2012***, 55*, 3364.
30. Spinks, D.; Torrie, L. S.; Thompson, S.; Harrison, J. R.; Frearson, J. A.; Read, K. D.; Fairlamb, A. H.; Wyatt, P. G.; Gilbert, I. H. *ChemMedChem*. **2012***, 7*, 95.
31. Mankad, N. P.; Toste, F. D. *Chem. Sci.* **2012***, 3*, 72.
32. Egbert, J. D.; Slawin, A. M. Z.; Nolan, S. P. *Organometallics* **2013***, 32*, 2271.

NMR Spectra

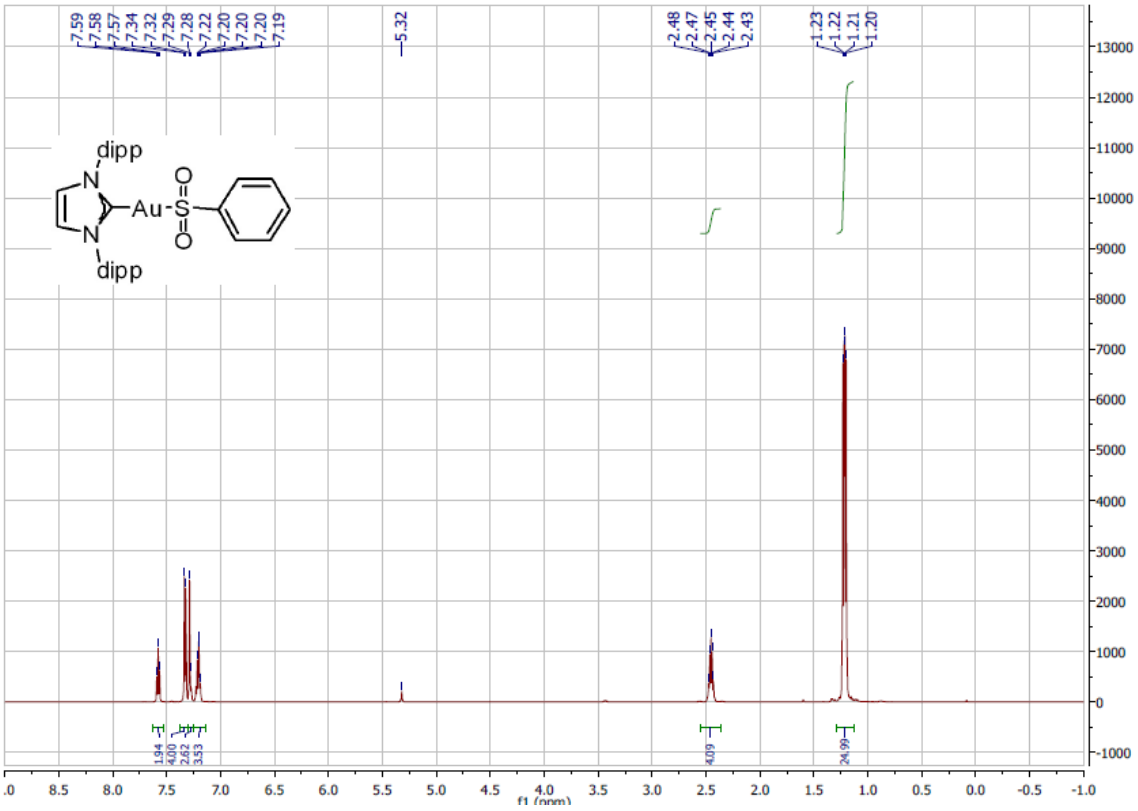
dipp
Au
S
O
dipp
7.59
7.58
7.57
7.34
7.32
7.29
7.28
7.22
7.20
7.20
7.20
7.19
5.32
2.48
2.47
2.45
2.44
2.43
1.23
1.22
1.21
1.20
1.94
4.00
2.62
3.53
4.09
24.99
f1 (ppm)

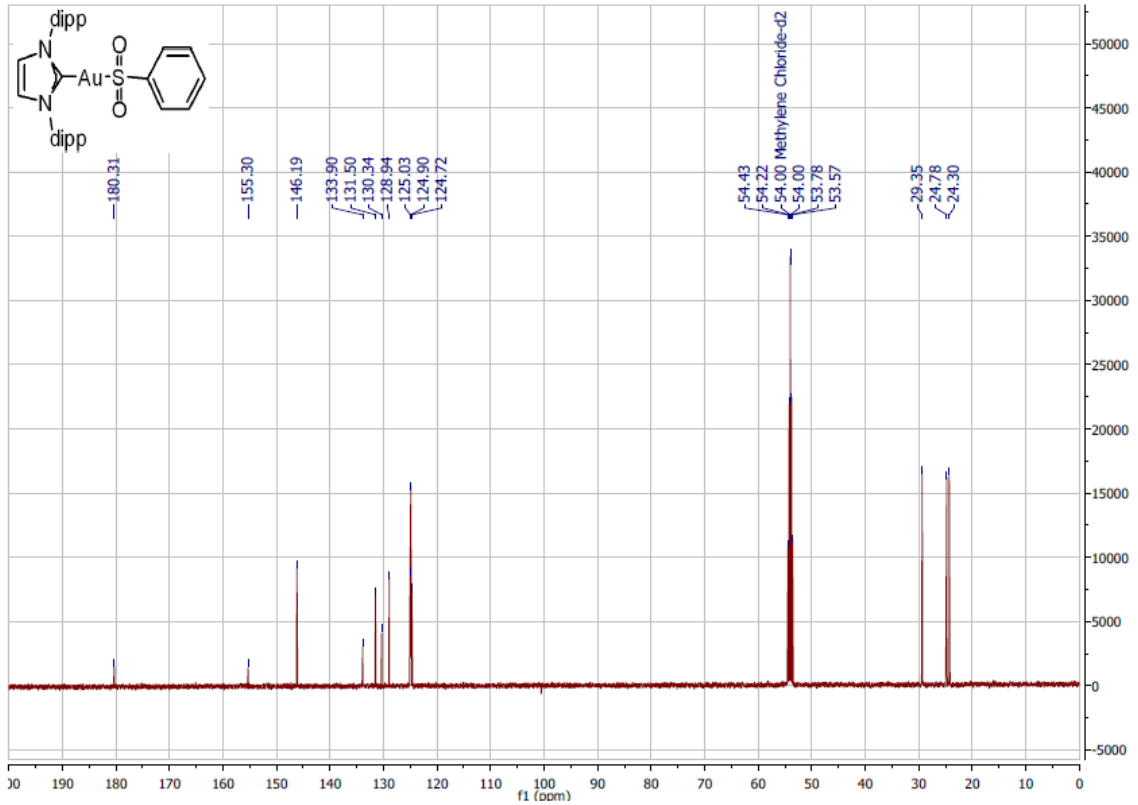
dipp
Au
S
O
dipp
180.31
155.30
146.19
133.90
131.50
130.34
128.94
125.03
124.90
124.72
54.43
54.22
54.00 Methylene Chloride-d2
54.00
53.78
53.57
29.35
24.78
24.30
f1 (ppm)

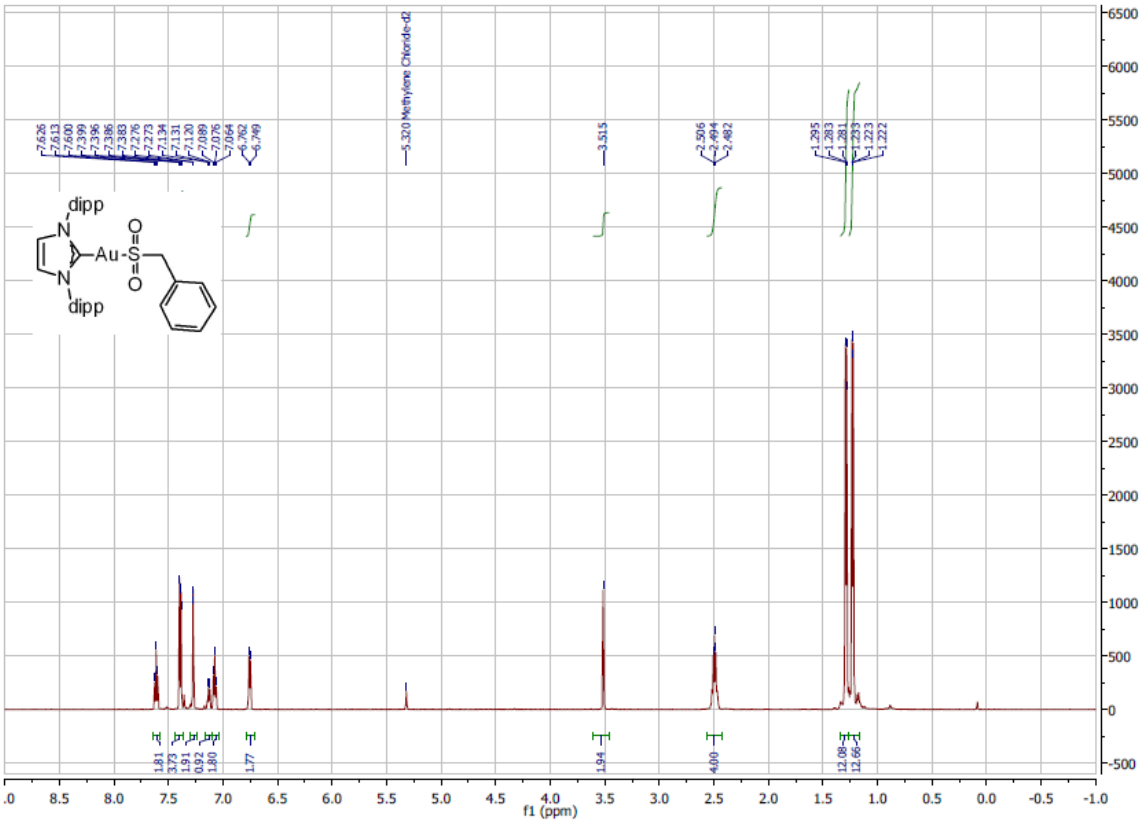
dipp
Au
dipp
f1 (ppm)

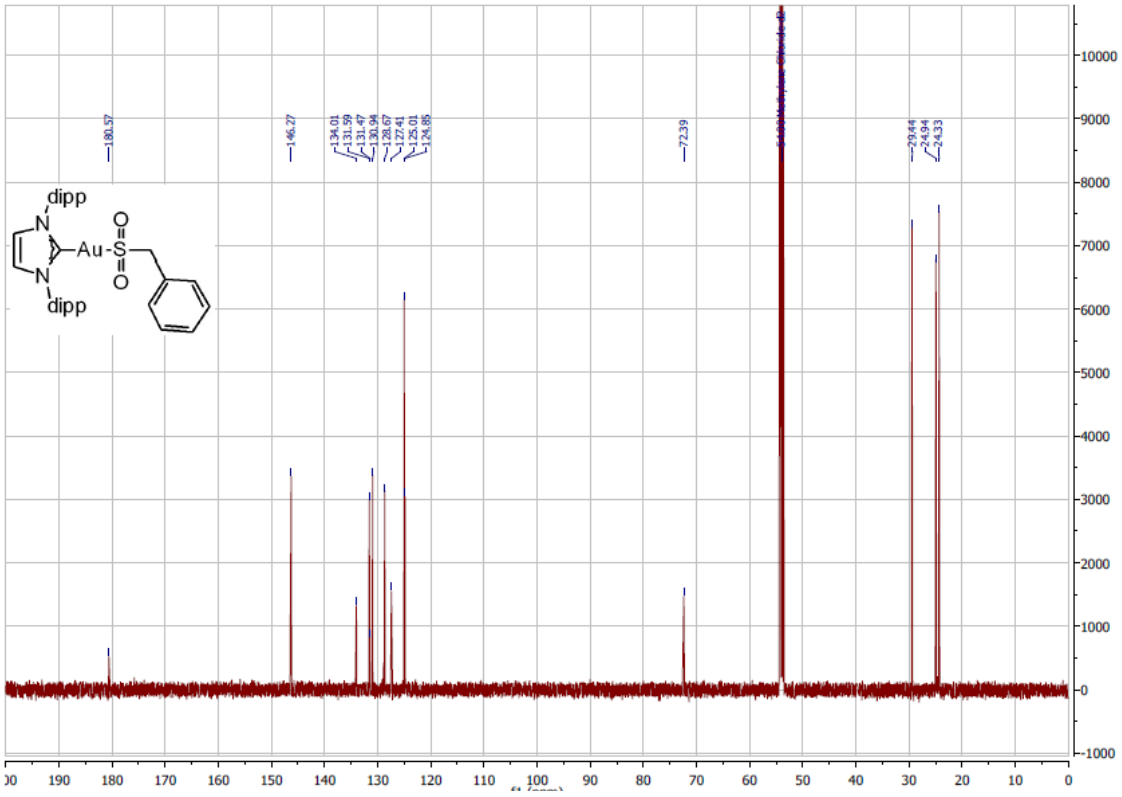
dipp
Au
dipp

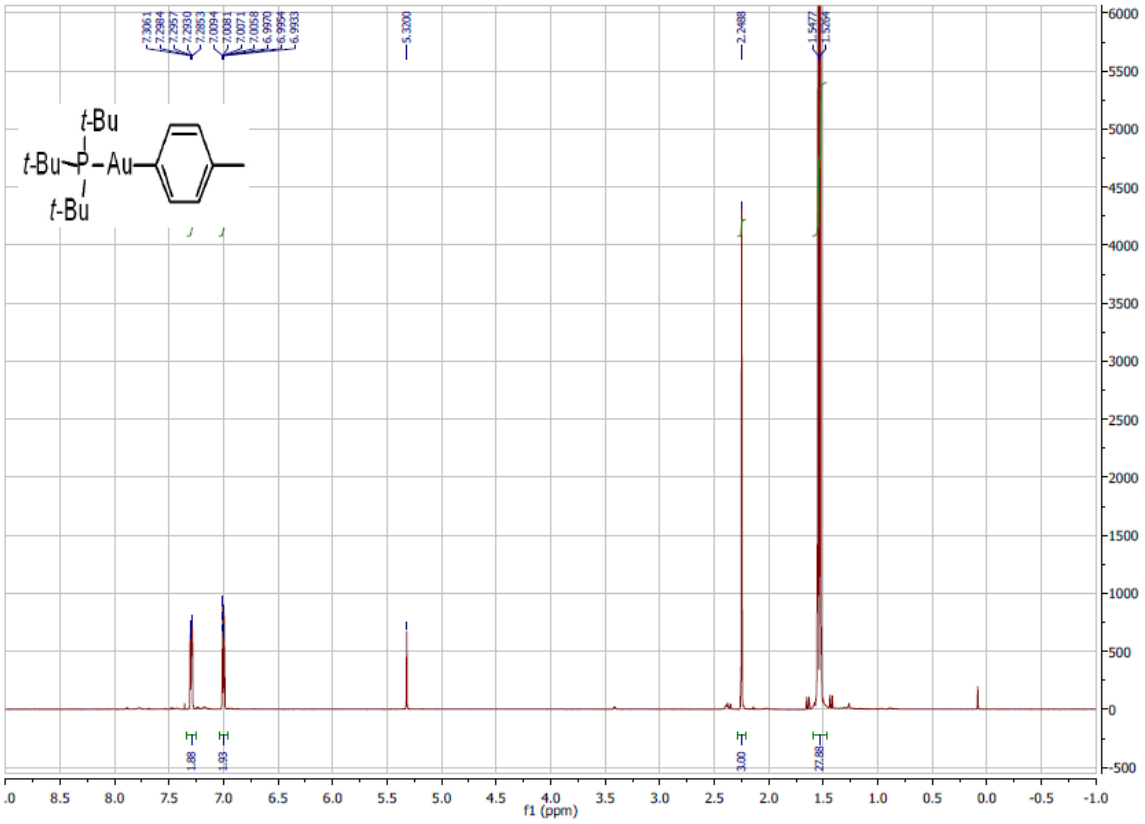
7.3061
7.2984
7.2957
7.2930
7.2853
7.0094
7.0081
7.0071
7.0058
6.9970
6.9954
6.9933
5.3200
2.2488
1.5477
1.5264
t-Bu
t-Bu
P
Au
t-Bu
1.88
1.93
3.00
27.88
f1 (ppm)

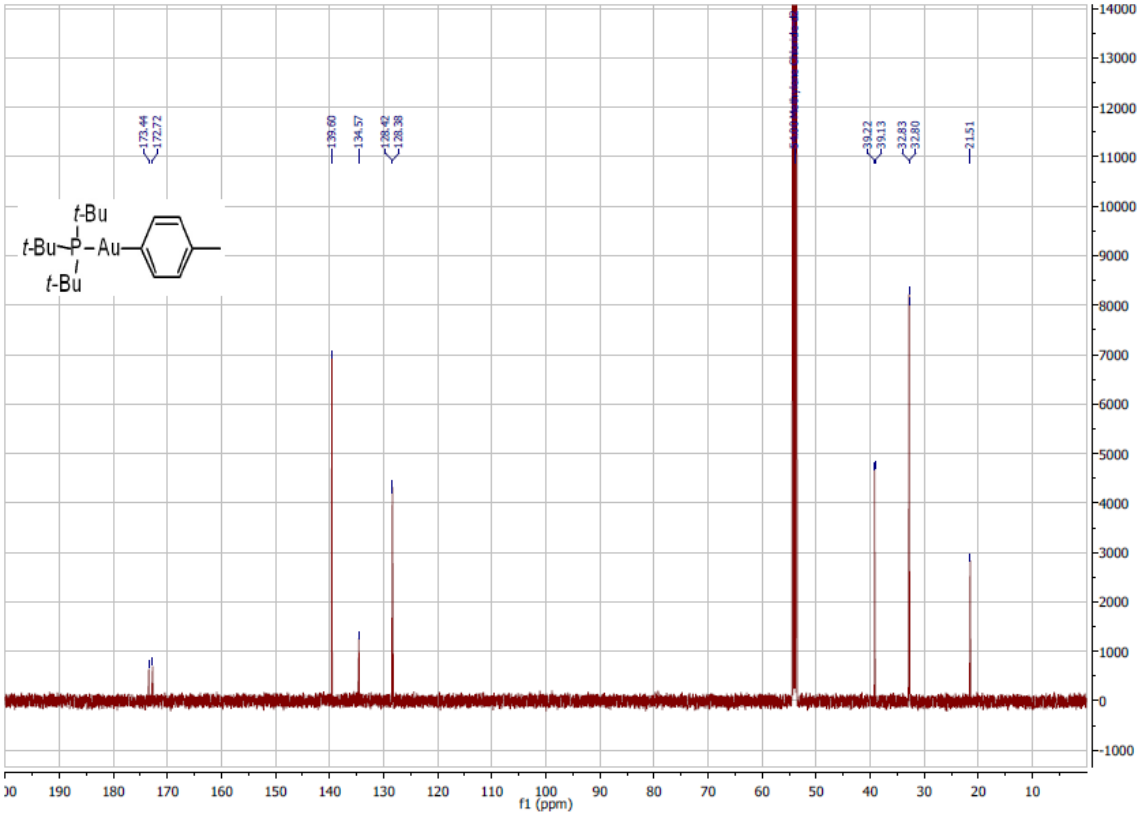
173.44
172.72
139.60
134.57
128.42
128.38
39.22
39.13
32.83
32.80
21.51
t-Bu
t-Bu
P
Au
t-Bu
f1 (ppm)

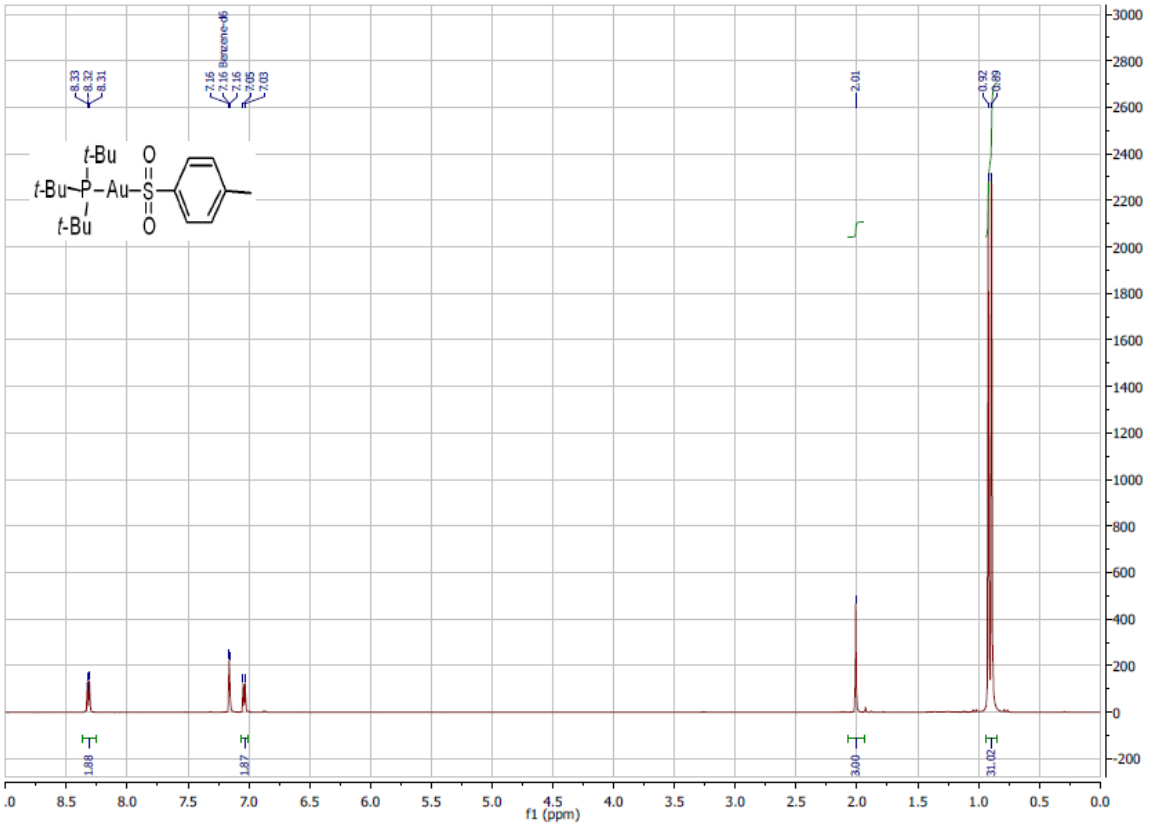
8.33
8.32
8.31
7.16
Benzene-d6
2.16
2.16
7.05
7.03
2.01
0.92
0.89
1.88
1.87
3.00
31.02
f1 (ppm)

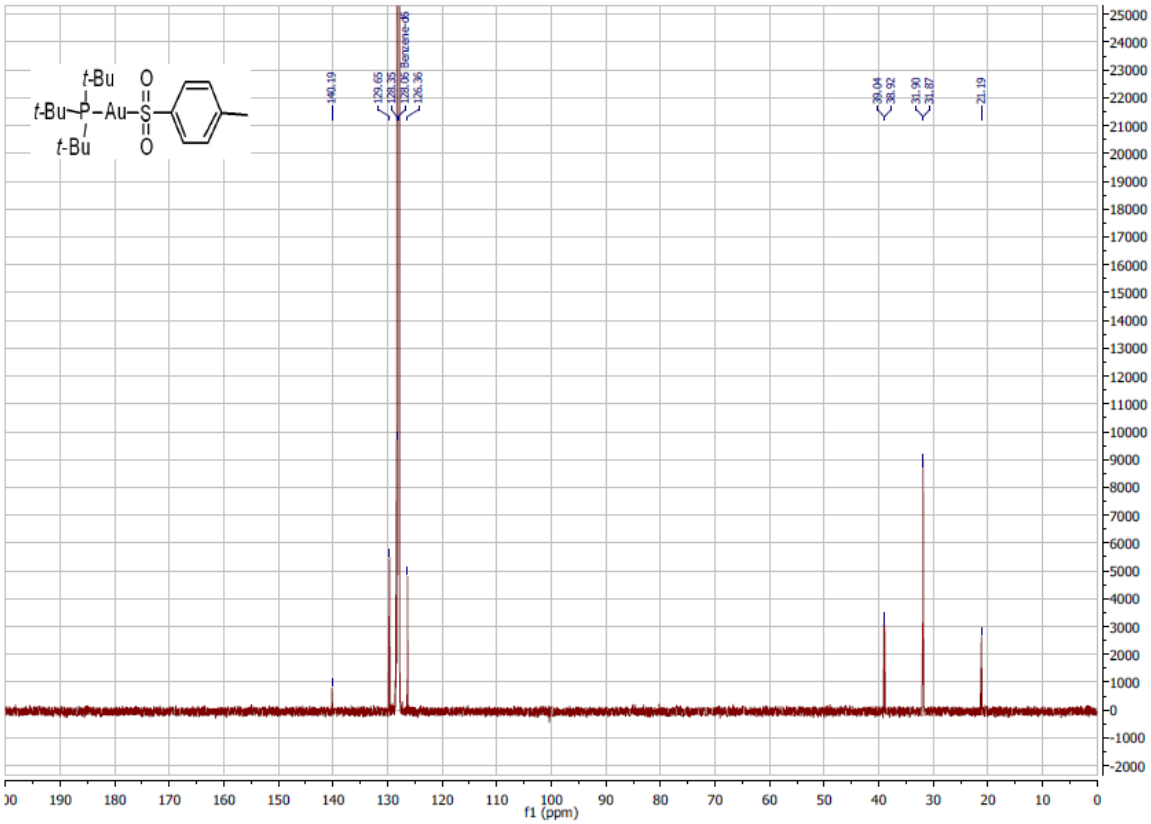
140.19
129.65
129.35
128.05
Benzene-d6
126.36
39.04
38.92
31.90
31.87
21.19
f1 (ppm)

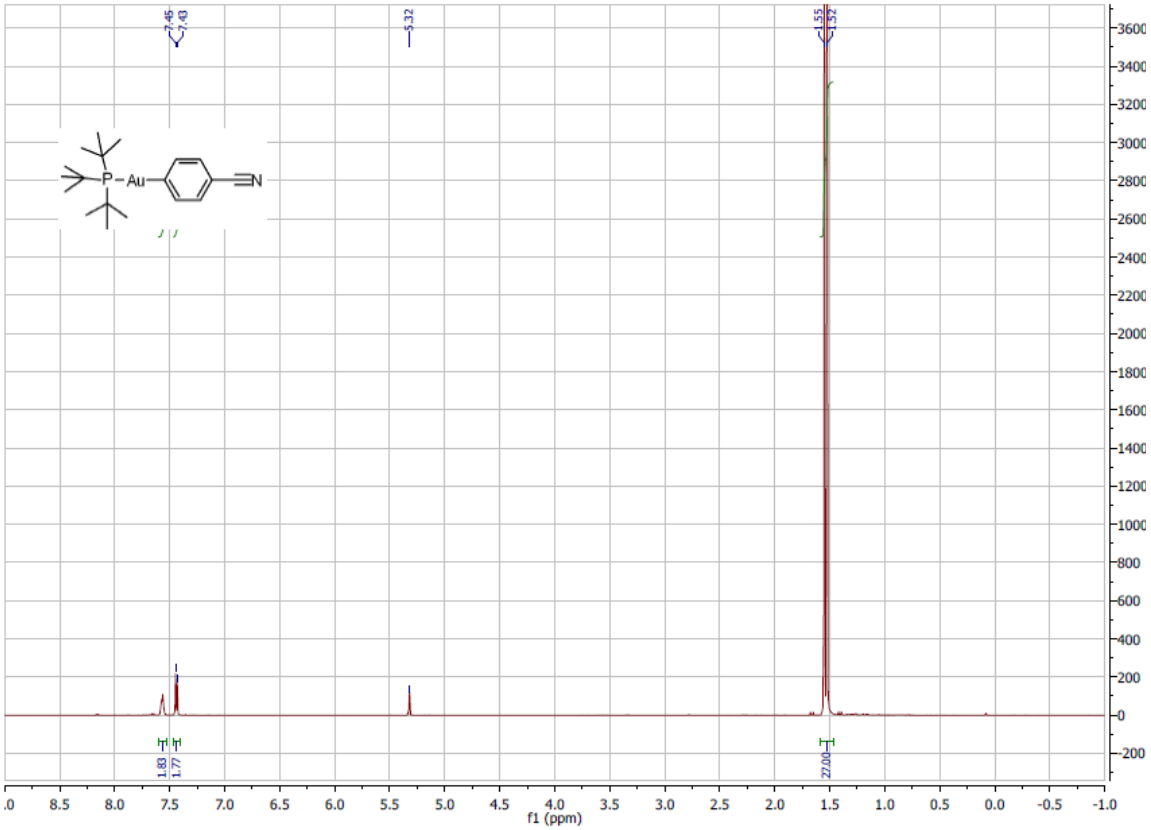
7.45
7.43
5.32
1.55
1.52
1.83
1.77
27.00
f1 (ppm)

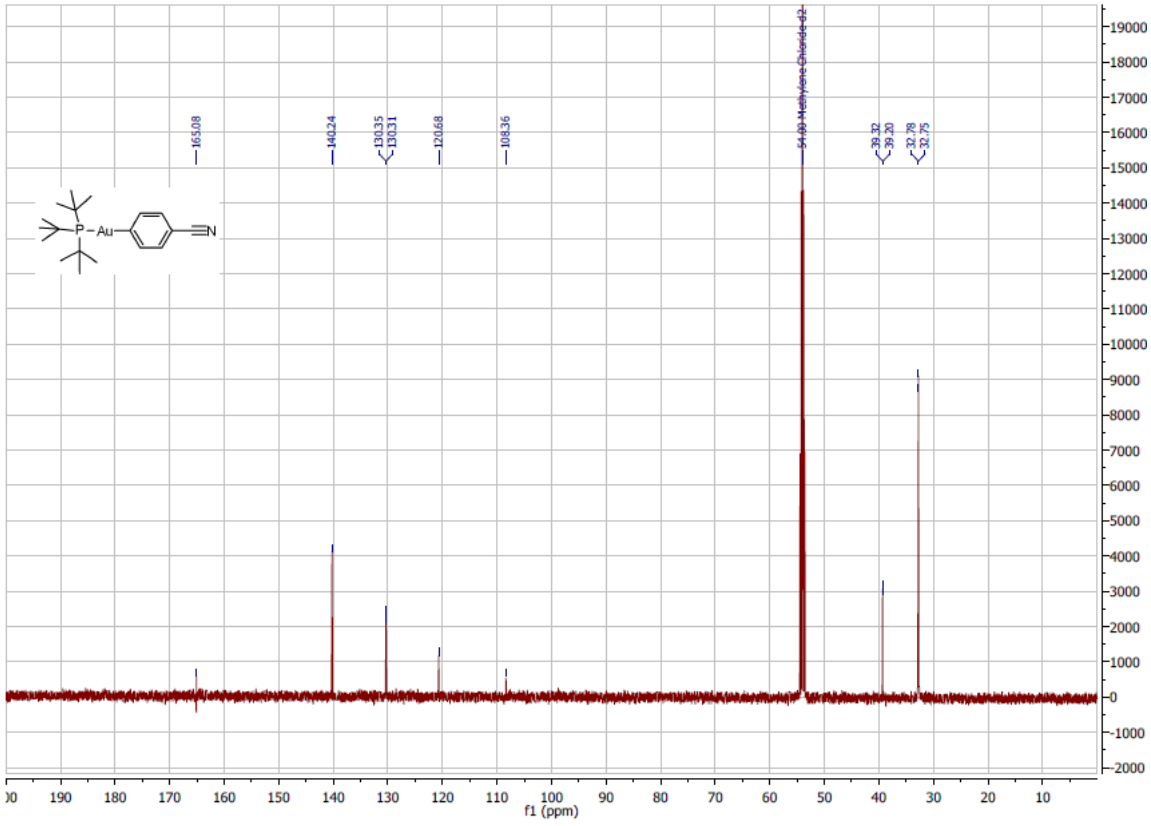
165.08
140.24
130.35
130.31
120.68
108.36
54.00 Methylene Chloride-d2
39.32
39.20
32.78
32.75
f1 (ppm)

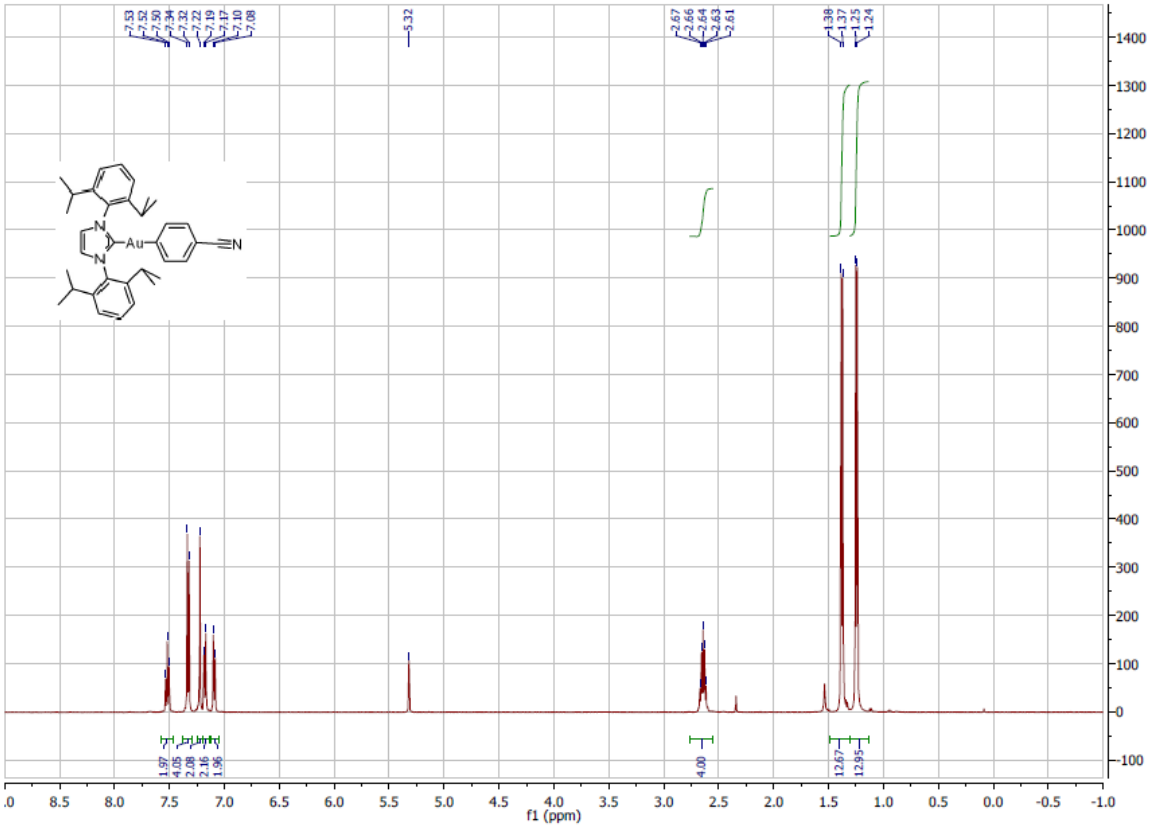
7.53
7.52
7.50
7.34
7.32
7.22
7.19
7.17
7.10
7.08
5.32
2.67
2.66
2.64
2.63
2.61
1.38
1.37
1.25
1.24
Au
N
CN
1.97
4.05
2.08
2.16
1.96
4.00
12.67
12.95
f1 (ppm)

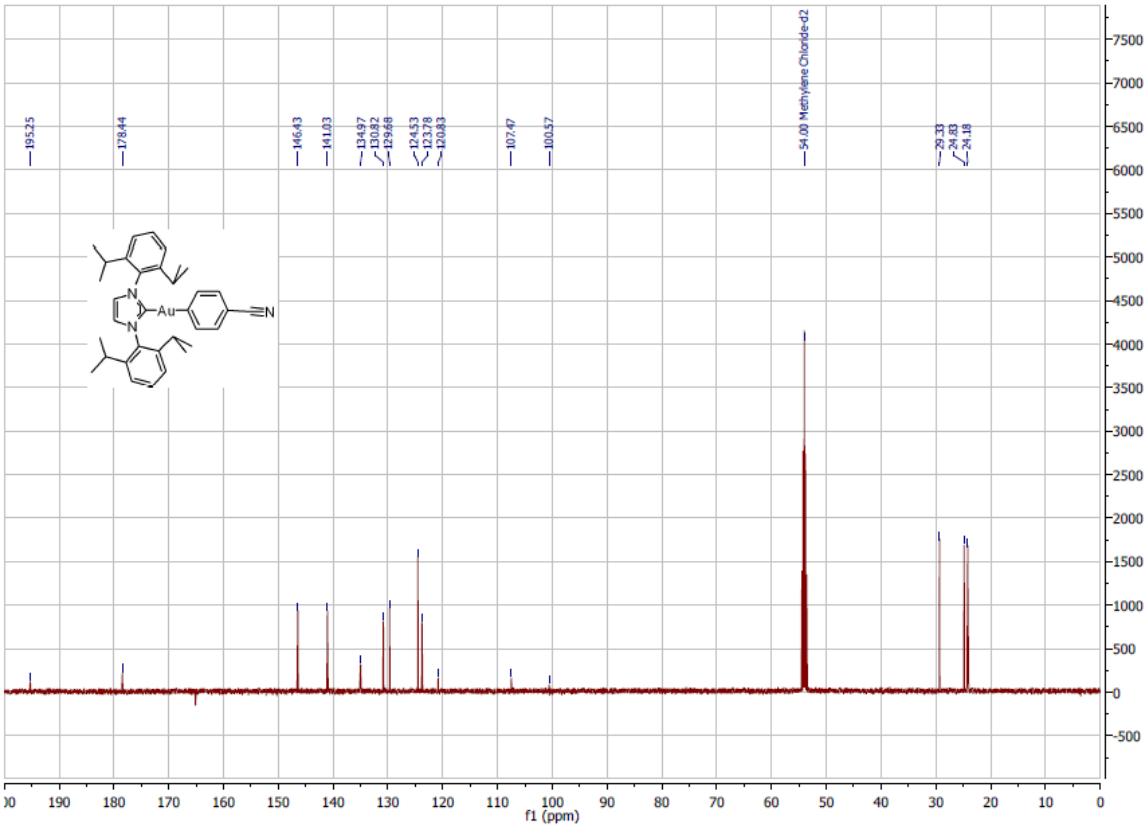
195.25
178.44
146.43
141.03
134.97
130.82
129.68
124.53
123.78
120.83
107.47
100.57
54.00 Methylene Chloride-d2
29.33
24.83
24.18
Au
N
CN
f1 (ppm)

X-Ray Crystallographic Tables

Complex 1

Table 1. Crystal data and structure refinement for iprau(so2)ph.

Identification code	shelxl	
Empirical formula	C34 H43 Au Cl2 N2 O2 S	
Formula weight	811.63	
Temperature	100(2) K	
Wavelength	0.71073 ≈	
Crystal system	Orthorhombic	
Space group	Pbca	
Unit cell dimensions	a = 19.409(2) ≈	α= 90∞.
	b = 14.6754(19) ≈	β= 90∞.
	c = 23.628(3) ≈	γ = 90∞.
Volume	6730.0(14) ≈^{3}	
Z	8	
Density (calculated)	1.602 Mg/m^3	
Absorption coefficient	4.625 mm^{-1}	
F(000)	3248	
Crystal size	0.08 x 0.03 x 0.03 mm^3	
Theta range for data collection	1.72 to 25.42∞.	
Index ranges	-23<=h<=23, -17<=k<=17, -22<=l<=28	
Reflections collected	192672	
Independent reflections	6165 [R(int) = 0.0602]	
Completeness to theta = 25.00∞	99.9 %	
Absorption correction	Semi-empirical from equivalents	
Max. and min. transmission	0.8737 and 0.7086	
Refinement method	Full-matrix least-squares on F^2	
Data / restraints / parameters	6165 / 0 / 387	
Goodness-of-fit on F^2	1.149	
Final R indices [I>2sigma(I)]	R1 = 0.0282, wR2 = 0.0534	
R indices (all data)	R1 = 0.0474, wR2 = 0.0638	
Largest diff. peak and hole	1.043 and -0.980 e.≈$^{-3}$	

Table 2. Atomic coordinates (x 10^4) and equivalent isotropic displacement parameters (≈^{2}x 10^3)
for iprau(so2)ph. U(eq) is defined as one third of the trace of the orthogonalized U^{ij} tensor.

	x	y	z	U(eq)
C(1)	3834(2)	808(3)	3142(2)	12(1)
C(2)	3976(2)	923(3)	4178(2)	15(1)
C(3)	4962(2)	766(3)	2892(2)	16(1)
C(4)	4934(2)	805(3)	3463(2)	14(1)
C(5)	3926(2)	148(3)	4521(2)	17(1)
C(6)	3647(2)	268(4)	5061(2)	22(1)
C(7)	3437(2)	1128(4)	5246(2)	24(1)
C(8)	3504(2)	1879(4)	4900(2)	22(1)
C(9)	3781(2)	1804(3)	4352(2)	18(1)
C(10)	4372(3)	3305(4)	4246(2)	35(1)
C(11)	3864(2)	2642(3)	3982(2)	22(1)
C(12)	3177(3)	3114(4)	3870(2)	34(1)
C(13)	4522(3)	-1349(4)	4766(2)	26(1)
C(14)	4144(2)	-794(3)	4313(2)	20(1)
C(15)	3519(3)	-1306(4)	4100(2)	34(1)
C(16)	4072(2)	744(3)	2114(2)	12(1)
C(17)	4074(2)	1553(3)	1805(2)	14(1)
C(18)	3864(2)	1497(3)	1238(2)	19(1)
C(19)	3652(2)	675(3)	1005(2)	19(1)
C(20)	3654(2)	-108(3)	1326(2)	18(1)
C(21)	3870(2)	-106(3)	1893(2)	15(1)
C(22)	4335(2)	-1704(3)	1968(2)	21(1)
C(23)	3866(2)	-980(3)	2235(2)	18(1)
C(24)	3127(2)	-1338(3)	2305(2)	23(1)
C(25)	4729(3)	3050(4)	1706(2)	29(1)
C(26)	4247(2)	2468(3)	2071(2)	19(1)
C(27)	3576(3)	2976(4)	2193(2)	30(1)
C(28)	1359(2)	905(3)	3881(2)	15(1)
C(29)	1836(2)	1011(3)	4309(2)	22(1)

C(30)	1602(3)	1093(4)	4866(2)	29(1)
C(31)	912(3)	1041(4)	4984(2)	27(1)
C(32)	440(2)	928(4)	4553(2)	25(1)
C(33)	658(2)	858(4)	3996(2)	23(1)
C(34)	2075(3)	1406(4)	1611(2)	26(1)
N(1)	4245(2)	831(3)	3607(1)	12(1)
N(2)	4286(2)	772(2)	2703(1)	12(1)
O(1)	1332(2)	1611(2)	2871(1)	24(1)
O(2)	1305(2)	-49(2)	2960(1)	25(1)
S(1)	1616(1)	806(1)	3149(1)	12(1)
Au(1)	2800(1)	806(1)	3131(1)	13(1)
Cl(1)	1769(1)	280(1)	1545(1)	27(1)
Cl(2)	1998(1)	2020(1)	965(1)	34(1)

Complex 2

Table 1. Crystal data and structure refinement for iprau(so2)bn_npm.

Identification code	npm046	
Empirical formula	C34 H43 Au N2 O2 S	
Formula weight	740.73	
Temperature	102(2) K	
Wavelength	0.71073 ≈	
Crystal system	Triclinic	
Space group	P-1	
Unit cell dimensions	a = 9.9184(3) ≈	α= 86.603(2)∞.
	b = 10.2997(3) ≈	β= 86.516(2)∞.
	c = 16.7473(5) ≈	γ = 71.061(2)∞.
Volume	1613.82(8) ≈^{3}	
Z	2	
Density (calculated)	1.524 Mg/m^3	
Absorption coefficient	4.654 mm^{-1}	
F(000)	744	
Crystal size	0.10 x 0.08 x 0.03 mm^3	
Theta range for data collection	2.09 to 36.35∞.	
Index ranges	-16<=h<=16, -16<=k<=16, 0<=l<=27	
Reflections collected	13585	
Independent reflections	13585 [R(int) = 0.0000]	
Completeness to theta = 36.35∞	86.7 %	
Absorption correction	Semi-empirical from equivalents	
Max. and min. transmission	0.8730 and 0.6533	
Refinement method	Full-matrix least-squares on F^2	
Data / restraints / parameters	13585 / 0 / 370	
Goodness-of-fit on F^2	0.310	
Final R indices [I>2sigma(I)]	R1 = 0.0384, wR2 = 0.0866	
R indices (all data)	R1 = 0.0461, wR2 = 0.0999	
Largest diff. peak and hole	7.926 and -1.717 e.≈$^{-3}$	

Table 2. Atomic coordinates (x 10^4) and equivalent isotropic displacement parameters ($\approx^2$x 10^3)
for iprau(so2)bn_npm. U(eq) is defined as one third of the trace of the orthogonalized U^{ij} tensor.

	x	y	z	U(eq)
Au(1)	5193(1)	6175(1)	7454(1)	14(1)
S(1)	2840(1)	6436(1)	7324(1)	18(1)
O(1)	2393(4)	6878(4)	6505(2)	28(1)
O(2)	2564(4)	5182(4)	7634(3)	27(1)
C(1)	7323(4)	5743(4)	7491(2)	13(1)
C(2)	9609(4)	5051(5)	7851(3)	16(1)
C(3)	9598(4)	5425(5)	7062(3)	17(1)
C(4)	7707(4)	5000(4)	8907(2)	14(1)
C(5)	7606(5)	5977(5)	9470(3)	17(1)
C(6)	7097(5)	5736(5)	10246(3)	22(1)
C(7)	6690(6)	4584(6)	10428(3)	23(1)
C(8)	6820(5)	3627(5)	9858(3)	21(1)
C(9)	7351(5)	3810(5)	9078(3)	16(1)
C(10)	7966(5)	7283(5)	9266(3)	20(1)
C(11)	9048(6)	7469(6)	9822(4)	29(1)
C(12)	6597(7)	8527(6)	9265(5)	40(2)
C(13)	7527(5)	2708(5)	8476(3)	20(1)
C(14)	8663(6)	1370(6)	8731(4)	28(1)
C(15)	6107(6)	2488(6)	8345(3)	26(1)
C(16)	7689(4)	6277(4)	6055(2)	13(1)
C(17)	7275(5)	7678(5)	5847(3)	17(1)
C(18)	6840(5)	8065(5)	5066(3)	19(1)
C(19)	6816(5)	7096(5)	4533(3)	20(1)
C(20)	7207(5)	5712(5)	4768(3)	18(1)
C(21)	7663(4)	5269(4)	5542(2)	15(1)
C(22)	7261(5)	8744(5)	6437(3)	21(1)
C(23)	8407(6)	9396(7)	6214(5)	38(2)
C(24)	5785(6)	9830(7)	6518(4)	35(1)
C(25)	8003(5)	3767(5)	5806(3)	19(1)

C(26)	9198(6)	2846(5)	5281(3)	24(1)
C(27)	6643(6)	3362(6)	5816(4)	33(1)
C(28)	1696(5)	7785(5)	7935(3)	23(1)
C(29)	2009(5)	9129(5)	7825(3)	19(1)
C(30)	2838(6)	9469(5)	8370(3)	24(1)
C(31)	3111(6)	10718(6)	8287(3)	26(1)
C(32)	2549(6)	11654(6)	7663(4)	28(1)
C(33)	1734(6)	11313(6)	7110(4)	30(1)
C(34)	1482(6)	10057(6)	7188(3)	27(1)
N(1)	8191(4)	5250(4)	8100(2)	13(1)
N(2)	8189(4)	5837(4)	6852(2)	13(1)

Chapter 3. Development of an Enantioselective Hydroazidation of Allenes Catalyzed by Gold(I)

Introduction

The catalytic hydrofunctionalization of unsaturated substrates – the addition of an H-X bond across a double or triple bond - is important for both its atom economy and the availability of a vast pool of unsaturated substrates (eq 1). As a result, this has become an area of intense research.[1] Despite the numerous reports of hydrofunctionalization, the subfield of hydroazidation (eq 2), specifically asymmetric hydroazidation, remains underexplored.

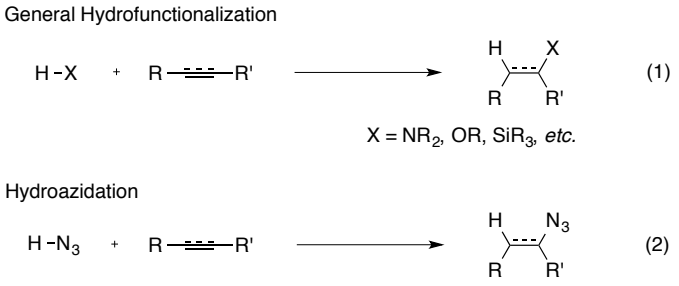

The azidation (as opposed to *hydro*azidation) of an unsaturated substrate is common. This process has been dominated by the Tsuji-Trost reaction, in which an allylic leaving group is substituted for an azide *via* a π-allyl intermediate (eq 3). This method has over twenty years of proven utility, and the reaction proceeds with predictable stereochemistry depending on the nature of the nucleophile;[2-5] however, this method requires an activated substrate and has never been rendered enantioselective for azidation.

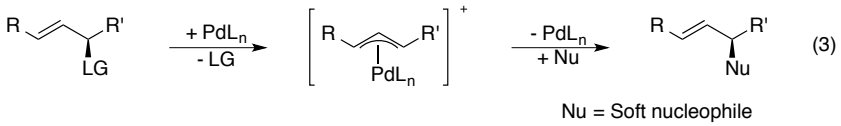

Catalytic hydroazidation has been accomplished with both metal-based and organic catalysts (Figure 1). Carreira and co-workers have employed cobalt catalysts in the hydroazidation of olefins,[6,7] but this transformation has yet to be rendered enantioselective, likely due to the radical mechanism by which it proceeds (Figure 1a). Jacobsen has developed an enantioselective hydroazidation using aluminum salen catalysts; however, only α,β–unsaturated amides are viable substrates as the reaction occurs *via* conjugate addition (Figure 1b).[8] Enantioselective hydroazidation has also been realized using peptides as catalysts, but again with a scope limited to α,β–unsaturated amides (Figure 1c).[9]

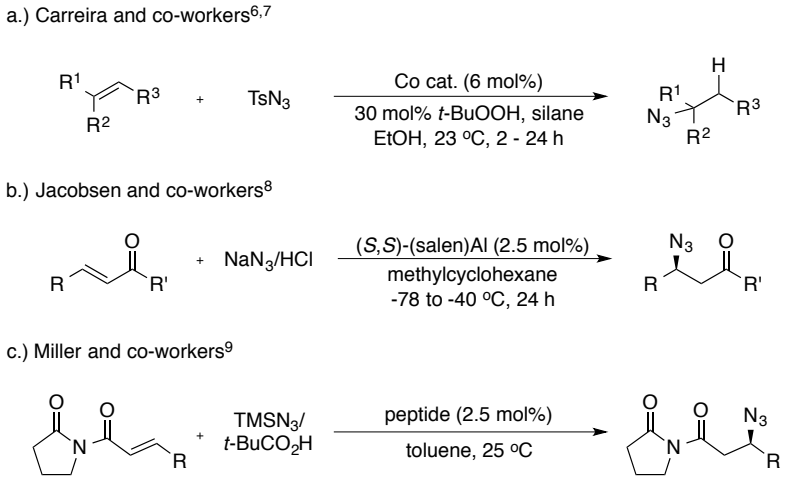

Figure 1. Methods for catalytic hydroazidation

Despite the progress made in hydroazidation, enantioselective methods for the hydroazidation of unactivated double bonds have not yet been reported, to the best of our knowledge. In part, this may be attributed to two factors: undesired ligation of the azide to the catalyst (in the case of metal-catalyzed reactions) and susceptibility of the enantioenriched product toward racemization. To address the first issue, a metal that does not readily form strong bonds with azides would be ideal. Gold, a very soft metal, forms bonds with azides under conditions that employ thallium as a halide abstracting agent or by reaction of a preformed gold acetate with $TMSN_3$ (Scheme 1).[10] The harsh conditions required to form an Au-N_3 bond suggest that catalyst death due to the formation of this linkage is unlikely. The prominence of gold in other areas of hydrofunctionalization makes it a natural candidate for hydroazidation.[11] In fact, during the development of the method described in this chapter, Muñoz and co-workers independently demonstrated the hydroazidation of allenes with gold(I) catalysts to form racemic mixtures of regioisomers (eq 4).[12]

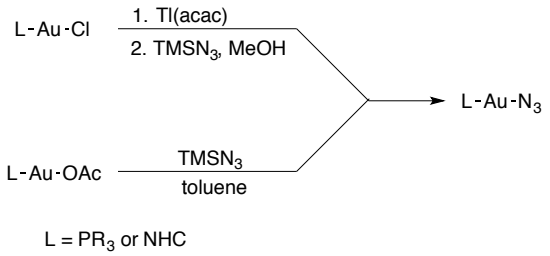

Scheme 1. Synthesis of gold(I) azides[12]

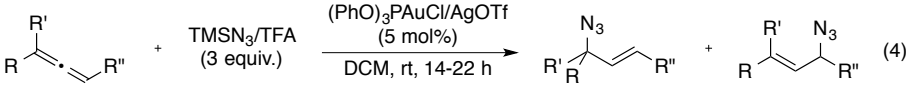

Choice of substrate would be integral in developing a gold-catalyzed enantioselective hydroazidation. Both the hydroazidation of alkenes and allenes pose considerable challenges. Gold has been employed in hydroamination of alkenes but the

high temperatures required for turnover disfavor kinetic control.[13] Hydroazidation of allenes results in a mixture of regioisomers; however, judicious choice of allene could eliminate the problem of multiple products.

The possible formation of two regioisomers of an allyl azide could be a result of the Winstein rearrangement (Figure 2).[14-16] This [3,3]-sigmatropic rearrangement is likely a concerted process, and not an ionization event, as demonstrated by the negative entropy of the rearrangement and a lack of dependence on solvent polarity; however, the existence of a tight ion pair has cannot to date be discounted. A single regioisomer can be favored through trapping[17] but an unelaborated allyl azide would be preferred, as it would possess potential for further manipulation (for instance, subsequent hydrogenations or cycloadditions). Inspection of the literature reveals that cinnamyl azides may be isolated as a single regioisomer.[18] Though these compounds may undergo this rearrangement, the stereospecifity of the reaction would not erode a stereocenter.

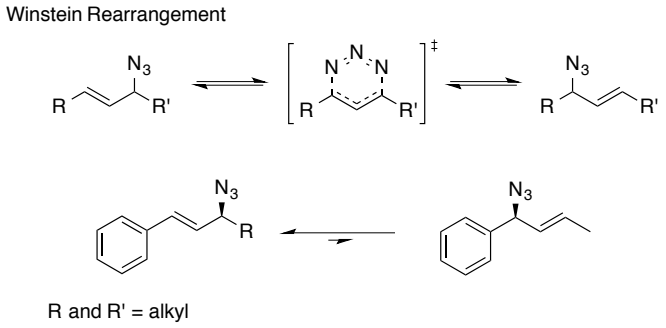

Figure 2. The Winstein rearrangement

This chapter relates the progress achieved in developing an enantioselective hydroazidation to form cinnamyl azides. Reaction optimization and mechanistic studies that provide insight into the factors necessary to effect this transformation are presented.

Results

The feasibility of the desired transformation was first evaluated using achiral [1,3-bis(2,6-diisopropylphenyl)imidazol-2-ylidene]gold(I) triflate (IPrAuOTf) (Table 1). This catalyst was chosen due to its high solubility and its lack of a strongly ligating X-type ligand, obviating the need for a halide abstracting agent. Trimethylsilyl azide ($TMSN_3$) was chosen as the azide source since the hydrazoic acid, the hydroazidation agent, and innocuous trimethylsilyl fluoride would form upon treatment with a source of hydrofluoric acid (HF). A survey of various HF sources showed that hydroazidation in the presence of gold(I) was indeed possible with 1-phenyl-1,2-butadiene (**1**) (Table 1). In the absence of catalyst, no background reaction was observed with triethylamine trihydrofluoride (3 HF-TEA) (entry 1) but three turnovers were achieved in the presence of IPrAuOTf to form the cinnamyl azide **3** (entry 2). Other HF sources proved inferior (entries 3 and 4).

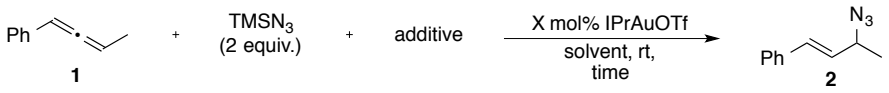

entry	solvent	additive (equiv.)	time (h)	X	conv (%)[a]
1	DCM-d_2	3 HF•TEA (1.4)	24	0	0
2	DCM-d_2	3 HF•TEA (1.7)	5	10	29
3	DCM-d_2	TASF (1.0	17	10	< 5
4	$MeNO_2$-d_3	KHF_2 (2.0)	17	10	17

[a] Percent conversion to desired product determined by ^{1}H NMR

Table 1. Preliminary hydroazidation with various fluoride sources

These promising first results prompted reevaluation of the hydrazoic acid source. A more innocuous byproduct would be preferred, as TEA could easily ligate to gold(I) and thus block the open coordination site needed for catalysis. Carboxylic acids were identified as a potential replacement due to literature reports of their use in forming HN_3 from $TMSN_3$.[9] Trifluoroacetic acid (TFA) was chosen, since its conjugate base would be less likely to ligate to gold(I) than would weaker acids. No background reaction was observed when allene **1** was treated with a TFA/$TMSN_3$ mixture (Table 2, entry 1). In the presence of gold, modest turnover was achieved upon simultaneous additions of catalyst and TFA/$TMSN_3$ mixture (entry 2). When TFA and $TMSN_3$ were incubated for approximately 20 min before the addition of gold, the reaction yield increased dramatically (entry 3). The presence of unreacted TFA might result in ligation of trifluoroacetate to gold, necessitating a slight excess of $TMSN_3$ and that catalyst be added following all other reagents.

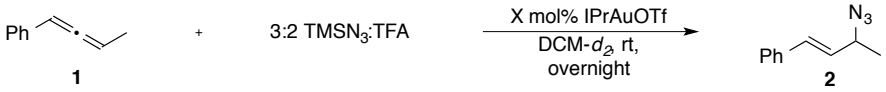

entry	X	yield (%)[a]
1	0	0
2[b]	5	20
3	5	77

[a] Determined by ^{1}H NMR versus 1,4-dioxane as a standard
[b] Catalyst was added immediately after addition of $TMSN_3$/TFA

Table 2. Hydroazidation using $TMSN_3$/TFA

With the reactivity of this system established, focus shifted to rendering the transformation enantioselective. This phase of investigation was initially hindered by irreproducible results, specifically highly variable levels of enantioselectivity. To rationalize these data, it was then posited that the catalyst may epimerize the product. This was tested by subjection of enantioenriched **1** to IPrAuOTf (Table 3). Indeed, a precipitous drop in enantiomeric excess was observed in less than an hour using DCM as

solvent. Racemization was not observed using dioxane as solvent, even after 11 h, nor in the absence of IPrAuOTf for either solvent. These results indicated that judicious choice of catalyst and solvent were both needed in order to achieve enantioselectivity and prevent erosion of enantiomeric excess.

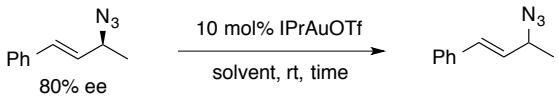

time (h)	DCM ee (%)	dioxane ee (%)
0	80	80
0.5	52	80
1	46	80
4	40	78
11	36	76

Table 3. Racemization of enantioenriched **1**

The ability of various chiral gold(I) catalysts to induce enantioselectivity was canvassed (Table 4). Common catalysts employed in enantioselective gold(I) catalysis were investigated, but in all cases only moderate yield and low enantioselectivity were achieved (entries 1-3). Use of a bimetallic acyclic diaminocarbene (ADC) gold(I) catalyst (**5**), based on a scaffold previously utilized by the Toste group,[19] resulted in good enantioselectivity and moderate yield (entry 5). When the enantioselectivity of the reaction was monitored over a number of time points, it was found that no erosion of enantiomeric excess was observed over the course of 16 h (Table 5).

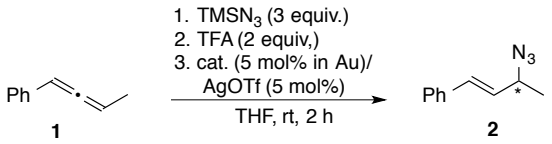

entry	cat.	yield (%)[a]	ee (%)
1	R-DM SEGPHOS	50	20
2	R-DTBM BINAP	49	10
3	**3**	35	2
4	**4**	0	-
5	**5**	33	60

[a] Determined by ^{1}H NMR versus 1,3,5-trimethoxybenzene as a standard

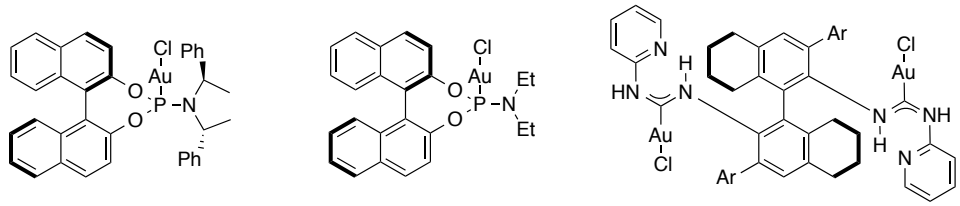

3 **4** **5**

Table 4. Catalyst survey for enantioselective hydroazidation

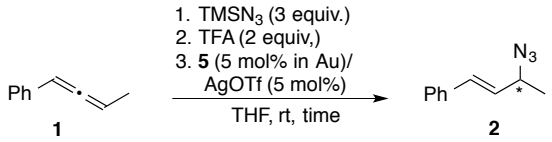

entry	time (h)	ee (%)
1	1	57
2	2	60
3	16	60

Table 5. Enantiomeric excess of **2** as a function of time

Conclusion

The first enantioselective hydroazidation of an unactivated π-bond has been achieved using a bimetallic ADC gold(I) catalyst. Studies on this transformation are ongoing. Further optimization and expansion of substrate scope are required to enhance the utility of this transformation. Additionally, mechanistic experiments centered on interactions between the catalyst and product will provide valuable insight as to why this

particular catalyst does not erode enantiomeric excess, where similar NHC gold(I) catalysts do.

Experimental

General Information

All experiments were conducted in a fume hood without precautions to exclude air or moisture. All NMR spectra were obtained at ambient temperature using Bruker AV-600, DRX-500, AV-500, AVB-400, AVQ-400, or AV-300 spectrometers. Enantiomeric excesses were determined using a Shimadzu Chiral HPLC. ^{1}H NMR chemical shifts (δ) are reported in parts per million (ppm) relative to residual solvent peaks (5.32 ppm for CD_2Cl_2 and 7.26 ppm for $CDCl_3$).

Materials

Reagents were purchased from commercial suppliers, checked for purity and used without further purification unless otherwise noted. Tetrahydrofuran and methylene chloride were dried and purified by passage through a column of activated alumina (type A2, 12 x 32, UOP LLC). IPrAuOTf[20] and 1-phenyl-1,2-butadiene[21] were prepared according to literature methods. Synthesis of complex **5** is adapted from a literature procedure.[19,22] Enantioenriched **1** was prepared by a literature method.[3]

Reactivity Studies (Tables 1 and 2)

All reactions in Tables 1 and 2 were performed in a J. Young tube and monitored by ^{1}H NMR. The sole exception is entry 4 of Table 1 in which the reaction mixture was stirred in a 1-dram vial due to heterogeneity. The ^{1}H NMR properties of the product matched those in the literature.[18]

Enantioselectivity Studies

Racemization Experiment (Table 3)

Enantioenriched azide in solvent (0.1 M) was stirred in a 1-dram vial with IPrAuOTf (10 mol%). Periodically, an aliquot of the reaction mixture was removed *via* pipette and analyzed by chiral HPLC.

Catalyst Screen (Tables 4 and 5)

Allene **1** (13 mg, 0.10 mmol) was dissolved in THF (0.5 mL) in a 1-dram vial. To the stirred solution was sequentially added $TMSN_3$ (40 μL, 0.30 mmol) and TFA (15 μL, 0.20 mmol). In a separate vial, catalyst (5 mol% in Au) and AgOTf (5 mol%) in THF (0.5 mL) were sonicated for approximately 1 min. The resulting heterogeneous mixture was filtered *via* syringe filter directly into the vial containing the allene solution. The reaction mixture was stirred for 2 h, at which time it was concentrated and passed through a short plug of silica using 9:1 EtOAc:hexanes. The resulting crude product was dissolved in $CDCl_3$ with 1,3,5-trimethoxybenzene (0.011 mmol) as a standard, and the

reaction yield determined by ^{1}H NMR. The sample was then concentrated and analyzed by chiral HPLC to determine enantiomeric excess.

(*E*)-(3-azidobut-1-en-1-yl)benzene

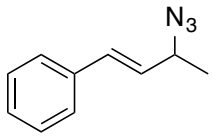

The ^{1}H NMR properties of this compound matched those in the literature.[18] HPLC (Whelk column) 100:0 (hexane:*i*-PrOH) 0.5 mL/min; T_{major} (17.0 min), T_{minor} (16.1 min); 60% *ee*.

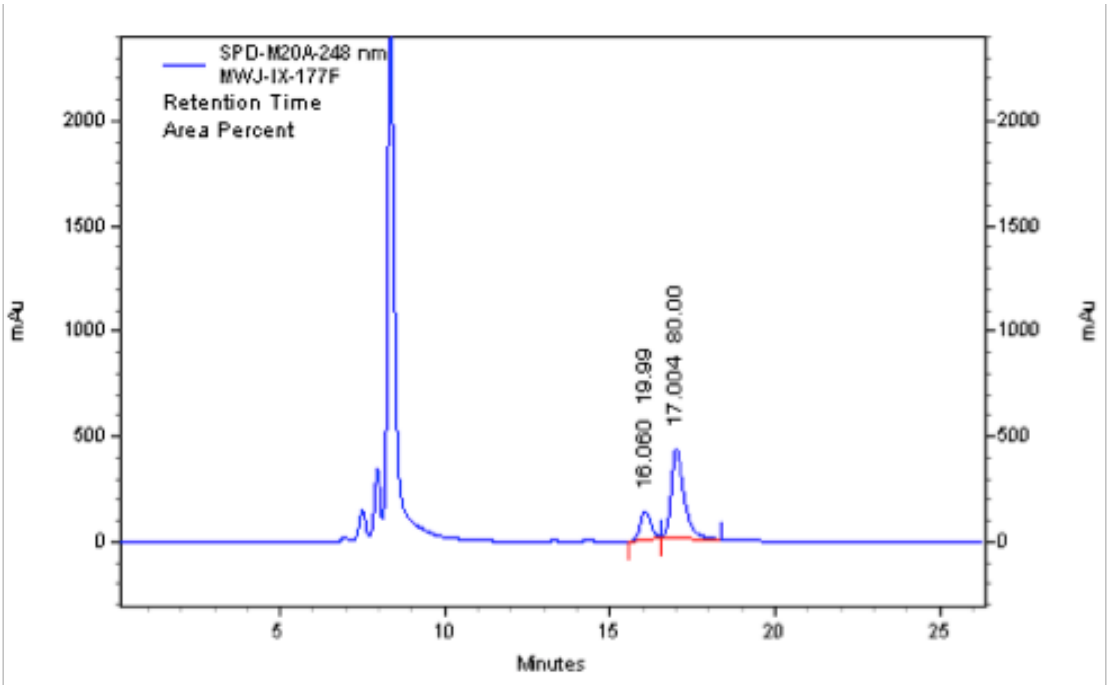

References

1. Ananikov, V. P.; Tanaka, M. *Top. Organomet. Chem.* **2013***, 43*, 1.
2. Murahashi, S.; Taniguchi, Y.; Imada, Y.; Tanigawa, Y. *J. Org. Chem.* **1989***, 54*, 3292.
3. Schuster, M.; He, W.; Blechert, S. *Tetrahedron Lett.* **2001***, 42*, 2289.
4. Le Bras, J.; Muzart, J. *Tetrahedron Lett.* **2011***, 52*, 5217.
5. Safi, M.; Fahrang, R.; Sinou, D. *Tetrahedron Lett.* **1990***, 31*, 527.
6. Waser, J.; Nambu, H.; Carreira, E. *J. Am. Chem. Soc.* **2005***, 127*, 8294.
7. Waser, J.; Gaspar, B.; Nambu, H.; Carreira, E. M. *J. Am. Chem. Soc.* **2006***, 128*, 11693.
8. Myers, J.; Jacobsen, E. *J. Am. Chem. Soc.* **1999***, 121*, 8959.
9. Guerin, D.; Miller, S. *J. Am. Chem. Soc.* **2002***, 124*, 2134.
10. Partyka, D. V.; Robilotto, T. J.; Updegraff, J. B., III; Zeller, M.; Hunter, A. D.; Gray, T. G. **2009***, 28*, 795.
11. Corma, A.; Leyva-Perez, A.; Sabater, M. J. *Chem. Rev.* **2011***, 111*, 1657.
12. Hurtado-Rodrigo, C.; Hoehne, S.; Munoz, M. P. *Chem. Commun.* **2014***, 50*, 1494.
13. Zhang, Z.; Lee, S. D.; Widenhoefer, R. A. *J. Am. Chem. Soc.* **2009***, 131*, 5372.
14. Gagneux, A.; Winstein, S.; Young, W. *J. Am. Chem. Soc.* **1960***, 82*, 5956.
15. Vander Werf, C. A.; Heasley V. L *J. Org. Chem.* **1966***, 31*, 3534.
16. Craig, D.; Harvey, J. W.; O'Brien, A. G.; White, A. J. P. *Org. Biomol. Chem.* **2011***, 9*, 7057.
17. Feldman, A.; Colasson, B.; Sharpless, K.; Fokin, V. *J. Am. Chem. Soc.* **2005***, 127*, 13444.
18. Rueping, M.; Vila, C.; Uria, U. *Org. Lett.* **2012***, 14*, 768.
19. Wang, Y.; Kuzniewski, C. N.; Rauniyar, V.; Hoong, C.; Toste, F. D. *J. Am. Chem. Soc.* **2011***, 133*, 12972.
20. Tsui, E. Y.; Mueller, P.; Sadighi, J. P. *Angew. Chem., Int. Ed.* **2008***, 47*, 8937.
21. Myers, A.; Zheng, B. *J. Am. Chem. Soc.* **1996***, 118*, 4492.
22. Khrakovsky, D.; Toste, F. D. *Unpublished results*

Chapter 4. Synthesis of Stable Gold(III) Pincer Complexes with Anionic Heteroatom Donors

Introduction

Coordination compounds of gold(III) are valuable in medicine,[1-5] materials science,[6,7] and catalysis.[8-10] Despite the utility of this high valent metal, gold(III) remains underexplored compared to gold(I), due in part to the propensity of gold(III) complexes to undergo decomposition *via* reduction[11-13] and protodemetallation.[14] The development of new stabilizing ligands would improve understanding and better enable harnessing the potential of this metal center.

Pincer ligands, members of a ligand class that have been exploited for decades in catalysis and structurally remarkable[15-17] compounds across the transition metals, have received relatively little attention in advancing the chemistry of gold(III). The works of Che, Yam, and Bochmann have demonstrated that cyclometallated 2,6-diphenylpyridine complexes of gold(III) exhibit electronic properties of interest in the development of photoluminescent materials[7,18-20] and the capacity to support highly reactive ligands.[21-23] The chemistry of other pincer ligands on gold(III) has not been explored to such depth.[5,24] Surprisingly, X-type heteroatom ligands are utilized in only a few examples of gold(III) pincer complexes[9,24] even though bidentate 2-pyridyl carboxylate[25] and 2-pyridyl amidate complexes[26,27] of gold(III) show catalytic and biological activity, respectively. Tridentate analogues of the ligands that support these compounds are well-documented in stabilizing other d^8 metal centers[28-31] and yet, to our knowledge, have not been extended to gold(III). This precedent and the use of other X_2L-type ligands to stabilize highly electrophilic metals suggest that bis(anionic) heteroatom-rich ligands[32] may serve as excellent ancillary ligands for gold(III). In addition, such ligands may prevent the reduction of gold(III) to gold(I), which would be of value as the oxidation state of gold catalysts can have a profound impact on product distributions in catalysis[33,34] and the potency of gold-containing therapeutics.[1,35]

Herein we report the synthesis, structural characterization, electrochemical analysis, and reactivity studies of gold(III) pincer complexes stabilized by gold-heteroatom bonds. The results of this study demonstrate that gold(III) complexes supported by iminothiolate and amidate pincer ligands are remarkably stable and less susceptible to reduction than analogues with carboxylate linkages. These findings in turn can inform ligand design for the diverse applications of gold(III) complexes.

Results and Discussion

All pincer complexes were accessed *via* salt metathesis of commercially available tetrahaloaurate salts (Scheme 1). The reaction of 2,6-dipicolinic acid **1** with $KAuCl_4$ in the presence of Ag_2CO_3 yielded the desired compound **2**, albeit in low yield. The identity of the compound was confirmed by ^1H NMR, elemental analysis, and the diagnostic infrared spectrum of the complex, which exhibited a strong absorption band at 1707 cm^{-1} for the carbonyl stretch, as has been observed for other gold(III) picolinate compounds.[36] Dipotassium bis(amidate) ligands **3** and **4** underwent salt metathesis with $KAuCl_4$ to yield complexes **5** and **6**, respectively. Similarly, bis(iminothiolate) complexes **8** and **9** were prepared in moderate to good yield by metallation of **7** with the appropriate tetrahaloaurate salt. For all compounds, one linkage isomer was formed, and the

structures of **5**, **8**, and **9** were confirmed unambiguously by single crystal X-ray diffraction (Figure 1).

Scheme 1. Synthesis of Gold(III) Pincer Complexes

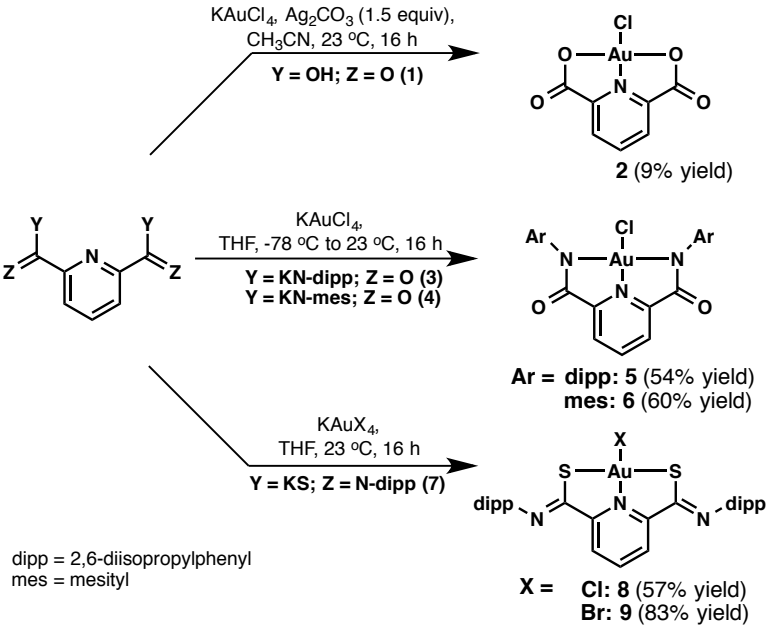

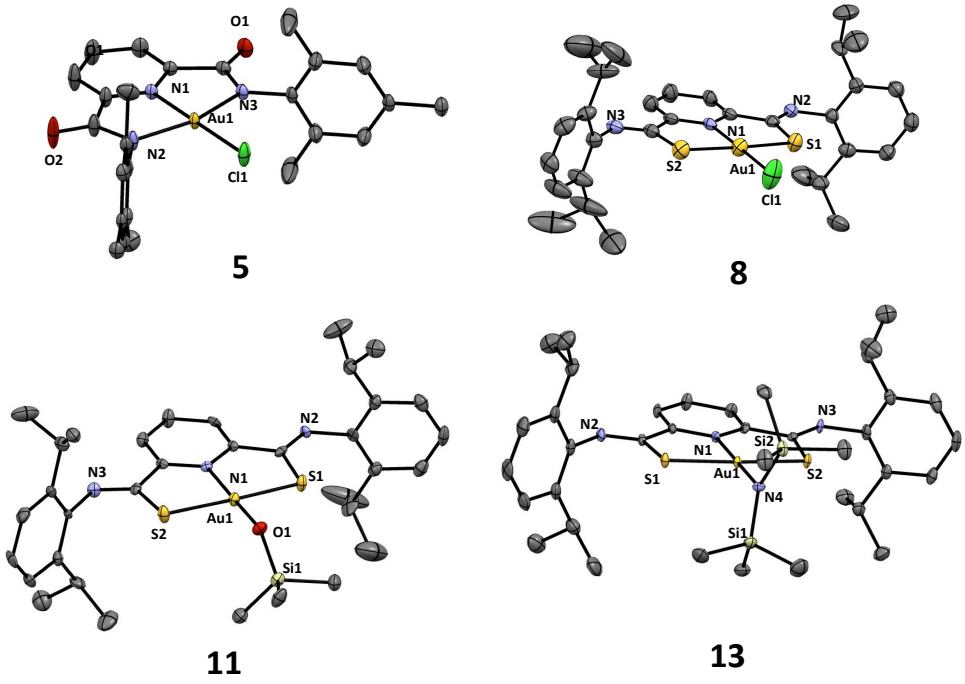

Figure 1. Solid-state structures of complexes **5**, **8**, **11**, and **13**. Thermal ellipsoids are shown at the 50% probability level. Hydrogen atoms and solvent molecules are omitted for clarity.

We first sought to probe the fundamental reactivity of these new complexes. Attempts to add new ligands to **5** and **6** *via* transmetallation were unsuccessful, presumably due to projection of the amidate aryl rings around the chloride; however, the less sterically congested coordination sphere of **8** permitted access to a variety of ligand substitutions. For example, complex **8** was treated with diphenylzinc to yield the organometallic compound **10** (Figure 2). Given our groups' interest in the reactivity of gold-heteroatom bonds, we next attempted substitution of the chloride with X-type heteroatom donors. An initial survey of various alkyl and aryl thiolates, amides and oxides led to no reaction or decomposition. Though previously reported methods designed to install heteroatom donors were unsuccessful, [37,38] it was found that salt metathesis with silyl amides, thiolates, and oxides yielded the first examples of gold(III) complexes with silyl-substituted heteroatoms as ligands (**11-13**), and silanoate **12** and silylamide **14** were subsequently characterized by X-ray diffraction in the solid state (Figure 1). The marked difference in reactivity between these ligands and their hydrocarbyl analogues remains unclear but may be attributed to attenuation of electron density at the heteroatom, which may in turn prevent reduction at the metal center.

Scheme 2. Ligand exchange with **4**.

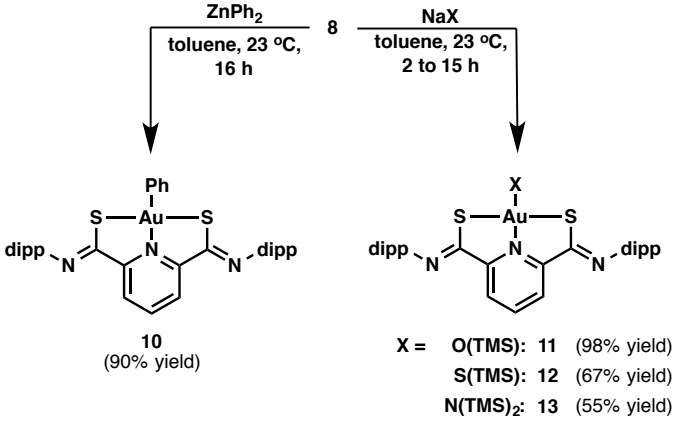

Our interest in using these complexes to effect catalytic transformations led us to examine a number of reactions known to involve gold(III) precatalysts, such as C-H activation [39] and cycloadditions. [40,41] Halide abstraction from complexes **5**, **6**, **8**, and **9** to open a coordination site were unsuccessful and treatment of complexes **10**-**14** with a host of electrophiles led to no reaction or decomposition. Surprisingly, reaction of **8** even with triflic acid did not lead to protonolysis to form benzene. Treatment of **5** and **8** with excess trifluoroacetic acid resulted in no reaction and reversible protonation at the ligand, respectively, even though similar conditions are known to cleave the Au—C bond of cyclometallated 2,6-diphenylpyridine gold(III) complexes. [42] In the course of canvassing the reactivity these new complexes, it was discovered that **2** was reduced to gold(0) in the presence of amine bases while the other complexes were not. This prompted us to consider the susceptibility of these new compounds to reduction.

Electrochemical profiles of each of these complexes were investigated by cyclic voltammetry in order to determine their reduction potentials (Figure 2). Complexes **5** and **6** underwent reduction only at very negative potentials (-1.06 and -1.05 V, respectively),

as did **8** and **9** (-0.96 and -0.95 V, respectively). In all cases these first reduction events were quasi-reversible. In contrast, complex **2** underwent an irreversible reduction at 0.15 V. (2-picolinato)gold(III) dichloride **14** and the 2-pyridyl amidate complex **15** were analyzed as well (Figure 3). The former was also reduced at a relatively anodic potential (-0.07 V), whereas the latter underwent reduction at -0.92 V. Though these data have not been definitively identified as being ligand- or metal-based reductions, they show the minimal potential at which these gold complexes are reduced and, given that these events are not fully reversible regardless of scan rate, the point at which these compounds begin to decompose. These data suggest that amidate, bidentate or tridentate, and iminothiolate complexes of gold(III) less susceptible to reduction, whereas carboxylate-supported complexes are reduced at relatively positive potentials. There are two major implications for these results. The first is that the identity of gold(III) picolinate catalysts is complicated by their high reduction potential, as Hashmi and co-workers have alluded to in a previous study focused on the induction period observed with this class of pre-catalysts.[25] A second insight is the importance of gauging the susceptibility to reduction of gold(III) complexes based on the context in which they are used. Just as picolinate complexes serve as excellent pre-catalysts for many transformations, their lack of other applications may be attributed to their ease of reduction. This idea is particularly important given recent advances in controlled reduction of gold(III) to gold(I) for delivering biological probes,[5] and the divergent reactivity between gold(I) and gold(III) catalysts.[33]

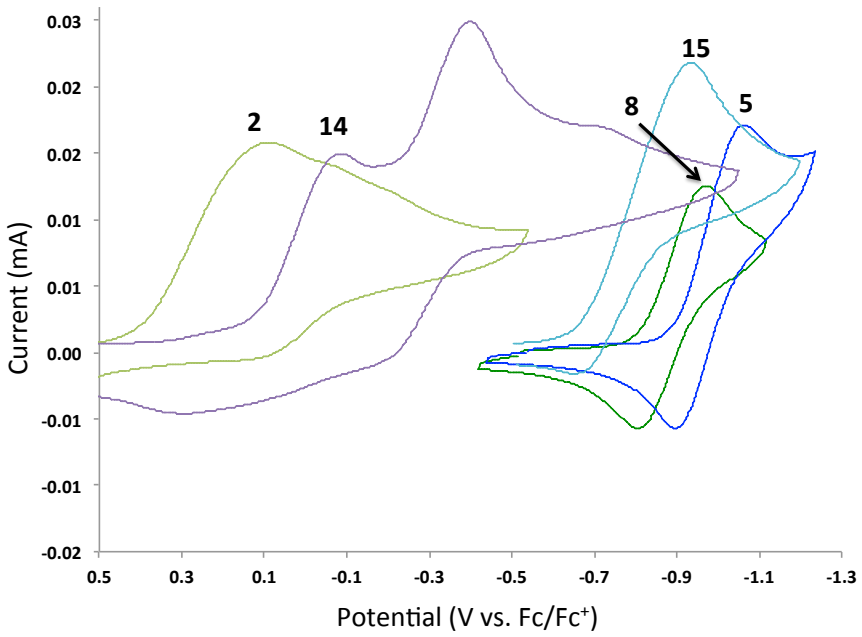

Figure 2. Cyclic voltammogram of complexes **2**, **5, 8**, **14**, and **15** in THF. Conditions: 0.1 M *n*-Bu_4NPF_6; working electrode: glassy carbon; counter electrode: Pt; Reference electrode: Ag/AgCl; scan rate 100 mV/s.

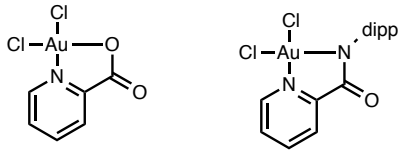

Figure 3. Structures of complexes **14** (left) and **15** (right).

Conclusion

In conclusion, a series of novel gold(III) complexes with ancillary pincer ligands bound by heteroatom linkages has been prepared. The bis(iminothiolate) scaffold was competent in stabilizing a number of complexes with varied substitution in the fourth coordination site. The stability of the pincer complexes with iminothiolate and amidate groups appears to preclude the use of these compounds is catalysis. This in turn led us to examine the electrochemistry of these pincer compounds and conclude that iminothiolate- and amidate-supported complexes have reduction potentials nearly a volt more cathodic than their carboxylate analogues. We hope that these compounds will be exploited in other fields that require discrete gold(III) complexes.

Experimental

General Information

All reactions were carried out using standard Schlenk technique or in a nitrogen-filled drybox unless otherwise noted. Glassware was oven-dried overnight or flame-dried under vacuum. All NMR spectra were obtained at ambient temperature using Bruker AV-600, DRX-500, AV-500, AVB-400, AVQ-400, or AV-300 spectrometers. ^{1}H NMR chemical shifts (δ) are reported in parts per million (ppm) relative to residual solvent peaks (5.32 ppm for CD_2Cl_2, 7.26 ppm for $CDCl_3$, 7.16 ppm for C_6D_6, 2.50 DMSO-d_6). ^{13}C NMR chemical shifts were also reported relative to deuterated solvent peaks (54.00 ppm for CD_2Cl_2, 77.23 ppm for $CDCl_3$, 128.06 for C_6D_6, 39.51 ppm for DMSO-d_6). Infrared (IR) spectra were recorded on a Nicolet Avatar FT-IR spectrometer. High-resolution mass spectral data were obtained from the Micromass/Analytical Facility operated by the College of Chemistry, University of California, Berkeley using a Thermo LTQ-FT (ESI) or Waters AutoSpec Premier (EI). X-ray structural analysis was conducted at the University of California, Berkeley CHEXRAY facility (details in the X-ray section below). Combustion analysis data were obtained at the Micro-Mass Facility at the University of California, Berkeley.

Materials

Reagents were purchased from commercial suppliers, checked for purity and used without further purification unless otherwise noted. Pentane, hexane, diethyl ether, toluene, tetrahydrofuran, and methylene chloride were dried and purified by passage through a column of activated alumina (type A2, 12 x 32, UOP LLC), and sparged with N_2 prior to use. Methylene chloride-d_2 and benzene-d_6 were distilled from CaH_2 and degassed *via* three freeze-pump-thaw cycles prior to use. Acetonitrile was distilled from calcium hydride prior to use. Complex **14** was purchased from Aldrich. NaS(TMS) was prepared according to a literature procedure. [43]

Electrochemistry

All electrochemical experiments were conducted under an argon atmosphere with a 0.1 M [*n*-Bu_4N][PF_6] solution in THF. A BASI's Epsilon potentiostat was used in all cases. The working electrode was a glassy carbon disk (3.0 mm diameter) and the working electrode was a platinum wire. The pseudoreference electrode consisted of a silver wire in a porous Vycor tip glass tube filled with 0.1 M [*n*-Bu_4N][PF_6] in CH_3CN. All potentials were referenced versus ferrocene/ferrocenium as an external standard.

2,6-pyridinedicarboxylato gold(III) chloride (2)

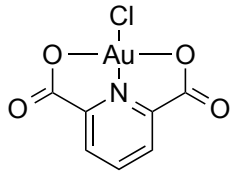

In a fume hood, Ag_2CO_3 (82.1 mg, 0.298 mmol) was added to an acetonitrile solution (10 mL) containing $KAuCl_4$ (75.6 mg, 0.200 mmol) and 2,6-pyridinedicarboxylic acid (36.6 mg, 0.220 mmol). The heterogeneous yellow reaction mixture was stirred for 16 h at room temperature at which time it was passed through Celite. The solution was concentrated to a crude yellow solid and washed with methanol. The desired product was isolated as an analytically pure yellow solid (7.0 mg, 0.018 mmol, 9% yield).

^{1}H NMR (500 MHz, CD_3CN) δ (ppm) 8.69 (t, *J* = 7.9 Hz, 1H), 8.19 (d, *J* = 8.0 Hz, 2H). ^{13}C NMR analysis was hampered by the poor solubility of the title compound. Anal. Calcd. for $C_7H_3AuClNO_4$: C, 21.15; H, 0.76; N, 3.52. Found: C, 20.95; H, 0.63; N, 3.38. IR (ATR): ν_{max}(cm^{-1}): 1707 (C=O), 1291, 1087, 756, 660, 471.

Dipotassium N,N'-bis(2,6-diisopropylphenyl)-2,6-pyridinedicarboxamidate (3)

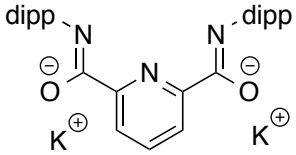

The title compound was prepared according to the procedure of Erker and coworkers.[44] Its ^{1}H NMR data match those found in this procedure.

N,N'-Bis(1,3,5-trimethylphenyl)-2,6-pyridinedicarboxamide

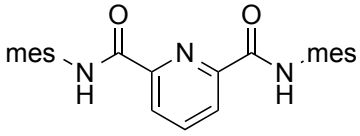

The title compound was prepared according to a literature procedure[44] and its ^{1}H NMR data match those in the literature.[45]

Dipotassium N,N'-Bis(1,3,5-trimethylphenyl)-2,6-pyridinedicarboxamidate (4)

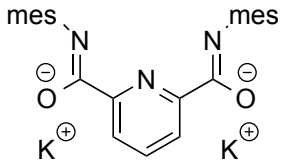

The title compound was prepared analogously to **3**. ^{1}H NMR (500 MHz, DMSO-d_6): δ (ppm) 8.13 (d, *J* = 7.6 Hz, 2H), 7.60 (t, *J* = 7.6 Hz, 1H), 6.64 (s, 4H), 2.15 (s, 6H), 2.01 (s, 12H). ^{13}C NMR (126 MHz, DMSO-d_6): δ (ppm) 162.4, 158.4, 151.3, 134.4, 129.2, 127.1, 125.8, 121.7, 20.6, 19.1. HRMS (ESI) (*m/z*) calculated for $[C_{25}H_{25}O_2N_3 + H - 2K]^-$: 400.2031, found 400.2029.

N,N'-Bis(2,6-diisopropylphenyl)-2,6-pyridinedicarboxamidate gold(III) chloride (5)

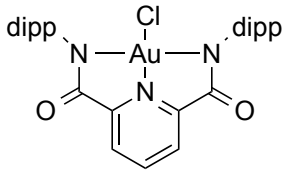

A Schlenk flask was charged with **3** (283 mg, 0.504 mmol) and THF (15 mL) in a glovebox. The flask was cooled to -78 °C on a Schlenk line and $KAuCl_4$ (187 mg, 0.494 mmol) added as a single portion. The reaction mixture turned red overnight as it was warmed to room temperature. The heterogeneous red solution was filtered through Celite and the resulting red solution concentrated to a solid. The crude material was purified by column chromatography (silica, 1:1 EtOAc:hexanes). The product was isolated as an analytically pure orange solid (192 mg, 0.268 mmol, 54% yield). ^{1}H NMR (600 MHz, $CDCl_3$): δ (ppm) 8.57 (t, *J* = 7.9 Hz, 1H), 8.27 (d, *J* = 7.9 Hz, 2H), 7.29 (t, *J* = 7.7 Hz, 2H), 7.16 (d, *J* = 7.8 Hz, 4H), 3.26 (h, *J* = 6.9 Hz, 4H), 1.25 (d, *J* = 6.8 Hz, 12H), 1.21 (d, *J* = 6.9 Hz, 12H). ^{13}C NMR (151 MHz, $CDCl_3$): δ (ppm) 168.2, 146.2, 145.8, 145.1, 138.6, 129.4, 129.1, 123.5, 29.2, 24.4, 23.2. IR (ATR): ν_{max}(cm^{-1}): 2958, 1645 (C=O), 1440, 1347, 1139, 1103, 833, 799, 746, 663. HRMS (ESI) (*m/z*) calculated for $[C_{31}H_{37}O_2N_3AuCl+H]^+$: 716.2313, found: 716.2318. Anal. Calcd. for $C_{31}H_{37}AuClN_3O_2$: C, 52.00; H, 5.21; N, 5.87. Found: C, 51.94; H, 5.36; N, 5.78.

N,N'-Bis(2,4,6-trimethylphenyl)-2,6-pyridinedicarboxamidate gold(III) chloride (6)

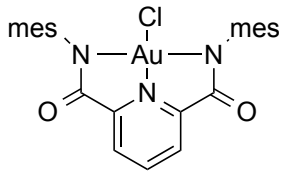

The title compound was synthesized analogously to **5** but with **4** (239 mg, 0.501 mmol). The product was isolated as an analytically pure orange solid (192 mg, 0.303 mmol, 60% yield) following column chromatography (3:1 EtOAc:hexanes). X-ray quality crystals were grown by diffusion of pentane into a DCM solution of **6** at -25 °C. ^{1}H NMR (600 MHz, $CDCl_3$): δ (ppm) 8.54 (t, *J* = 7.8 Hz, 1H), 8.24 (d, *J* = 7.8 Hz, 2H), 6.90 (s, 4H), 2.27 (s, 12H), 2.27 (s, 6H). ^{13}C NMR (151 MHz, $CDCl_3$): δ (ppm) 167.6, 146.1, 145.7, 139.1, 137.9, 134.6, 129.2, 129.0, 21.3, 18.9. IR (ATR): ν_{max}(cm^{-1}): 2916, 1640 (C=O), 1599, 1477, 11436, 1350, 1102, 756, 558. HRMS (ESI) (*m/z*) calculated for $[C_{25}H_{25}O_2N_3AuCl+H]^+$: 632.1374, found 632.1372. Anal. Calcd. for $C_{25}H_{25}AuClN_3O_2$: C, 47.52; H, 3.99; 6.65. Found: C, 47.61; H, 4.27; N, 6.53.

N,N'-Bis(2,6-diisopropylphenyl)-2,6-pyridinedithioamide

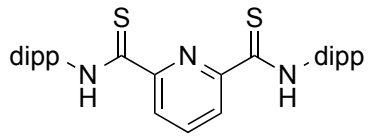

A round-bottom flask was charged with L (972 mg, 2.00 mmol), Lawesson's reagent (2.40 g, 5.93 mmol), and toluene (20 mL). The reaction mixture was heated at 100 °C for 20 h and then cooled to room temperature. The heterogeneous orange mixture was filtered on a medium frit and the white solid washed with toluene. The filtrate was concentrated to an orange oil and subjected to column chromatography (5-10% EtOAc/hex) and a yellow band eluted. The desired product was isolated as a yellow solid (980 mg, 1.90 mmol, 95% yield). ^{1}H NMR (600 MHz, $CDCl_3$)): δ (ppm) 10.75 (s, 2H), 9.06 (d, *J* = 7.9 Hz, 2H), 8.13 (t, *J* = 7.9 Hz, 1H), 7.43 (t, *J* = 7.8 Hz, 2H), 7.29 (d, *J* = 7.7 Hz, 4H), 3.02 (sept, *J* = 6.9 Hz, 4H), 1.28 (d, *J* = 6.9 Hz, 12H), 1.15 (d, *J* = 6.9 Hz, 12H). ^{13}C NMR (126 MHz, $CDCl_3$): δ (ppm) 191.9 149.1, 145.6, 138.8, 133.7, 129.5, 128.1, 124.2, 29.2, 24.6, 23.2. IR (ATR): ν_{max}(cm^{-1}): 3317, 3281, 2958, 2925, 1697, 1486, 1350, 1073, 802. HRMS (ESI) (*m/z*) calculated for $[C_{31}H_{39}N_3S_2+H]^+$: 518.2658, found 518.2659.

Dipotassium N,N'-Bis(2,6-diisopropylphenyl)-2,6-pyridinedithioamidate (7)

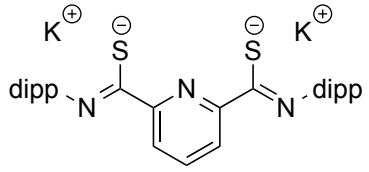

Ligand **L** (3.64 g, 7.34 mmol) was dissolved in THF (40 mL) in a glovebox. To the solution was added KH (589 mg, 14.7 mmol). Rapid gas evolution was observed and the reaction mixture was stirred for 4 h. The resulting precipitate was isolated on a fine frit, washed with hexanes, and residual solvent stripped under vacuum. (Note: Approximately 13% THF by mass remains even after prolonged exposure to vacuum and heating). The product was isolated as a pale yellow solid (3.13 g, 5.23 mmol). ^{1}H NMR (500 MHz, DMSO-d_6): δ (ppm) 8.09 (d, *J* = 7.7 Hz, 2H), 7.66 (t, *J* = 7.7 Hz, 1H), 6.95 (d, *J* = 7.6 Hz, 4H), 6.81 (t, *J* = 7.6 Hz, 2H), 3.04 (sept, *J* = 6.9 Hz, 4H), 1.18 (d, *J* = 6.9 Hz, 12H), 1.05 (d, *J* = 6.9 Hz, 12H). ^{13}C NMR (126 MHz, DMSO-d_6): δ (ppm) 182.9, 161.2, 151.6, 137.3, 134.7, 121.8, 120.4, 27.4, 24.0 , 23.8 (one aromatic carbon was not detected). HRMS (ESI) (*m/z*) calculated for $[C_{31}H_{37}N_3S_2K_2–2K + H]^-$: 516.2513, found 516.2501.

N,N'-Bis(2,6-diisopropylphenyl)-2,6-pyridinediiminothiolate gold(III) chloride (8)

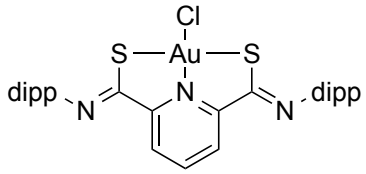

To a solution of $KAuCl_4$ (131 mg, 0.347 mmol) in THF (7 mL) was added **7** (206 mg, 0.347 mmol) in a glovebox with assistance of THF (3 mL). The red reaction mixture was stirred for 18 h and then passed through a thin pad of alumina. Methylene chloride was used to wash the alumina until the solvent eluted was colorless, indicating that none of the product remained on the alumina pad. The resulting solution was concentrated to an analytically pure red solid (147mg, 0.197 mmol, 57% yield). X-ray quality crystals were grown by diffusion of pentane into a DCM solution of **8** at -25 °C. ^{1}H NMR (600 MHz, $CDCl_3$): δ (ppm) 8.63 (d, *J* = 7.9 Hz, 2H), 8.37 (t, *J* = 7.9 Hz, 1H), 7.22-7.18 (m, 6H), 2.76 (sept., *J* = 7.7, 7.2 Hz, 5H), 1.26 (d, *J* = 7.0 Hz, 12H), 1.14 (d, *J* = 6.8 Hz, 12H). ^{13}C NMR (126 MHz, CD_2Cl_2): δ (ppm) 165.4, 157.9, 144.5, 141.5, 136.9, 129.5, 126.0, 124.0, 29.3, 23.9, 23.5. IR (ATR): ν_{max}(cm^{-1}): 3060, 2957, 2924, 2864, 1574 (C=N), 1465, 1291, 1184, 1096, 1047, 952, 758. HRMS (ESI) (*m/z*) calculated for $[C_{31}H_{37}N_3AuClS_2+H]^+$: 748.1856, found: 748.1863. Anal. Calcd. for $C_{31}H_{37}AuClN_3S_2$: C, 49.76; H, 4.98; N, 5.62; S, 8.57. Found: C, 50.10; H, 4.92; N, 5.49; S, 8.16.

N,N'-Bis(2,6-diisopropylphenyl)-2,6-pyridinediiminothiolate gold(III) bromide (9)

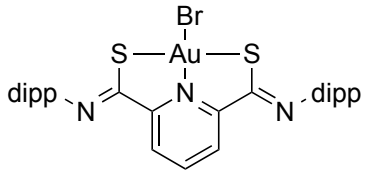

The title complex was prepared analogously to **8** using $KAuBr_4$•$2H_2O$ (59.0 mg, 0.100 mmol) and **7** (68.0 mg, 0.114 mmol). The desired product was isolated as an analytically pure orange solid (65.5 mg, 0.826 mmol, 83% yield). X-ray quality crystals were grown by layering a DCM solution of **9** with hexane and storing at -20 °C. ^{1}H NMR (500 MHz, CD_2Cl_2): δ 8.61 (d, *J* = 7.9 Hz, 2H), 8.35 (t, *J* = 7.9 Hz, 1H), 7.35-6.95 (m, 6H), 2.80 (sept, *J* = 6.9 Hz, 4H), 1.26 (d, *J* = 6.9 Hz, 12H), 1.14 (d, *J* = 6.8 Hz, 12H). ^{13}C NMR (126 MHz, CD_2Cl_2): δ 166.9, 157.0, 144.5, 141.4, 136.8, 129.4, 125.9, 124.0, 29.3, 23.9, 23.5. IR (ATR): ν_{max}(cm^{-1}): 2956, 1569 (C=N), 1460, 1288, 948, 759. HRMS (ESI) (*m/z*) calculated for $[C_{31}H_{37}N_3AuBrS_2+H]^+$: 792.1351, found 792.1368. Anal. Calcd. for $C_{31}H_{37}AuBrN_3S_2$: C, 46.97; H, 4.71; N, 5.30. Found: C, 46.80; H, 4.64; N, 5.18.

N,N'-Bis(2,6-diisopropylphenyl)-2,6-pyridinediiminothiolate gold(III) phenyl (10)

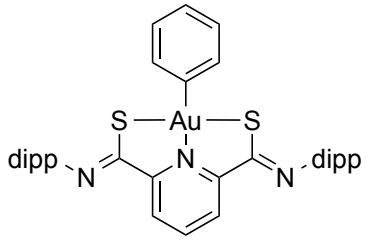

Ph_2Zn (5.9 mg, 0.027 mmol) was added to **8** (37.7 mg, 0.050 mmol) with the assistance of toluene (2.5 mL) in a glovebox. The reaction mixture became opaque and yellow with stirring overnight. The reaction mixture was passed through Celite and the pad washed with toluene until the solvent eluted was colorless. The solution was concentrated to an analytically pure yellow solid (35.6 mg, 0.045 mmol, 90% yield). ^{1}H NMR (600 MHz, CD_2Cl_2): δ (ppm) 8.62 (d, *J* = 7.9 Hz, 2H), 8.32 (t, *J* = 7.9 Hz, 1H), 7.30 (d, *J* = 7.6 Hz, 2H), 7.20 (d, *J* = 7.5 Hz, 4H), 7.17 – 7.11 (m, 2H), 7.10-7.00 (m, 3H), 2.86 (sept, *J* = 7.1 Hz, 4H), 1.26 (d, *J* = 6.8 Hz, 12H), 1.15 (d, *J* = 6.8 Hz, 12H). ^{13}C NMR (151 MHz, CD_2Cl_2): δ (ppm) 167.8, 155.9, 145.7, 140.2, 136.9, 135.2, 130.6, 129.6, 127.8, 127.5, 125.4, 123.9, 29.3, 23.9, 23.6. IR (ATR):

ν_{max}(cm^{-1}): 2956, 1569 (C=N), 1461, 1291, 954. HRMS (ESI) (*m/z*) calculated for [C37H42AuN3S2+Na]$^+$: 812.2378, found: 812.2392. Anal. Calcd. for for $C_{37}H_{42}AuN_3S_2$: C, 56.58; H, 5.53; N, 5.18; S, 7.79. Found: C, 56.26; H, 5.36; N, 5.32; S, 8.12.

N,N'-Bis(2,6-diisopropylphenyl)-2,6-pyridinediiminothiolate gold(III) trimethylsilanoate (11)

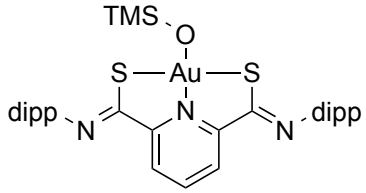

A scintillation vial was charged with **8** (148 mg, 0.198 mmol) and toluene (10 mL) in a glovebox. To the solution was added NaOTMS (24.0 mg, 0.214 mmol). The resulting homogeneous, pale red solution was stirred for 1.5 h at which time it was filtered via syringe filter and concentrated. The resulting crude solid was washed with hexane and placed under vacuum. The desired product was isolated as a spectroscopically pure yellow solid (156 mg, 0.195 mmol, 98% yield). X-ray quality crystals were grown from a DCM/acetonitrile solution at -20 °C. ^{1}H NMR (500 MHz, CD_2Cl_2): δ (ppm) 8.57 (d, *J* = 7.9 Hz, 2H), 8.32 (t, *J* = 7.9 Hz, 1H), 7.28-7.10 (m, 6H), 2.82 (sept, *J* = 6.9 Hz, 4H), 1.27 (d, *J* = 6.9 Hz, 12H), 1.14 (d, *J* = 6.8 Hz, 12H), -0.01 (s, 9H). ^{13}C NMR (126 MHz, methylene chloride-d_2): δ (ppm) 165.3, 158.5, 144.9, 141.0, 137.0, 128.8, 125.8, 124.0, 29.3, 23.9, 23.6, 3.30. IR (ATR): ν_{max}(cm^{-1}): 2957, 1575 (C+N, 1464, 958, 914, 754, 744. HRMS (ESI) (*m/z*) calculated for [$C_{34}H_{46}ON_3AuS_2Si$+Na]$^+$: 824.2430, found 824.2409. Anal. Calcd. for $C_{34}H_{46}AuN_3OS_2Si$: C, 50.92; H, 5.78; N, 5.24. Found: C, 48.74; H, 5.45; N, 4.96. Combustion analysis was consistently high in carbon despite multiple attempts at further purification.

N,N'-Bis(2,6-diisopropylphenyl)-2,6-pyridinediiminothiolate gold(III) trimethylthiolate (12)

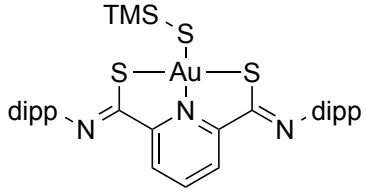

A scintillation vial was charged with **X** (37.0 mg, 0.049 mmol) and toluene (4 mL) in a glovebox. To the solution was added NaSTMS (19.6 mg, 0.153 mmol). The reaction mixture immediately became dark red and was stirred overnight. The orange solution was filtered *via* syringe filter and concentrated to an orange solid. Following trituration with pentane, the desired product was isolated as an analytically pure orange solid (27.1 mg, 0.033 mmol, 67% yield). ^{1}H NMR (500 MHz, C_6D_6): δ (ppm) 7.88 (d, *J* = 7.9 Hz, 2H), 7.20 (m, 6H), 6.76 (t, *J* = 7.9 Hz, 1H), 3.09 (sept, *J* = 7.0 Hz, 4H), 1.41 (d, *J* = 6.9 Hz, 12H), 1.29 (d, *J* = 6.8 Hz, 12H), 0.32 (s, 9H). ^{13}C NMR (126 MHz, C_6D_6) : δ (ppm) 168.42 , 155.36 , 145.22 , 139.11 , 136.44 , 127.58 , 125.80 , 124.01 , 29.20 , 24.07 , 23.56 , 4.77 . IR (ATR): ν_{max}(cm^{-1}): 3062, 2957, 1574 (C=N), 1460, 945, 836. HRMS (ESI) (*m/z*) calculated for [$C_{34}H_{46}N_3AuS_3Si$+Na]$^+$: 840.2181, found 840.2166. Anal. Calcd. for $C_{34}H_{46}AuN_3S_3Si$: C, 49.92; H, 5.67; N, 5.14. Found: C, 50.28; H. 5.67; N, 4.89.

N,N'-Bis(2,6-diisopropylphenyl)-2,6-pyridinediiminothiolate gold(III) bis(trimethylsilyl)amide (13)

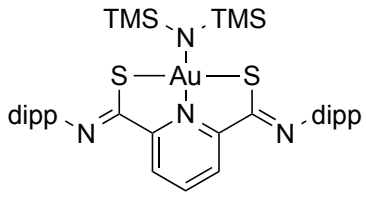

A scintillation vial was charged with **8** (38.2 mg, 0.051 mmol) and toluene (4 mL) in a glovebox. To the solution was added NaHMDS (10.2 mg, 0.056 mmol). The resulting homogeneous, dark red solution was stirred for 15 h at which time it was concentrated to a crude red solid. The solid was dissolved in hexane, filtered *via* syringe filter, and concentrated to yield the desired product (25.1 mg, 0.028 mmol, 55% yield) as a spectroscopically pure red solid. Analytically pure material was isolated through precipitation from pentane at -20 °C, but at greatly reduced yield due to the high solubility of **13** even in hydrocarbons. X-ray quality crystals were grown from a saturated hexane solution at -20 °C. ^{1}H NMR (500 MHz, CD_2Cl_2): δ (ppm) 8.59 (d, J = 7.9 Hz, 2H), 8.27 (t, J = 7.9 Hz, 1H), 7.27-7.02 (m, 6H), 2.85 (sept, J = 6.8 Hz, 4H), 1.27 (d, J = 6.9 Hz, 12H), 1.15 (d, J = 6.8 Hz, 12H), 0.07 (s, 9H). ^{13}C NMR (126 MHz, CD_2Cl_2): δ (ppm) 167.3, 157.1, 145.4, 140.5, 137.0, 128.4, 125.5, 124.0, 29.2, 23.9, 23.8, 5.32. IR (ATR): ν_{max}(cm^{-1}): 2958, 1572 (C=N), 1461, 1245, 965, 871, 819, 756. HRMS (ESI) (*m/z*) calculated for $[C_{37}H_{55}N_4AuSSi_2+H]^+$: 873.3145, found: 873.3146. Anal. Calcd. for $C_{37}H_{55}AuN_4S_2Si_2$: C, 50.90; H, 6.35; N, 6.42. Found: C, 51.20; H, 6.36; N, 6.29.

N-(2,6-diisopropylphenyl)-2-pyridinecarboxamide

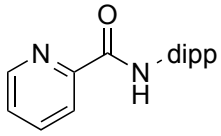

The title compound was prepared according to the procedure of Bazan and coworkers. [46]

Potassium N-(2,6-diisopropylphenyl)-2-pyridinecarboxamidate

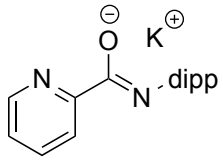

A round-bottom flask was charged with N-(2,6-diisopropylphenyl)-2-pyridinecarboxamide (984 mg, 3.48 mmol) and THF (20 mL) in a glovebox. KH (141 mg, 3.52 mmol) was added, resulting in the rapid evolution of gas. The reaction mixture was stirred overnight and then concentrated to approximately 10 mL in volume to promote precipitation. The precipitate was collected on a fine frit and washed with hexane. Residual solvent was removed under vacuum to yield the desired product as a beige solid (647 mg, 2.02 mmol, 58% yield). ^{1}H NMR (500 MHz, DMSO-d_6): δ (ppm) 8.46 (d, J = 3.5 Hz, 1H), 8.20 (d, J = 7.9 Hz, 1H), 7.69 (td, J = 7.6, 1.8 Hz, 1H), 7.30-7.09 (m, 1H), 6.87 (d, J = 7.5 Hz, 2H), 6.71 (t, J = 7.5 Hz, 1H), 3.20 (sept, J = 6.9 Hz, 4H), 1.06 (d, J = 6.9 Hz, 6H). ^{13}C NMR (126 MHz, DMSO-d_6): δ (ppm) 162.7, 147.7, 139.8, 135.2, 123.2, 122.2, 121.1, 119.0, 27.6, 23.6. HRMS (ESI) (*m/z*) calculated for $[C_{18}H_{21}ON_2K - K]^-$: 281.1659, found 281.1657.

N-(2,6-diisopropylphenyl)-2-pyridinecarboxamidate gold(III) dichloride (15)

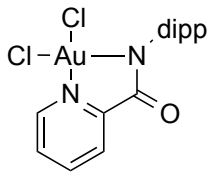

A Schlenk flask was charged with potassium N-(2,6-diisopropylphenyl)-2-pyridinecarboxamidate (42.8 mg, 0.134 mmol) and THF (5 mL) in a glovebox. The flask was cooled to -78 °C on a Schlenk line and $KAuCl_4$ (48.6 mg, 0.129 mmol) added as a single portion. The reaction mixture became yellow within two hours and red overnight as it was warmed to room temperature. The reaction mixture was concentrated and the crude solid filtered through Celite using DCM. The filtered solution was concentrated to a red solid and purified by column chromatography (1:1 EtOAc:hexanes). The product was isolated as a spectroscopically pure orange solid (17.9 mg, 0.033 mmol, 26% yield). X-ray quality crystals were obtained by hexane diffusion into a DCM solution at -20 °C. ^{1}H NMR (600 MHz, $CDCl_3$): δ (ppm) 9.63 (d, J = 5.8 Hz, 1H), 8.41 (t, J = 7.7 Hz, 1H), 8.28 (d, J = 7.7 Hz, 1H), 7.95 (t, J = 6.9 Hz, 1H), 7.41 (app t, J = 7.8, 2.1 Hz, 1H), 7.21 (app d, J = 7.8, 2.1 Hz, 2H), 3.24 (sept, J= 7.5 Hz, 2H), 1.31 (d, J = 6.9 Hz, 6H), 1.17 (d, J = 6.8 Hz, 6H). ^{13}C NMR (151 MHz, $CDCl_3$): δ 168.8, 149.0, 146.0, 145.0, 144.2, 138.6, 129.7, 129.4, 129.3, 123.4, 29.2, 24.4, 23.2. IR (ATR): ν_{max}(cm^{-1}): 2960, 1652 (C=O), 1610, 1354, 792, 753, 669. HRMS (ESI) (*m/z*) calculated for $[C_{18}H_{21}ON_2AuCl_2+H]^+$: 549.0769, found: 549.0770. Anal. Calcd. for $C_{18}H_{21}AuCl_2N_2O$: C, 39.36; H, 3.85; N, 5.10. Found: C, 40.25; H, 3.80; N, 4.99. Combustion analysis was high in carbon despite multiple attempts.

References

1. Maiore, L.; Aragoni, M. C.; Deiana, C.; Cinellu, M. A.; Isaia, F.; Lippolis, V.; Pintus, A.; Serratrice, M.; Arca, M. *Inorg. Chem.* **2014**, *53*, 4068-4080.
2. Sivararn, H.; Tan, J.; Huynh, H. V. *Organometallics* **2012**, *31*, 5875-5883.
3. Liu, W.; Bensdorf, K.; Proetto, M.; Hagenbach, A.; Abram, U.; Gust, R. *J. Med. Chem.* **2012**, *55*, 3713-3724.
4. Lum, C. T.; Sun, R. W.; Zou, T.; Che, C.-M. *Chem. Sci.* **2014**, *5*, 1579-1584.
5. Zou, T.; Lum, C. T.; Chui, S. S.; Che, C.-M. *Angew. Chem., Int. Ed.* **2013**, *52*, 2930-2933.
6. Lai, S.-L.; Wang, L.; Yang, C.; Chan, M.-Y.; Guan, X.; Kwok, C.-C.; Che, C.-M. *Adv. Funct. Mat.* **2014**, *10.1002/adfm.201400082*.
7. Wong, K. M.; Hung, L.; Lam, W. H.; Zhu, N.; Yam, V. W. *J. Am. Chem. Soc.* **2007**, *129*, 4350-4365.
8. Boronat, M.; Corma, A.; Gonzalez-Arellano, C.; Iglesias, M.; Sanchez, F. *Organometallics* **2010**, *29*, 134-141.
9. Debono, N.; Iglesias, M.; Sanchez, F. *Adv. Synth. Catal.* **2007**, *349*, 2470-2476.
10. Kung, K. K.; Lo, V. K.; Ko, H.; Li, G.; Chan, P.; Leung, K.; Zhou, Z.; Wang, M.; Che, C.-M.; Wong, M. *Adv. Synth. Catal.* **2013**, *355*, 2055-2070.
11. Wolf, W. J.; Winston, M. S.; Toste, F. D. *Nature Chem.* **2014**, *6*, 159-164.
12. Scott, V. J.; Labinger, J. A.; Bercaw, J. E. *Organometallics* **2010**, *29*, 4090-4096.
13. Garg, J. A.; Blacque, O.; Fox, T.; Venkatesan, K. *Inorg. Chem.* **2010**, *49*, 11463-11472.
14. Smith, D. A.; Rosca, D.; Bochmann, M. *Organometallics* **2012**, *31*, 5998-6000.
15. van Koten, G; Milstein, D. *Top. Organomet. Chem.* **2013**, *40*, 1-356.
16. Morales-Morales, D.; Jensen, C. M. *The Chemistry of Pincer Compounds;* Elsevier Science: Oxford, 2007.
17. Choi, J.; MacArthur, A. H. R.; Brookhart, M.; Goldman, A. S. *Chem. Rev.* **2011**, *111*, 1761-1779.
18. Au, V. K.; Lam, W. H.; Wong, W.; Yam, V. W. *Inorg. Chem.* **2012**, *51*, 7537-7545.
19. To, W.; Tong, G. S.; Lu, W.; Ma, C.; Liu, J.; Chow, A. L.; Che, C. *Angew. Chem., Int. Ed.* **2012**, *51*, 2654-2657.
20. Wong, K.; Cheung, K.; Chan, M.; Che, C. *Organometallics* **1998**, *17*, 3505-3511.
21. Rosca, D.; Smith, D. A.; Hughes, D. L.; Bochmann, M. *Angew. Chem., Int. Ed.* **2012**, *51*, 10643-10646.
22. Rosca, D.; Smith, D. A.; Bochmann, M. *Chem. Commun.* **2012**, *48*, 7247-7249.
23. Savjani, N.; Rosca, D.; Schormann, M.; Bochmann, M. *Angew. Chem., Int. Ed.* **2013**, *52*, 874-877.
24. Ortner, K.; Hilditch, L.; Zheng, Y.; Dilworth, J.; Abram, U. *Inorg. Chem.* **2000**, *39*, 2801-2806.
25. Hashmi, A.; Weyrauch, J.; Rudolph, M.; Kurpejovic, E. *Angew. Chem., Int. Ed.* **2004**, *43*, 6545-6547.
26. Fan, D.; Yang, C.; Ranford, J.; Vittal, J. *Dalton Trans.* **2003**, 4749-4753.
27. Wilson, C. R.; Fagenson, A. M.; Ruangpradit, W.; Muller, M. T.; Munro, O. Q. *Inorg. Chem.* **2013**, *52*, 7889-7906.
28. Begum, R.; Powell, D.; Bowman-James, K. *Inorg. Chem.* **2006**, *45*, 964-966.

29. Wang, Q.; Begum, R. A.; Day, V. W.; Bowman-James, K. *J. Am. Chem. Soc.* **2013***, 135*, 17193-17199.
30. Huang, D.; Holm, R. H. *J. Am. Chem. Soc.* **2010***, 132*, 4693-4701.
31. Zhou, X.; Kostic, N. *Inorg. Chem.* **1988***, 27*, 4402-4408.
32. Golisz, S. R.; Bercaw, J. E. *Macromolecules* **2009***, 42*, 8751-8762.
33. Sromek, A.; Rubina, M.; Gevorgyan, V. *J. Am. Chem. Soc.* **2005***, 127*, 10500-10501.
34. Xia, Y.; Dudnik, A. S.; Gevorgyan, V.; Li, Y. *J. Am. Chem. Soc.* **2008***, 130*, 6940-6941.
35. Liu, W.; Bensdorf, K.; Proetto, M.; Hagenbach, A.; Abram, U.; Gust, R. *J. Med. Chem.* **2012***, 55*, 3713-3724.
36. Dar, A.; Moss, K.; Cottrill, S.; Parish, R.; McAuliffe, C.; Pritchard, R.; Bealey, B.; Sandbank, J. *J. Chem. Soc. Dalton Trans.* **1992**, 1907-1913.
37. Cinellu, M. A.; Minghetti, G.; Pinna, M. V.; Stoccoro, S.; Zucca, A.; Manassero, M. *Eur. J. Inorg. Chem.* **2003**, 2304-2310.
38. Cinellu, M.; Minghetti, G.; Pinna, M.; Stoccoro, S.; Zucca, A.; Manassero, M. *J. Chem. Soc. Dalton Trans.* **1999**, 2823-2831.
39. Kharasch, M.; Isbell, H. *J. Am. Chem. Soc.* **1931***, 53*, 3053-3059.
40. Shapiro, N. D.; Shi, Y.; Toste, F. D. *J. Am. Chem. Soc.* **2009***, 131*, 11654-11655.
41. Shapiro, N. D.; Toste, F. D. *J. Am. Chem. Soc.* **2008***, 130*, 9244-9245.
42. Smith, D. A.; Rosca, D.; Bochmann, M. *Organometallics* **2012***, 31*, 5998-6000.
43. Do, Y.; Simhon, E.; Holm, R. *Inorg. Chem.* **1983***, 22*, 3809-3812.
44. Wasilke, J.; Wu, G.; Bu, X.; Kehr, G.; Erker, G. *Organometallics* **2005***, 24*, 4289-4297.
45. Smit, T. M.; Tomov, A. K.; Britovsek, G. J. P.; Gibson, V. C.; White, A. J. P.; Williams, D. J. *Cat. Sci. & Tech.* **2012***, 2*, 643-655.
46. Lee, B.; Bu, X.; Bazan, G. *Organometallics* **2001***, 20*, 5425-5431.

NMR Spectra

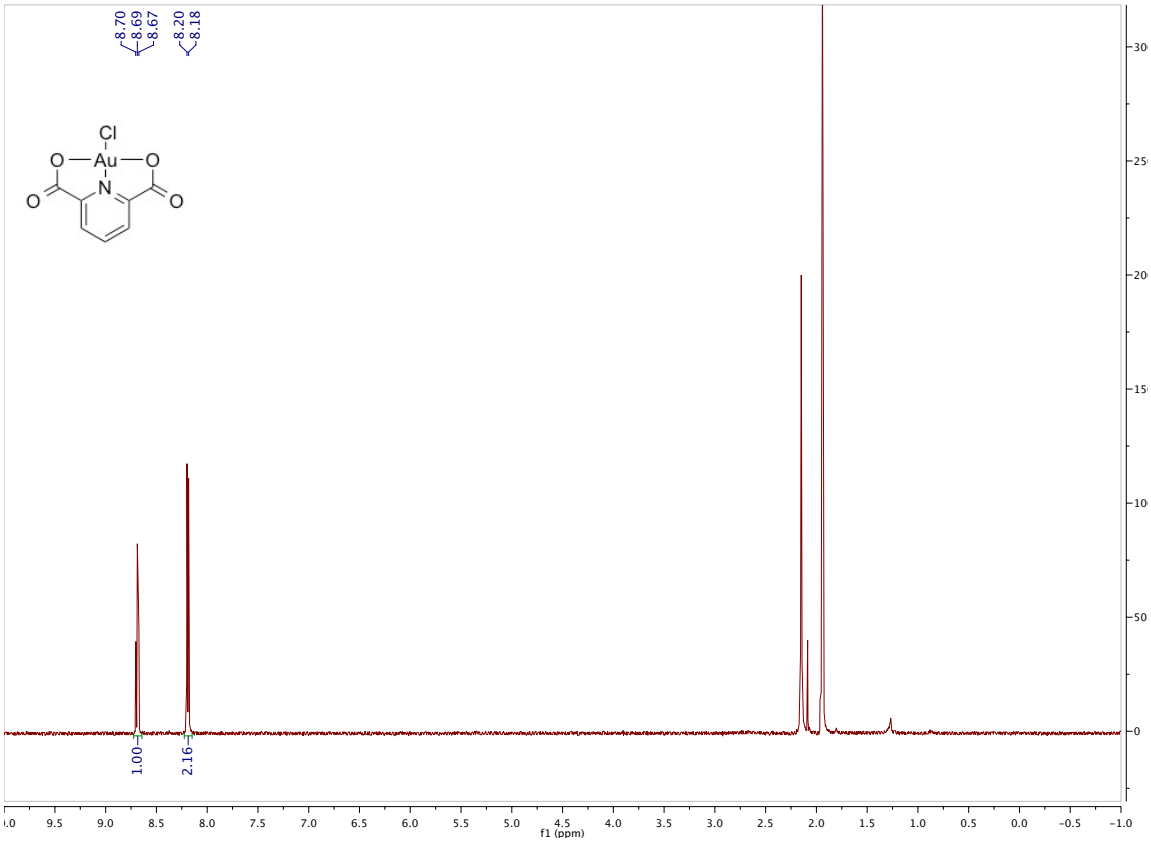

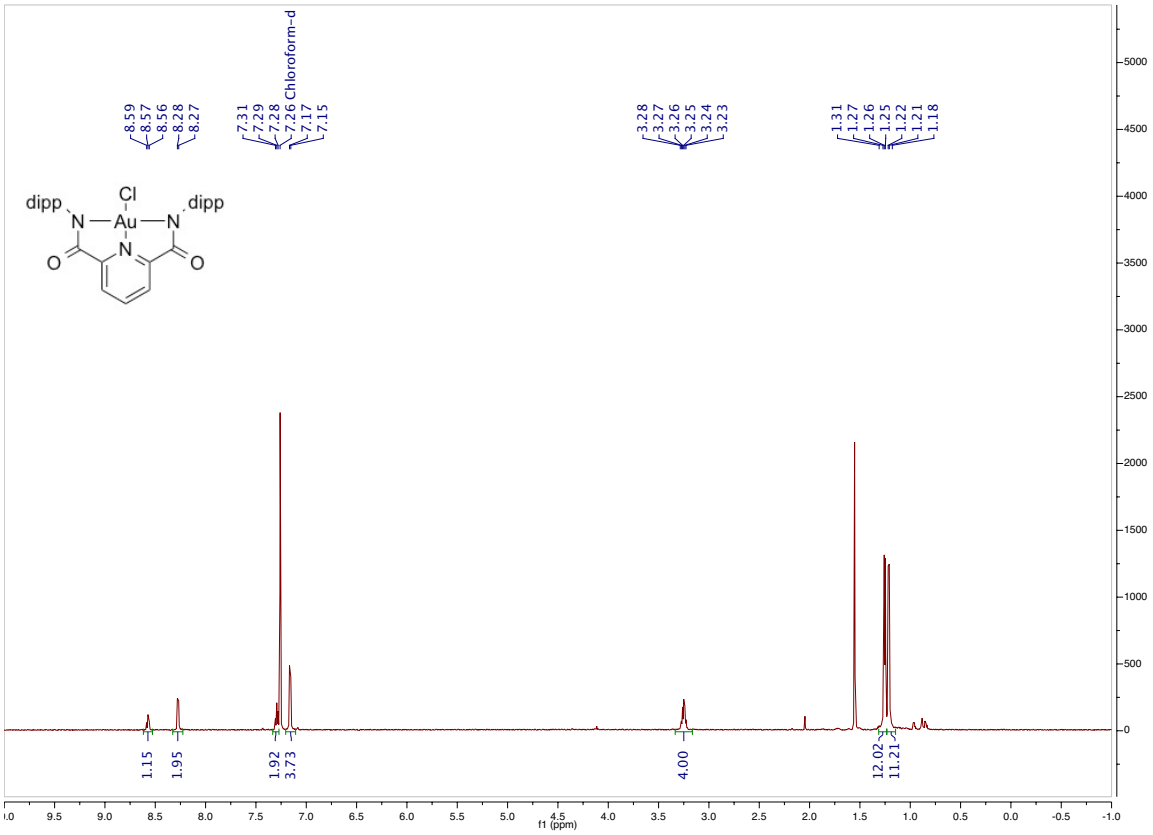
8.59
8.57
8.56
8.28
8.27
7.31
7.29
7.28
7.26 Chloroform-d
7.17
7.15
3.28
3.27
3.26
3.25
3.24
3.23
1.31
1.27
1.26
1.25
1.22
1.21
1.18
dipp
Cl
Au
N
O
1.15
1.95
1.92
3.73
4.00
12.02
11.21
f1 (ppm)

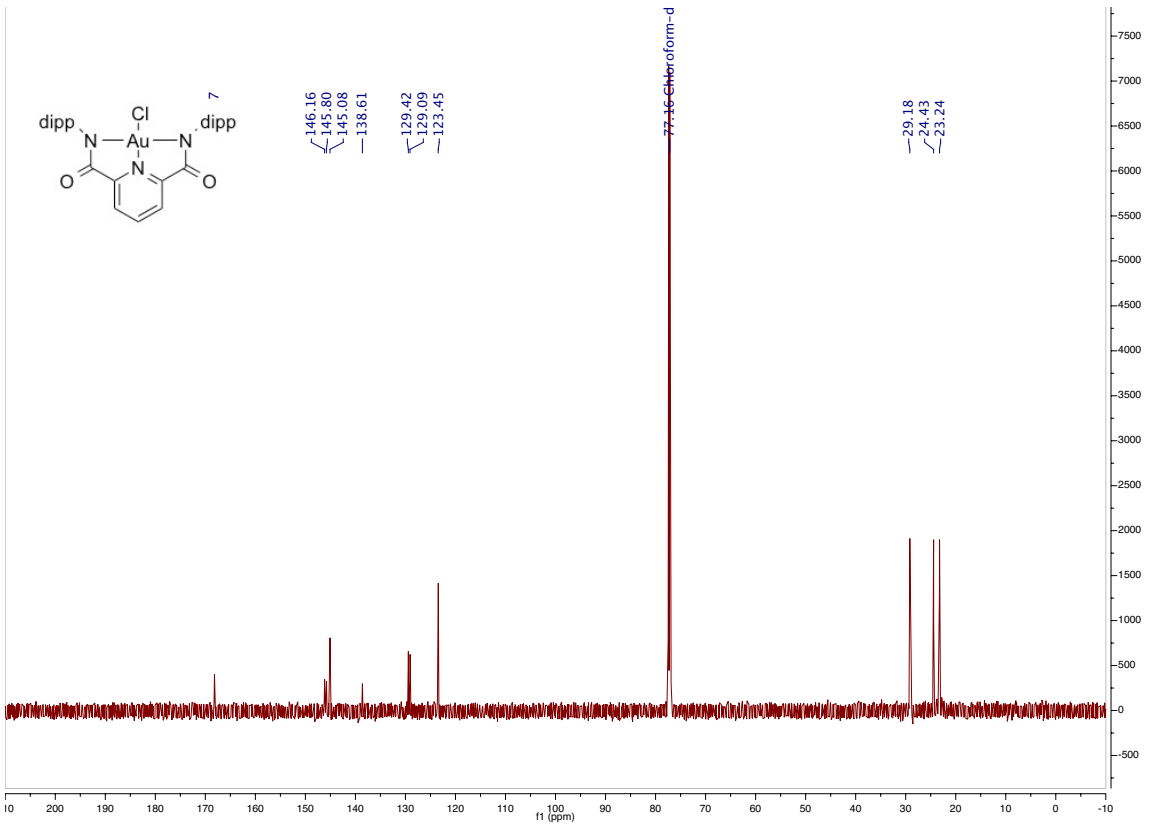
dipp
Cl
Au
N
O
146.16
145.80
145.08
138.61
129.42
129.09
123.45
77.16 Chloroform-d
29.18
24.43
23.24
f1 (ppm)

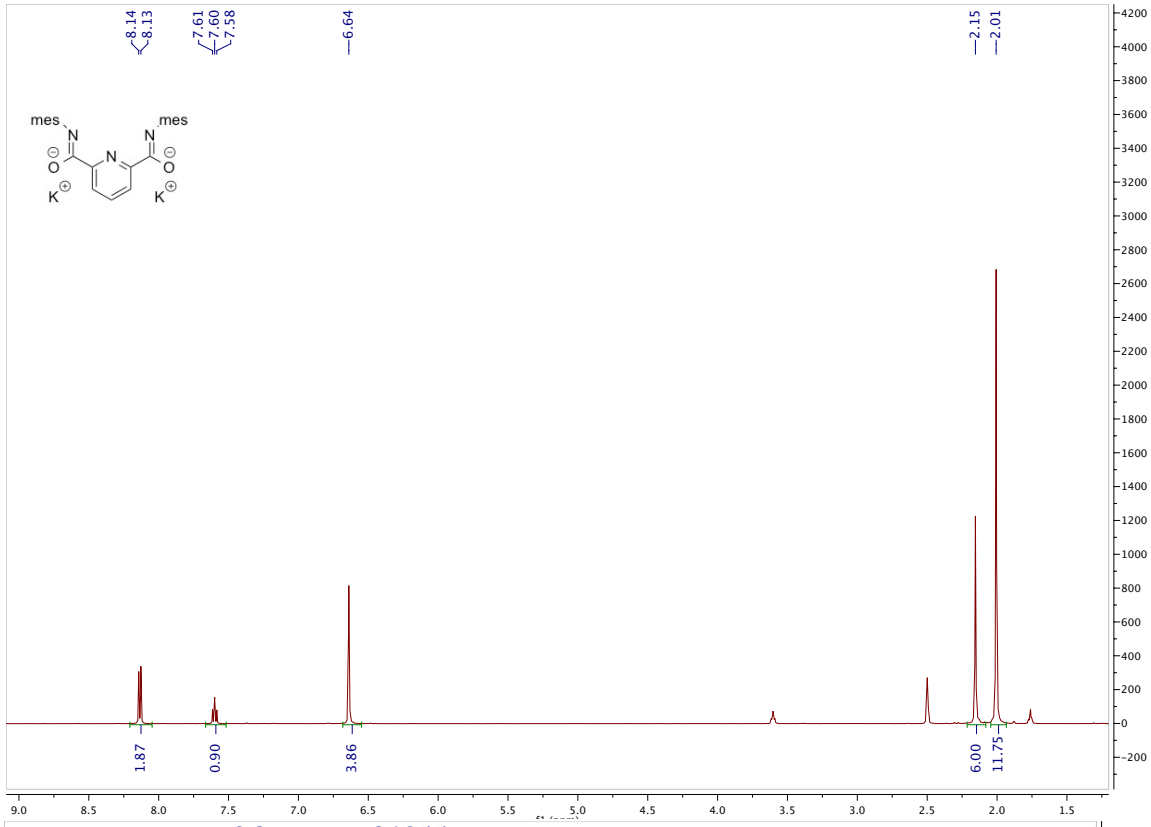
8.14
8.13
7.61
7.60
7.58
6.64
2.15
2.01
mes
mes
1.87
0.90
3.86
6.00
11.75

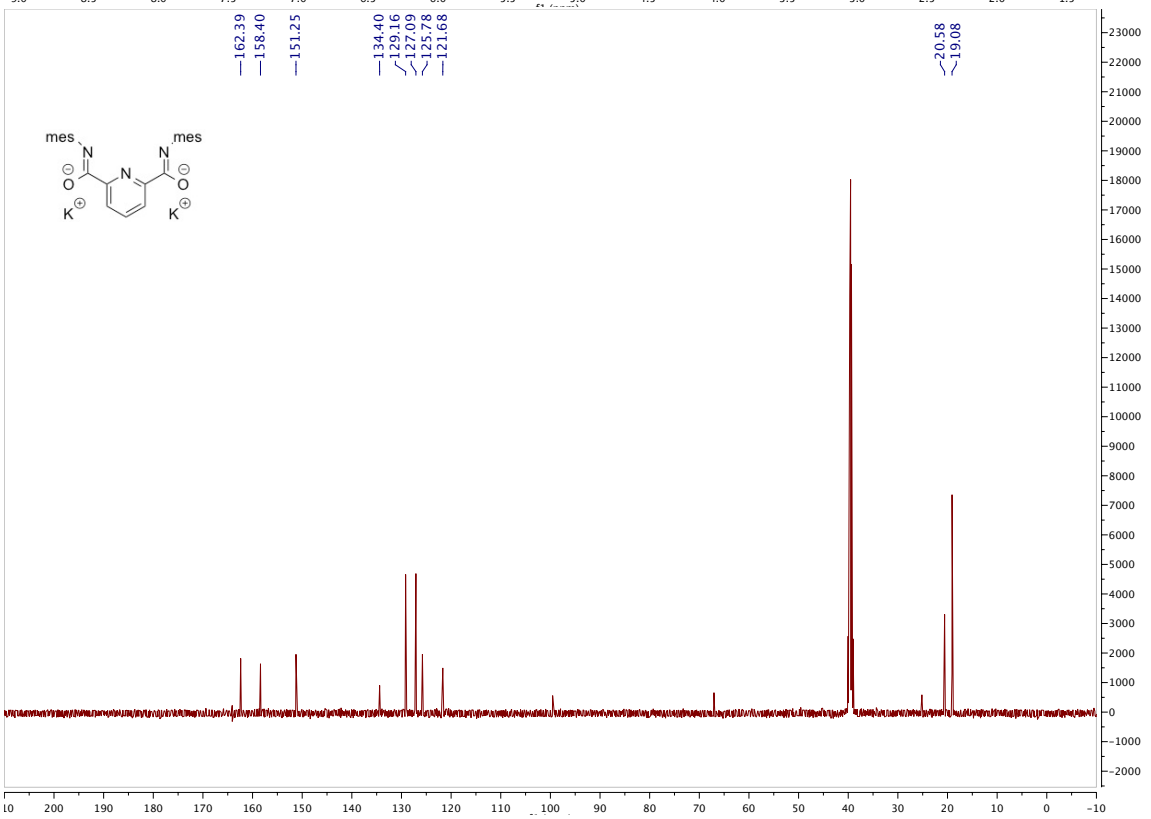
162.39
158.40
151.25
134.40
129.16
127.09
125.78
121.68
20.58
19.08
mes
mes

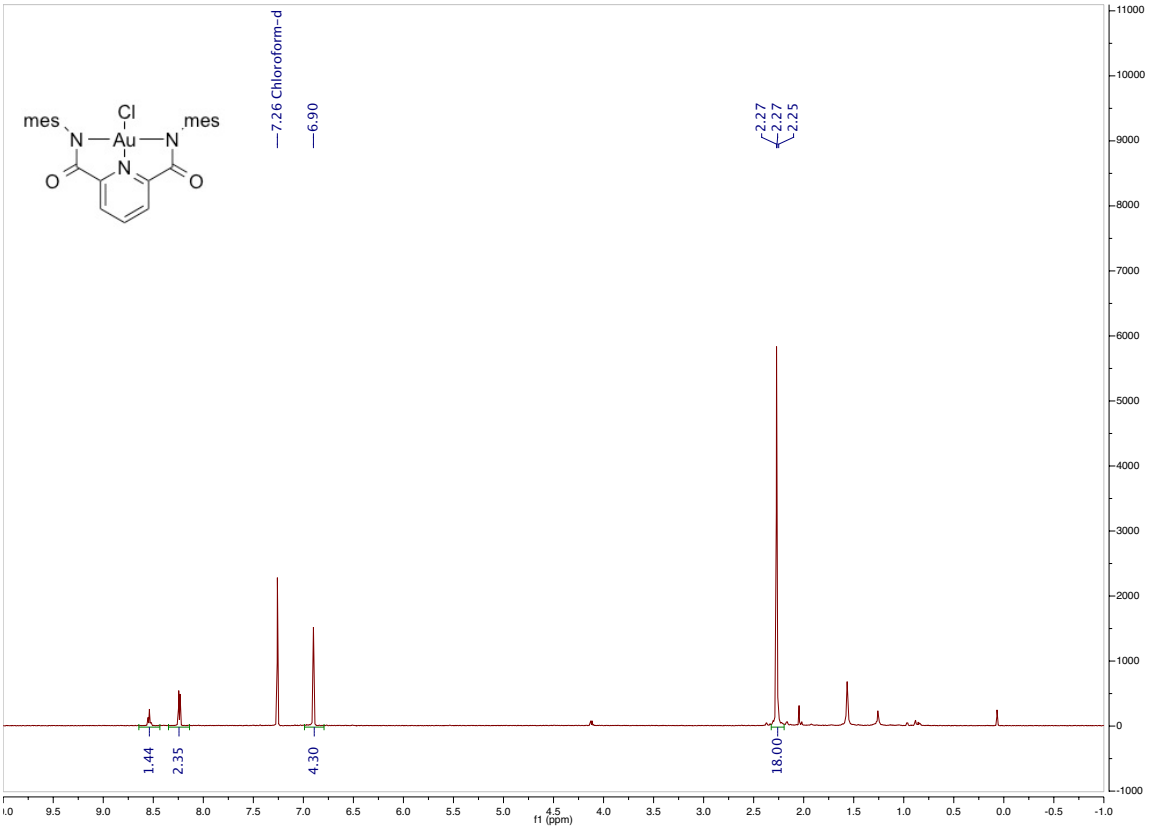
mes
Cl
mes
N
Au
N
O
O
N
7.26 Chloroform-d
6.90
2.27
2.27
2.25
1.44
2.35
4.30
18.00
f1 (ppm)

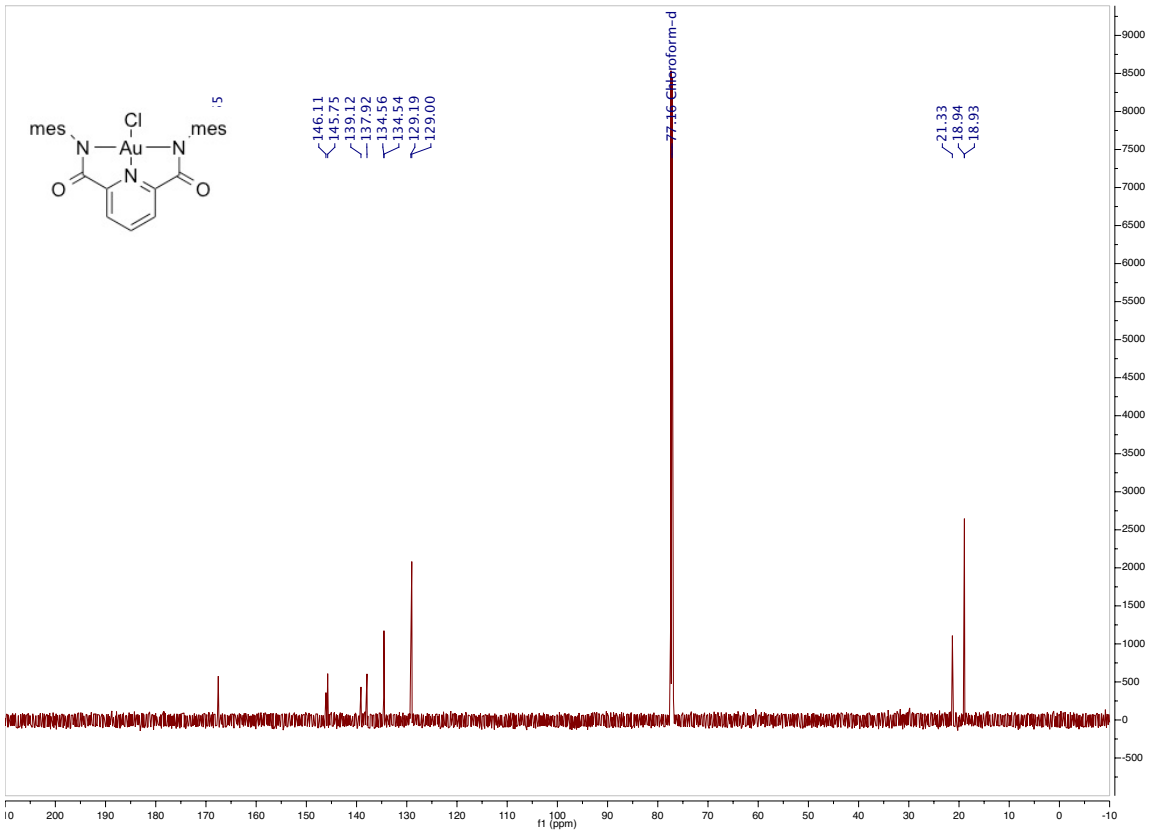
mes
Cl
mes
N
Au
N
O
O
N
146.11
145.75
139.12
137.92
134.56
134.54
129.19
129.00
77.16 Chloroform-d
21.33
18.94
18.93
f1 (ppm)

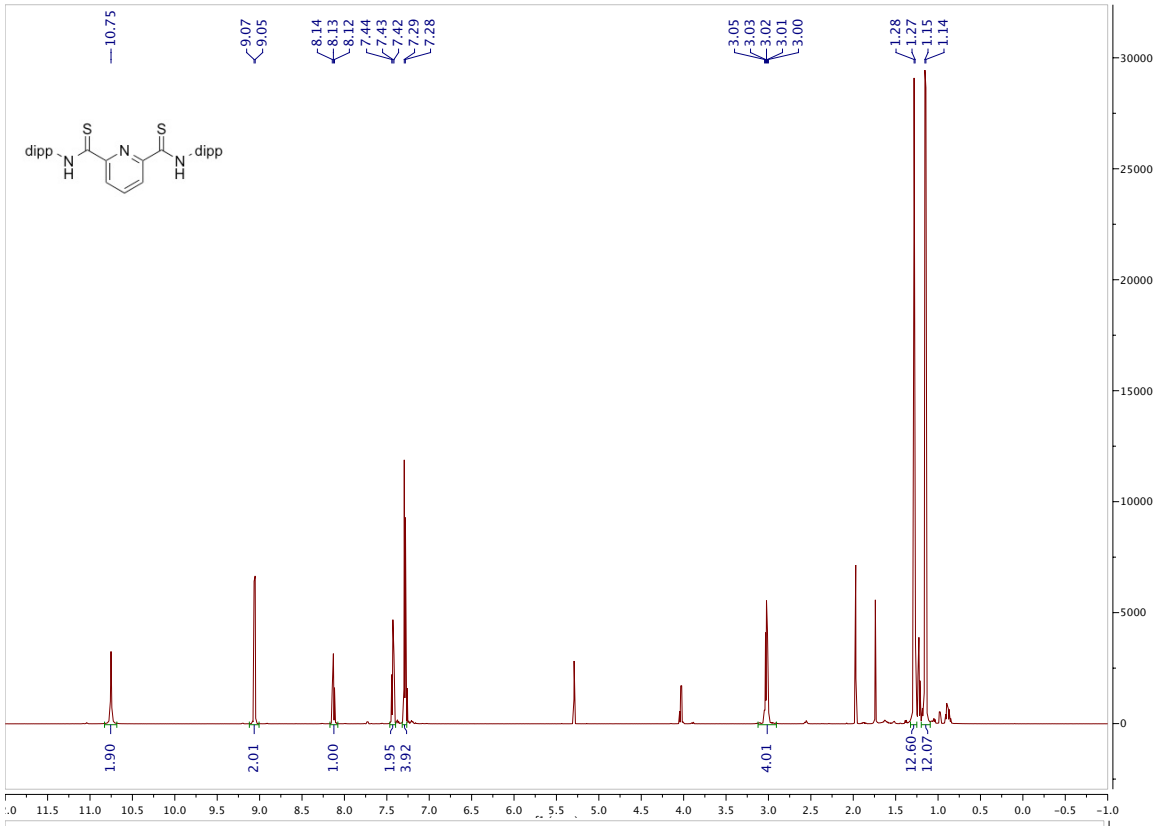
10.75
9.07
9.05
8.14
8.13
8.12
7.44
7.43
7.42
7.29
7.28
3.05
3.03
3.02
3.01
3.00
1.28
1.27
1.15
1.14
dipp
dipp
1.90
2.01
1.00
1.95
3.92
4.01
12.60
12.07

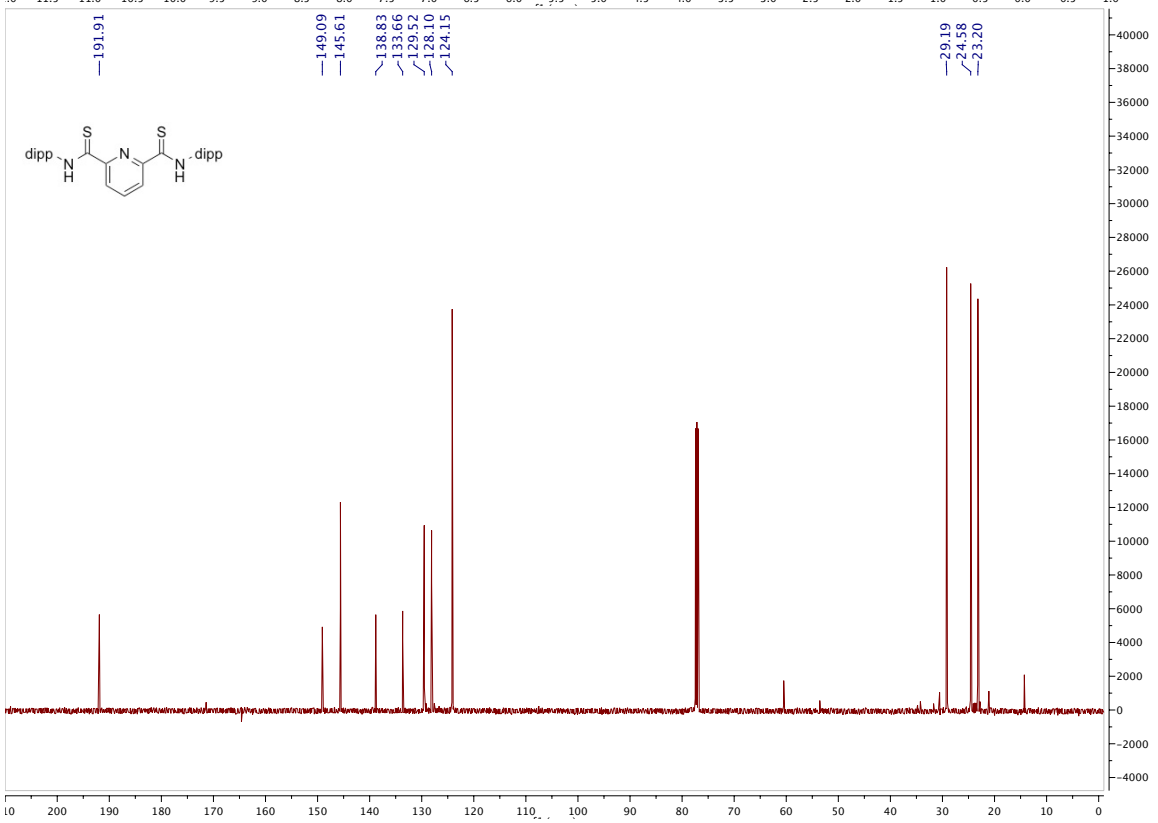
191.91
149.09
145.61
138.83
133.66
129.52
128.10
124.15
29.19
24.58
23.20
dipp
dipp

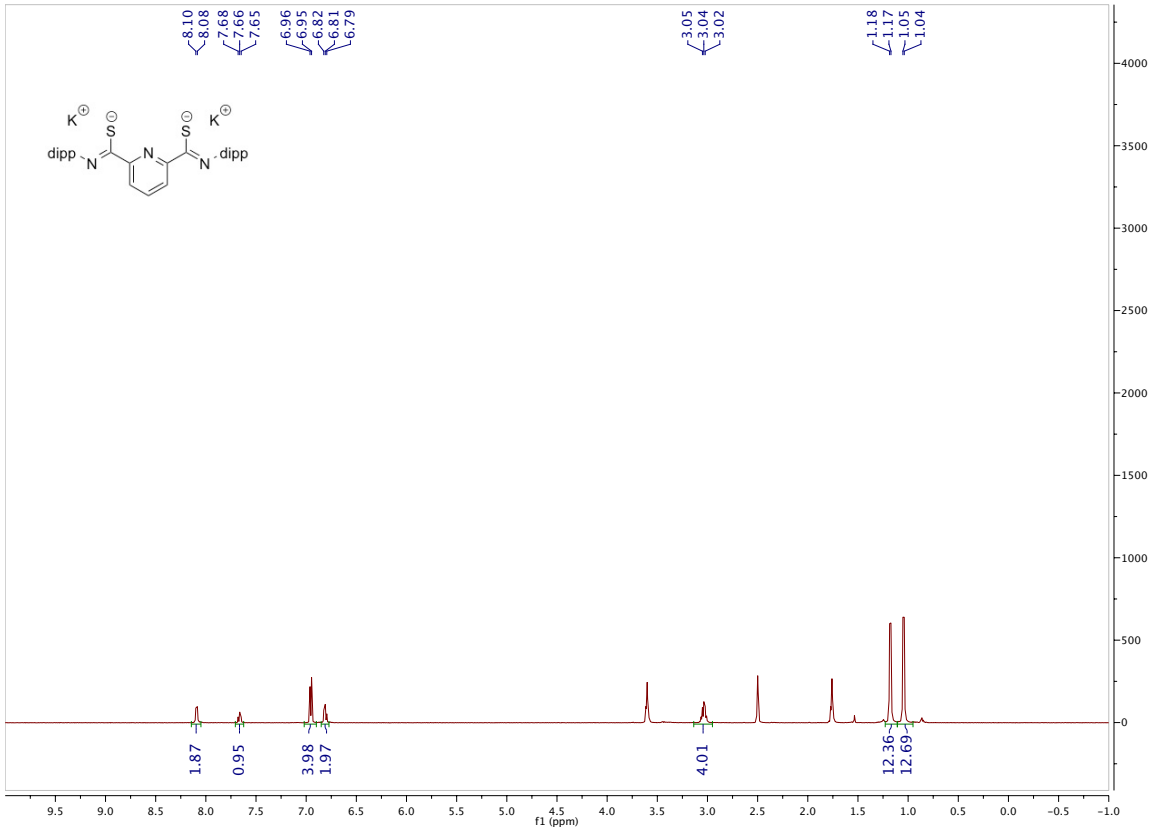
8.10
8.08
7.68
7.66
7.65
6.96
6.95
6.82
6.81
6.79
3.05
3.04
3.02
1.18
1.17
1.05
1.04
K
S
N
dipp
1.87
0.95
3.98
1.97
4.01
12.36
12.69
f1 (ppm)

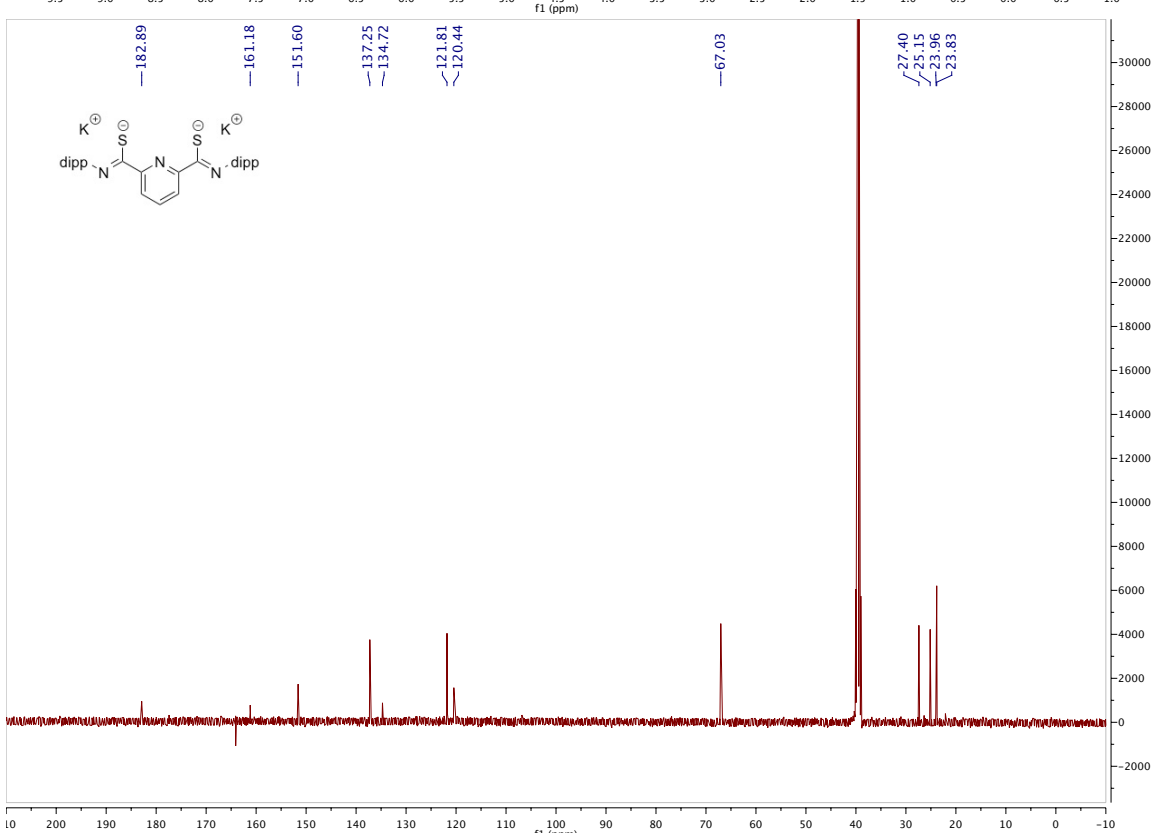
182.89
161.18
151.60
137.25
134.72
121.81
120.44
67.03
27.40
25.15
23.96
23.83
K
S
N
dipp

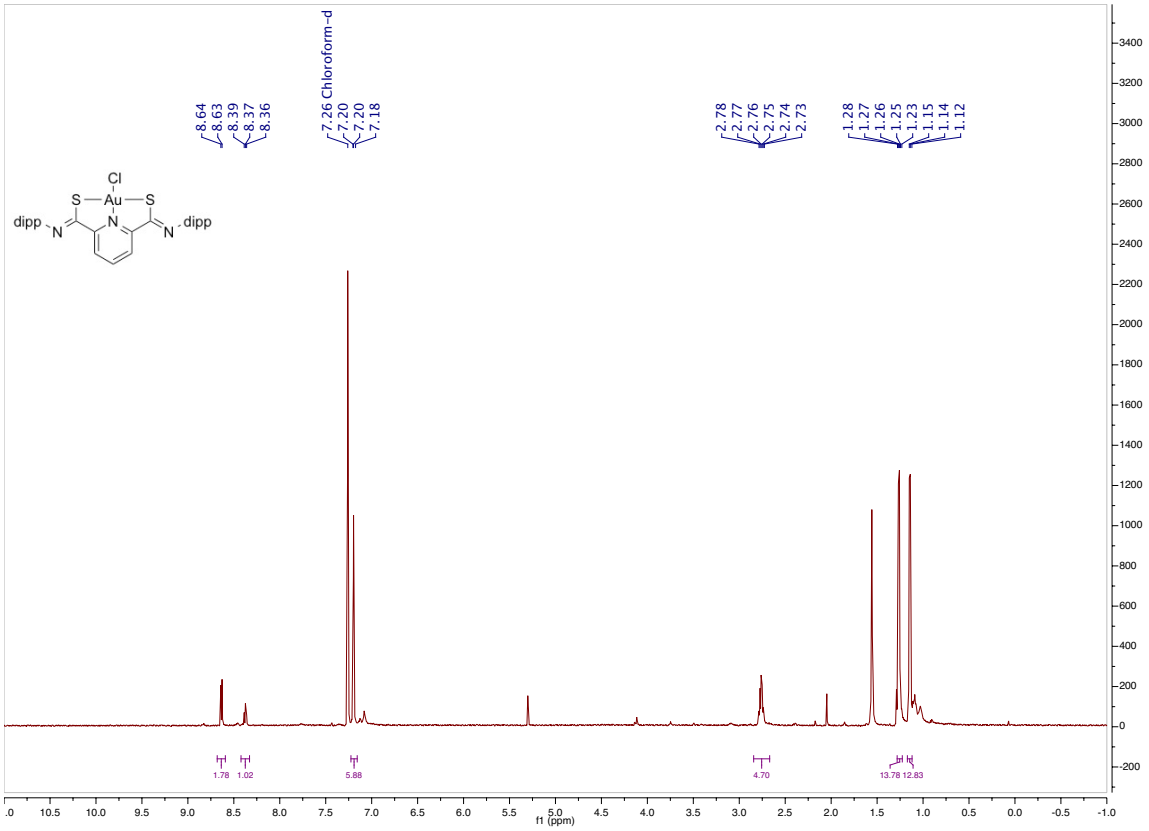
8.64
8.63
8.39
8.37
8.36
7.26 Chloroform-d
7.20
7.20
7.18
2.78
2.77
2.76
2.75
2.74
2.73
1.28
1.27
1.26
1.25
1.23
1.15
1.14
1.12
Cl
S
Au
S
N
dipp
dipp
1.78
1.02
5.88
4.70
13.78
12.83
f1 (ppm)

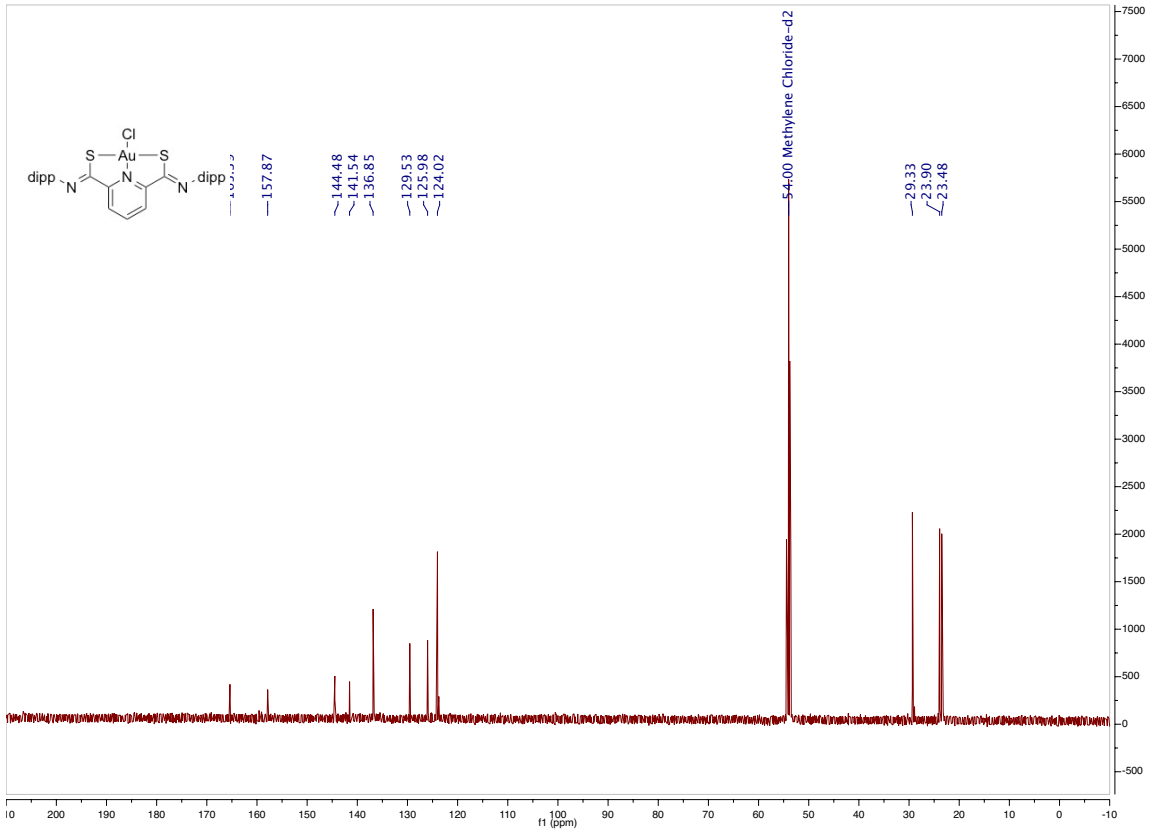
157.87
144.48
141.54
136.85
129.53
125.98
124.02
54.00 Methylene Chloride-d2
29.33
23.90
23.48
Cl
S
Au
S
N
dipp
dipp
f1 (ppm)

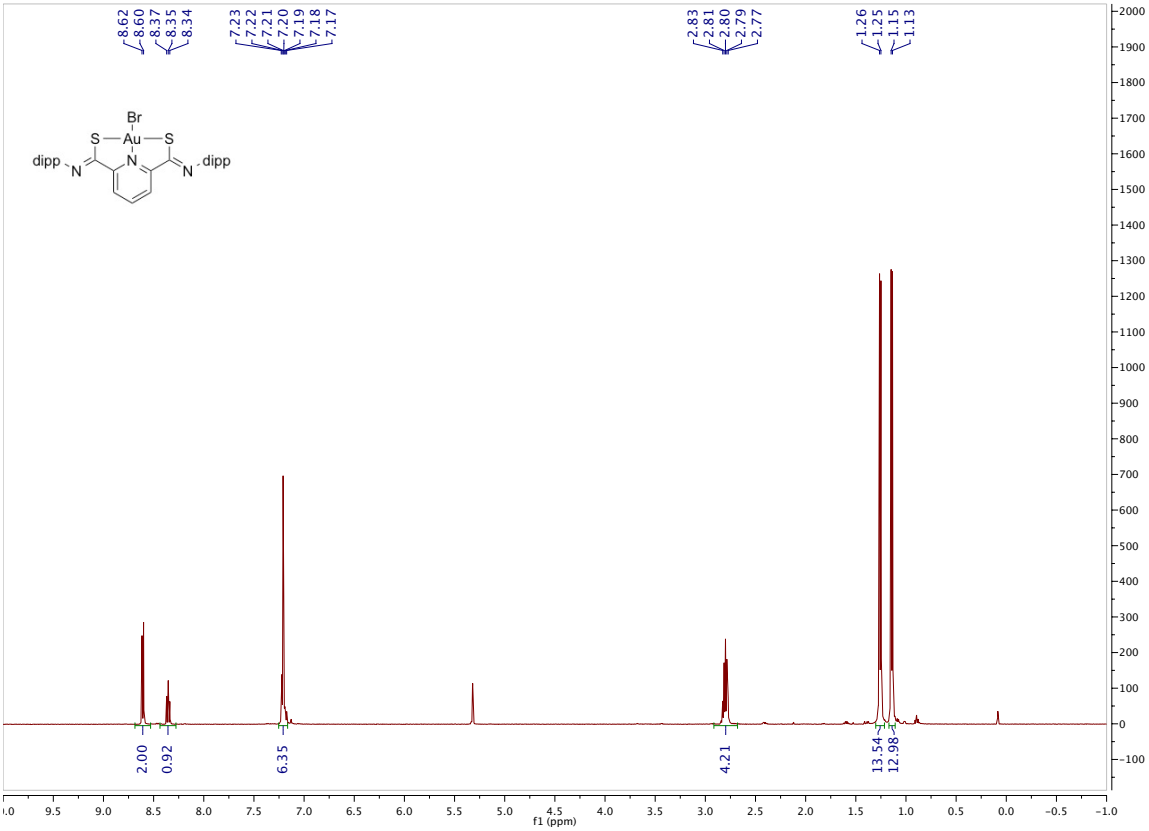
8.62
8.60
8.37
8.35
8.34
7.23
7.22
7.21
7.20
7.19
7.18
7.17
2.83
2.81
2.80
2.79
2.77
1.26
1.25
1.15
1.13
Br
S
Au
S
dipp
N
N
N
dipp
2.00
0.92
6.35
4.21
13.54
12.98
f1 (ppm)

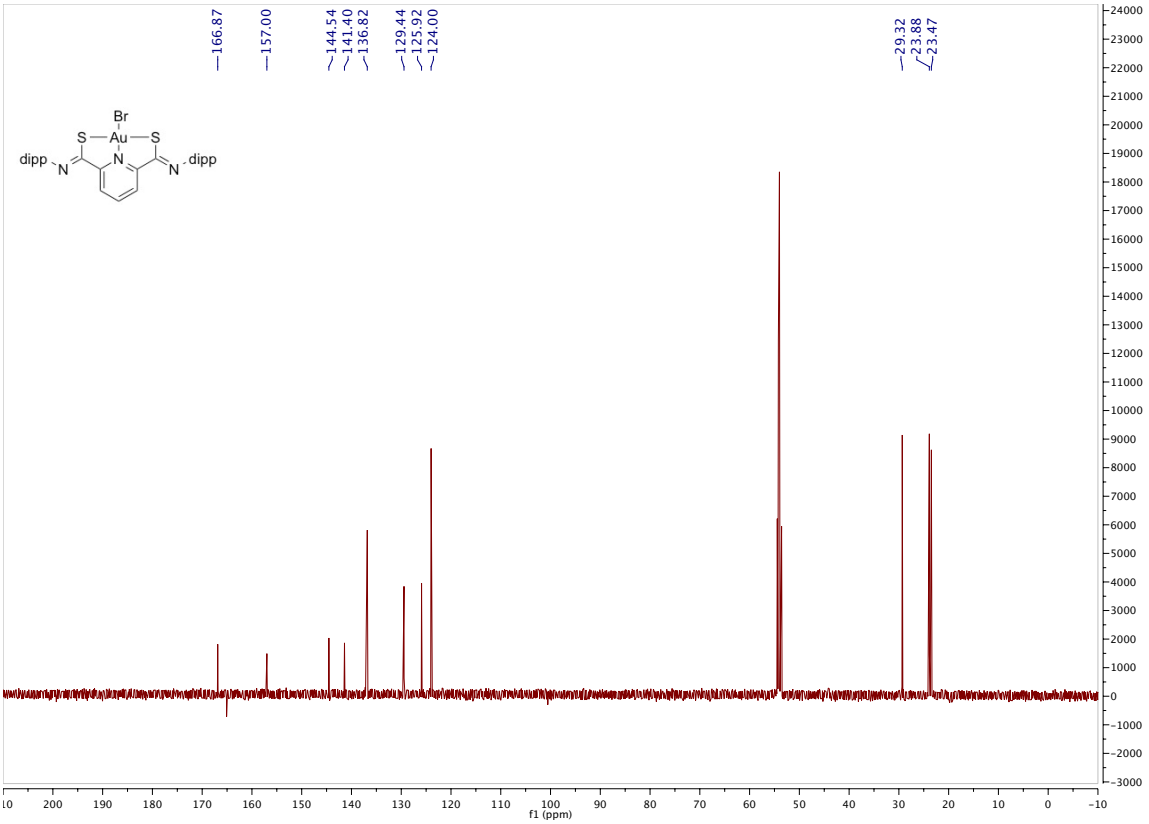
166.87
157.00
144.54
141.40
136.82
129.44
125.92
124.00
29.32
23.88
23.47
Br
S
Au
S
dipp
N
N
N
dipp
f1 (ppm)

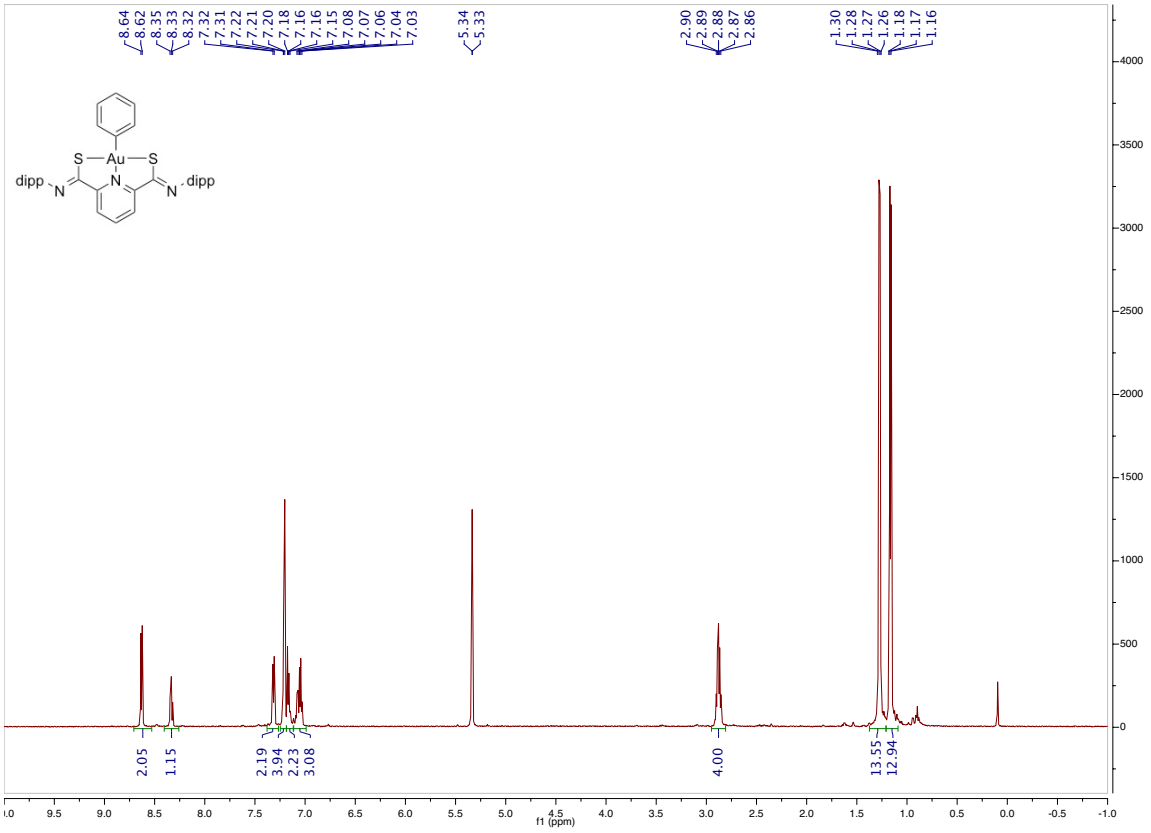
8.64
8.62
8.35
8.33
8.32
7.32
7.31
7.22
7.21
7.20
7.18
7.16
7.16
7.15
7.08
7.07
7.06
7.04
7.03
5.34
5.33
2.90
2.89
2.88
2.87
2.86
1.30
1.28
1.27
1.26
1.18
1.17
1.16
dipp
dipp
2.05
1.15
2.19
3.94
2.23
3.08
4.00
13.55
12.94
f1 (ppm)

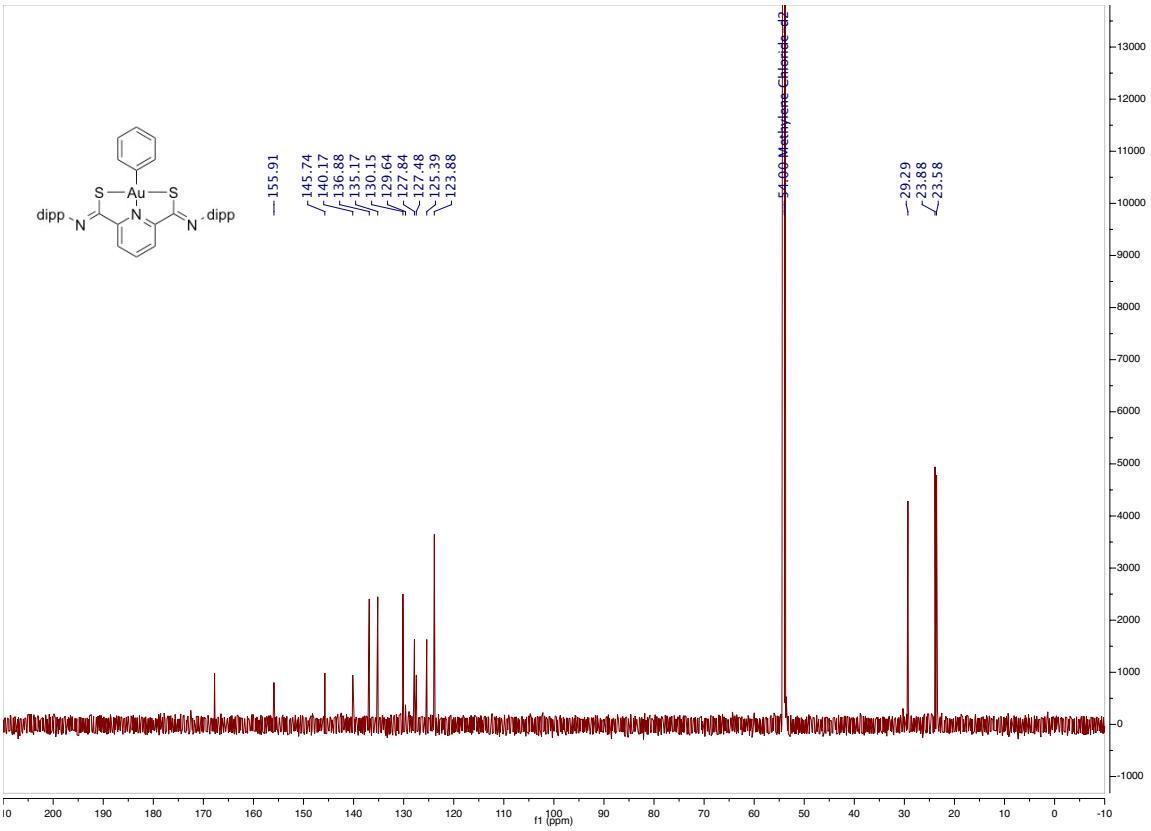
155.91
145.74
140.17
136.88
135.17
130.15
129.64
127.84
127.48
125.39
123.88
54.00 Methylene Chloride-d2
29.29
23.88
23.58
dipp
dipp
f1 (ppm)

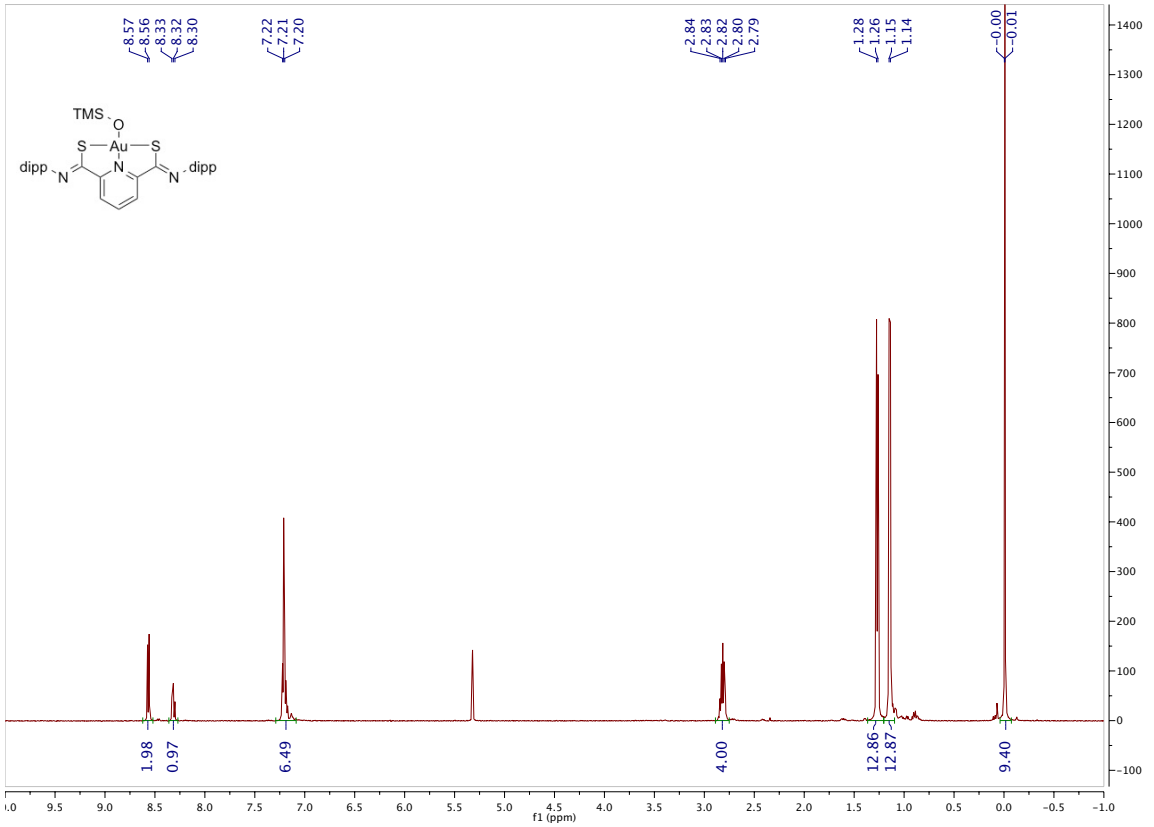
8.57
8.56
8.33
8.32
8.30
7.22
7.21
7.20
2.84
2.83
2.82
2.80
2.79
1.28
1.26
1.15
1.14
0.00
0.01
TMS
O
S
Au
S
N
dipp
N
N
dipp
1.98
0.97
6.49
4.00
12.86
12.87
9.40
f1 (ppm)

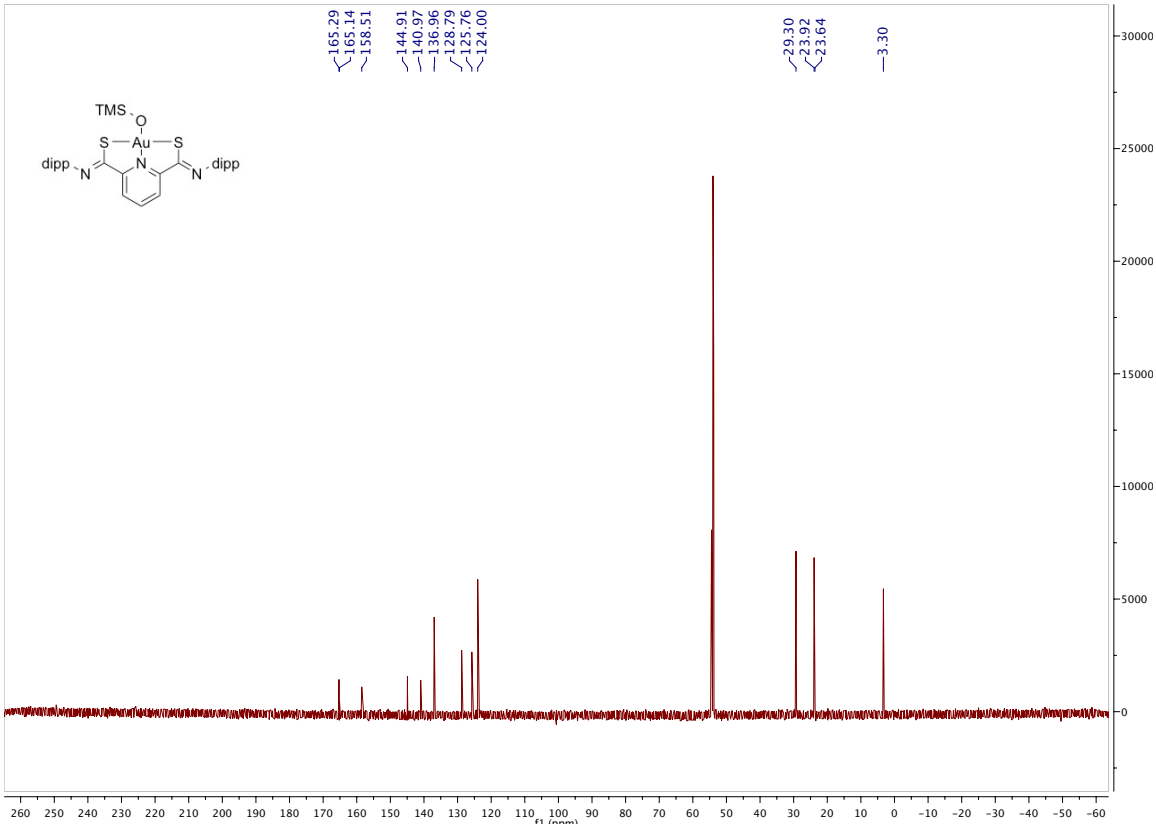
165.29
165.14
158.51
144.91
140.97
136.96
128.79
125.76
124.00
29.30
23.92
23.64
3.30
TMS
O
S
Au
S
N
dipp
N
N
dipp
f1 (ppm)

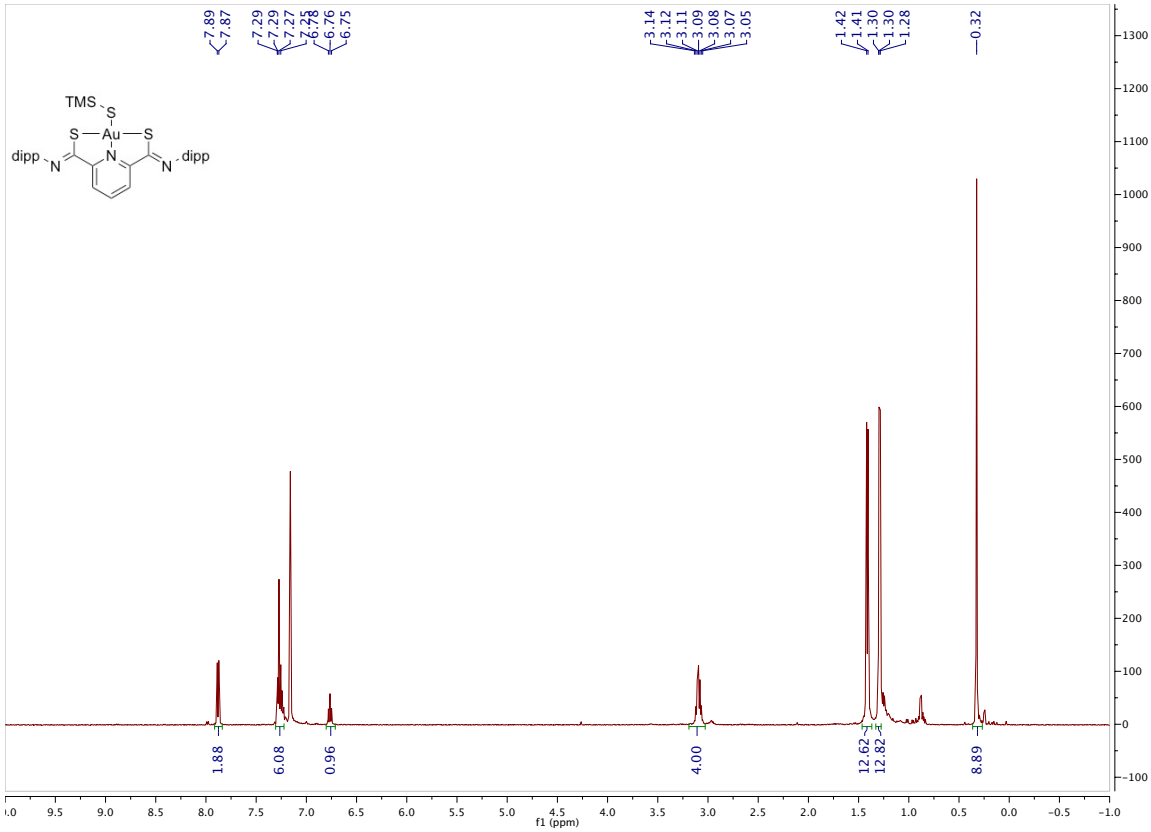
7.89
7.87
7.29
7.29
7.27
7.25
6.76
6.75
3.14
3.12
3.11
3.09
3.08
3.07
3.05
1.42
1.41
1.30
1.30
1.28
0.32
TMS
S
S
Au
S
dipp
N
N
N
dipp
1.88
6.08
0.96
4.00
12.62
12.82
8.89
f1 (ppm)

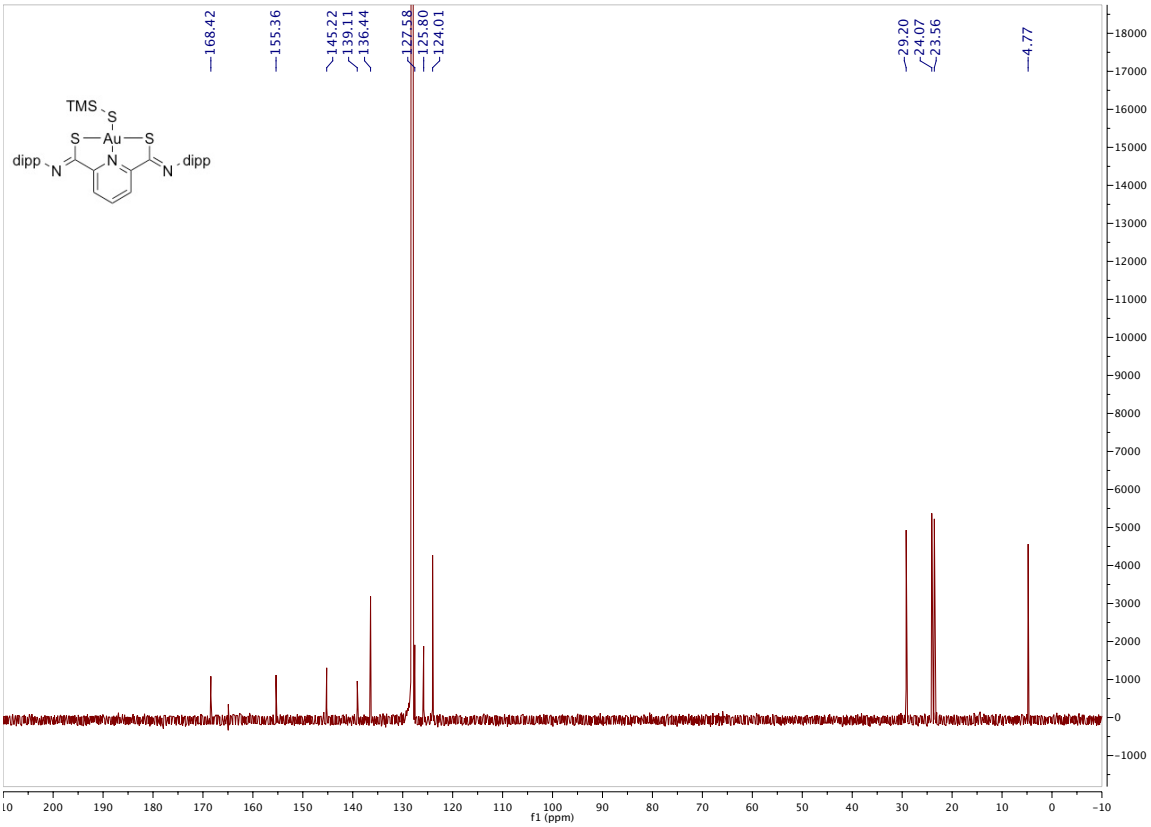
168.42
155.36
145.22
139.11
136.44
127.58
125.80
124.01
29.20
24.07
23.56
4.77
TMS
S
S
Au
S
dipp
N
N
N
dipp
f1 (ppm)

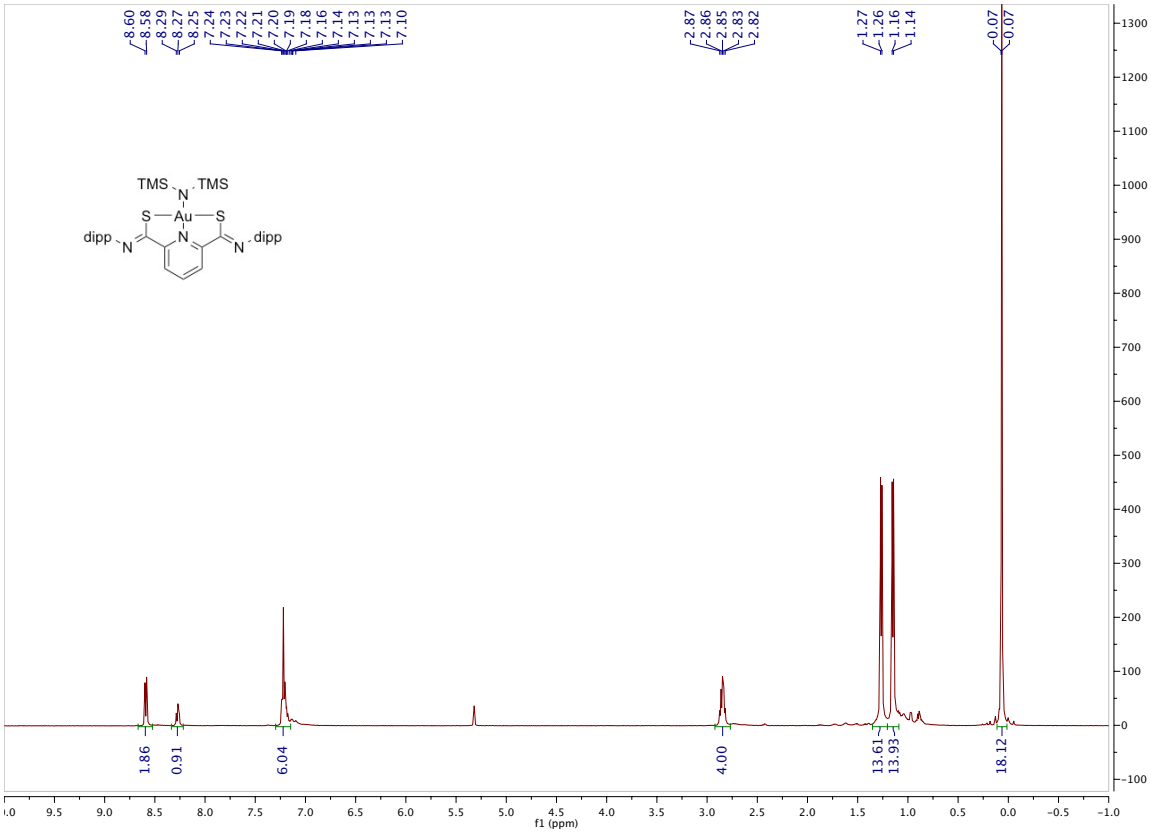
8.60
8.58
8.29
8.27
8.25
7.24
7.23
7.22
7.21
7.20
7.19
7.18
7.16
7.14
7.13
7.13
7.13
7.10
2.87
2.86
2.85
2.83
2.82
1.27
1.26
1.16
1.14
0.07
0.07
TMS
N
TMS
S
Au
S
dipp
N
N
N
dipp
1.86
0.91
6.04
4.00
13.61
13.93
18.12
f1 (ppm)

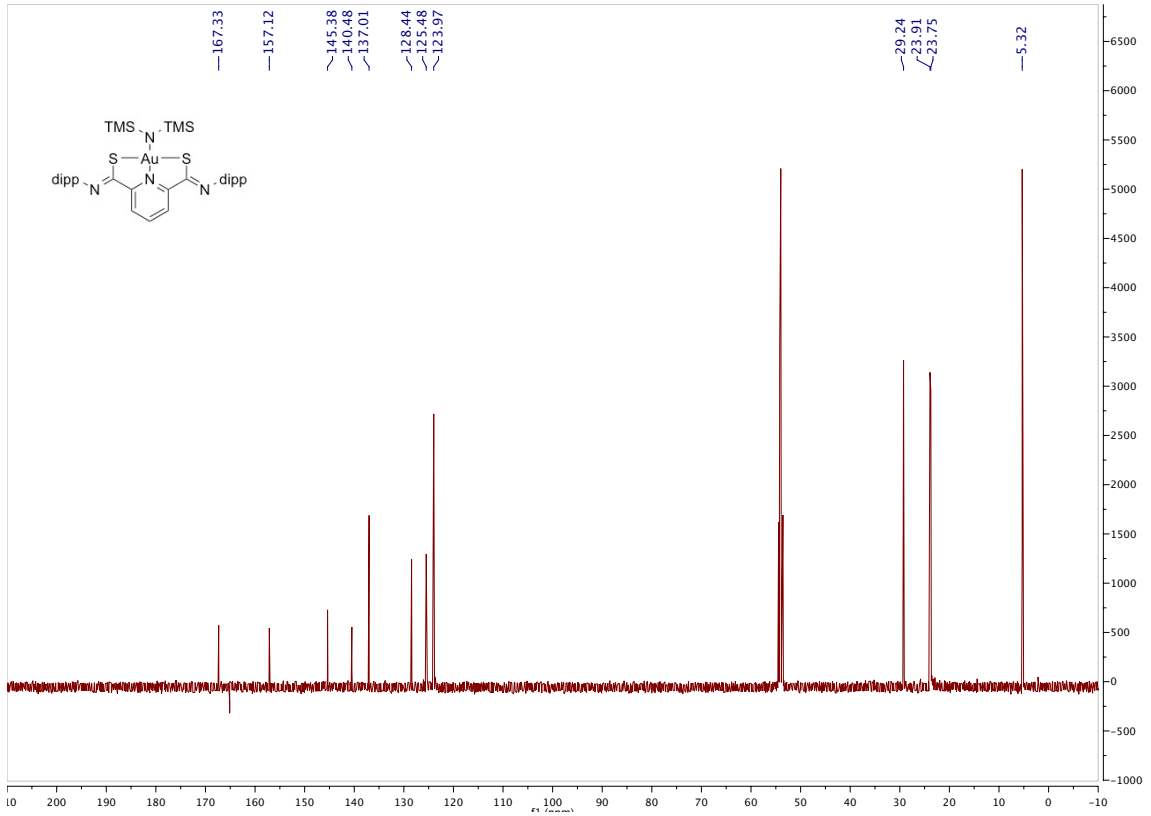
167.33
157.12
145.38
140.48
137.01
128.44
125.48
123.97
29.24
23.91
23.75
5.32
TMS
N
TMS
S
Au
S
dipp
N
N
N
dipp
f1 (ppm)

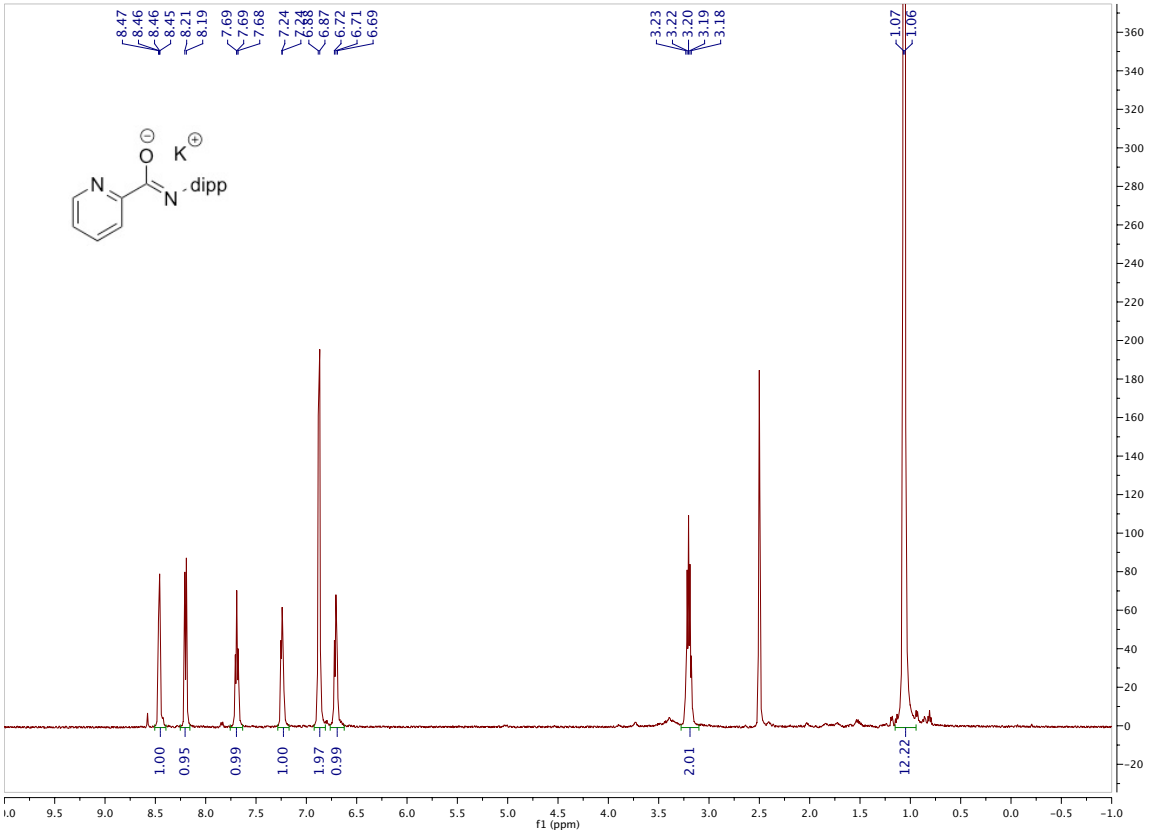
8.47
8.46
8.46
8.45
8.21
8.19
7.69
7.69
7.68
7.24
7.24
6.88
6.87
6.72
6.71
6.69
3.23
3.22
3.20
3.19
3.18
1.07
1.06
O
K
N
N
dipp
1.00
0.95
0.99
1.00
1.97
0.99
2.01
12.22
f1 (ppm)

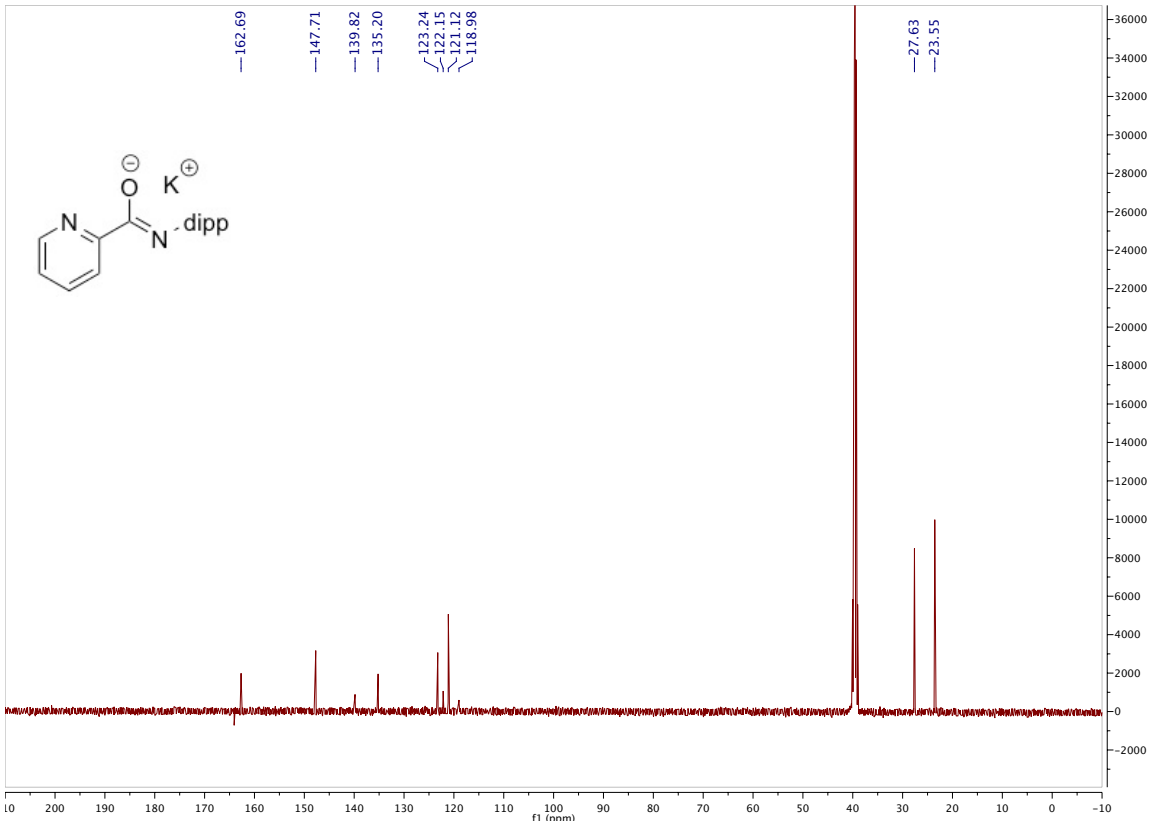
162.69
147.71
139.82
135.20
123.24
122.15
121.12
118.98
27.63
23.55
O
K
N
N
dipp
f1 (ppm)

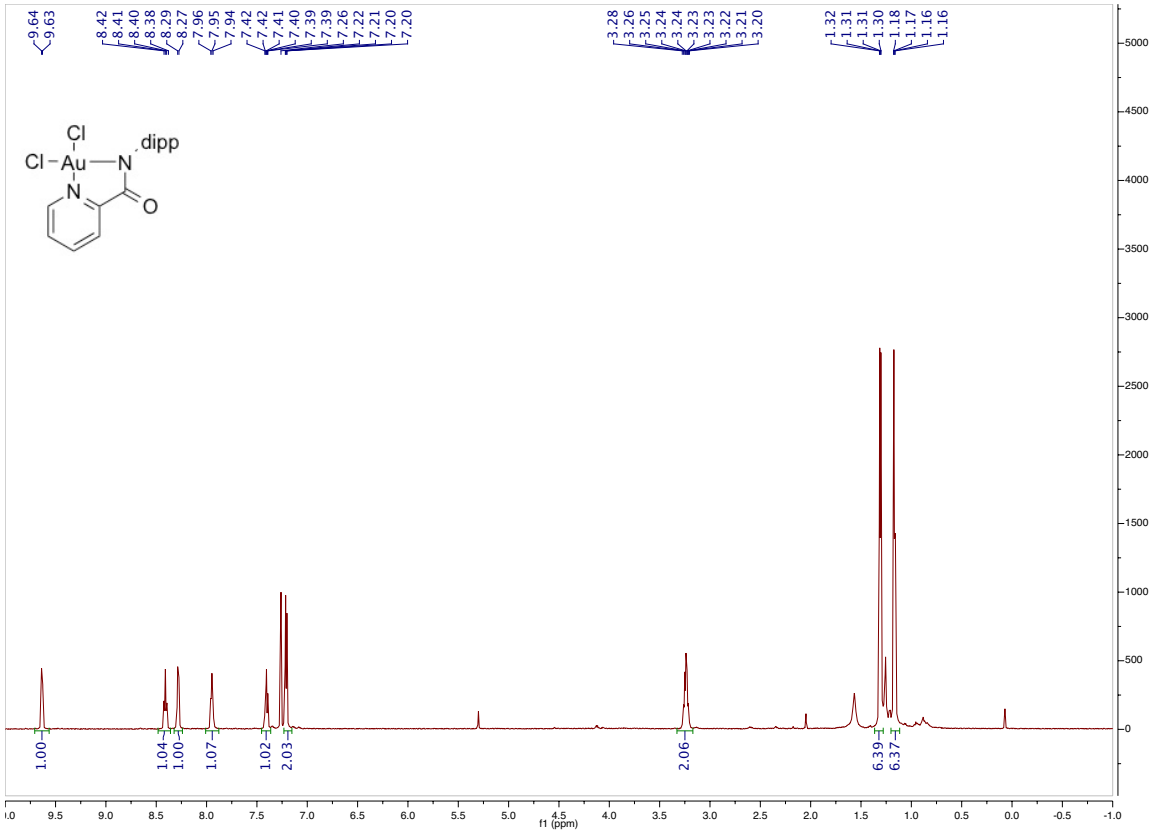
9.64
9.63
8.42
8.41
8.40
8.38
8.29
8.27
7.96
7.95
7.94
7.42
7.42
7.41
7.40
7.39
7.39
7.26
7.22
7.21
7.20
7.20
3.28
3.26
3.25
3.24
3.24
3.23
3.23
3.22
3.21
3.20
1.32
1.31
1.31
1.30
1.18
1.17
1.16
1.16
Cl
Cl–Au–N
dipp
N
O
1.00
1.04
1.00
1.07
1.02
2.03
2.06
6.39
6.37
f1 (ppm)

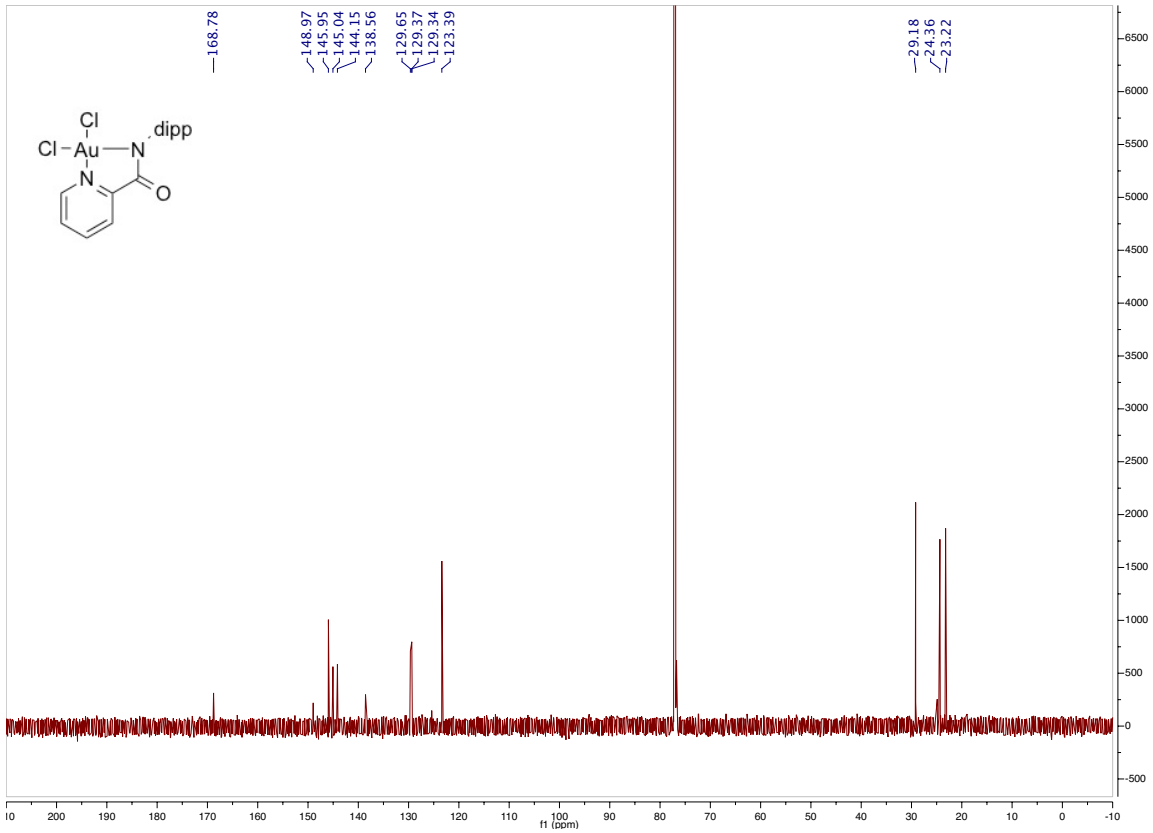
168.78
148.97
145.95
145.04
144.15
138.56
129.65
129.37
129.34
123.39
29.18
24.36
23.22
Cl
Cl–Au–N
dipp
N
O
f1 (ppm)

X-Ray Crystallographic Tables

Complex 9

Table 1. Crystal data and structure refinement for toste103.

X-ray ID	toste103	
Sample/notebook ID	Au(III)Br	
Empirical formula	C31.90 H38.80 Au Br Cl1.80 N3 S2	
Formula weight	869.08	
Temperature	100(2) K	
Wavelength	0.71073 Å	
Crystal system	Triclinic	
Space group	P -1	
Unit cell dimensions	a = 10.6673(5) Å	α= 101.749(3)°.
	b = 12.8317(6) Å	β= 102.660(3)°.
	c = 14.8811(7) Å	γ = 105.925(3)°.
Volume	1834.05(15) $Å^3$	
Z	2	
Density (calculated)	1.574 Mg/m^3	
Absorption coefficient	5.369 mm^{-1}	
F(000)	855.6	
Crystal size	0.040 x 0.020 x 0.020 mm^3	
Theta range for data collection	1.720 to 25.378°.	
Index ranges	-12<=h<=12, -15<=k<=15, -17<=l<=17	
Reflections collected	41255	
Independent reflections	6669 [R(int) = 0.0553]	
Completeness to theta = 25.000°	99.9 %	
Absorption correction	Analytical	
Max. and min. transmission	0.990 and 0.789	
Refinement method	Full-matrix least-squares on F^2	
Data / restraints / parameters	6669 / 0 / 377	
Goodness-of-fit on F^2	1.071	
Final R indices [I>2sigma(I)]	R1 = 0.0393, wR2 = 0.0964	
R indices (all data)	R1 = 0.0516, wR2 = 0.1029	
Extinction coefficient	n/a	
Largest diff. peak and hole	2.443 and -1.241 $e.Å^{-3}$	

Table 2. Atomic coordinates (x 10^4) and equivalent isotropic displacement parameters ($Å^2$x 10^3) for toste103. U(eq) is defined as one third of the trace of the orthogonalized U^{ij} tensor.

	x	y	z	U(eq)
C(1)	823(6)	2331(5)	-216(4)	13(1)
C(2)	943(6)	2605(5)	834(4)	14(1)
C(3)	657(7)	1783(5)	1286(5)	21(2)
C(4)	831(7)	2087(6)	2271(5)	26(2)
C(5)	1295(7)	3221(5)	2772(5)	21(2)
C(6)	1556(6)	4034(5)	2287(4)	15(1)
C(7)	2008(6)	5256(5)	2783(4)	15(1)
C(8)	296(7)	929(5)	-1660(4)	19(1)
C(9)	1349(7)	702(6)	-1981(5)	29(2)
C(10)	1099(8)	264(6)	-2961(5)	33(2)
C(11)	-158(8)	20(6)	-3604(5)	31(2)
C(12)	-1202(8)	229(5)	-3262(5)	24(2)
C(13)	-1017(7)	682(5)	-2298(4)	19(1)
C(14)	2731(8)	937(8)	-1273(6)	45(2)
C(15)	3813(10)	1913(9)	-1393(10)	77(4)
C(16)	3168(10)	-111(9)	-1357(8)	60(3)
C(17)	-2158(7)	899(6)	-1908(5)	25(2)
C(18)	-2642(8)	92(6)	-1333(6)	32(2)
C(19)	-3381(8)	862(6)	-2686(5)	33(2)
C(20)	2628(7)	6692(5)	4211(4)	18(1)
C(21)	1642(7)	7128(5)	4436(5)	19(1)
C(22)	2049(7)	8244(6)	4989(5)	28(2)
C(23)	3414(7)	8912(6)	5320(5)	29(2)
C(24)	4378(7)	8458(6)	5102(5)	28(2)
C(25)	4011(7)	7342(6)	4554(5)	23(2)
C(26)	142(7)	6400(6)	4096(5)	26(2)
C(27)	-496(9)	6404(8)	4911(6)	48(2)
C(28)	-660(8)	6773(8)	3321(6)	48(2)
C(29)	5116(7)	6855(7)	4357(6)	37(2)
C(30)	6078(11)	7578(10)	3946(10)	81(4)
C(31)	5886(14)	6662(14)	5257(9)	109(6)

C(32)	5220(30)	4330(20)	1192(19)	74(7)
C(33)	6840(20)	3042(19)	3028(17)	57(6)
N(1)	1376(5)	3708(4)	1343(3)	12(1)
N(2)	466(5)	1290(4)	-653(4)	16(1)
N(3)	2215(5)	5537(4)	3684(4)	18(1)
S(1)	1201(2)	3445(1)	-741(1)	20(1)
S(2)	2199(2)	6214(1)	2088(1)	25(1)
Cl(1)	4310(7)	2865(6)	1179(5)	86(2)
Cl(2)	5036(8)	5247(7)	1671(6)	94(3)
Cl(3)	7895(8)	3206(7)	2591(6)	89(3)
Cl(4)	6378(10)	4163(8)	3538(7)	109(3)
Br(1)	2036(1)	6328(1)	-201(1)	24(1)
Au(1)	1692(1)	4903(1)	629(1)	16(1)

Complex 11

Table 1. Crystal data and structure refinement for toste109.

X-ray ID	toste109	
Sample/notebook ID	Au(III)OTMS	
Empirical formula	C34 H46 Au N3 O S2 Si	
Formula weight	801.91	
Temperature	100(2) K	
Wavelength	0.71073 Å	
Crystal system	Triclinic	
Space group	P -1	
Unit cell dimensions	a = 10.7510(5) Å	α= 106.618(2)°.
	b = 13.3542(6) Å	β= 105.324(2)°.
	c = 14.9418(6) Å	γ = 97.809(2)°.
Volume	1929.93(15) $Å^3$	
Z	2	
Density (calculated)	1.380 Mg/m^3	
Absorption coefficient	3.978 mm^{-1}	
F(000)	808	
Crystal size	0.030 x 0.030 x 0.020 mm^3	
Theta range for data collection	1.501 to 25.370°.	
Index ranges	-12<=h<=12, -16<=k<=16, -17<=l<=18	
Reflections collected	21746	
Independent reflections	7009 [R(int) = 0.0598]	
Completeness to theta = 25.000°	99.8 %	
Absorption correction	Semi-empirical from equivalents	
Max. and min. transmission	0.862 and 0.734	
Refinement method	Full-matrix least-squares on F^2	
Data / restraints / parameters	7009 / 0 / 390	
Goodness-of-fit on F^2	1.013	
Final R indices [I>2sigma(I)]	R1 = 0.0389, wR2 = 0.0712	
R indices (all data)	R1 = 0.0569, wR2 = 0.0769	
Extinction coefficient	n/a	
Largest diff. peak and hole	1.018 and -1.132 $e.Å^{-3}$	

Table 2. Atomic coordinates (x 10^4) and equivalent isotropic displacement parameters ($Å^2$x 10^3) for toste109. U(eq) is defined as one third of the trace of the orthogonalized U^{ij} tensor.

	x	y	z	U(eq)
C(1)	5632(5)	2107(4)	4747(4)	14(1)
C(2)	5804(5)	2470(4)	5810(4)	11(1)
C(3)	5606(5)	1763(4)	6302(4)	15(1)
C(4)	5786(6)	2177(4)	7317(4)	20(1)
C(5)	6185(5)	3261(4)	7801(4)	18(1)
C(6)	6384(5)	3946(4)	7290(4)	12(1)
C(7)	6851(5)	5137(4)	7782(4)	13(1)
C(8)	5046(6)	696(4)	3236(4)	14(1)
C(9)	3772(6)	524(4)	2594(4)	17(1)
C(10)	3548(6)	26(4)	1590(4)	24(1)
C(11)	4575(6)	-278(4)	1250(4)	26(2)
C(12)	5819(6)	-79(4)	1889(4)	25(2)
C(13)	6103(6)	417(4)	2900(4)	19(1)
C(14)	2663(6)	854(4)	2978(4)	22(1)
C(15)	1604(6)	1125(5)	2233(4)	30(2)
C(16)	2030(7)	-22(6)	3296(6)	51(2)
C(17)	7500(6)	657(5)	3609(5)	37(2)
C(18)	8564(8)	1064(7)	3207(7)	77(3)
C(19)	7798(8)	-265(7)	3887(8)	107(4)
C(20)	7628(5)	6631(4)	9213(4)	11(1)
C(21)	8998(6)	7081(4)	9552(4)	16(1)
C(22)	9444(6)	8170(4)	10098(4)	22(1)
C(23)	8569(6)	8803(5)	10306(4)	24(1)
C(24)	7213(6)	8341(5)	9941(4)	24(1)
C(25)	6713(5)	7256(4)	9393(4)	15(1)
C(26)	9977(5)	6412(5)	9318(4)	23(1)
C(27)	10694(6)	6797(6)	8669(5)	42(2)
C(28)	10994(6)	6425(5)	10254(5)	38(2)
C(29)	5246(6)	6769(4)	9033(4)	22(1)
C(30)	4425(6)	7456(4)	8580(4)	24(1)
C(31)	4797(7)	6532(5)	9848(5)	45(2)

C(32)	7809(6)	4956(5)	3410(4)	27(2)
C(33)	7646(6)	7251(4)	4330(4)	27(2)
C(34)	9337(6)	6171(5)	5577(4)	26(1)
N(1)	6185(4)	3542(3)	6307(3)	12(1)
N(2)	5264(4)	1090(3)	4284(3)	13(1)
N(3)	7169(4)	5493(3)	8721(3)	16(1)
O(1)	6484(4)	5586(3)	4855(3)	18(1)
Si(1)	7796(2)	5961(1)	4560(1)	17(1)
S(1)	5911(2)	3066(1)	4181(1)	18(1)
S(2)	6918(2)	5940(1)	7043(1)	19(1)
Au(1)	6389(1)	4560(1)	5567(1)	13(1)

Complex 13

Table 1. Crystal data and structure refinement for toste104.

X-ray ID	toste104	
Sample/notebook ID	Au(III)HMDS	
Empirical formula	C43 H67 Au N4 S2 Si2	
Formula weight	957.27	
Temperature	100(2) K	
Wavelength	0.71073 Å	
Crystal system	Monoclinic	
Space group	P 21/n	
Unit cell dimensions	a = 14.9748(13) Å	α= 90°.
	b = 20.5171(19) Å	β= 90.033(4)°.
	c = 17.0555(14) Å	γ = 90°.
Volume	5240.1(8) $Å^3$	
Z	4	
Density (calculated)	1.213 Mg/m^3	
Absorption coefficient	2.962 mm^{-1}	
F(000)	1968	
Crystal size	0.050 x 0.040 x 0.020 mm^3	
Theta range for data collection	1.553 to 25.406°.	
Index ranges	-18<=h<=17, -24<=k<=24, -20<=l<=20	
Reflections collected	94545	
Independent reflections	9411 [R(int) = 0.0533]	
Completeness to theta = 25.000°	98.4 %	
Absorption correction	Analytical	
Max. and min. transmission	0.985 and 0.873	
Refinement method	Full-matrix least-squares on F^2	
Data / restraints / parameters	9411 / 0 / 484	
Goodness-of-fit on F^2	1.095	
Final R indices [I>2sigma(I)]	R1 = 0.0310, wR2 = 0.0769	
R indices (all data)	R1 = 0.0456, wR2 = 0.0841	
Extinction coefficient	n/a	
Largest diff. peak and hole	1.694 and -1.052 $e.Å^{-3}$	

Table 2. Atomic coordinates (x 10^4) and equivalent isotropic displacement parameters ($Å^2$x 10^3) for toste104. U(eq) is defined as one third of the trace of the orthogonalized U^{ij} tensor.

	x	y	z	U(eq)
C(1)	3912(3)	6272(2)	8448(2)	10(1)
C(2)	4157(3)	5881(2)	7747(2)	10(1)
C(3)	4140(3)	5213(2)	7743(2)	15(1)
C(4)	4391(3)	4874(2)	7080(3)	16(1)
C(5)	4650(3)	5215(2)	6418(3)	14(1)
C(6)	4651(3)	5888(2)	6438(2)	12(1)
C(7)	4896(3)	6287(2)	5737(2)	10(1)
C(8)	3531(3)	6322(2)	9772(3)	16(1)
C(9)	4236(3)	6519(2)	10260(3)	21(1)
C(10)	4014(4)	6824(3)	10961(3)	29(1)
C(11)	3149(4)	6929(3)	11173(3)	32(1)
C(12)	2456(4)	6745(3)	10679(3)	29(1)
C(13)	2633(3)	6432(2)	9969(3)	20(1)
C(14)	5207(3)	6404(3)	10045(3)	28(1)
C(15)	5764(4)	7048(3)	10005(3)	36(1)
C(16)	5651(4)	5928(3)	10622(3)	35(1)
C(17)	1894(3)	6216(3)	9417(3)	27(1)
C(18)	1012(4)	6579(3)	9536(3)	36(1)
C(19)	1740(4)	5495(3)	9481(4)	41(2)
C(20)	5274(3)	6345(2)	4416(2)	14(1)
C(21)	4573(3)	6504(2)	3908(3)	18(1)
C(22)	4798(4)	6825(2)	3207(3)	24(1)
C(23)	5663(4)	6971(2)	3022(3)	23(1)
C(24)	6354(3)	6810(2)	3538(3)	19(1)
C(25)	6173(3)	6488(2)	4243(3)	14(1)
C(26)	3606(3)	6351(3)	4102(3)	27(1)
C(27)	3059(4)	6958(3)	4206(3)	39(2)
C(28)	3182(4)	5894(3)	3488(3)	33(1)
C(29)	6912(3)	6305(2)	4820(3)	18(1)
C(30)	7781(3)	6668(3)	4684(3)	26(1)
C(31)	7083(3)	5564(2)	4800(3)	27(1)

C(32)	6241(3)	7953(3)	7640(3)	25(1)
C(33)	5036(4)	8802(3)	8596(3)	29(1)
C(34)	5664(4)	9277(3)	7014(3)	34(1)
C(35)	2556(3)	7946(2)	6586(3)	23(1)
C(36)	3105(4)	9254(3)	7225(3)	28(1)
C(37)	3768(4)	8796(3)	5621(3)	27(1)
C(38)	778(6)	5742(5)	6203(6)	89(3)
C(39)	1475(5)	6008(4)	5700(5)	74(2)
C(40)	2315(5)	6055(4)	6192(5)	62(2)
C(41)	1986(6)	6114(4)	7049(5)	78(3)
C(42)	960(6)	6113(5)	6988(6)	90(3)
C(43)	-214(6)	5798(7)	5919(6)	132(5)
N(1)	4409(2)	6210(2)	7094(2)	10(1)
N(2)	3731(2)	5966(2)	9073(2)	14(1)
N(3)	5077(2)	5979(2)	5109(2)	11(1)
N(4)	4396(2)	8190(2)	7108(2)	11(1)
Si(1)	5294(1)	8544(1)	7575(1)	17(1)
Si(2)	3495(1)	8535(1)	6647(1)	16(1)
S(1)	3905(1)	7136(1)	8375(1)	13(1)
S(2)	4915(1)	7145(1)	5824(1)	12(1)
Au(1)	4408(1)	7198(1)	7101(1)	9(1)